ISSN 0021-9673

VOL. 665 NO. 1 APRIL 8, 1994

9th Int. Symp. Advances and Applications of Chromatography in Industry Bratislava, Aug. 29–Sept. 3, 1993

JOURNAL OF CHROMATOGRAPHY A

INCLUDING ELECTROPHORESIS AND OTHER SEPARATION METHODS

SYMPOSIUM VOLUMES

ELSEVIER

JOURNAL OF CHROMATOGRAPHY A

INCLUDING ELECTROPHORESIS AND OTHER SEPARATION METHODS

Scope. The *Journal of Chromatography A* publishes papers on all aspects of **chromatography, electrophoresis** and related methods. Contributions consist mainly of research papers dealing with chromatographic theory, instrumental developments and their applications. In the *Symposium volumes*, which are under separate editorship, proceedings of symposia on chromatography, electrophoresis and related methods are published. *Journal of Chromatography B: Biomedical Applications* —This journal, which is under separate editorship, deals with the following aspects: developments in and applications of chromatographic and electrophoretic techniques related to clinical diagnosis or alterations during medical treatment; screening and profiling of body fluids or tissues related to the analysis of active substances and to metabolic disorders; drug level monitoring and pharmacokinetic studies; clinical toxicology; forensic medicine; veterinary medicine; occupational medicine; results from basic medical research with direct consequences in clinical practice.

Submission of Papers. The preferred medium of submission is on disk with accompanying manuscript (see *Electronic manuscripts* in the Instructions to Authors, which can be obtained from the publisher, Elsevier Science B.V., P.O. Box 330, 1000 AH Amsterdam, Netherlands). Manuscripts (in English; *four* copies are required) should be submitted to: Editorial Office of *Journal of Chromatography A*, P.O. Box 681, 1000 AR Amsterdam, Netherlands, Telefax (+31-20) 5862 304, or to: The Editor of *Journal of Chromatography B: Biomedical Applications*, P.O. Box 681, 1000 AR Amsterdam, Netherlands. Review articles are invited or proposed in writing to the Editors who welcome suggestions for subjects. An outline of the proposed review should first be forwarded to the Editors for preliminary discussion prior to preparation. Submission of an article is understood to imply that the article is original and unpublished and is not being considered for publication elsewhere. For copyright regulations, see below.

Publication information. *Journal of Chromatography A* (ISSN 0021-9673): for 1994 Vols. 652–682 are scheduled for publication. *Journal of Chromatography B: Biomedical Applications* (ISSN 0378-4347): for 1994 Vols. 652–662 are scheduled for publication. Subscription prices for *Journal of Chromatography A*, *Journal of Chromatography B: Biomedical Applications* or a combined subscription are available upon request from the publisher. Subscriptions are accepted on a prepaid basis only and are entered on a calendar year basis. Issues are sent by surface mail except to the following countries where air delivery via SAL is ensured: Argentina, Australia, Brazil, Canada, China, Hong Kong, India, Israel, Japan, Malaysia, Mexico, New Zealand, Pakistan, Singapore, South Africa, South Korea, Taiwan, Thailand, USA. For all other countries airmail rates are available upon request. Claims for missing issues must be made within six months of our publication (mailing) date. Please address all your requests regarding orders and subscription queries to: Elsevier Science B.V., Journal Department, P.O. Box 211, 1000 AE Amsterdam, Netherlands. Tel.: (+31-20) 5803 642; Fax: (+31-20) 5803 598. Customers in the USA and Canada wishing information on this and other Elsevier journals, please contact Journal Information Center, Elsevier Science Inc., 655 Avenue of the Americas, New York, NY 10010, USA, Tel. (+1-212) 633 3750, Telefax (+1-212) 633 3764.

Abstracts/Contents Lists published in Analytical Abstracts, Biochemical Abstracts, Biological Abstracts, Chemical Abstracts, Chemical Titles, Chromatography Abstracts, Current Awareness in Biological Sciences (CABS), Current Contents/Life Sciences, Current Contents/Physical, Chemical & Earth Sciences, Deep-Sea Research/Part B: Oceanographic Literature Review, Excerpta Medica, Index Medicus, Mass Spectrometry Bulletin, PASCAL-CNRS, Referativny Zhurnal, Research Alert and Science Citation Index.

US Mailing Notice. *Journal of Chromatography A* (ISSN 0021-9673) is published weekly (total 52 issues) by Elsevier Science B.V., (Sara Burgerhartstraat 25, P.O. Box 211, 1000 AE Amsterdam, Netherlands). Annual subscription price in the USA US$ 4994.00 (US$ price valid in North, Central and South America only) including air speed delivery. Second class postage paid at Jamaica, NY 11431. **USA POSTMASTERS**: Send address changes to *Journal of Chromatography A*, Publications Expediting, Inc., 200 Meacham Avenue, Elmont, NY 11003. Airfreight and mailing in the USA by Publications Expediting.

See inside back cover for Publication Schedule, Information for Authors and information on Advertisements.

0021-9673/94/$07.00

Printed in the Netherlands

For Contents see p. VII.

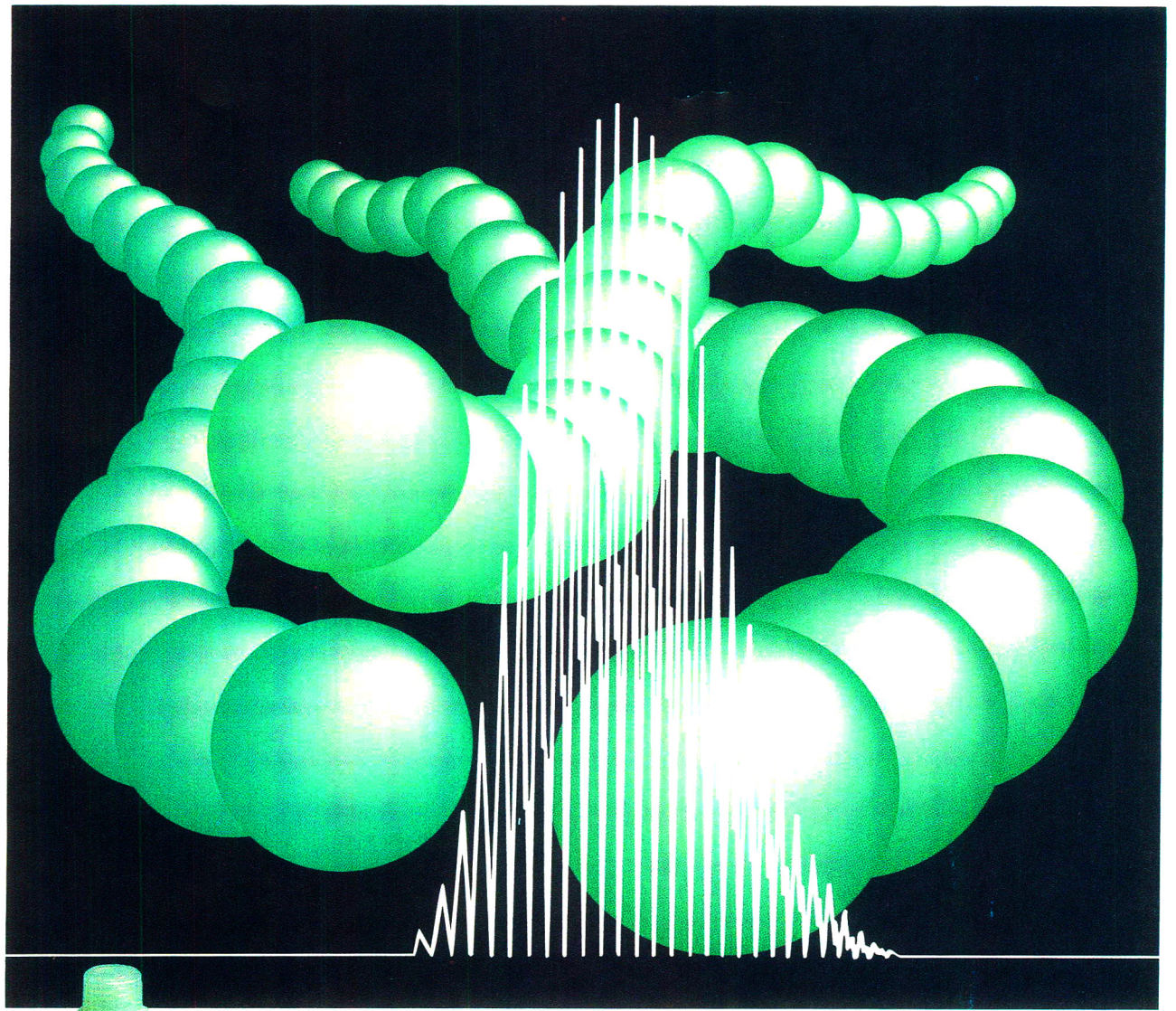

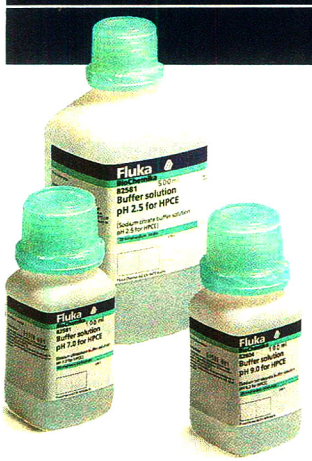

Ready-to-use reagents for capillary electrophoresis

Fluka is the first company to introduce a comprehensive series of ready-to-use reagents for capillary electrophoresis. The analyst can now choose from among a broad range of buffers between pH 2.5 and 11. These reagents, together with capillary wash solutions and special HPCE grade water, will facilitate the analyst's daily tasks and therefore allow him to spend additional time on more creative work.

Fluka reagents for capillary electrophoresis have to pass specially developed tests. This rigorous analytical control gives the researcher the certainty of buying top-quality products.

Fluka guarantees that these reagents have
- no insoluble residues,
- limited absorbance over a wide wave-length range (e. g. 200-800 nm),
- virtually no fluorescent impurities,
- and have been tested for application.

Capillary electrophoresis reagents are handled very carefully and packed under clean-room conditions. This exludes contamination at any stage of the production process.
Ask for a free copy of our HPCE leaflet.

Fluka

Chemika-BioChemika

Switzerland: Fluka Chemie AG, Industriestrasse 25, CH-9470 Buchs/Switzerland, Telephone 081 755 25 11, Telex 855 282, Fax 081 756 54 49

Benelux: Fluka Chemie, B-2880 Bornem, Tel. (03) 899 13 01 France: Fluka Chimie, F-38297 St.Quentin Fallavier, Tél. 74 82 28 00
Germany: Fluka Chemie, D-89231 Neu-Ulm, Tel. (0731) 973-3200 Great Britain: Fluka Chemicals Gillingham, Tel. (0747) 82 30 97
Italy: Fluka Chimica, I-20151 Milano, Tel. (02) 33417-310 Japan: Fluka Fine Chemical, Chiyoda-Ku, Tokyo, Tel. 81-03-3255-4787
Spain: Fluka Química, E-28100 Alcobendas, Tel. (91) 661 99 77 USA: Fluka Chemical Corp., Ronkonkoma, N.Y., Tel. 516-467-0980

Send your article on floppy disk!

All articles may now be submitted on computer disk, with the eventual aim of reducing production times and improving the reliability of proofs still further. Please follow the guidelines below.

With revision, your disk plus one final, printed and exactly matching version (as a printout) should be submitted together to the editor. **It is important that the file on disk to be processed and the printout are identical.** Both will then be forwarded by the editor to Elsevier.

The accepted article will be regarded as final and the files will be processed as such. Proofs are for checking typesetting/editing: only printer's errors may be corrected. No changes in, or additions to the edited manuscript will be accepted.

Illustrations should be provided in the usual manner and, if possible, on a **separate** floppy disk as well.

Please follow the general instructions on style/arrangement and, in particular, the reference style of this journal as given in the "Guide for Authors".

The preferred storage medium is a 5¼ or 3½ inch disk in MS-DOS or Macintosh format, although other systems are also welcome.

Please label the disk with your name, the software & hardware used and the name of the file to be processed.

For further information on the preparation of compuscripts please contact:

Elsevier Science B.V.
Journal of Chromatography A
P.O. Box 330
1000 AH Amsterdam, The Netherlands
Phone: (+31-20) 5862 793 Fax: (+31-20) 5862459

ELSEVIER
SCIENCE

Chiral HPLC Column

Application Guide for Chiral HPLC Column Selection

SECOND EDITION!

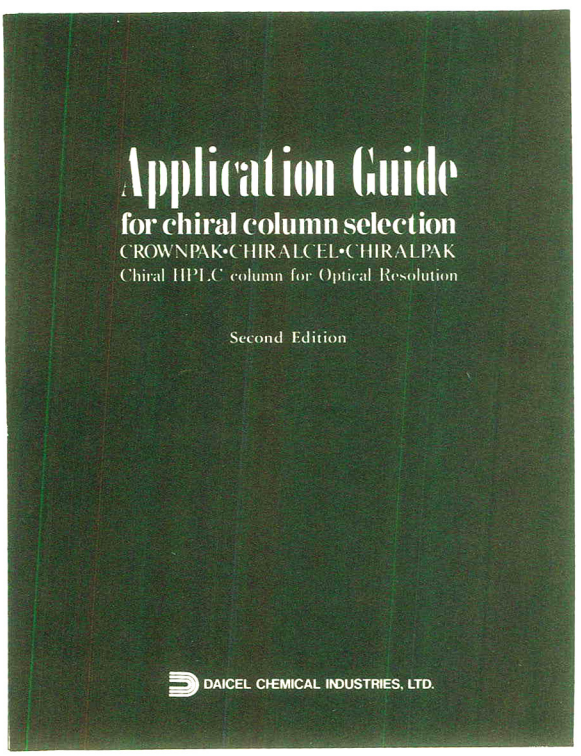

GREEN BOOK

The 112-page green book contains chromatographic resolutions of over 350 chiral separations, cross-indexed by chemical compound class, structure, and the type of chiral column respectively. This book also lists chromatographic data together with analytical conditions and structural information. A quick reference guide for column selection from a wide range of DAICEL chiral HPLC columns is included.

To request this book, please let us know by fax or mail.

DAICEL CHEMICAL INDUSTRIES, LTD.

AMERICA

CHIRAL TECHNOLOGIES, INC.

730 Springdale Drive, P.O. Box 564, Exton, PA 19341
Phone: +1-215-594-2100
Facsimile: +1-215-594-2325

EUROPE

DAICEL (EUROPA) GmbH

Oststr. 22
D-40211 Düsseldorf, Germany
Phone: + 49-211-369848
Facsimile: + 49-211-364429

ASIA/OCEANIA

DAICEL CHEMICAL INDUSTRIES, LTD.
CHIRAL CHEMICALS NDD
8-1, Kasumigaseki 3-chome,
Chiyoda-ku, Tokyo 100, JAPAN
Phone: +81-3-3507-3151
Facsimile: +81-3-3507-3193

Intelligent Software for Chemical Analysis

Edited by **L.M.C. Buydens** and **P.J. Schoenmakers**

Data Handling in Science and Technology Volume 13

Various emerging techniques for automating intelligent functions in the laboratory are described in this book. Explanations on how systems work are given and possible application areas are suggested. The main part of the book is devoted to providing data which will enable the reader to develop and test his own systems. The emphasis is on expert systems; however, promising developments such as self-adaptive systems, neural networks and genetic algorithms are also described.

Contents:

1. Introduction. Automation and intelligent software. Expert systems. Neural networks and genetic algorithms. Reader's guide. Concepts. Conclusions. **2. Knowledge-based Systems in Chemical Analysis** (P. Schoenmakers). Computers in analytical chemistry. Sample preparation. Method selection. Method development. Instrument control and error diagnosis. Data handling and calibration. Data interpretation. Validation. Laboratory management. Concluding remarks. Concepts. Conclusions. Bibliography. **3. Developing Expert Systems** (H. van Leeuwen). Introduction. Prerequisites. Knowledge acquisition. Knowledge engineering. Inferencing. Explanation facilities. The integration of separate systems. Expert-system testing validation and evaluation. Concepts. Conclusions. Bibliography. **4. Expert-System-Development Tools** (L. Buydens, H. van Leeuwen, R. Wehrens). Tools for implementing expert systems. Tool selection. Knowledge-acquisition tools. Concepts. Conclusions. Bibliography. **5. Validation and Evaluation of Expert Systems for HPLC Method Development - Case Studies** (F. Maris, R. Hindriks). Introduction. Case study I: Expert systems for method selection and selectivity optimization. Case study II: System-optimization expert system. Case study III: Expert system for repeatability testing, applied for trouble-shooting in HPLC. Case study IV: Ruggedness-testing expert system. General comments on the evaluations. Concepts. Conclusions. Bibliography. **6. Self-adaptive Expert Systems** (R. Wehrens). Introduction - maintaining expert systems. Self-adaptive expert systems: Methods and approaches. The refinement approach of SEEK. Examples from analytical chemistry. Concluding remarks. Concepts. Conclusions. Bibliography. **7. Inductive Expert Systems** (R. Wehrens, L. Buydens). Introduction. Inductive classification by ID3. Applications of ID3 in analytical chemistry. Concluding remarks. Concepts. Conclusions. Bibliography. **8. Genetic Algorithms and Neural Networks** (G. Kateman). Introduction. Genetic algorithms. Artificial neural networks. Concepts. Conclusions. Bibliography. **9. Perspectives.** Limitations of Intelligent Software. Dealing with intelligent software. Potential of intelligent software. **Index.**

© 1993 366 pages Hardbound
Price: Dfl. 350.00 (US $ 200.00)
ISBN 0-444-89207-9

ORDER INFORMATION

For USA and Canada
ELSEVIER SCIENCE INC.
P.O. Box 945
Madison Square Station
New York, NY 10160-0757
Fax: (212) 633 3880

In all other countries
ELSEVIER SCIENCE B.V.
P.O. Box 330
1000 AH Amsterdam
The Netherlands
Fax: (+31-20) 5862 845

US$ prices are valid only for the USA & Canada and are subject to exchange rate fluctuations; in all other countries the Dutch guilder price (Dfl.) is definitive. Customers in the European Community should add the appropriate VAT rate applicable in their country to the price(s). Books are sent postfree if prepaid.

ELSEVIER SCIENCE B.V.

JOURNAL OF CHROMATOGRAPHY A

VOL. 665 (1994)

JOURNAL OF CHROMATOGRAPHY A

INCLUDING ELECTROPHORESIS AND OTHER SEPARATION METHODS

SYMPOSIUM VOLUMES

ELSEVIER

AMSTERDAM — LONDON — NEW YORK — TOKYO

Bratislava, 1720–1750
(by F.B. Werner–M. Engelbrecht)

0021-9673/94/$07.00

Printed in the Netherlands

SYMPOSIUM ISSUE

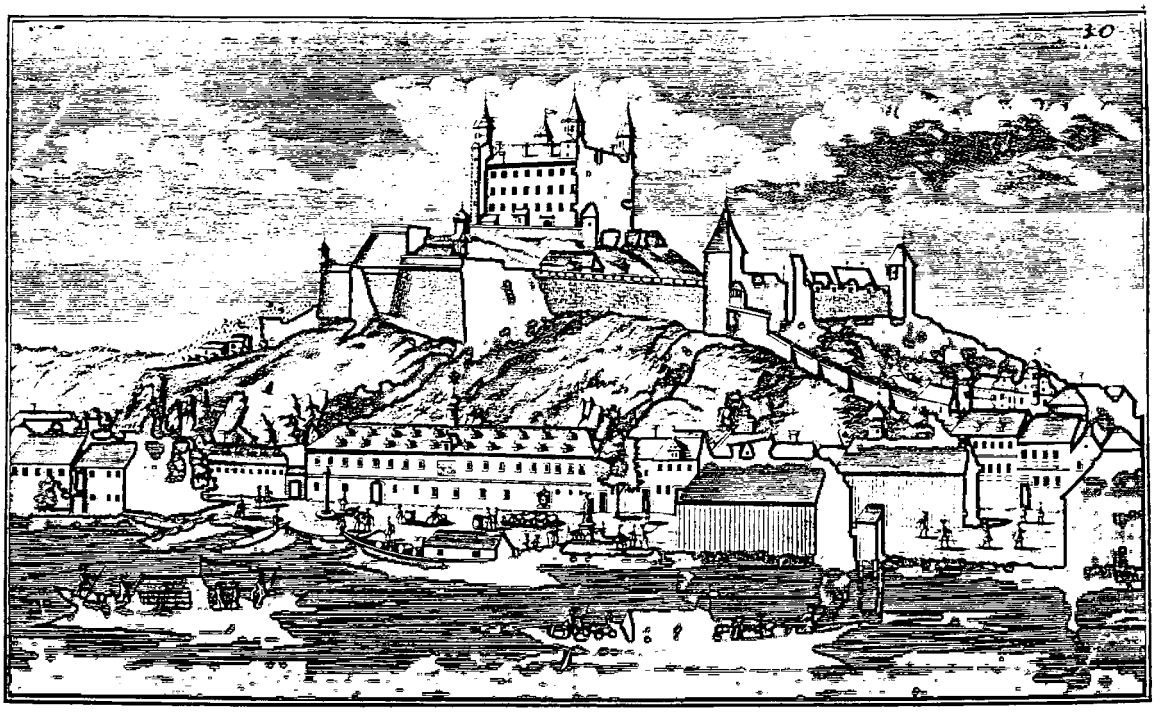

9TH INTERNATIONAL SYMPOSIUM ON ADVANCES AND APPLICATIONS OF CHROMATOGRAPHY IN INDUSTRY

Bratislava (Slovak Republic), August 29–September 3, 1993

Guest Editor

JÁN KRUPCÍK

(Bratislava, Slovak Republic)

VOL. 665, NO. 1 JOURNAL OF CHROMATOGRAPHY A APRIL 8, 1994

CONTENTS

9TH INTERNATIONAL SYMPOSIUM ON ADVANCES AND APPLICATIONS OF CHROMATOGRAPHY IN INDUSTRY, BRATISLAVA, AUGUST 29–SEPTEMBER 3, 1993

ELSEVIER

Journal of Chromatography A, 665 (1994) 1

JOURNAL OF CHROMATOGRAPHY A

Preface

The *9th International Symposium on Advances and Applications of Chromatography in Industry* was held in Bratislava, Slovak Republic, from August 29th to September 3rd, 1993. The Symposium Chairman was Associate Professor Jozef Polonský and the Symposium Secretary was Dipl. Ing. Eva Benická. The organizers were the Faculty of Chemical Technology of the Slovak Technical University, the Slovak Chemical Society at the Slovak Academy of Sciences, the Institute of Polymers of the Slovak Academy of Sciences, the Faculty of Natural Sciences of Comenius University and the Slovak Society for Industrial Chemistry at Slovnaft, all in Bratislava. The location of the Symposium was the Faculty of Chemical Technology of the Slovak Technical University in Bratislava.

The scientific programme included 41 oral presentations in five morning sessions as plenary lectures and in afternoon sessions as main lectures dealing with the theory and practice of gas chromatography, liquid chromatography (with two special sections devoted to gel permeation chromatography), supercritical fluid chromatography, electromigration methods, coupled techniques and other methods (advances, new separation systems, identification of substances, optimization, detection systems) and their applications in industry, biochemistry, clinical chemistry, biotechnology and environmental and trace analysis. In addition, three poster sessions including over 137 posters provided space and time for direct discussions in small groups on all aspects of separation methods.

There were over 270 registered participants from nineteen countries, who contributed to the symposium with lectures, posters and discussions and many of whom submitted manuscripts for this special issue.

Fourteen companies took part in an exhibition of chromatographic and electrophoretic instruments, columns, accessories and chemicals.

The social programme also contributed to creating a friendly atmosphere and establishing personal contacts during the Symposium. The Gala Concert by SĽUK (Slovak Folk-Art Ensemble) was a great experience for everybody.

It is my pleasure to thank all the organizations and individuals who helped in any form to the success of this Symposium. Finally, I express my appreciation to Associate Professor Zdeněk Deyl for his effort and care in producing this special issue.

Bratislava (Slovak Republic) Jozef Polonský

SSDI 0021-9673(93)E1061-4

ELSEVIER

Journal of Chromatography A, 665 (1994) 3–8

JOURNAL OF CHROMATOGRAPHY A

Evaluation of separation quality with a novel threshold criterion☆

J. Hrouzek*, Š. Hatrík, J. Krupčík, E. Benická

Department of Analytical Chemistry, Faculty of Chemical Technology, Slovak Technical University, Radlinského 9, 812 37 Bratislava, Slovak Republic

Abstract

A novel threshold criterion based on the degree of peak overlap is proposed. It can be used for the evaluation of the degree of separation for simple or complex mixtures. The criterion considers quality of separation for relevant peaks only. Non-symmetrical peak shapes, different peak-height ratios and the influence of other peaks on the separation are also considered. The proposed criterion was tested on overlapped peaks of complex chromatograms obtained by capillary gas chromatography.

1. Introduction

The analysis of complex mixtures cannot be successful without using a powerful separation technique (*e.g.*, gas, liquid or supercritical chromatography or capillary electrophoresis). There are problems, however, with the measurement of separation quality. The conventional approach, which relies on the intuition of the chromatographer as the only means of obtaining good separation, should by changed to a more objective method.

In general, the aim of the development of a separation method is to obtain the required separation of all sample components of interest in a reasonable analysis time [1]. This means that each peak of interest corresponds to a single component, no significant overlap between peaks takes place and the cost of separation is as low as possible. It is important that the measurement of the quality of a separation is independent of the technique or conditions used to obtain the separation. Several aspects should be considered in the evaluation of separation quality. First, the required separation should be considered. Second, the other factors such as the total analysis time and consumption of mobile phase are also very important. Considering these requirements, both the required separation and the cost of separation should be included in a criterion expressing the quality of separation.

There are several different methods in chromatography and electrophoresis that are used to describe the degree of separation of the components of a mixture, but usually they do not adequately consider peak asymmetry and the cost of separation. Any criteria that have to judge separation quality should condense the information from all of the chromatogram into a single number. The main problem with such evaluation is to define a criterion that adequately quantifies the peak overlap. The chromatograph-

* Corresponding author.

☆ Part of this paper was presented at *15th International Symposium on Capillary Chromatography, Riva del Garda, May 24–27, 1993.*

0021-9673/94/$07.00
SSDI 0021-9673(93)E1129-N

ic resolution $R_{i,j}$ [2], Kaiser's criterion P [3], separation factor S [4], Trennzahl TZ [5] and selectivity factor α are commonly used to describe the separation quality of two peaks. The elementary criteria already mentioned consider neither the influence of other peaks on the separation nor, except for Kaiser's criterion, the peaks-height ratio and peak shapes. The fraction overlap parameter [6] is more suitable to describe peak overlap, but it considers two neighbouring peaks only.

The aims of the chromatographer vary according to the analytical problem encountered and the technique chosen to solve it. One, several preferred or all components of the recorded signal can be of interest [7]. The resolution of all the peaks composing the mixture is, however, only a rare situation in practice. The question to be answered in each instance is what the chromatographer thinks is a good (or at least acceptable) separation. This varies widely for qualitative or quantitative analysis or preparative chromatography. Therefore, specific goals of a particular problem should be built in into the criteria proposed.

The aim of this paper is to define a threshold criterion that considers peak asymmetry, peak-height ratio and influence of other peaks on the separation. The value of the threshold criterion is affected only by the separation quality of relevant peaks. The cost of separation is considered for evaluation of equal separation quality obtained under different conditions.

2. Theoretical

The separation of one component from the other solutes in a mixture can be calculated in different ways. The most advantageous is the calculation of the overlapped area of the peak of interest with adjacent peaks in a chromatogram. Information about overlapped and total peak areas gives an outline of the separation quality of the peak investigated.

If there are m peaks expected on the chromatogram, the total overlapped area O_k of peak k can be defined as

$$O_k = O_{1,k} + \cdots + O_{k-1,k} + O_{k+1,k} + \cdots + O_{m,k}$$

where $O_{i,k}$ is a particular overlap of peak k with peak i in area units. The degree of overlap DO_k of peak k with m adjacent peaks can be defined as the ratio of overlapped area O_k to the total peak area A_k (see Fig. 1):

$$DO_k = \frac{O_k}{A_k} \cdot 100\%$$

The DO_k value expresses the overlapped area of peak k in pure peak k area units. O_k represents an addition of all contributions, and therefore the DO_k value lies in the $(<0; \infty)$ interval. In a comparison of a procedure based on peak overlap with those using the chromatographic resolution factor $R_{i,j}$, a significant increase in the degree of overlap, DO_A, is shown in Fig. 2 for peak A with increasing peak-height ratio h_B/h_A, while $R_{A,B} = 1$ in all instances. In the Fig. 3, the dependence of DO_A on the peak-height ratio h_B/h_A for two simulated Gaussian peaks ($R_{A,B} = 1$) is presented. The course of the curve depends, however, both on the value of the resolution factor and on the peak shapes.

The difference in above-mentioned approaches can be more clearly illustrated for the peak doublet and triplet in Fig. 4a and b, respectively. The chromatographic resolution factors are equal ($R_{A,B} = R_{B,C} = 1$), but the degrees of overlap DO_B are different in Fig. 4a and b. The overlapped area reflects the influence of all peaks on the separation quality of the investigated peak.

The separation quality of peak k describes via DO_k eliminates problems connected with non-symmetrical peak shapes, different height ratios of overlapped peaks and influences of other

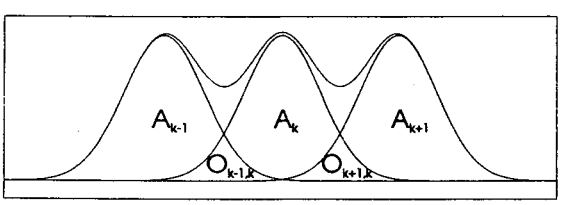

Fig. 1. Peak areas for degree of overlap calculation.

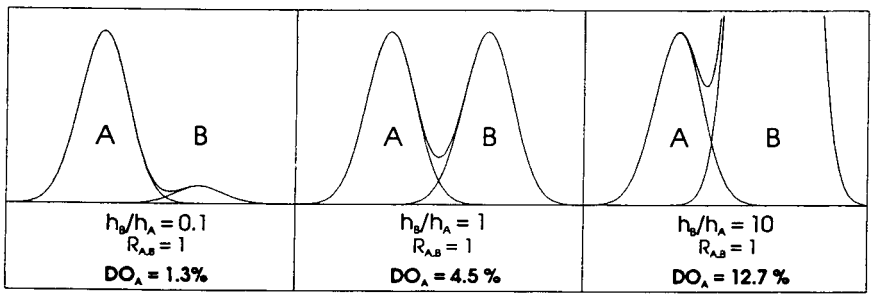

Fig. 2. Comparison of the degree of overlap DO_k approach with the chromatographic resolution factor $R_{i,j}$ method.

peaks on the separation. By setting a threshold value P_k (*e.g.*, 5%) for each relevant peak k, below which the degree of overlap DO_k is acceptable, a term I_k can be defined:

$I_k = 1$ if $DO_k \leq P_k$

$I_k = 0$ if $DO_k > P_k$

The value of P_k is a numerical expression of the required separation of peak k and therefore the choice of P_k depends on the required peak purity. When the relevant peaks are separated better than the required P_k value, $I_k = 1$, and if the separation is worse, then $I_k = 0$. Based on this, a primary part of the proposed threshold criterion can be defined as

$$F_1 = \sum_{k=1}^{N} I_k$$

where N is the number of peaks of interest. The primary part of the criterion can be a whole number from the interval (<0; N>) and is affected by the quality of the relevant peak

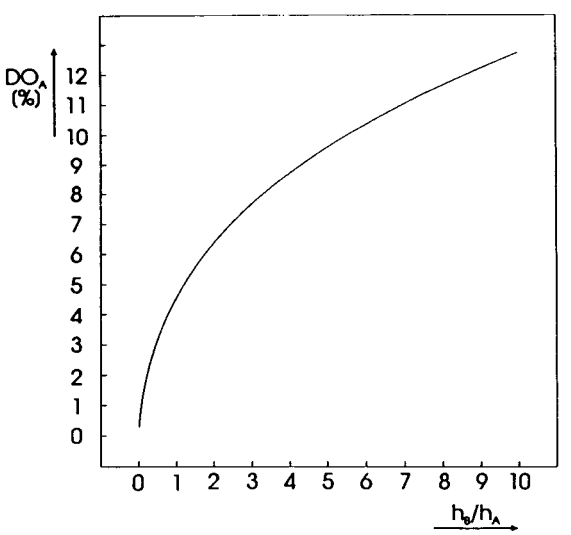

Fig. 3. Dependence of DO_A on peak-height ratio h_B/h_A for two Gaussian peaks ($R_{A,B}$) = 1.

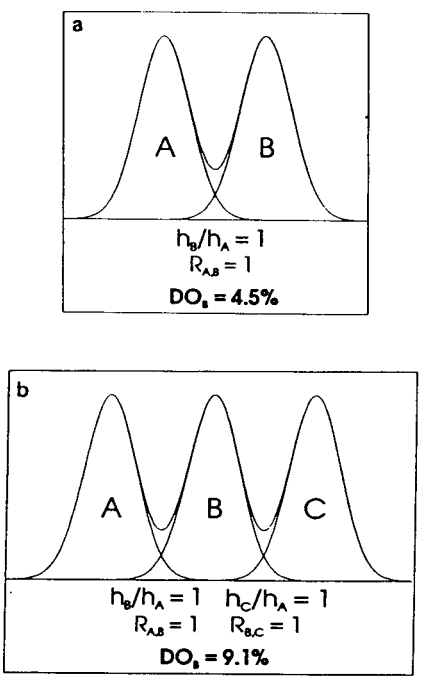

Fig. 4. Degree of overlap of peak B (DO_B) calculated for (a) one and (b) two adjacent peaks while $R_{A,B} = R_{B,C} = 1$.

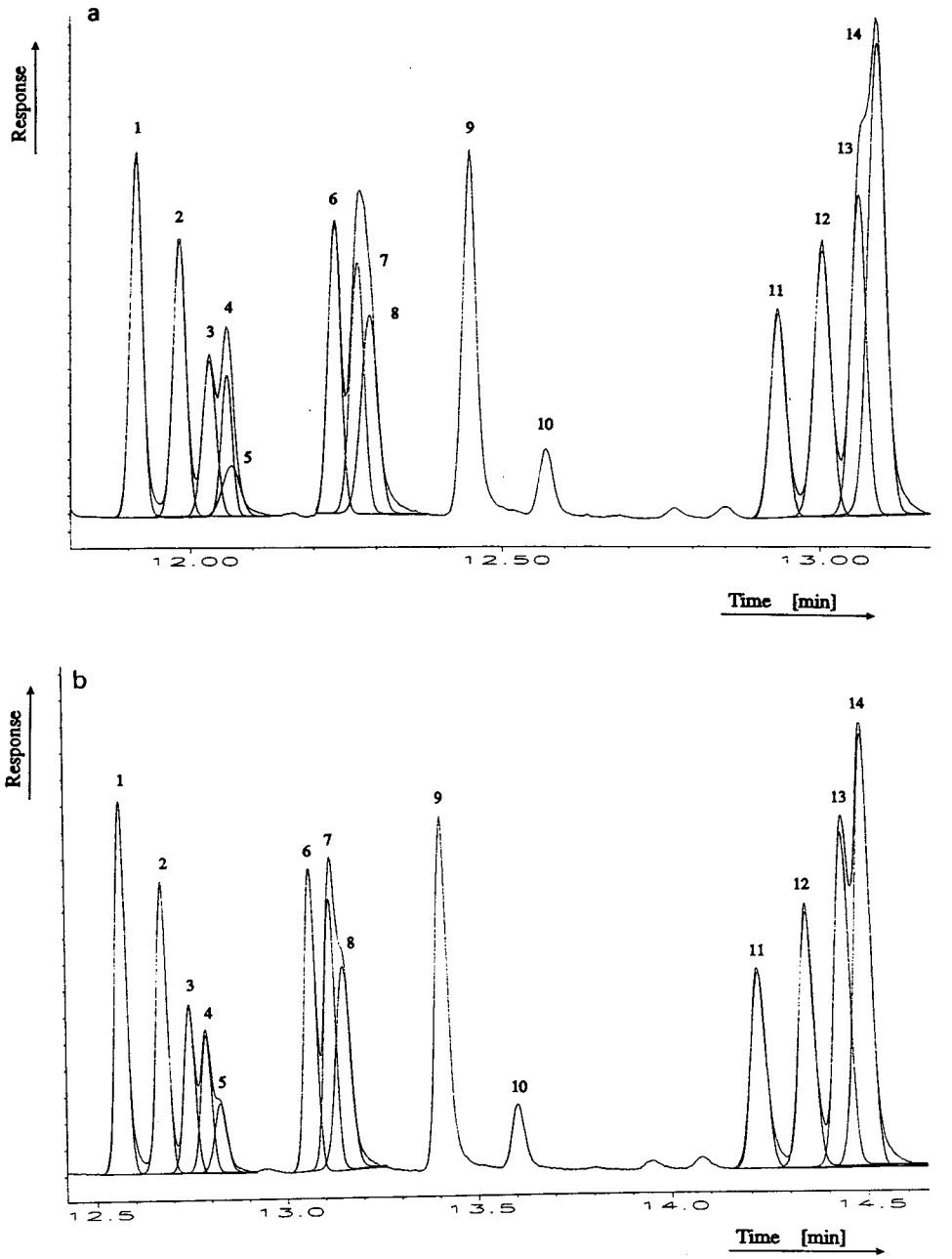

Fig. 5. Two chromatograms of the test mixture recorded using slightly different temperature programmes. The pure peaks are also depicted.

separation only. The separation of irrelevant components does not affect the F_1 value. With the choice of P_k we can fine tune the criterion with regard to the separation goals.

The cost of analysis is often an important factor in practice. The time needed to realize any separation can play a very important role in routine analysis and if the analysis is too long a worse separation (from the point of view of resolution) is sometimes accepted. Factors affecting the cost of separation (such as the analysis time and consumption of mobile phase) can be included in the proposed criterion as a secondary part. The threshold criterion can be found, as we recently showed [8], from the equation

$$F = \sum_{k=1}^{N} I_k + \frac{\text{cost}_{\max} - \text{cost}}{\text{cost}_{\max}}$$

The chosen maximum acceptable cost of analysis ($\text{cost}_{\max}$) should be higher than the real cost. The cost of a real analysis is never zero and therefore the ratio $(\text{cost}_{\max} - \text{cost})/(\text{cost}_{\max})$ is always less than 1. The secondary part of this criterion therefore distinguishes between different separations when an equal number of relevant compounds are separated between as required but the separation costs are different. The higher the criterion value for recorded signal, the better is the separation and the cheaper the analysis. The use of the threshold criterion in computer-assisted optimization procedures will be published separately [9].

3. Verification

The validity of the proposed threshold criterion was verified by an evaluation of the separation quality two example chromatograms obtained by capillary gas chromatography. The chromatograms differ slightly in appearance owing to variations in the temperature programme. The calculations of the primary part of the criterion, corresponding to selected peaks from a fraction of a complex chromatogram, are presented in Fig. 5a and b, is shown in Table 1. For calculation of the degree of peak overlap a deconvolution procedure was used [9]. Fourteen peaks were detected in both fractions of the chromatograms. Twelve of them were selected as a relevant ($N = 12$) and corresponding P_k values were set. Six peaks have a degree of overlap $DO_k > P_k$ and therefore they were not counted as pure enough. Six were acceptably pure ($F_{1A} = F_{1B} = 6$) as for these $DO_k \leqslant P_k$. The elution

Table 1
Calculation of the primary part of the criterion for the chromatograms in Fig. 5a and b

Peak number (k)	Is peak relevant?	P_k (%)	Fig. 5a		Fig. 5b	
			DO_k (%)	I_k	DO_k (%)	I_k
1	Yes	5	0.04	1	0.01	1
2	Yes	5	1.71	1	0.86	1
3	Yes	5	25.20	0	11.71	0
4	Yes	10	66.97	0	30.45	0
5	Yes	10	106.05	0	27.13	0
6	Yes	10	8.35	1	7.17	1
7	No	–	44.91	–	30.98	–
8	Yes	10	41.37	0	29.09	0
9	No	–	0.00	–	0.00	–
10	Yes	7	0.00	1	0.00	1
11	Yes	7	0.54	1	0.11	1
12	Yes	7	2.56	1	1.54	1
13	Yes	7	31.90	0	19.81	0
14	Yes	7	20.48	0	13.68	0
	$N = 12$			$F_1 = 6$		$F_1 = 6$

times of the last peaks in the chromatograms in Fig. 5a and b were 25 and 42 min, respectively, which correspond to the costs of analyses. For $cost_{max} = 60$ min the values $F = 6.58$ for Fig. 5a and $F = 6.30$ for Fig. 5b were found using the data given in Table 1, which means that the separation in Fig. 5a is superior to that in Fig. 5b.

By setting other threshold P_k values ($P_k = 15\%$ for all peaks), other F values were found: $F = 6.58$ for Fig. 5a and $F = 8.30$ for Fig. 5b, from which the separation in Fig. 5b is superior to that in Fig. 5a. Hence the criterion can be tuned by the choice of the threshold values P_k. From the above examples it follows that the objectives of the separation should be well defined in order to make a reliable decision.

4. Acknowledgement

The authors thank the Slovak Ministry of Education for a grant, No. 1/990927/92.

5. References

[1] S.N. Demming, J.M. Palasota, J. Lee and L. Sun, *J. Chromatogr.*, 485 (1989) 15.
[2] L.R. Snyder and J.J. Kirkland, *An Introduction to Modern Liquid Chromatography*, Wiley, New Yor, 2nd ed., 1979.
[3] R. Kaiser, *Gas Chromatographie*, Geest and Portig, Leipzig, 1960, p. 33.
[4] A.C.J.H. Drouen, P.J. Schoenmakers, H.A.H. Billiet and L. de Galan, *Chromatographia*, 16 (1982) 48.
[5] K.J. Hyver and P. Sandra (Editors), *High Resolution Gas Chromatography*, Hewlett-Packard, Avondale, PA, 3rd ed., 1988, p. 10.
[6] P.J. Schoenmakers, *Optimization of Chromatographic Selectivity*, Elsevier, Amsterdam, 1986.
[7] R. Cella, C.G. Barroso and J.A. Pérez-Bustamante, *J. Chromatogr.*, 485 (1989) 477.
[8] J. Hrouzek, Š. Hatrík and J. Krupčík, in P. Sandra (Editor), *15th International Symposium on Capillary Chromatography*, Vol. 1, Hüthig, Heidelberg 1993, p. 141.
[9] Š. Hatrík, J. Hrouzek, J. Lehotay and J. Krupčík, *J. Chromatogr. A*, 665 (1994) 9.

ELSEVIER

Journal of Chromatography A, 665 (1994) 9–15

JOURNAL OF CHROMATOGRAPHY A

Use of a threshold criterion in the computer-assisted optimization of chromatographic separations

Š. Hatrík*, J. Hrouzek, J. Lehotay, J. Krupčík

Department of Analytical Chemistry, Faculty of Chemical Technology, Slovak Technical University, Radlinského 9, Bratislava 812 37, Slovak Republic

Abstract

A threshold criterion based on the calculation of the degree of overlap of adjacent peaks was used for the computer-based optimization of the binary mobile phase composition in HPLC. The procedure was applied to the chromatographic separation of selected phenylurea herbicides and some of their aniline degradation products. The optimization procedure was based on the modelling of retention, peak widths and peak shapes by the general exponential function, which allows non-symmetrical tailed peaks also to be described. The results from the optimization were presented as a contour map, which gives a good impression of the quality of separation over the whole range of two-dimensional space.

1. Introduction

Computer-based optimization methods in chromatography have been encouraged by a need to define method development strategies for automated chromatographic instruments. A number of optimization strategies have been developed specifically for chromatographic systems [1]. The primary purpose of optimization methods in chromatography is to obtain an adequate separation of the solutes of interest from all the other components in a reasonable analysis time. The procedures for the efficient location of the optimum in chromatographic optimization can be broadly divided into three categories: simultaneous grid-search methods, self-finding sequential methods such as the simplex method and interpretative methods [2]. Grid-search methods require large numbers of experiments, inevitable for finding the optimum [3] and the simplex procedure often locates a secondary, local maximum rather than the global optimum [4]. Regression designs start from the individual retention times and are based on the fact that a few well chosen chromatograms suffice to fit a simple model [5–10]. Many more criteria for optimization in chromatography have been discussed in the literature [3].

In this work, we used a threshold criterion introduced recently [11] in a computer-assisted optimization of the binary mobile phase composition in the HPLC of six phenylurea herbicides and some of their substituted aniline degradation products.

2. Experimental

2.1. Apparatus

Reversed-phase HPLC was performed using a Waters Model 501 pump with a Vydac 5-μm C_{18}

* Corresponding author.

0021-9673/94/$07.00
SSDI 0021-9673(94)00021-Z

column (250 × 4.6 mm I.D.) and a Waters Model 484 variable-wavelength UV detector. The flow-rate of the mobile phase was 1.5 ml/min in all experiments. The detection wavelength was 250 nm. Chromatograms were recorded and translated into ASCII code by a Waters Baseline 810 integrator.

2.2. Chemicals

Methanol was of spectrophotometric grade and was supplied by Janssen Chimia (Brussels, Belgium). The standards of phenylurea herbicides (monolinuron, linuron, isoproturon, chlorbromuron, metbromuron and chlortoluron) were supplied by the Research Institute of Chemical Technology (Bratislava, Slovak Republic). Substituted anilines (*o*-chloro-*m*-methylaniline, *p*-chloroaniline, *p*-bromaniline, isopropylaniline and 3,4-dichloroaniline) were supplied by the Department of Organic Chemistry of the Pharmaceutical Faculty of Comenius University (Bratislava, Slovak Republic).

2.3. Computer program

We used a laboratory-written computer program for the optimization, which consists of a deconvolution procedure and optimization procedure for finding the optimum. The program was written in PASCAL and runs on IBM-PC computers.

3. Optimization method

3.1. Criterion

The optimization criterion that was used in the optimization procedure is based on the quantification of the degree of overlap of K adjacent peaks. The criterion can be expressed by the following equation:

$$F = \sum_{1}^{N} I_k + \frac{c_{max} - c}{c_{max}}$$

where N is the number of components, I_k is a Boolean expression and equals one if the degree of overlap is under the threshold value p_k and zero in the opposite case, c_{max} is the maximum acceptable cost of analysis and c is the cost of an individual analysis. The degree of overlap of peak K is defined as the ratio of the overlapped area of the peak with m adjacent peaks and the total area of peak K. In the secondary part of the criterion analysis time, consumption of the mobile phase, etc., can be included. The criterion is discussed in detail elsewhere [12].

3.2. Optimization procedure

The optimization procedure requires the following information: the retention curves of all components; the peak parameters (obtained by a deconvolution procedure); and the dependences between capacity factors and the peak widths. All steps of the optimization procedure are described below.

4. Results and discussion

4.1. Modelling of retention

The retention was modelled with changing solvent composition. It is generally recognized that for most solutes the dependence between ln k' and φ (percentage of methanol in the mobile phase) is not linear when considering the full range of eluent compositions and therefore it may become necessary to express the functional dependence of ln k' on φ as a second-order polynomial, but over the limited range of methanol–water compositions ($1 < k' < 10$) the ln k'–φ dependence of most solutes is linear according to [13].

$$\ln k' = \ln k_0 - S\varphi \quad (1)$$

The correlation coefficients of the linear dependences (mostly higher than 0.99) and the slopes and intercepts of Eq. 1 for individual compounds are given in Table 1.

Table 1
Determination of slopes and intercepts of the dependences in Eqs. 1 and 2 and the choice of the shape parameters a and b included in the GEX function

Compound	Ln k_0	S	Correlation coefficient, r	A (min)	B (min)	Correlation coefficient, r	a	b
o-Chloro-*m*-methylaniline	2.065	5.09	0.99456	0.0945	0.1096	0.99956	0.90	5.00
p-Chloroaniline	3.837	7.20	0.99921	0.0995	0.1128	0.99325	1.55	5.00
p-Bromoaniline	4.395	7.86	0.99875	0.0997	0.1199	0.99762	1.80	5.10
Monolinuron	5.000	8.44	0.99936	0.0889	0.1109	0.99744	1.80	5.05
Isopropylaniline	4.762	7.70	0.99653	0.0890	0.1160	0.98532	1.95	5.05
Metbromuron	5.395	8.81	0.99921	0.0986	0.1199	0.99936	1.88	4.95
Isoproturon	5.337	8.63	0.99962	0.0950	0.1090	0.99712	2.03	4.90
Chlortoluron	5.884	9.28	0.99935	0.0897	0.1138	0.98965	1.76	5.00
3,4-Dichloroaniline	5.624	9.00	0.99982	0.0982	0.1173	0.99351	1.50	5.25
Linuron	6.572	9.89	0.99957	0.0986	0.1170	0.99663	1.87	5.00
Chlorbromuron	6.751	9.97	0.99952	0.0908	0.1184	0.98796	2.06	4.90

4.2. Modelling of peak shapes

Peak asymmetry can arise from a variety of instrumental and chromatographic sources. They include incomplete resolution of sample components, slow kinetic processes, chemical reactions and also the formation of column voids [14]. In reversed-phase chromatography the presence of tailing peaks of basic compounds can be explained by their interactions with acidic sites on reversed stationary phases by ion-exchange processes. Therefore, the peaks of substituted anilines are non-Gaussian but right tailed. Any peak in a chromatogram is characterized by several parameters such as retention time, peak height, peak width and shape parameters. We have described all peaks in a chromatogram by the generalized exponential function (GEX) [15]. This function is shown to be very general. For a given set of K peaks it may be represented by

$$h = \sum_{i=1}^{K} \left\{ h_{m,i} t_i^{(b_i-1)} \exp\left[\frac{b_i - 1}{a_i} \cdot (1 - t_i^{a_i}) \right] \right\}$$

where

$t_i = (t - t_{0,i})/(t_{R,i} - t_{0,i})$
$t_{0,i}$ = start of a peak i in minutes;
$t_{R,i}$ = retention time of a peak i;
$h_{m,i}$ = height of a peak i;
a_i, b_i = shape parameters of a peak i;
h = signal of a peak i at time t.

The retention time $t_{R,i}$ can be calculated from the ln k'–φ dependences relatively accurately (see Table 2). The start of a peak was calculated according to the experimentally measured dependence between $t_{R,i} - t_{0,i}$ and the capacity factor as

$$t_{R,i} - t_{0,i} = A + Bk' \quad (2)$$

Eq. 2 follows from basic chromatographic theory. Assuming that the start of a peak is a fixed number C of standard deviations away from its top, we obtain

$$t_{R,i} - t_{0,i} = C\sigma_i = C \cdot \frac{t_{R,i}}{\sqrt{N_i}}$$

$$t_{R,i} - t_{0,i} = C \cdot \frac{t_d}{\sqrt{N_i}} + C \cdot \frac{t_d}{\sqrt{N_i}} \cdot k'_i$$

This equation predicts the slope B and intercept A to be equal. Table 2 shows that this bears out reasonably in practice. As can be seen from Table 2, this dependence is linear for all the solutes tested. Peak heights were calculated from the individual peak areas, which were the inputs to the optimization procedure. The peak

Table 2
Comparison of experimentally measured and predicted values of capacity factors and degrees of overlap under the global optimum conditions

Compound	k'		DO_k	
	Predicted	Experimental	Predicted	Experimental
o-Chloro-*m*-methylaniline	0.69	0.67	0.00	0.00
p-Chloroaniline	1.46	1.48	0.28	0.40
p-Bromoaniline	1.87	1.88	0.31	0.42
Monolinuron	2.59	2.61	2.07	3.12
Metobromuron	3.20	3.18	60.40	67.96
Isoproturon	3.30	3.29	54.60	61.90
Chlortoluron	4.17	4.19	1.09	0.99
3,4-dichloroaniline	3.67	3.68	3.81	2.93
Isopropylaniline	2.90	2.89	5.92	5.99
Linuron	6.21	6.29	0.04	0.073
Chlorobromuron	7.16	7.21	0.03	0.057

asymmetry was calculated for all peaks with changing mobile phase composition and hence with changing capacity factors. We observed that the peak asymmetry varied only very slightly or not at all over the limited range of capacity factors. Therefore, only one deconvolution procedure was needed for obtaining the shape parameters a and b (see Table 1).

The algorithm of the deconvolution procedure is shown in Fig. 1 [16], where x is a vector of parameters of function $f(x)$, ε is the precision of the minimization procedure, k is a constant which prevents the method from accumulating errors due to the method of calculation of vector h, ω specifies the method of minimization (ω = 0, Fletcher–Reeves; $\omega = 1$, Polak–Rieber), i is a counter, g and h are the vectors and OPTIM(x, h) is a function which optimizes the value of λ for which the function $f(x+\lambda h)$ has a minimum. For a chromatogram consisting of m data points [(h_i, t_i) and $i = 1, 2, \ldots, m$] and K overlapping peaks, the function $f(x)$ from Fig. 1 may now be written as

$$f(x) = \sum_{i=1}^{m} (h_i - h_{\mathrm{exp},i})^2$$

where $h_i = \Sigma_{j=1}^{K} h_{j,i}$, $h_{\mathrm{exp},i}$ is the value of the recorded signal in a chromatogram at time t_i and h_i represents the sum of K GEX functions at the same time.

The deconvolution program was interfaced with a Baseline 810 workstation and loading of data was done automatically. A typical deconvolution using our program for four peaks takes *ca.* 2 min on a PC-AT 386 computer, which is an acceptable run time. With all the above-mentioned parameters, the optimization program can calculate the degree of overlap for an individual peak at a given composition of mobile phase and also the value of the F criterion.

Fig. 2 shows the result of optimization (x-axis = degree of overlay, y-axis = mobile phase composition, z-axis = F criterion). The figures in the middle of the zone indicate the number of sufficiently resolved peaks in this zone, meaning the number of peaks with a degree of overlap equal to or smaller than the given value of the threshold p_k. The choice of p_k depends on the required peak purities (*e.g.*, acceptable error of the method). To understand better the meaning of p_k, the dependence of the chromatographic resolution of the degree of overlap DO_A or DO_B of two equal Gaussian peaks is shown in Fig. 3. The p_k value can be selected analogously to the threshold values of other threshold criteria (*e.g.*, min $k_\omega \cap R_{s,\min} \geq x$). The slice of Fig. 2 for a given value of threshold 10% (which is responsible for a chromatographic resolution of *ca.* 0.85) is shown in Fig. 4. The optimum (nine peaks were separated with a degree of overlap ≤

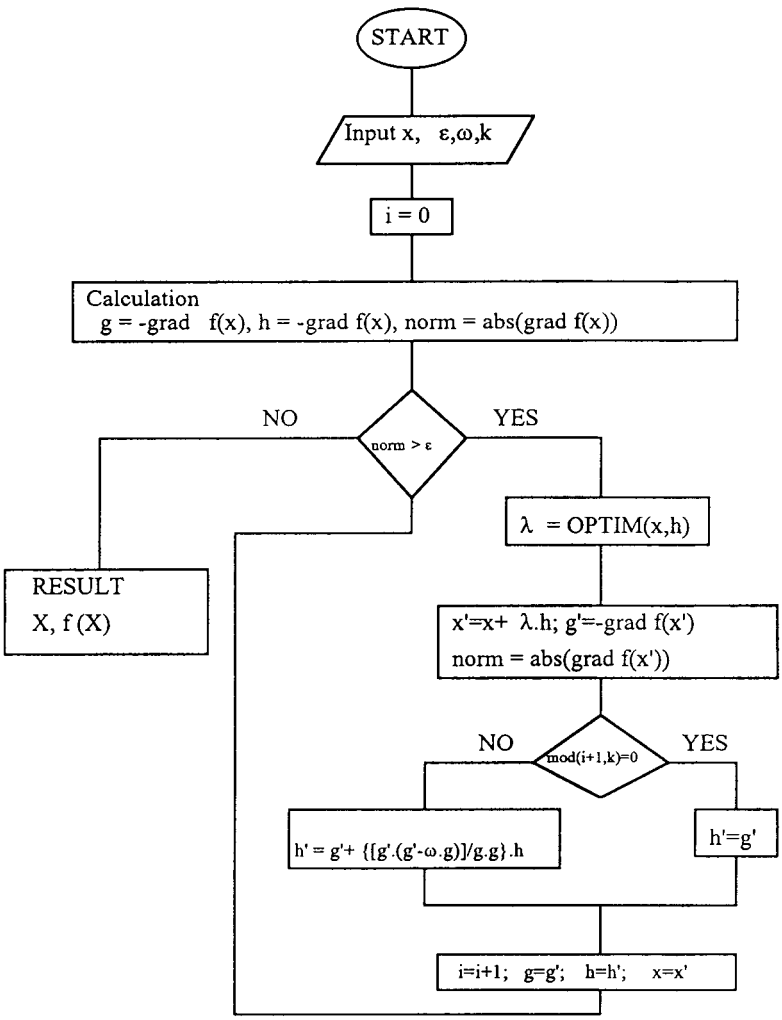

Fig. 1. Algorithm of the minimization procedure included in the deconvolution procedure [17].

10%) lies between 45 and 51% of methanol in the mobile phase. The global optimum for eleven components was found at $x = 6\%$, $y = 48\%$, $z = 9$. Two peaks (metbromuron and isoproturon) were strongly overlapped, but the degree of overlap for the other components was below 6% of the total area of the peak. Real and simulated chromatograms of ten components (metbromuron was excluded) measured with 48% of methanol in the mobile phase are shown in Figs. 5 and 6. In Table 3, the individual degrees of overlap for the set of measured and simulated chromatograms are compared.

5. Conclusions

The threshold criterion was used for the computer-assisted optimization of the binary mobile phase composition for the HPLC separation of selected phenylurea herbicides and some of their aniline degradation products. The F criterion counts the number of sufficiently resolved peaks realistically. It also reflects the height ratio of adjacent peaks and also the influence of other peaks that can interfere with the peak being investigated. The presentation of results as in Fig. 2 gives a good indication of the quality of

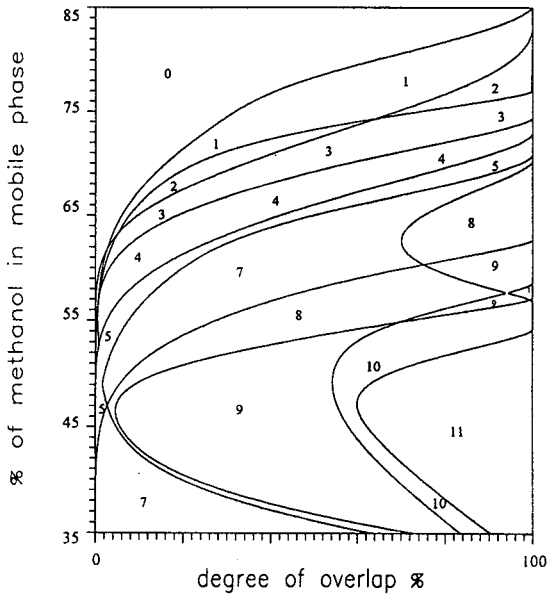

Fig. 2. Results of optimization procedure for eleven components. For details, see text.

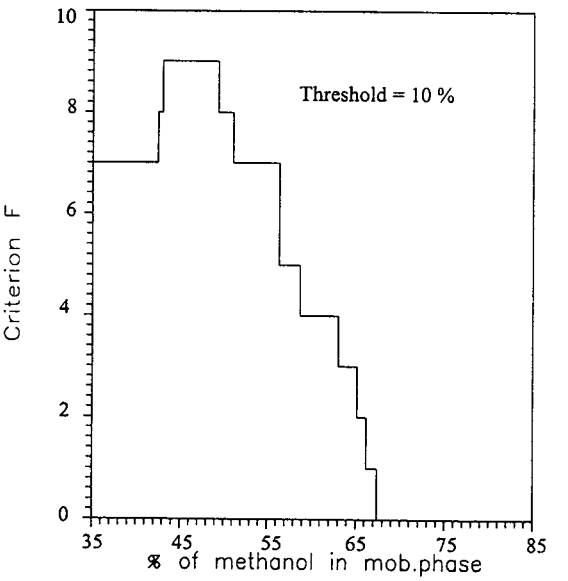

Fig. 4. Dependence of F criterion on the mobile phase composition if the threshold p_k is chosen to be 10% of the total area of the peak investigated.

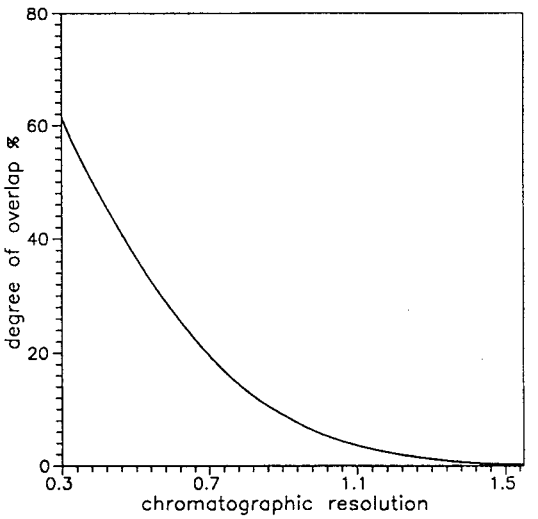

Fig. 3. Dependence of chromatographic resolution on the degree of overlap of two equal Gaussian peaks.

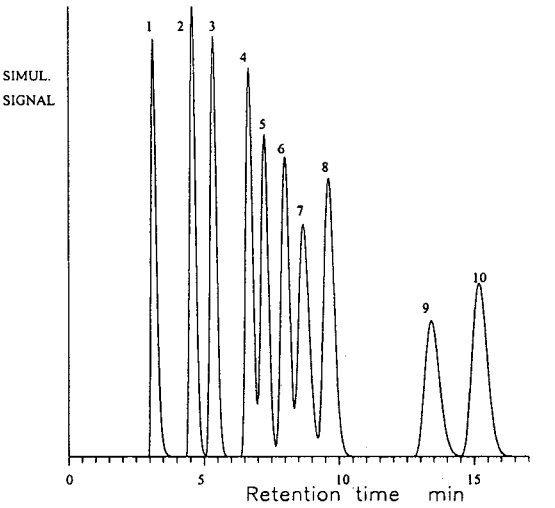

Fig. 5. Chromatogram simulated with the parameters corresponding to the global optimum (48% of methanol in the mobile phase). Peaks: 1 = *o*-chloro-*m*-methylaniline; 2 = *p*-chloroaniline; 3 = *p*-bromoaniline; 4 = monolinuron; 5 = isopropylaniline; 6 = isoproturon; 7 = 3,4-dichloroaniline; 8 = chlortoluron; 9 = linuron; 10 = chlorbromuron.

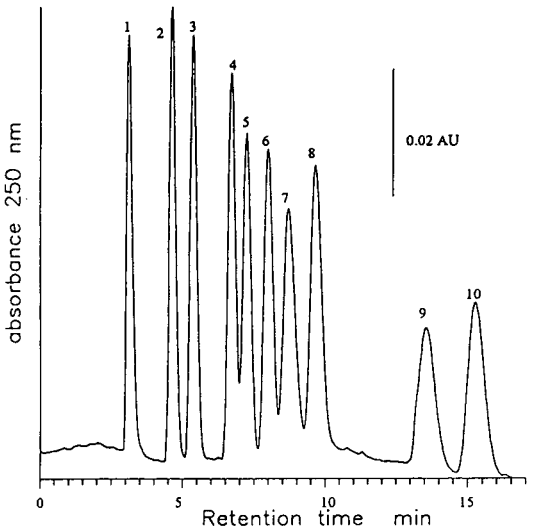

Fig. 6. Experimentally measured chromatogram under the global optimum conditions. Column, Vydac C_{18}, 5 μm (250 × 4.6 mm I.D.); flow-rate, 1.5 ml/min; UV detection at 250 nm. Peaks as in Fig. 5.

separation not only for the given value of the threshold but also over the whole range of p_k values. The results presented indicate relatively good agreement between the simulations and experiments.

6. References

[1] S.N. Deming, J.M. Palasota, J. Lee and L. Sun, *J. Chromatogr.*, 485 (1989) 15.
[2] P.J. Naish-Chamberlain and R.J. Lynch, *Chromatographia*, 29 (1990) 79.
[3] P.J. Schoenmakers, *Optimization of Chromatographic Selectivity*, Elsevier, Amsterdam, 1986.
[4] H.A.H. Billiet and L. de Galan, *J. Chromatogr.*, 485 (1989) 27.
[5] J.L. Glajch, J.J. Kirkland, K.M. Squire and J.M. Minor, *J. Chromatogr.*, 199 (1980) 57.
[6] Q.S. Wang, R.Y. Gao and H.Y. Wang, *J. High Resolut. Chromatogr.*, 13 (1990) 173.
[7] R.M. Marce, M. Callul and J.C. Olucha, *J. Chromatogr.*, 542 (1991) 277.
[8] O. Busto, J. Olucha and F. Borrul, *Chromatographia*, 32 (1991) 566.
[9] J. Vialle, P. Navarro, T.T. Nguyet, P. Lanteri and R. Longeray, *J. Chromatogr.*, 549 (1991) 159.
[10] J. Hrouzek and J. Krupčík, *Ropa Uhlie*, 34 (1992) 361.
[11] J. Hrouzek, Š. Hatrík and J. Krupčík, in *15th International Symposium on Capillary Chromatography*, Vol. 1, 1993, p. 141.
[12] J. Hrouzek, Š. Hatrík, J. Krupčík and E. Benická, *J. Chromatogr. A*, 665 (1994) 3.
[13] D.P. Herman, H.A.H. Billiet and L. de Galan, *J. Chromatogr.*, 463 (1989) 1.
[14] C.F. Poole and S.K. Poole, *Chromatography Today*, Elsevier, Amsterdam, 1991, p. 26.
[15] R.A. Vaidya and R.D. Hester, *J. Chromatogr.*, 287 (1984) 231.
[16] V. Kvasnička and Š. Varga, *Mathematics Vol. I, Vol. II*, SNTL, Prague, 1992, p. 31.

ELSEVIER

Journal of Chromatography A, 665 (1994) 17–25

JOURNAL OF CHROMATOGRAPHY A

Charge-transfer chromatographic study of the interaction of non-ionic surfactants with hydroxypropyl-β-cyclodextrin

Tibor Cserháti*, Esther Forgács

Central Research Institute for Chemistry, Hungarian Academy of Sciences, P.O. Box 17, 1525 Budapest, Hungary

Abstract

The interaction of 38 ethoxylated and one non-ethoxylated non-ionic surfactants with hydroxypropyl-β-cyclodextrin (HPBCD) was studied by reversed-phase charge-transfer chromatography. The relative strength of interaction, the hydrophobicity and the specific hydrophobic surface area of the surfactants and the effect of methanol concentration on the strength of interaction were calculated. The presence of a phenyl group and the length of the alkyl chain in the hydrophobic moiety of the surfactants have the greatest impact on their hydrophobic character, and the role of the length of the polar ethylene oxide chain is negligible. Surfactants with a tributylphenol hydrophobic moiety did not form complexes with HPBCD, the cavity of HPBCD probably being too small for the insertion of the bulky tributylphenol group. Most surfactants formed complexes with HPBCD, but the strength of interaction varied considerably. Stepwise regression analysis indicated that both the hydrophobicity and the specific hydrophobic surface area of the surfactants significantly influenced the strength of interaction, demonstrating the importance of hydrophobic interactions in inclusion complex formation between non-ionic surfactants and HPBCD.

1. Introduction

Non-ionic surfactants show various types of biological activity. Polyethoxylated non-ionic surfactants with no similarities in the hydrophobic moiety are able to reverse multi-drug resistance in a human leukaemic cell line [1] and nonylphenyl nonylethoxylate breaks down the polymer aggregates of scleroglucan [2]. Tween 80 enhances the intestinal absorption of the anthelminthic drug albendazole in rat gut [3], and Polysorbate 80 and Polyoxyl 40 markedly influence the transport of drugs in monolayers of human intestinal epithelial (Caco-2) cells [4]. Nearly quantitative conversion of linoleic acid into its hydroperoxide was achieved in microemulsions containing non-ionic surfactants, water and an organic solvent [5]. Non-ionic surfactants enhanced the systemic absorption of α-melanocyte-stimulating hormone via the ocular route in rabbits [6]. Non-ionic surfactants derived from tris(hydroxymethyl)aminomethane performed well in the solubilization of subcellular proteins of rat hepatocytes and membrane antigens from tumour cells [7]. Triton X-100 stimulated the ATPase activity of P-glycoprotein at low concentration and inhibited it at higher concentrations [8]. Triton X-100 activated the lecithin:cholesterol acyltransferase enxyme [9].

Non-ionic surfactants also show toxic side-effects. Surfactants are cytotoxic, the cytotoxicity order being cationic > anionic = amphoteric > non-ionic. Triton X-100 had a ranking similar to

* Corresponding author.

0021-9673/94/$07.00
SSDI 0021-9673(93)E1071-7

anionic surfactants [10]. Triton X-100 and Triton XR suppressed spore germination and germ tube growth of *Mucor mucedo* [11]. Polyethoxylated non-ionic surfactants inhibit the transport of 2,4-dinitrophenylglutathione from intact human erythrocytes. Surfactants possibly modify the arrangement of integral membrane proteins such as P glycoprotein and presumably the glutathione transporters [12]. Non-ionic surfactants inhibit the mineralization of phenanthrene in soil–water systems, probably by interacting with the membrane of soil microflora [13].

The biological activity of surfactants depends on the molecular structure. The toxicity of polyoxyethylene alkyl ethers decreased with increasing length of the alkyl chain and increased with increasing length of the polyoxyethylene head group [14]. The complex stability of 2-(1-naphthyl)acetic acid (NAA) with non-ionic surfactant micelles decreased with increasing logarithm of the length of the ethylene oxide chain for the Triton X series. The undissociated form of NAA formed more stable complexes [15].

Owing to their capacity to form inclusion complexes, cyclodextrins (CDs) are used in the stabilization and formulation of drugs, flavours and fragrances and also in agrochemistry [16]. Methylated CDs, but not CDs themselves, have surface activity [17]. Many surface-active agents can form inclusion complexes with CDs, resulting in striking changes in critical micelle concentration and surface tension [18,19]. The formation of inclusion complexes of some non-ionic surfactants with CDs decreases their phytotoxicity [20].

Charge-transfer reversed-phase chromatography has frequently been used to study various molecular interactions [21] such as the interaction of non-ionic surfactants with CDs [22] and with highly water-soluble CD derivatives [23].

The objectives of the work were the study the interaction of non-homologous series of non-ionic surfactants with a hydroxypropyl-β-CD derivative by charge-transfer chromatography and to find relationships between physico-chemical parameters, molecular structures and the relative strength of complex formation of surfactants.

2. Experimental

Charge-transfer chromatography was performed on Kieselgel 60 plates (Merck, Darmstadt, Germany) preimpregnated with *n*-hexane–paraffin oil (95:5, v/v). The structures of the non-ionic surfactants studied are given in Table 1. The surfactants were dissolved in methanol (20 mg/ml) and 4-μl volumes of solutions were spotted on the plates. The eluent was aqueous methanol with methanol concentrations between 50 and 80% (v/v) in steps of 5% (v/v). Hydroxypropyl-β-cyclodextrin (HPBCD) was purchased from Cyclolab Research and Development Laboratory (Budapest, Hungary) and was added to the eluent at concentrations of 0–37.5 mg/ml. After development the plates were dried at room temperature and the surfactants were detected with iodine vapour. Each determination was run in quadruplicate. The R_M value [$\log(1/R_F - 1)$], which characterizes the molecular lipophilicity in reversed-phase thin-layer chromatography, was calculated for each surfactant and eluent.

To separate the effects of methanol and HPBCD on the lipophilicity of surfactants and to take into consideration the effect of methanol concentration on inclusion complex formation, the following equation was fitted to the experimental data:

$$R_M = R_{M0} + b_1C_1 + b_2C_2 + b_3C_1C_2 \quad (1)$$

where R_M is the R_M value for a surfactant determined at given methanol and HPBCD concentrations, R_{M0} is the R_M value extrapolated to zero methanol and HPBCD concentrations, b_1 is the decrease in the R_M value caused by a 1% increase in methanol concentration in the eluent (related to the specific hydrophobic surface area of the surfactant [24]), b_2 is the decrease in the R_M value caused by a 1 mg/ml change in the HPBCD concentration in the eluent (related to the relative strength of interaction), b_3 is the effect of methanol concentration on the complex formation and C_1 and C_2 are the concentrations of methanol and HPBCD, respectively. Eq. 1 was applied separately for each surfactant. When the relative standard deviation of parallel de-

Table 1
Structure of non-ionic surfactants: $Q-O(C_2H_4O)_{n_e}-H$

No.	Trade name	Q	n_e (average)
1	Tween 20	Sorbitan monolaurate	20
2	Tween 40	Sorbitan monopalmitate	20
3	Tween 60	Sorbitan monostearate	20
4	Tween 80	Sorbitan monooleate	20
5	Tween 61	Sorbitan monostearate	4
6	Tween 81	Sorbitan monooleate	5
7	Tween 65	Sorbitan tristearate	20
8	Tween 85	Sorbitan trioleate	20
9	Brij 30	Lauryl alcohol	4
10	Brij 35	Lauryl alcohol	23
11	Brij 56	Oleyl/cetylalcohol	10
12	Brij 76	Stearyl alcohol	10
13	Brij 78	Stearyl alcohol	20
14	Brij 96	Oleyl alcohol	10
15	Arkopal N50	Nonylphenol	5
16	Arkopal N60		6
17	Arkopal N80		8
18	Arkopal N90		9
19	Arkopal N100		10
20	Arkopal N110		11
21	Arkopal N150		15
22	Arkopal N230		23
23	Arkopal N300		30
24	Sapogenate T40	Tributylphenol	4
25	Sapogenate T60		6
26	Sapogenate T80		8
27	Sapogenate T100		10
28	Sapogenate T110		11
29	Sapogenate T130		13
30	Sapogenate T180		18
31	Sapogenate T300		30
32	Sapogenate T 500		50
33	Myrj 45	Stearic acid	8
34	Myrj 49		20
35	Myrj 51		30
36	Myrj 52		40
37	Myrj 53		50
38	Myrj 59		100
39	Span 80	Sorbitan monooleate	0

terminations was higher than 8%, the data were omitted from the calculations.

To test the validity of the hypothesis that with homologous series of solutes the slope and intercept values (b_1 and R_{M0} in Eq. 1) are strongly intercorrelated [25,26], the linear correlation was calculated between the two physico-chemical parameters:

$$R_{M0} = A + Bb_1 \quad (2)$$

To find the relationships between the physico-chemical parameters (lipophilicity and specific hydrophobic surface area) and the molecular substructures of surfactants, and to select the physico-chemical parameters and molecular substructures of the surfactants that significantly

Table 2
Parameters of multilinear correlations between R_M values of surfactants and concentrations of methanol (C_1) and hydroxypropyl-β-cyclodextrin (C_2) in the eluent: $R_M = R_{M0} + b_1C_1 + b_2C_2 + b_3C_1C_2$

Parameter	Surfactant[a]														
	1	2	3	4	5	6	7	8	9	10	11	12	13	14	15
n	15	15	15	15	15	15	15	15	15	15	15	15	15	15	15
R_{M0}	3.89	5.02	4.89	5.01	5.74	5.63	5.63	5.94	4.52	4.76	4.91	5.94	5.46	4.63	4.22
$-b_1 \cdot 10^{-2}$	4.36	6.06	5.81	5.99	6.85	6.91	6.78	7.23	6.05	6.14	6.00	7.21	6.61	5.56	5.61
$s_{b_1} \cdot 10^{-2}$	0.62	0.35	0.48	0.44	0.91	0.45	0.48	0.37	0.38	0.47	0.40	0.60	0.46	0.47	0.51
$-b_2 \cdot 10^{-2}$	–	7.26	6.64	7.55	–	8.28	8.23	8.94	7.99	7.39	8.16	10.17	8.26	5.82	6.98
$s_{b_2} \cdot 10^{-2}$	–	0.98	1.33	1.21	–	1.24	1.32	1.04	1.06	1.31	1.10	1.68	1.28	1.32	1.41
$b_3 \cdot 10^{-3}$	–	10.71	9.86	11.67	–	12.62	12.54	13.59	12.06	11.24	11.91	14.85	11.86	8.68	10.12
$s_{b_3} \cdot 10^{-3}$	–	1.66	2.24	2.04	–	2.09	2.23	1.75	1.78	2.21	1.85	2.83	2.16	2.22	2.38
b_1 (%)	–	16.54	17.15	15.58	–	16.33	16.18	15.93	15.11	16.28	14.94	14.47	16.12	18.37	16.13
b_2 (%)	–	45.60	45.13	45.15	–	45.02	45.16	47.20	45.88	45.08	46.69	46.93	46.37	44.48	46.18
b_3 (%)	–	37.86	37.72	39.27	–	38.65	38.66	36.87	39.01	38.64	38.37	38.60	37.51	37.15	37.69
$F_{calc.}$	–	104.55	53.69	70.01	–	88.76	74.40	136.63	88.79	62.15	78.29	48.28	71.05	52.22	42.20
r^2	0.7923	0.9661	0.9361	0.9502	0.8360	0.9603	0.9530	0.9739	0.9603	0.9443	0.9553	0.9294	0.9509	0.9344	0.9201
	16	17	18	19	20	21	22	23	24	25	26	27	28	29	30.
n	15	15	15	15	15	15	15	15	15	15	15	15	15	15	15
R_{M0}	3.89	4.29	3.76	3.77	3.86	3.75	3.60	3.23	3.77	3.58	3.23	3.41	3.40	3.39	3.14
$-b_1 \cdot 10^{-2}$	5.14	5.78	5.03	5.06	5.15	4.98	4.68	3.98	5.01	4.69	4.22	4.41	4.39	3.36	3.99
$s_{b_1} \cdot 10^{-2}$	0.46	0.48	0.37	0.45	0.34	0.34	0.33	0.44	0.30	0.30	0.26	0.35	0.35	0.31	0.30
$-b_2 \cdot 10^{-2}$	6.86	8.03	6.68	6.96	7.45	7.44	6.27	5.37	–	–	–	–	–	–	–

	31	32	33	34	35	36	37	38	39						
$s_{b_2} \cdot 10^{-2}$	1.27	1.35	1.04	1.26	0.94	0.94	0.93	1.23	–	–	–	–	–	–	–
$b_3 \cdot 10^{-3}$	10.00	11.87	9.80	10.25	11.26	11.37	9.62	8.22	–	–	–	–	–	–	–
$s_{b_3} \cdot 10^{-3}$	2.14	2.27	1.75	2.12	1.58	1.58	1.56	2.08	–	–	–	–	–	–	–
b_1 (%)	15.18	14.59	15.19	14.72	13.97	13.52	14.83	14.75	–	–	–	–	–	–	–
b_2 (%)	46.58	46.60	46.44	47.70	50.99	46.46	45.70	45.77	–	–	–	–	–	–	–
b_3 (%)	38.24	38.81	38.37	37.58	35.04	40.02	39.47	39.48	–	–	–	–	–	–	–
$F_{calc.}$	43.28	48.44	61.86	42.23	79.35	74.16	70.24	28.55	–	–	–	–	–	–	–
r^2	0.9219	0.9296	0.9440	0.9592	0.9558	0.9529	0.9504	0.8862	0.9548	0.9491	0.9529	0.9240	0.9249	0.9350	0.9308
n	15	15	14	9	15	15	15	12	14						
R_{M0}	3.34	2.57	3.75	5.29	4.97	4.61	4.95	5.04	3.65						
$-b_1 \cdot 10^{-2}$	4.17	2.87	4.28	6.20	6.14	5.53	5.89	6.37	4.55						
$s_{b_1} \cdot 10^{-2}$	0.23	0.20	0.76	1.26	0.45	0.38	0.56	0.78	0.89						
$-b_2 \cdot 10^{-2}$	–	–	–	–	7.39	5.06	6.92	–	–						
$s_{b_2} \cdot 10^{-2}$	–	–	–	–	1.24	1.06	1.55	–	–						
$b_3 \cdot 10^{-3}$	–	–	–	–	11.21	8.20	10.47	–	–						
$s_{b_3} \cdot 10^{-3}$	–	–	–	–	2.09	1.80	2.61	–	–						
b_1 (%)	–	–	–	–	16.30	17.62	16.66	–	–						
b_2 (%)	–	–	–	–	45.15	44.83	45.01	–	–						
b_3 (%)	–	–	–	–	38.55	37.55	38.33	–	–						
$F_{calc.}$	–	–	–	–	69.38	98.37	41.22	–	–						
r^2	0.9789	0.9433	0.7264	0.7748	0.9498	0.9531	0.9183	0.8685	0.6838						

[a] Numbers 1–39 refer to surfactants in Table 1.

influence their complex-forming capacity, stepwise regression analysis was applied [27]. Stepwise regression analysis was applied four times:

(1) lipophilicity (R_{M0} in Eq. 1) being the dependent and the molecular substructures being the independent variables;

(2) specific hydrophobic surface area (b_1 in Eq. 1) being the dependent and the molecular substructures being the independent variables;

(3) relative strength of interaction (b_2 in Eq. 1) being the dependent and the R_{M0} and b_1 values being the independent variables; and

(4) relative strength of interaction (b_2 in Eq. 1) being the dependent and the R_{M0}, b_1 values and the molecular substructures being the independent variables.

In each instance the number of accepted independent variables was not limited and the acceptance limit was set to the 95% significance level.

3. Results and discussion

The simultaneous effects of methanol and HPBCD concentrations of the R_M values of surfactants 11 and 22 are shown in Figs. 1 and 2, respectively. The R_M values decrease in each instance with increase in methanol concentration, *i.e.*, these compounds do not show any anomalous retention behaviour in this concentration range that would invalidate the evaluation using Eq. 1. An increase in HPBCD concentration also caused a decrease in R_M values, indicating complex (probably inclusion complex) formation. Interaction of the more hydrophilic HPBCD with the surfactant decreases the lipophilicity of the latter. This finding suggests that the biological properties (adsorption, uptake, half-life, etc.) of surfactant–HPBCD complexes may be different from that of uncomplexed surfactants, resulting in modified effectivity.

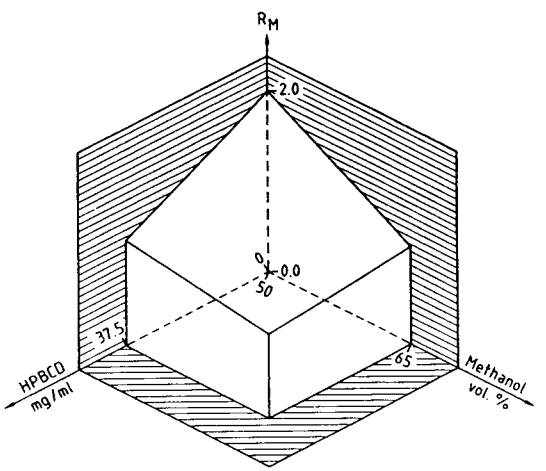

Fig. 1. Effects of methanol and hydroxypropyl-β-cyclodextrin (HPBCD) concentrations on the R_M value of surfactant 11 in Table 1.

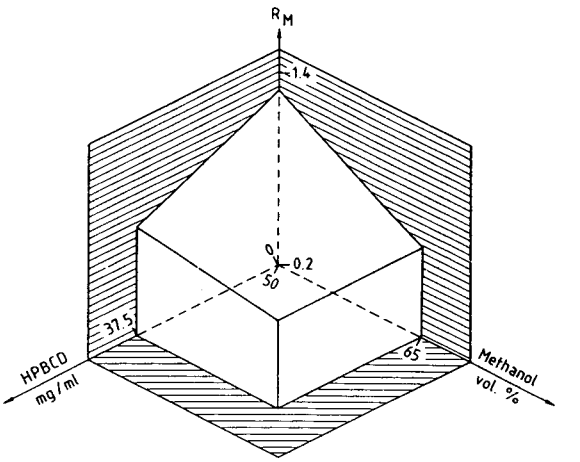

Fig. 2. Effects of methanol and hydroxypropyl-β-cyclodextrin (HPBCD) concentrations on the R_M value of surfactant 22 in Table 1.

The parameters of Eq. 1 are compiled in Table 2. Blank entries in Table 2 indicate that these independent variables did not significantly influence the R_M value of the surfactant. The equation fits the experimental data well, the significance levels in each instance being over 95% (see calculated F values). The ratios of variance explained were about 68–97% (see r^2 values). Most of the surfactants interact with HPBCD (the b_2 values differ significantly from zero), which means that in cosmetics and pesticide formulations containing both surfactants and HPBCD their possible interaction has to be taken into consideration. The parameters of Eq. 1 show large variations between the surfactants, demonstrating that the lipophilicity (R_{M0}),

specific hydrophobic surface area (b_1) and the capacity of surfactants to form inclusion complexes with HPBCD (b_2) differ considerably. This finding suggests also that the inclusion complex formation may influence differently the biological effects of individual surfactants. The complex-forming capacity of surfactants with HPBCD decreases considerably with increasing concentration of methanol in the eluent (see b_3 values). This result can be explained by the supposition that methanol also forms inclusion complexes with HPBCD. This complex is probably very weak; however, methanol is present at a higher concentration than the surfactant and the competition for the HPBCD cavity results in a decrease in the stability of surfactant–HPBCD complexes at higher methanol concentrations. The path coefficients (b_i values) indicate that changes in methanol concentration have the smallest and changes in HPBCD concentration the largest effect on the retention behaviour of surfactants.

A significant linear correlation was found between the intercept (lipophilicity) and slope (specific hydrophobic surface area) values of surfactants (Fig. 3). This finding indicates that from a chromatographic point of view these surfactants behave as a homologous series of compounds, although their hydrophobic moieties are considerably different. This surprising result

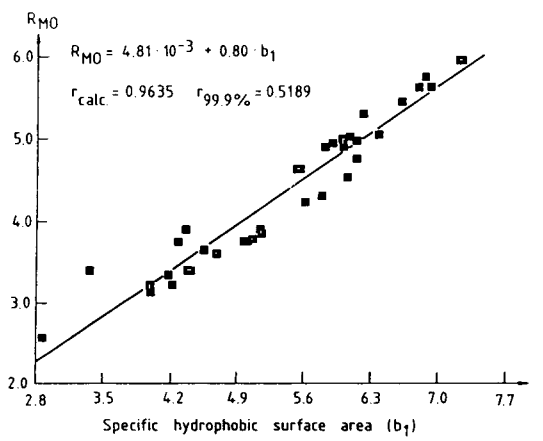

Fig. 3. Relationship between the lipophilicity (R_{MO}) and specific hydrophobic surface (b_1) of surfactants.

suggests that the hydrophilic ethylene oxide chains determine the retention behaviour of ethoxylated surfactants and the character of the hydrophobic moiety is of negligible importance. This can be explained by the assumption that the ethylene oxide chains point towards the polar mobile phase and the area of the hydrophobic surface of surfactants in contact with the non-polar support depends on the capacity of ethylene oxide chains to draw away the hydrophobic moiety from the non-polar support. This effect is really independent of the character of the hydrophobic moiety and depends only on the length of the ethylene oxide chain.

Each stepwise regression analysis found a significant relationship between the chromatographic parameter and molecular substructures (Table 3). The lipophilicity depends on the length of the alkyl chain and on the number of phenyl groups in the hydrophobic moiety of the surfactants (Eq. 3 in Table 3). These two hydrophobic substructures account for most of the change in lipophilicity (see r^2 values), the effect of the phenyl group being the stronger (see B values). The character of the relationship between the specific hydrophobic surface area and substructures is similar (Eq. 4), but the ratio of variance is markedly lower. This results suggests that other molecular characteristics not included in the calculation may also influence the specific hydrophobic surface area of surfactants. The fact that the hydrophobic molecular parameters account for most of the change in the complex-forming capacity of surfactants emphasizes the predominant role of hydrophobic forces in the inclusion complex formation (Eq. 5).

The best relationship describing the dependence of complex-forming capacity on the various parameters of surfactants includes both physico-chemical and structural characteristics (Eq. 6). The effects of the specific hydrophobic surface area and the number of phenyl groups have been discussed above. However, the significant role of the ester bonds need some explanation. It is well known that this substructure markedly modifies the spacial arrangement of the hydrophobic and hydrophilic moieties. This structural change may decrease the contact sur-

Table 3
Relationships between the lipophilicity (R_{M0}), specific hydrophobic surface area (b_1), complex-forming capacity (b_2) and molecular substructures of surfactants[a,b]

$$R_{M0} = a + B_I x_I + B_{II} x_{II} \quad (3)$$

$$b_1 = a + B_I x_{II} \quad (4)$$

$$b_2 = a + B_I R_{M0} + B_{II} b_1 \quad (5)$$

$$b_2 = a + B_I b_1 + B_{II} x_{II} + B_{III} x_{III} \quad (6)$$

Parameter	Equation No.			
	3	4	5	6
n	39	39	24	24
a	4.48	6.02	−0.55	−3.51
B_I	$2.39 \cdot 10^{-2}$	−1.44	−2.08	1.74
s_{B_I}	$1.03 \cdot 10^{-2}$	0.26	0.67	0.20
B_{II}	−1.16	–	3.02	0.60
$s_{B_{II}}$	0.20	–	0.65	0.27
B_{III}	–	–	–	1.04
$s_{B_{III}}$	–	–	–	0.36
B_I (%)	28.36	–	39.75	63.17
B_{II} (%)	71.64	–	60.25	13.56
B_{III} (%)	–	–	–	23.27
$F_{calc.}$	36.98	–	28.30	30.18
r^2	0.6726	0.4627	0.7294	0.8191

[a] Results of stepwise regression analysis. Surfactants not interacting with hydroxypropyl-β-cyclodextrin were omitted from Eq. 5 and 6.
[b] x_I = Length of alkyl chain in the hydrophobic moiety of surfactants; x_{II} = number of phenyl groups in the hydrophobic moiety of surfactants; x_{III} = number of ether bonds in the hydrophobic moiety of surfactants.

face between the surfactants and the non-polar surface of the HPBCD cavity, resulting in a modified complex-forming capacity.

4. Acknowledgement

This work was supported by a grant for Cooperation in Science and Technology with Central and Eastern European Countries: "Enhanced removal and prevention of environmental pollution by attachment and immobilization of bacteria at surfaces".

5. References

[1] D.M. Woodcock, M.E. Linsenmeyer, G. Chojnowski, A.B. Kriegler, V. Nink, L.K. Webster and W.H. Sawyer, *Br. J. Cancer*, 66 (1992) 62.
[2] T.E. Ouriaghli, J. Francois, D. Sarazin and N.T. Dinh, *Carbohydr. Polym.*, 17 (1992) 305.
[3] J.L. Del Estal, A.I. Alvarez, C. Villaverde, P. Corenel, S. Fabra and J.G. Prieto, *J. Pharm. Biomed. Anal.*, 9 (1991) 1161.
[4] E.K. Anderberg, C. Nystrom and P. Artursson, *J. Pharm. Sci.*, 81 (1992) 879.
[5] G.J. Piazza, *Biotechnol. Lett.*, 14 (1992) 1153.
[6] G.C.Y. Chiou, Z.F. Shen, Y.Q. Zheng and Y.J. Chen, *Drug Dev. Res.*, 27 (1992) 177.
[7] J.C. Maurizis, A.A. Pavia and B. Pucci, *Bioorg. Med. Chem. Lett.*, 3 (1993) 161.
[8] C.A. Doige, X. Yu and F.J. Sharom, *Biochim. Biophys. Acta*, 1146 (1993) 65.
[9] F.A. Bonelli and A. Jonas, *Biochim. Biophys. Acta*, 1166 (1993) 92.
[10] R.L. Grant, C. Yao, D. Gabaldon and D. Acosta, *Toxicology*, 76 (1992) 153.
[11] A.A. Reyes, *Microbios.*, 71 (1992) 235.
[12] P.G. Board, *FEBS Lett.*, 315 (1993) 298.
[13] S. Laha and R.G. Luthy, *Biotechnol. Bioeng.*, 40 (1992) 1367.

[14] H.E.J. Hofland, J.A. Bowstra, J.C. Verhoef, G. Buckton, B.Z. Chowdry, M. Ponec and H.E. Junginger, *J. Pharm. Pharmacol.*, 44 (1992) 287.
[15] A. Heredia and M.J. Bukovac, *J. Agric. Food Chem.*, 40 (1992) 2290.
[16] J. Szejtli, in J.L. Atwood, J.E. Davis and D.D. McNicoll (Editors), *Inclusion Compounds*, Vol. III, Academic Press, London, 1984, p. 331.
[17] T. Cserháti and J. Szejtli, *Tenside Deterg.*, 22 (1985) 237.
[18] J. Koch, in J. Szejtli (Editor), *Proceedings of the 1st International Symposium on Cyclodextrins*, Akadémiai Kiadó, Budapest, 1982, p. 487.
[19] K. Kralova, L. Mitterhauszova and J. Szejtli, *Tenside Deterg.*, 20 (1983) 37.
[20] G. Oros, T. Cserháti and J. Szejtli, *Acta Agric. Hung.*, 38 (1989) 211.
[21] T. Cserháti and J. Szögyi, *Chem. Anal. (Warsaw)*, 36 (1991) 267.
[22] T. Cserháti and M. Szejtli, *Carbohydr. Res.*, 224 (1992) 165.
[23] T. Cserháti, E. Fenyvesi and J. Szejtli, *J. Inclus. Phenom.*, 14 (1992) 181.
[24] C. Horváth, W. Melander and I. Molnár, *J. Chromatogr.*, 125 (1976) 129.
[25] T. Cserháti, *Chromatographia*, 18 (1984) 318.
[26] K. Valkó, *J. Liq. Chromatogr.*, 7 (1984) 1405.
[27] H. Mager, *Moderne Regressionanalyse*, Salle, Sauerlander, Frankfurt am Main, 1982, p. 135.

ELSEVIER

Journal of Chromatography A, 665 (1994) 27–32

JOURNAL OF CHROMATOGRAPHY A

Use of a novel carbon sorbent for the adsorption of organic compounds from water

S. Škrabáková[a], E. Matisová*[,a], E. Benická[a], I. Novák[b], D. Berek[b]

[a]*Department of Analytical Chemistry, Faculty of Chemical Technology, Slovak Technical University, Radlinského 9, 812 37 Bratislava, Slovak Republic*

[b]*Slovak Academy of Sciences, Polymer Institute, 842 36 Bratislava, Slovak Republic*

Abstract

A porous carbon sorbent prepared by pyrolysis of cellulose in the presence of porogens was tested for the preconcentration of volatile organic pollutants (particularly hydrocarbons in the gasoline range) from water matrices by the purge-and-trap method. The trapped components were desorbed by carbon disulphide and measured by high-resolution capillary gas chromatography with on-column injection. The studied concentration range of individual hydrocarbons in water was 10 ppb–10 ppm. Drinking water, spring water and gasoline-contaminated water are given as examples of real sample analysis.

1. Introduction

The investigation of the contamination of water with low concentrations of compounds is a complex problem that can only be solved by using isolation and preconcentration procedures prior to the determination. There are many techniques that can be used for the isolation and preconcentration of the considered pollutants from environmental samples that have been described in several reviews [1–4]. One of the most commonly used techniques, especially for volatile organic compounds (VOCs), is the determination of the purgeable priority pollutants listed by the US Environmental Protection Agency (EPA) involving the purge-and-trap technique, first introduced by Bellar and Lichtenberg [5].

The commonly used sorbents for trace enrichment purposes have been reviewed by Liška *et al.* [4]. In recent years, organic polymers of the Tenax variety and various carbon materials have mostly been used. Comparison between the collection efficiency of Carbopack B and Tenax GC [6] and Tenax TA and Carbotrap [7] shows that for all VOCs additional adsorbents or methods must be considered. Therefore, volatile compounds are in many instances trapped on selective adsorbents connected in series, *e.g.*, Tenax TA–Chromosorb 106–Spherocarb [8], Tenax GC–silica gel–charcoal [9,10] or Carbopack B–Carbosieve [11], or multi-bed carbonaceous sorbents such as Vocarb 4000 and Vocarb 3000 [12].

The development of new types of sorbents for solid-phase extraction (SPE) is growing rapidly. Among the materials that have been investigated in recent years are tailored sorbents. They have attracted attention because of their potential for the optimum solution of separation problems. Second-generation sorbents with a predominant-

* Corresponding author.

0021-9673/94/$07.00
SSDI 0021-9673(93)E1300-O

ly carbonaceous matrix should be mentioned in this context. The advantages of these materials are their thermal stability, chemical resistance and stability over a wide pH range. The method employed for the preparation of many porous carbons [13] is based on the pyrolysis of organic precursors on the surface and within the pores of macroparticulate silica gel. After pyrolysis the silica is removed by alkali digestion, leaving a carbonaceous material whose particle size, porosity and surface area are dependent on the silica gel used as a support.

The aim of this work was to evaluate the possibilities of trapping volatile organic compounds from water matrices on a novel porous carbon sorbent, prepared by pyrolysis of cellulose in the presence of porogens.

2. Experimental

All chemicals used were of the highest available purity and were obtained from different sources. A stock standard solution of the following *n*-alkanes and aromatic hydrocarbons was prepared in methanol: *n*-heptane, toluene, *n*-octane, ethylbenzene, *m*-xylene, *p*-xylene, *o*-xylene, *n*-nonane, 1,3,5-trimethylbenzene, *n*-decane, *n*-undecane, 2-methylnaphthalene and 1,6-dimethylnaphthalene (weighing of 10 μl of standard per 10 ml of methanol). Working standard solutions of lower concentration were prepared by dilution of the stock standard solution in CS_2.

Test solutions containing 10 ppb, 0.2 ppm and 10 ppm of each component were prepared by dilution of aliquots of the mixtures in doubly distilled, deionized water.

The tested carbon sorbent (Carb II) was prepared by controlled pyrolysis of cellulose beads in the presence of porogens [14] and had the following characteristics: particle size 180–400 μm, surface area 400 m^2/g, spherical particles.

The nitrogen purge gas with a flow-rate of 20 ml/min was dried and purified using molecular sieve 5A and $CaCl_2$ and transferred through a custom-made purge vessel. Organic compounds were stripped from 30 ml of water at 90°C for 15 min and the drying time was 5 min.

Adsorption cartridges were prepared by packing glass tubes (11 cm × 3 mm I.D.) with 150 mg of carbon sorbent activated by heating under a CO_2 atmosphere at 750°C for 15 min. The trapped components were desorbed by the addition of 1 ml of carbon disulphide to the glass vial with the transferred sorbent and the vial was placed in an ultrasonic bath for 20 min. The eluates were then analysed by high-resolution capillary gas chromatography (HRcGC).

GC measurements were performed on a Fractovap 4160 capillary gas chromatograph (Carlo Erba, Milan, Italy) equipped with a Grob-type cold on-column injector and a flame ionization detector. The analyses were carried out using two capillary columns, as follows.

An HP-1 fused-silica capillary column (Hewlett-Packard, Avondale, PA, USA) with a dimethylsiloxane phase (25 m × 0.2 mm I.D., 0.33-μm film thickness) was connected with a 1.4-m retention gap (0.53 mm I.D.). The temperature programme was 1 min isothermal at 35°C, increased at 8°C/min to 180°C, held for 5 min. Hydrogen was used as the carrier gas with a linear velocity 50 cm/s.

An HP-PONA fused-silica capillary column (Hewlett-Packard) (50 m × 0.2 mm I.D., 0.50-μm film thickness) was connected with a 1-m retention gap (0.53 mm I.D.). The temperature programme was 15 min isothermal at 40°C, then increased at 1.6°C/min to 190°C, held for 10 min. Hydrogen was used as the carrier gas with a linear velocity 35 cm/s (at 40°C).

The detector temperature was 300°C and the sample volume injected was 1 μl in both instances.

3. Results and discussion

In a recent paper [15] it was shown that a carbon sorbent prepared by pyrolysis of saccharose in a matrix of silica (Carb I) was suitable for the preconcentration of non-polar and slightly polar compounds from air samples. Preliminary experiments have shown the possibility of using

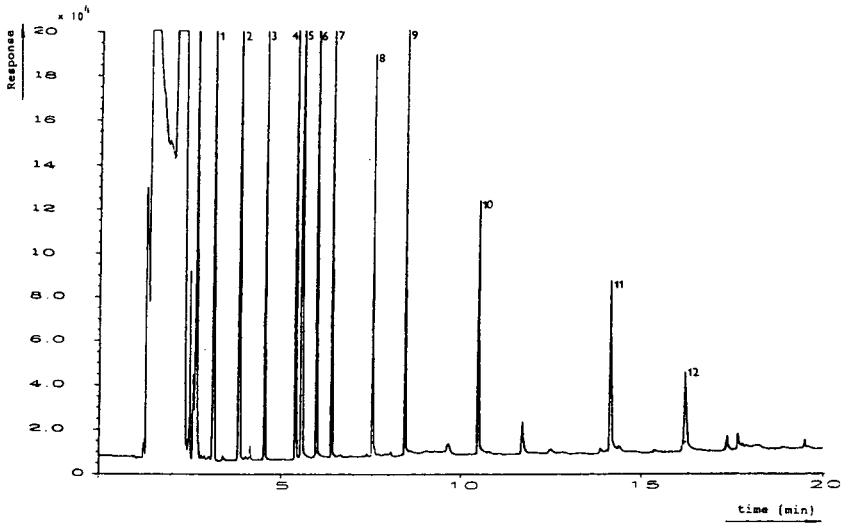

Fig. 1. Chromatogram of the separation of standard hydrocarbon mixture after preconcentration by the purge-and-trap method from water at a concentration of 0.2 ppm. Measurements were performed on the HP-1 column with hydrogen as carrier gas at 50 cm/s under temperature-programmed conditions: 35°C, held for 1 min, than increased at 8°C/min to 180°C, held for 5 min. On-column injection; flame ionization detection. Peaks: 1 = *n*-heptane; 2 = toluene; 3 = *n*-octane; 4 = ethylbenzene; 5 = *m*-, *p*-xylene; 6 = *o*-xylene; 7 = *n*-nonane; 8 = 1,3,5-trimethylbenzene; 9 = *n*-decane; 10 = *n*-undecane; 11 = 2-methylnaphthalene; 12 = 1,6-dimethylnaphthalene.

carbon sorbents prepared by pyrolysis of cellulose in the presence of porogens (Carb II) in the analysis of non-polar compounds trapped from air samples. In this work, we investigated the possibilities of using a carbon sorbent in the purge-and-trap technique and in the determination of volatile compounds in water samples, particularly hydrocarbons.

The sorbent was evaluated on the basis of calculated recoveries of the sorption–desorption procedure. Purge-and-trap recoveries of hydrocarbons were studied at concentrations of 10

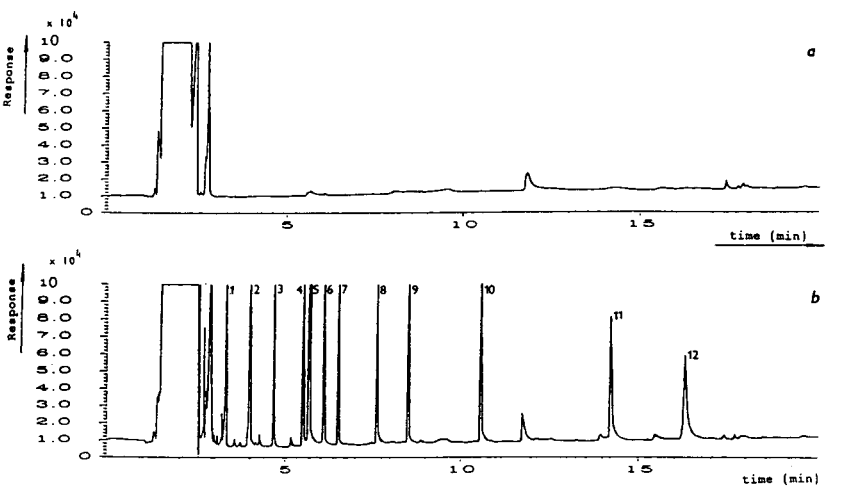

Fig. 2. Chromatogram of the separation of organic compounds after preconcentration by the purge-and-trap method from (a) spring water and (b) spring water with addition of standards (*ca.* 75 ppb). Chromatographic conditions and peak assignments as in Fig. 1.

ppm, 0.2 mg/kg and 10 μg/kg. A chromatogram of the separation of a standard mixture at the 0.2 ppm level after preconcentration is given in Fig. 1; chromatographic measurements were performed on an HP-1 non-polar chemically bonded dimethylsilicone column. The recovery R was calculated from the GC peak-areas ratio:

$$R\ (\%) = (A_i/A_i') \cdot 100$$

where A_i is the peak area determined in eluates after the stripping procedure and A_i' is the peak area of the model mixture of corresponding dilution (without preconcentration).

The recoveries under the given experimental conditions for hydrocarbons up to C_{10} approached 100%; for higher boiling compounds, particularly naphthalenes, they were significantly lower. When measuring lower concentrations (ppb level) the signal profile was slightly disturbed by the signals of the solvent and the sorbent blank itself. The analysis of higher boiling components was problematic.

The tested carbon sorbent was also applied to the determination of hydrocarbons in real samples (drinking water, spring water and water contaminated by gasoline). In drinking water and

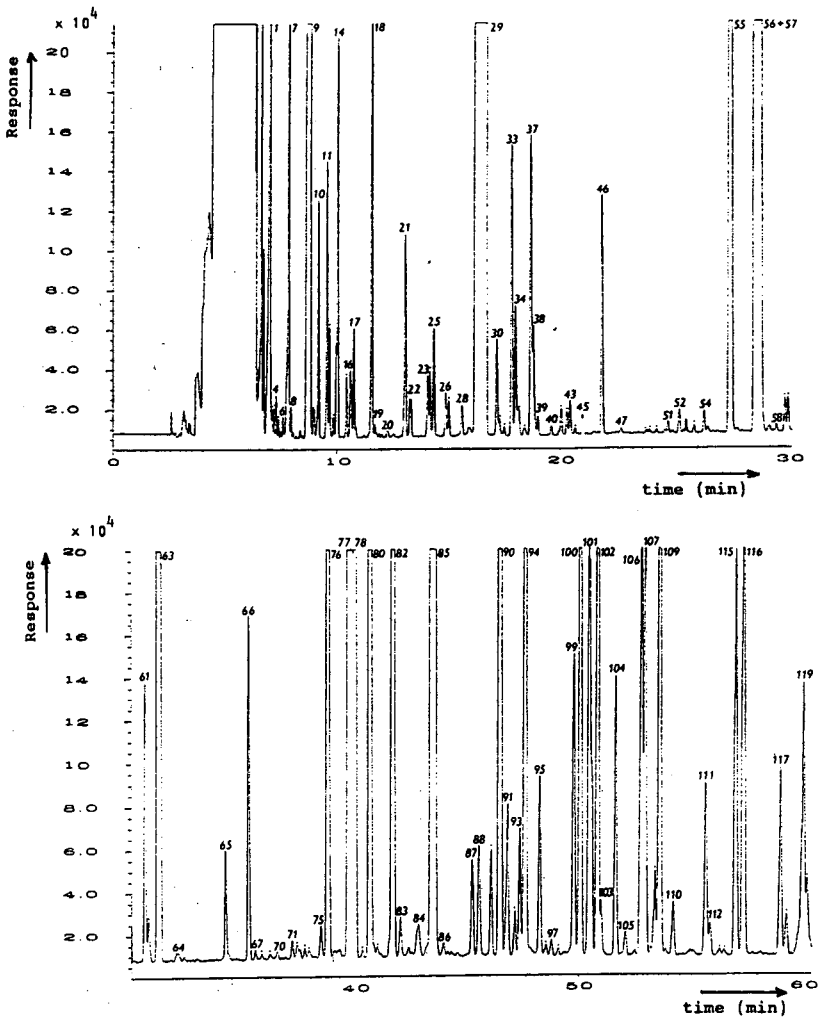

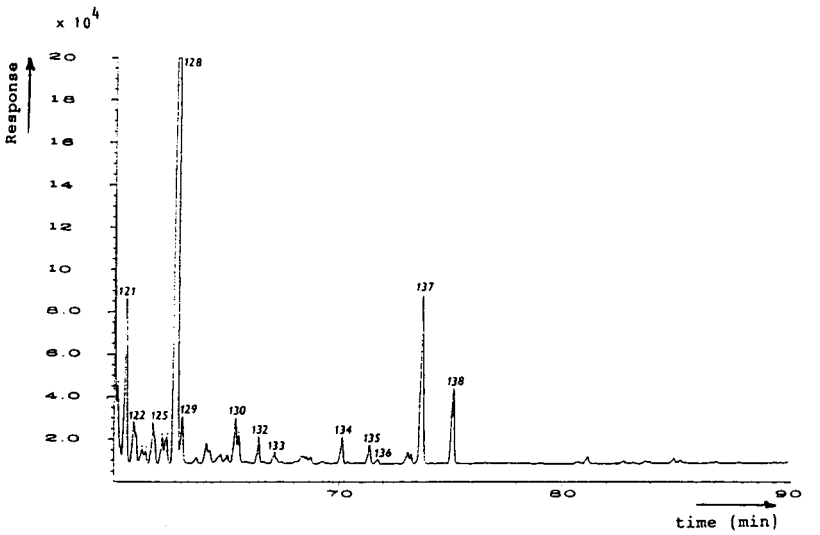

Fig. 3. Chromatogram of the separation of organic compounds stripped from gasoline-contaminated water. Measurements were performed on an HP-PONA column with hydrogen as carrier gas at 35 cm/s, under temperature-programmed conditions: 40°C, held for 15 min, then increased at 1.6°C/min to 190°C, held for 10 min. On-column injection; flame ionization detection. Peaks: 1 = *n*-hexane; 2 = *cis*-1-hexene/*trans*-2-hexene; 3 = 2-me-2-pentene; 4 = 3-me-cy-pentene; 5 = *cis*-2-hexene; 6 = 3-me-*trans*-2-pentene; 7 = me-cy-pentane; 8 = 2,2,3-tri-me-butane; 9 = benzene; 10 = cy-hexane; 11 = 2-me-hexane; 12 = 2,3-di-me-pentane; 13 = 1,1-di-me-cy-pentane; 14 = 3-me-hexane; 15 = 1-*cis*-3-di-me-cy-pentane; 16 = 1-*trans*-3-di-me-cy-pentane/3-et-pentane; 17 = 1-*trans*-2-di-me-cy-pentane; 18 = *n*-heptane; 19 = 3-me-*cis*-2-hexene/2-me-2-hexene; 20 = 3-me-*trans*-3-hexene; 21 = 1-*cis*-2-di-me-cy-pentane/me-cy-hexane; 22 = 2,2-di-me-hexane/1,1,3-tri-me-cy-pentane; 23 = et-cy-pentane; 24 = 2,5-di-me-hexane; 25 = 2,4-di-me-hexane/2,2,3-tri-me-pentane; 26 = 1-*trans*-2-*cis*-4-tri-me-cy-pentane; 27 = 3,3-di-me-hexane; 28 = 1-*trans*-2-*cis*-3-tri-me-cy-pentane; 29 = toluene; 30 = 1,1,2-tri-me-cy-pentane; 31 = 2-me-3-et-pentane; 32 = 2,5-di-me-2-hexene; 33 = 2-me-heptane; 34 = 4-me-heptane/3,4-di-me-hexane/3-me-3-et-pentane; 35 = 2,2,4,4-tetra-me-pentane; 36 = 1-*cis*-2-*trans*-4-tri-me-cy-pentane; 37 = 3-me-heptane; 38 = 3-et-hexane; 39 = 1-*trans*-4-di-me-cy-hexane; 40 = 1,1-di-me-cy-hexane; 41 = 1-me-*trans*-3-et-cy-pentane; 42 = 1-me-*cis*-3-et-cy-pentane; 43 = 1-me-*trans*-2-et-cy-pentane; 44 = 2,2,4-tri-me-hexane; 45 = 1-*trans*-2-di-me-cy-hexane; 46 = *n*-octane; 47 = iso-pro-cy-pentane; 48 = 2,3,5-tri-me-hexane/2,2,3,4-tetra-me-pentane; 49 = 1-me-*cis*-2-et-cy-pentane; 50 = 2,2-di-me-heptane; 51 = 2,4-di-me-heptane; 52 = *n*-pro-cy-pentane/et-cy-hexane; 53 = 1,1,3-tri-me-cy-hexane; 54 = 2,5-di-me-heptane/3,5-di-me-heptane; 55 = et-benzene; 56 = *m*-xylene; 57 = *p*-xylene; 58 = 4-et-heptane; 59 = 4-me-octane; 60 = 2-me-octane; 61 = 3-et-heptane; 62 = 3,3-di-et-pentane; 63 = *o*-xylene; 64 = 1-me-*cis*-3-et-cy-hexane; 65 = *n*-nonane; 66 = iso-pro-benzene; 67 = cy-nonane; 68 = 2-me-4-et-heptane/iso-pro-cy-hexane; 69 = cy-nonane; 70 = 2,2-di-me-octane; 71 = 3,5-di-me-octane; 72 = 2,5-di-me-octane; 73 = *n*-bu-cy-pentane; 74 = cy-decane; 75 = 3,3-di-me-octane/2,6-di-me-octane; 76 = *n*-pro-benzene; 77 = 3-et-toluene; 78 = 4-et-toluene; 79 = 1,1,3,4-tetra-me-cy-hexane; 80 = 1,3,5-tri-me-benzene; 81 = 4-et-octane; 82 = 2-et-toluene; 83 = 2-me-nonane; 84 = 3-me-nonane; 85 = 1,2,4-tri-me-benzene; 86 = iso-bu-cy-hexane/2,2,7-tri-me-octane/1,2,3,4-tetra-me-cy-hexane; 87 = iso-bu-benzene; 88 = *sec.*-bu-benzene; 89 = *n*-decane; 90 = C_{10} aromatic; 91 = 1-me-3-iso-pro-benzene; 92 = 1-me-4-iso-pro-benzene; 93 = 3,4,6-tri-me-octane; 94 = indane; 95 = 2,2-di-me-nonane/*sec.*-bu-cy-hexane; 96 = 1-me-2-iso-pro-benzene; 97 = 2,6-di-me-nonane; 98 = *n*-bu-cy-hexane; 99 = 1,3-di-et-benzene; 100 = 1-me-3-*n*-pro-benzene; 101 = 1-me-4-*n*-pro-benzene/1,4-di-et-benzene/C_{10} aromatic; 102 = 1,3-di-me-5-et-benzene; 103 = C_{10} aromatic; 104 = 1-me-2-*n*-pro-benzene; 105 = 2,3-di-me-nonane; 106 = 1,4-di-me-2-et-benzene; 107 = 1,3-di-me-4-et-benzene; 108 = C_{10} aromatic; 109 = 1,2-di-me-4-et-benzene; 110 = 3-me-decane; 111 = 1,2-di-me-3-et-benzene; 112 = 1-me-3-*sec.*-bu-benzene/1-et-3-iso-pro-benzene; 113 = C_{10} aromatic; 114 = 1-me-4-*sec.*-bu-benzene/1-et-4-iso-pro-benzene; 115 = *n*-undecane/C_{10} aromatic; 116 = C_{11} aromatic; 117 = aromatic; 118 = C_{11} aromatic; 119 = C_{11} aromatic/alkane; 120 = C_{11} aromatic; 121 = C_{10} aromatic; 122 = C_{11} aromatic/C_{12} aromatic; 123 = C_{11} aromatic; 124 = C_{12} aromatic; 125 = C_{12} aromatic; 126 = C_{11} aromatic/C_{12} aromatic; 127 = aromatic; 128 = naphthalene; 129 = C_{11} aromatic/C_{12} aromatic; 130 = C_{11} aromatic; 131 = C_{11} aromatic/C_{12} aromatic; 132 = C_{12} aromatic; 133 = *n*-dodecane; 134 = aromatic; 135 = aromatic; 136 = C_{11} aromatic; 137 = me-naphthalene; 138 = me-naphthalene. Abbreviations: me = methyl; et = ethyl; pro = propyl; bu = butyl; cy = cyclo.

spring water the organic components sought were not found at the studied concentration level. Chromatograms for the analysis of spring water and spring water with the addition of standards (*ca.* 75 ppb) are shown in Fig. 2a and b, respectively.

To obtain a better resolution of larger numbers of hydrocarbons expected in gasoline-contaminated water, GC measurements were performed on an HP-PONA capillary column, which is specially designed for the analysis of multi-component hydrocarbon mixtures [16–18]. Qualitative analysis was done by comparing the retention times of sample components with those of hydrocarbon mixtures of known composition (gasoline for pyrolysis and reformate). All chromatographic measurements were carried out with the optimized temperature programme. A chromatogram of compounds stripped from contaminated water is given in Fig. 3, where 163 compounds were identified, predominately aromatic hydrocarbons, cycloalkanes and alkanes. Quantitative analysis was performed by the internal standard method. The concentrations of individual components were found to be in the range 7 ppb–3.5 ppm.

4. Conclusions

The possibilities of the accumulation of non-polar volatile organic compounds from water matrices on a novel porous carbon sorbent, Carb II (prepared by the controlled pyrolysis of cellulose in the presence of porogens), were studied. The trapped components (*n*-alkanes and aromatics), after stripping, were desorbed by CS_2 and subjected to HRcGC. Good recoveries with the adsorption–desorption procedure (purge-and-trap method) were obtained at the studied concentration levels (10 ppb–10 ppm). The tested sorbent was also applied in the analysis of real samples (drinking water, spring water and gasoline-contaminated water).

5. References

[1] F.I. Onuška, *J. High Resolut. Chromatogr.*, 12 (1989) 4.
[2] J. Namiesnik, T. Górecki and M. Biziuk, *Anal. Chim. Acta*, 237 (1990) 1.
[3] S.K. Poole, T.A. Dean, J.W. Oudsema and C.F. Poole, *Anal. Chim. Acta*, 236 (1990) 3.
[4] I. Liška, J. Krupčík and P.A. Leclercq, *J. High Resolut. Chromatogr.*, 12 (1989) 577.
[5] T.A. Bellar and J.J. Lichtenberg, *J. Am. Water Works Assoc.*, 66 (1974) 739.
[6] P. Ciccioli, E. Brancaleoni, A. Cecinato, C. di Palo, A. Brachetti and A. Liberti, *J. Chromatogr.*, 351 (1986) 433.
[7] H. Rothweiler, P.A. Wager and Ch. Schlatter, *Atmos. Environ.*, 25B (1991) 231.
[8] A. Bianchi, M.S. Varney and J. Phillips, *J. Chromatogr.*, 467 (1989) 111.
[9] J.W. Eichelberger, T.A. Bellar, J.P. Donnelly and W.L. Budde, *J. Chromatogr. Sci.*, 28 (1990) 460.
[10] M.F. Mehran, M.G. Nickelsen, N. Golkar and W.J. Cooper, *J. High Resolut. Chromatogr.*, 13 (1990) 429.
[11] *Supelco Rep.*, 7, No. 5 (1988).
[12] *New Expanded Supelco Rep.*, 12 No. 1 (1993) 21.
[13] O. Chiantore, I. Novák and D. Berek, *Anal. Chem.*, 60 (1988) 638.
[14] I. Novák, D. Berek, J. Štamberg, J. Peška, B. Philipp, H. Gensrich, V. Grobe and D. Bratsch, *Czech. Pat.*, 230 297 (1984); *Ger. Pat.*, DD 21 864 (1985).
[15] S. Škrabáková, E. Matisová, M. Onderová, I. Novák and D. Berek, *Chem. Pap.*, in press.
[16] E. Matisová, L. Kubuš and E. Jurányiová, *J. High Resolut. Chromatogr.*, 14 (1991) 713.
[17] E. Matisová, E. Jurányiová, P. Kuráň, E. Brandšteterová, A. Kočan and Š. Holotík, *J. Chromatogr.*, 552 (1991) 301.
[18] E. Matisová, Š. Vodný, S. Škrabáková and M. Onderová, *J. Chromatogr.*, 629 (1993) 309.

ELSEVIER

Journal of Chromatography A, 665 (1994) 33–36

JOURNAL OF CHROMATOGRAPHY A

Short Communication

Structural inhomogeneities in wide-pore silica gels

I. Novák*, D. Berek

Polymer Institute, Slovak Academy of Sciences, Dúbravská cesta 9, 842 36 Bratislava, Slovak Republic

Abstract

The cause of a bimodal or multimodal pore-size distribution in wide-pore silica gels made by a calcination procedure were elucidated. It was found that the process of crystallization of salt out of the pores of the silica gel is influenced by the nature of the salt and by the rate of evaporation of water. If these parameters were optimized, the pore structure of wide-pore silica gel prepared by this method was more uniform and the batch-to-batch repeatability of the process was greatly improved.

1. Introduction

Silica gels still dominate HPLC applications and include macroporous and even gigaporous (wide-pore) particles with pore diameters of 10–100 nm and >100 nm, respectively. The most common applications are size-exclusion chromatography [1] and procedures in which the chromatographic functions are attached to macromolecules accommodated within the pores of carriers [2–9].

Wide-pore silica gels can be prepared by the controlled polycondensation of silicic acid, but the maximum pore size so far prepared in this direct way hardly exceeds 100 nm [10]. A more efficient way to prepare wide-pore silica gel is the indirect route, *e.g.*, by enlarging the pores of readily available mesoporous materials [11–15].

Tanaka *et al.* [16] investigated microscopically the texture of various commercial silica gels. They found that wide-pore silica gels ($D = 30$–400 nm) usually possessed pores of two or even several different sizes within the same sample. This resulted in wide or bimodal pore-size distribution curves of the silica gels as measured by different methods. The logical conclusion of Tanaka *et al.* [16] was that the samples studied were in fact mixtures of at least two different materials.

In this study, we tried to answer the question of whether such mixtures can be formed unintentionally in the course of wide-pore silica gel production and, if so, what the cause of these irregularities is and how they can be prevented.

2. Experimental

Scanning electron microscopy was carried out with a Jeol 35 SEM.

2.1. Silica gel

An experimental sample (SG-10) was prepared in this Institute with surface area, pore volume and particle diameter of 320 $m^2 g^{-1}$, 1.8

* Corresponding author.

0021-9673/94/$07.00
SSDI 0021-9673(93)E1231-N

$cm^3\ g^{-1}$ and 8–12 μm, respectively. Silica gel LiChrospher Si-100 (10 μm) was obtained from Merck (Darmstadt, Germany).

2.2. Preparation of wide-pore silica gel

A 25% aqueous solution of a suitable salt, typically NaCl, was slowly added to carefully stirred silica gel in a glass beaker to form only slightly wet material. This means that almost the whole volume of solution was soaked up by the pores of the silica gel. The mixture was transferred into an oven and dried at different temperatures above 110°C and under different arrangements. The dried materials were heated in a furnace at different temperatures and for different durations, typically at 700°C for 2 h. The salt was then leached out with an excess of distilled water and the remaining silica gel was dried after washing.

3. Results and discussion

We applied a calcination procedure for widening the pore size of conventional (6–20-nm) silica gels as introduced by Krebs and Heintz [17], as this method or its modifications are probably used by the producers of commercial wide-pore silica gels. It is based on filling the pores of silica gel with a neutral, thermostable inorganic salt with melting point above 300°C and calcinating the composite. At high temperatures, both the silica gel and the salt at least partially liquefy and phase separation occurs. The size and shape of the phases formed depend on the amount and nature of the salt and on the conditions of calcination. The phases solidify when the temperature drops and, subsequently, the salt phase is leached out, leaving wide-pore silica gel with pore diameters of $\geq$1000 nm.

Using the Krebs and Heintz method [17], we produced with a single procedure and from the same starting sample bimodal, "mixed" materials as reported by Tanaka *et al.* [16] (Figs. 1 and 2). Careful investigation of single particles of silica gels by scanning electron microscopy showed that the bimodal pore structure may be present even within single particles (Figs. 3 and 4). Sometimes, the particles contain shell or skin regions (Fig. 5). On the other hand, the regular sponge-like structure of wide-pore silica gels prepared by the Krebs and Heintz method [17] typically has a very narrow pore-size distribution (Fig. 6). This means that wide-pore silica gels prepared by the calcination method may inherently consist of mixtures of materials with different pore sizes, each possessing a narrow size distribution.

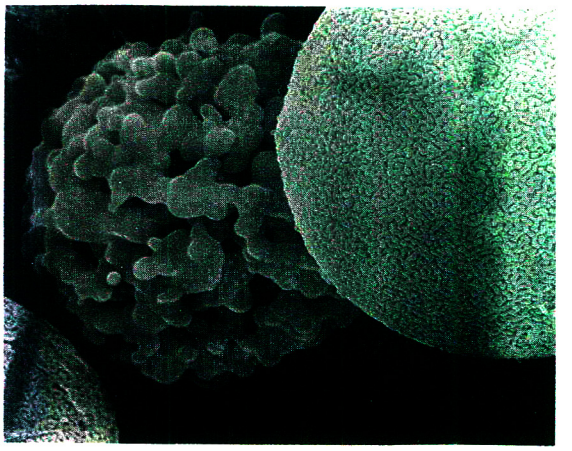

Fig. 1. Scanning electron micrograph of silica gel SG-10 soaked and dried with salt, heated at 800°C for 30 min, washed out with water and dried.

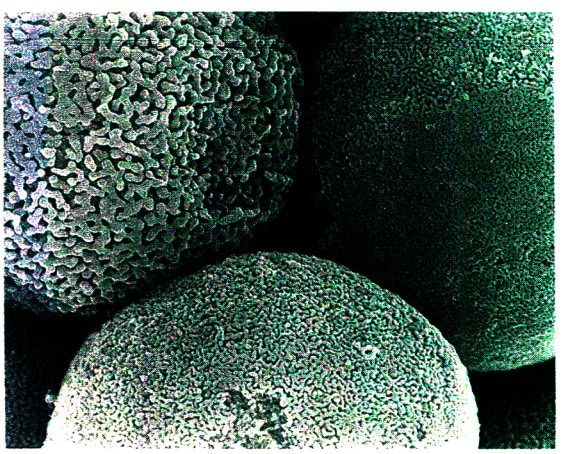

Fig. 2. Scanning electron micrograph of silica gel SG-10. Treatment as in Fig. 1.

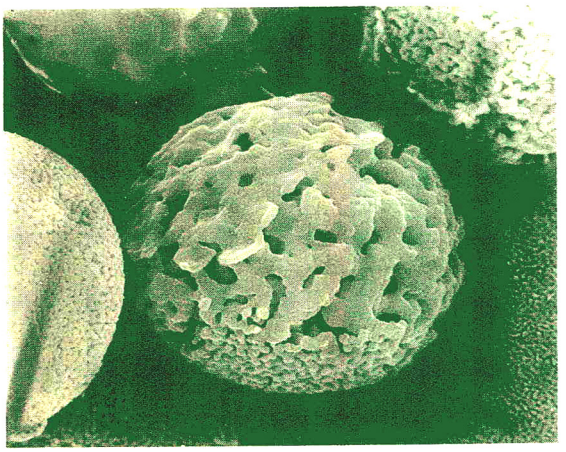

Fig. 3. Scanning electron micrograph of silica gel SG-10 soaked and dried with salt, heated at 700°C for 1 h, washed out with water and dried.

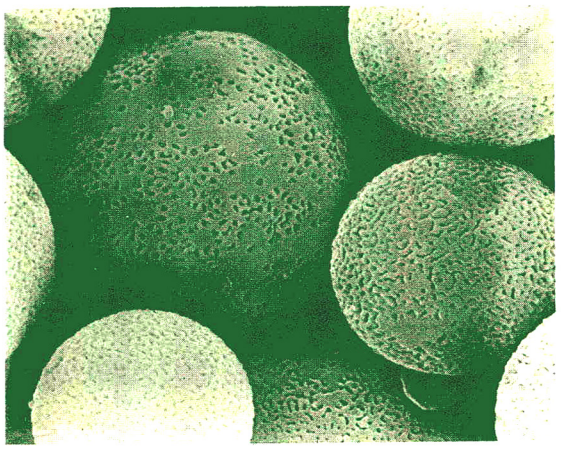

Fig. 5. Scanning electron micrograph of silica gel LiChrospher Si-100 treated with salt, heated at 700°C for 2 h, washed out with water and dried.

In order to explain the reasons for bimodal and multimodal structure formation, we also checked microscopically the raw material and the intermediate products formed under different experimental conditions. We found that a voluminous phase of fine wool-like crystals was formed on the surface of the layer of material during drying (Fig. 7) and in this instance the final silica gel possessed a bi- or multimodal pore structure. This means that during calcination

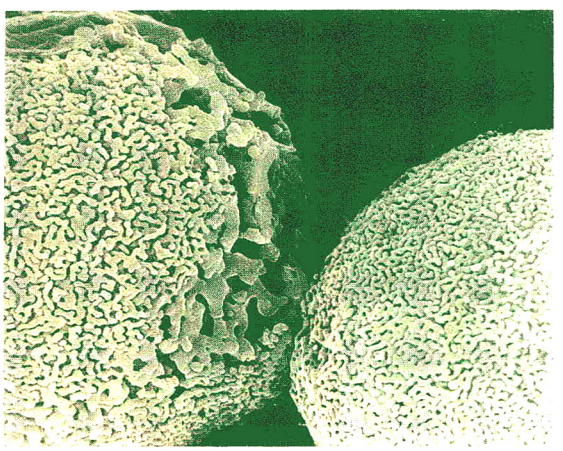

Fig. 4. Scanning electron micrograph of LiChrospher Si-100 treated with NaCl, heated at 750°C for 2 h, washed out with water and dried.

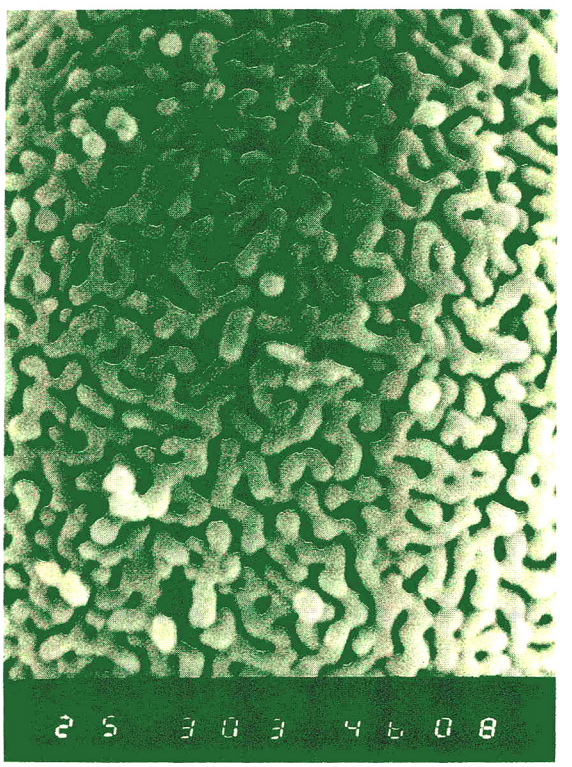

Fig. 6. Scanning electron micrograph of LiChrospher Si-100 soaked in NaCl solution and dried, heated at 800°C for 1 h, washed out with water and dried.

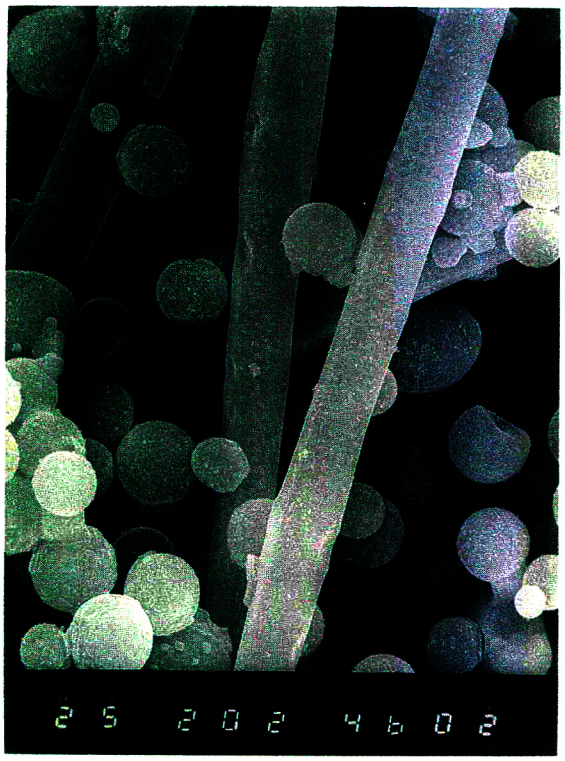

Fig. 7. Scanning electron micrograph of silica gel SG-10 after drying with the salt.

some pores were empty whereas others were filled only partly with salt, and only a small fraction of the pores was optimally saturated with salt. This could explain why pores with different structures are formed within one batch of silica gel or even within a single particle.

A possibility for improving the uniformity of wide-pore silica gel prepared by the calcination method is the cautious stirring of either the silica during water evaporation or dry silica gel containing crystals of salt so that the long needles are broken. In any event, the resulting dry mixture must be as homogeneous as possible so that salt melted during calcination can more easily re-enter the pores of the silica and the phase separation can proceed homogeneously.

4. References

[1] K.K. Unger, *Porous Silica (Journal of Chromatography Library*, Vol. 16), Elsevier, Amsterdam, 1979.
[2] Y. Okamoto, M. Kawashima and K. Hatada, *J. Am. Chem. Soc.*, 106 (1984) 5357.
[3] Y. Okamoto, M. Kawashima and K. Hatada, *J. Chromatogr.*, 363 (1986) 173.
[4] Y. Okamoto, *Chem. Technol.*, 17 (1987) 176.
[5] Y. Okamoto, R. Aburatani, Y. Kaida and K. Hatada, *Chem. Lett.*, (1988) 1125.
[6] Y. Okamoto, M. Yanagida and K. Hatada, *Polym. J.*, 21 (1989) 795.
[7] Y. Okamoto, H. Mohri and K. Hatada, *Polym. J.*, 21 (1989) 439.
[8] Y. Okamoto, Y. Kaida, H. Hayashida and K. Hatada, *Chem. Lett.*, (1990) 909.
[9] Y. Okamoto and Y. Kaida, *J. High Resolut. Chromatogr.*, 13 (1990) 708.
[10] I. Novák and D. Berek, unpublished results.
[11] N.V. Akshinskaya, A.V. Kiselev and Yu.S. Nikitin, *Zh. Fiz. Khim.*, 37 (1963) 927.
[12] A.V. Kiselev, V.M. Lukyanovich, Yu.S. Nikitin, E.B. Oganesyan and A.J. Sarakhov, *Kolloidn. Zh.*, 31 (1969) 388.
[13] A.V. Kiselev, Yu.S. Nikitin, A.J. Sarakhov and E.B. Oganesyan, *Kolloidn. Zh.*, 30 (1968) 842.
[14] M. Le Page and A. de Vries, *Fr. Pat.*, 1 475 929 (1967).
[15] D. Berek and I. Novák, *Chromatographia*, 30 (1990) 582.
[16] N. Tanaka, K. Hashidzume, M. Araki, H. Tsuchiya, A. Okuno, K. Iwaguchi, S. Ohnishi and N. Takai, *J. Chromatogr.*, 448 (1988) 95.
[17] K.F. Krebs and H. Heintz, *Ger. Pat.*, 2 042 910 (1970).

ELSEVIER

Journal of Chromatography A, 665 (1994) 37–45

JOURNAL OF CHROMATOGRAPHY A

Dextran-grafted silica gel for high-performance size-exclusion chromatography of proteins

M. Petro[a,b], P. Gemeiner[c], D. Berek*[,b]

[a]*Department of Analytical Chemistry, Faculty of Natural Sciences, Comenius University, Mlynská dolina CH-2, 842 15 Bratislava, Slovak Republic*

[b]*Polymer Institute, Slovak Academy of Sciences, Dúbravská cesta 9, 842 36 Bratislava, Slovak Republic*

[c]*Institute of Chemistry, Slovak Academy of Sciences, Dúbravská cesta 9, 842 38 Bratislava, Slovak Republic*

Abstract

A hydrophilic stationary phase for aqueous high-performance size-exclusion chromatography (HPSEC), *viz.*, dextran-grafted silica gel, was synthesized and tested. Using dextran or dextran derivatives covalently grafted on to epoxysilica gel, it was possible to achieve good hydrophilic shielding of the silica gel surface, preserving the unique physical properties of silica matrix. The retention of proteins on the stationary phase was studied to optimize the modification procedure. The undesired silica matrix effect was minimized by combination of three phenomena: chemical removal of silanols by silanization, steric shielding of residual silanols with grafted macromolecules and electrostatic compensation of SiO^- groups by a positively charged anchoring group. Optimized dextran-grafted silica is a suitable packing material for the HPSEC of proteins, operating with a wide range of ionic strength of the eluent.

1. Introduction

Numerous silica-based packing materials for aqueous high-performance size-exclusion chromatography (HPSEC) with high pressure stability and excellent flow properties have been prepared [1]. The main problem is that they often show undesirable interaction of residual surface silanols with many solutes [2].

To be suitable for the SEC of biopolymers, such as proteins, silica supports must therefore be well covered with a hydrophilic organic layer. This has been done mainly by the reaction of silanols on the silica surface with γ-glycidyloxypropyltrimethoxysilane to produce diol-bonded phases [3]. Better shielding of residual silanols has been achieved by the immobilization of hydrophilic organic macromolecules, such as polyvinylpyrrolidone [4], poly(ethylene oxide) [5], polysaccharides [6–9] and other polymers [10,11], on the silica gel. Additionally, the unfavourable interactions of proteins with residual silanols can be prevented by the presence of positively charged groups linked to the immobilized polymer, *e.g.*, diethylamino groups on dextran [8].

None of the individual approaches, chemical removal of silanols, steric shielding of residual silanols or electrostatic compensation of SiO^- groups, fully solves the fundamental problem of the undesired solute retention on silica-based materials in aqueous SEC. Hence the combination of these approaches should be considered.

In this paper, the preparation and characteri-

* Corresponding author.

0021-9673/94/$07.00
SSDI 0021-9673(93)E1205-E

zation of a hydrophilic stationary phase for the HPSEC of proteins with minimized protein–sorbent interactions are described. The material was prepared by covalent grafting of dextran molecules (native or derivatized with ethylenediamine) on to the silica surface via epoxy groups previously bonded to the silica surface.

The main difference between the dextran-grafted silica gel and silica gel coated with a layer of cross-linked dextran [7–9] is that dextran grafts may protrude further over the walls of pores than does the more or less intact layer of macromolecules. Protruding dextran chains may fit with the native conformation of separated proteins preserving their biological activity.

As it is known that electrostatic interactions decrease and hydrophobic interactions increase with increasing ionic strength [12,13], the dependence of the retention of selected proteins on the salt content in the eluent was studied to characterize the nature and the intensity of undesirable solute–sorbent interactions. Such information was used for optimization of the grafting procedure. The resulting dextran-grafted silica gel with optimized properties was used for the HPSEC of model proteins.

2. Experimental

2.1. Materials

Spherical silica gel SG-10-78 (mean particle diameter 8 μm; specific surface area 78 $m^2\ g^{-1}$, specific pore volume 1.3 ml g^{-1}) was prepared by modification of the laboratory-made base silica material designated SG-10 [14] to obtain larger pores. γ-Glycidyloxypropyltrimethoxysilane was supplied by Fluka (Buchs, Switzerland). Dextran with a relative molecular mass of $4 \cdot 10^4$ (Rheodextran, D-40) was obtained from Biotika (Slovenská Lupča, Slovak Republic).

Ethylenediamine (99%) was obtained from Janssen Chimica (Bruges, Belgium), sodium periodate from Carlo Erba (Milan, Italy), sodium borohydride from Metallgesellschaft (Frankfurt a.M., Germany), 2,4,6-trinitrobenzoic acid, (analytical-reagent grade) from Serva (Heidelberg, Germany) and 6-aminocaproic acid (99%) from Aldrich (Milwaukee, WI, USA).

Aminoethyl derivatives of dextran (AE-dextran, AE-D) were prepared by reductive alkylation [15,16] of dextran dialdehyde with ethylenediamine and sodium borohydride [15]. The degree of substitution of AE-D was controlled by the molar ratio of sodium periodate to dextran, whereby the generated aldehyde groups were subsequently reductively alkylated in the presence of a large excess of diamine. Primary amino groups of AE-D derivatives were determined spectrophotometrically at 360 and/or 420 nm by a procedure based on the reaction of free amino groups with 2,4,6-trinitrobenzenesulphonate (TNBS) [17,18]. Molar absorptivities ε_{360} = 11 000 l mol^{-1} cm^{-1} and ε_{420} = 18 320 l mol^{-1} cm^{-1} were determined by reaction of 6-aminocaproic acid with TNBS.

The protein standards (Table 1) were obtained from Pharmacia–LKB (Uppsala, Sweden), Boehringer (Mannheim, Germany) and Sigma (St. Louis, MO, USA). D,L-Alanine and deuterium oxide were purchased from Lachema (Brno, Czech Republic). Dextran standards for SEC calibration with relative molecular masses from $1 \cdot 10^3$ to $6.7 \cdot 10^5$ were obtained from Pharmacosmos (Viby, Denmark) and dextran with relative molecular mass $2 \cdot 10^6$ from Pharmacia–LKB.

2.2. LC experiments

The chromatograph used for the LC characterization of sorbents consisted of a Waters Model 510 HPLC pump (Waters–Millipore, Milford, MA, USA), a Rheodyne (Cotati, CA, USA) Model 7120 injector, an RIDK 101 differential refractometric detector, a Model 2563 UV–Vis detector and a TZ 4620 line recorder (Laboratory Instruments, Prague, Czech Republic). A Baseline 810 chromatography workstation (Dynamic Solutions, Division of Millipore, Ventura, USA) based on an NEC SX plus computer (purchased from Waters) was used for data acquisition and processing.

HPSEC separations were performed on a

Table 1
Protein calibration standards

Standard	Abbreviation	Supplier[a]	$M_r \times 10^{-3}$ [b]	Source[b]
Cytochrome *c*	CYT	B	12.5	Horse heart
Ribonuclease	RN	P	13.7	Bovine pancreas
Chymotrypsinogen A	CHT	P, B, S	25	Bovine pancreas
Ovalbumin	OVA	P, B	43, 45	Hen egg
Albumin	BSA	P, B	67, 68	Bovine serum
Aldolase	ALDO	P, B	158	Rabbit muscle
Catalase	CAT	P, B	232, 240	Bovine liver
Ferritin	FR	P, B	440, 450	House spleen
Thyroglobulin	TG	P	669	Bovine thyroid

[a] P = Pharmacia; B = Boehringer; S = Sigma.
[b] As given by the supplier.

liquid chromatograph consisting of a Model 2150 HPLC pump, a Model 2140 rapid spectral detector (both from LKB, Bromma, Sweden), a Rheodyne Model 7010 injector and an Acer computer with HPLC Analysis Program Wavescan EG (purchased from LKB).

Model mixtures were prepared from 1.0 mg ml^{-1} stock standard solutions of individual standards. The injection volumes were 20 or 10 μl. Low-molecular-mass alanine or deuterium oxide was used as a marker for the determination of the total volume of liquid within the column. The void volume was determined by injection of the highest molecular mass dextran standard. Each standard was injected individually into the particular column to calibrate it or to identify peaks on the chromatograms.

2.3. Sorbent preparation

Epoxysilica gel was prepared by modification of silica gel with γ-glycidyloxypropyltriethoxysilane in dry toluene according to a slightly modified procedure of Hermansson [19]. During silanization the reflux cooler was thermostated with water, the temperature being kept between the boiling points of methanol and toluene. After silanization for 8 h the epoxysilica was isolated by filtration, washed with toluene, acetone and methanol and dried at 110°C. The amount of bonded glycidyloxy groups was 3.2 μmol m^{-2} as calculated from elemental analysis data.

Diol-bonded silica gel was prepared from epoxysilica by opening the oxirane rings in an acidic environment. An aqueous suspension of epoxysilica was adjusted to pH 3 with 2% (v/v) nitric acid and stirred occasionally in an ultrasonic bath. About 10 min later the suspension was neutralized to pH 7 with sodium carbonate solution. The diol-silica obtained was filtered, washed with water and methanol and dried at 110°C.

To prepare dextran-grafted silica gels, dried epoxysilica gel was treated with aqueous solutions of dextran or AE-dextran at various pH values from 8 to 13.5. The volume of suspending solution was about twice the pore volume of added silica support. The suspension was stirred at 20°C for 48 h, then carefully adjusted to pH 3 with 2% (v/v) nitric acid. After several minutes the acidic solution was removed by washing the sorbent with water on a suction filter until the pH was 7. Finally, the dextran-grafted silica obtained was washed with methanol and dried at 105°C.

The amount of total immobilized organic phase was controlled by elemental analysis of treated supports during (Fig. 1) and after the grafting procedure (Table 2). The individual fractions of the sorbents were neutralized and thoroughly washed with water and methanol before elemental analysis.

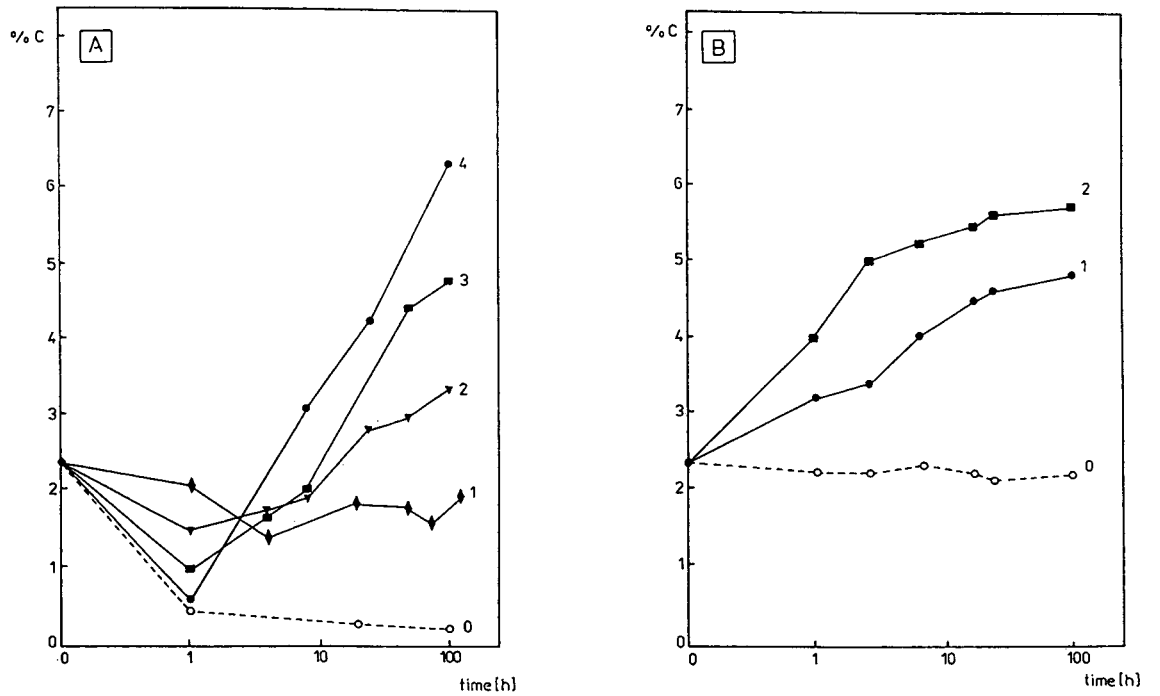

Fig. 1. Time dependence of total amount of immobilized organic phase, expressed as carbon percentage, during grafting dextran or its ethylenediamine derivatives on to epoxysilica gel. Content of dextran or its derivative in all grafting suspensions was 50% ($M_{dextran}/M_{support}$). Other conditions of reaction: (A) grafting native dextran at pH (1) 9.5, (2) 11.5, (3) 12.5 and (4) 13.5, and (0) reference experiment at pH 13.5 without dextran; (B) grafting ethylenediamine derivatives of dextran, (1) AE_3-D-40 and (2) AE_4-D-40, at pH 8.0, and (0) reference experiment at pH 8.0 without AE-dextran.

Table 2
Dextran-grafted silica gels

Sorbent	Immobilized dextran[a]	$\frac{M_{added\ dex.}}{M_{support}}$ [b]	$\frac{n_{NH_2}}{n_{AE\text{-}dextran}}$ [c]	pH at grafting	C (%)[d]
SG-d_1	D-40	1.0	–	13.5	6.4
SG-d_2	D-40	1.0	–	12.5	4.8
SG-d_3	D-40	1.0	–	11.5	3.4
SG-d_4	D-40	0.3	–	12.5	2.1
SG-d_5	D-40	0.3	–	9.5	2.0
SG-d_6	AE_1-D-40	0.5	0.2	11.5	2.2
SG-d_7	AE_2-D-40	0.5	1.0	11.5	4.0
SG-d_8	AE_3-D-40	0.5	2.2	8.0	4.8
SG-d_9	AE_4-D-40	0.5	5.7	8.0	5.8

[a] D-40 = Dextran with average molecular mass $40 \cdot 10^3$; AE-D-40 = Ethylenediamine derivative of D-40.
[b] Amount of dexran or dextran derivative in reaction mixture.
[c] Content of primary amino groups in the ethylenediamine derivatives of dextran used.
[d] As determined by elemental analysis.

2.4. Packing of columns

The sorbents were slurry packed into stainless-steel columns of dimensions 500 × 8 mm I.D., 250 × 8 mm I.D. and 100 × 4 mm I.D. using a Knauer (Berlin, Germany) pneumatic HPLC pump. To obtain well packed columns, the packing procedures needed to be optimized. We used either tetrachloroethylene–*n*-propanol [65:35 (v/v) before mixing] or toluene–cyclohexanol [40:60 (v/v) before mixing] as appropriate suspending liquids. As the pressing liquid we used methanol in both instances. The maximum packing pressure used was 30 MPa.

3. Results and discussion

3.1. Sorbent preparation

It was presumed that unmodified dextran reacts with oxirane groups bonded on the silica surface only in highly basic solutions (Fig. 1a). At pH 9.5 no important change in the carbon content of sorbent was observed, which indicates that virtually no dextran was immobilized under these conditions. At higher pH the unmodified dextran can be grafted on epoxysilica, but competition between cleavage of bonded glycidyloxypropyl groups and dextran grafting probably occurs. Hence it can be concluded that base-catalysed hydrolysis of Si–O–Si bonds prevails at the beginning but in the later stages of the reaction the silica surface is well shielded with grafted dextran. This prevents further splitting of residual silane-silica bonds and the grafting reaction prevails.

In the second approach the AE-dextrans with a controlled content of amino groups (Table 2) were grafted on epoxysilica at pH 8 (Fig. 1B). It seems that under these conditions the glycidyloxypropyl groups are not extensively cleaved. Therefore, the amount of grafted dextran could be approximately calculated from the difference between the carbon contents of the starting epoxybonded silica and the resulting dextran-grafted silica gel. For example, according to such a calculation, dextran-grafted silica composite sorbents SG-d_8 and SG-d_9 contain about 58.5 and 81 mg g^{-1} of immobilized dextran, respectively.

3.2. LC characterization of sorbents

Plots of the SEC distribution coefficient of the chromatographed proteins on the salt content in the mobile phase were used for the evaluation of both electrostatic and hydrophobic interactions of proteins with diol-bonded and dextran-grafted silica gels (Fig. 2).

The acidic protein ovalbumin and the basic protein chymotrypsinogen A were selected for a more detailed study of protein–sorbent interactions. These proteins have a relatively low molecular mass so that they can easily penetrate most pores of sorbents. The cation-exchange effect of residual silanols on both diol-bonded and dextran-grafted silicas increases the retention of chymotrypsinogen A, which is positively charged at pH 7. On the other hand, negatively charged ovalbumin is electrostatically repulsed and therefore it elutes from aqueous eluents with low ionic strength in a lower elution volume than predicted from the SEC calibration graph obtained under conditions of supressed solute–sorbent interactions (see Section 3.3). Both the retaining and repulsing electrostatic interactions can be easily supressed by adding salt to the eluent.

As shown in Fig. 2A, more effective shielding with the dextran layer may result in weakening of undesirable interactions of proteins with the silanols of the silica matrix as compared with diol-silica.

The effect of residual silanols is more effectively supressed by modification of epoxysilica gels with AE-dextran derivatives. The properties of the resulting sorbents depend, however, on the content of AE groups (Table 2) bonded on dextran prior its grafting on epoxysilica gel (Fig. 2B). Such a phenomenon is due to the prevention of the cation-exchange effect of silanols in the presence of positively charged amino groups. The optimum content of AE groups introduced on dextran is between 2 and 6 groups per

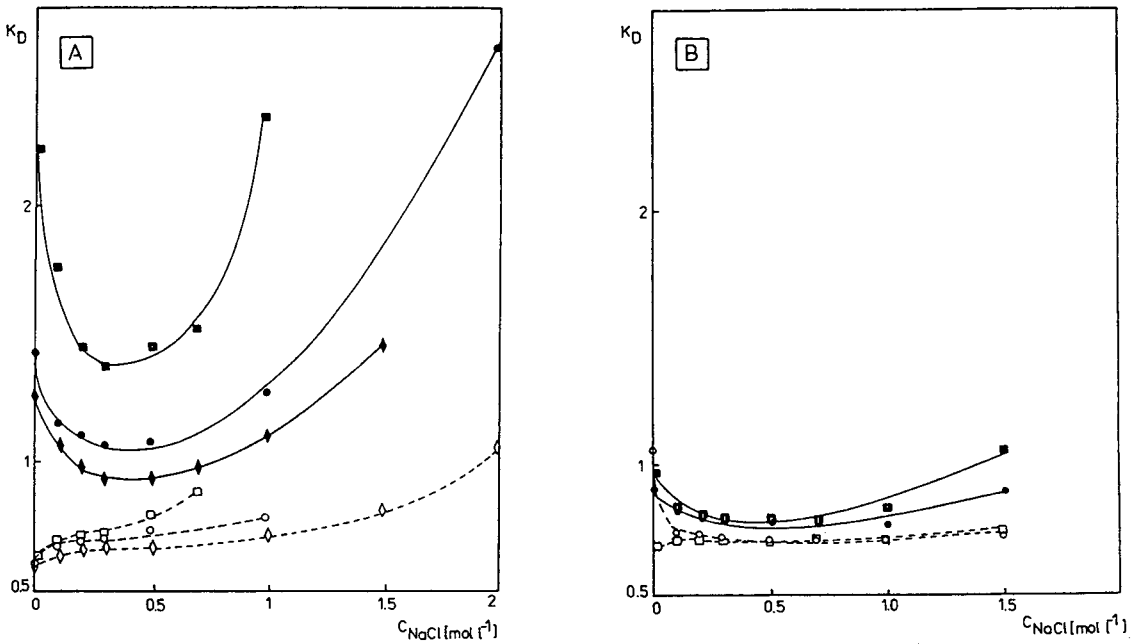

Fig. 2. Dependence of retention of ovalbumin (dashed lines) and chymotrypsinogen (solid lines) on salt concentration in the eluent obtained with various column packings. Eluent: 1/15 *M* phosphate buffer (pH 7.0) + NaCl additive. Retention was evaluated as SEC distribution coefficient $K_D = (V_e - V_0)/(V_t - V_0)$, where V_e is the elution volume of the protein, V_0 the void volume measured as the elution volume of dextran with molecular mass $2000 \cdot 10^3$ and V_t the total liquid volume in the column measured as the elution volume of deuterium oxide. Column packings: (A) ■, □ = diol-SG, ◆, ◇ = SG-d_2; ●, ○ = SG-d_6; (B) ■, □ = SG-d_8, ●, ○ = SG-d_9.

dextran molecule. The dextran-grafted silicas designated SG-d_8 and SG-d_9 in Table 2 show lower protein–sorbent interactions than other dextran-grafted silicas. In this respect, the resulting materials show properties comparable to those of some well known commercial silica-based column packings for protein SEC such as TSK SW sorbents [13]. If the content of AE groups in the grafted dextran is higher than a certain level, anion-exchange properties of such materials can be observed. These result in increasing ovalbumin retention at low salt content in the eluent.

The hydrophobic interactions between the sorbent and proteins, caused by the hydrocarbon part of the glycidyloxypropylsilane spacer, begin to prevail at salt concentrations in the buffer of about 1 mol l^{-1} and higher. It can be seen from Fig. 2 that in this area the protein retention increases with increasing salt content more steeply with diol-silica than with dextran-grafted silicas. This means that also the protein–sorbent hydrophobic interactions can be significantly supressed by a dextran covering. This may be important for separation of hydrophobic proteins, such as membrane proteins.

In Fig. 3, plots of ln k' *vs.* the number of carbon atoms in *n*-alkanols chromatographed on diol-silica and selected dextran-grafted silica gel with water as eluent are compared. The lower selectivity of the separation of *n*-alkanols on dextran-silica under these reversed-phase conditions indicates its higher hydrophilicity in comparison with diol-silica prepared from the same starting epoxysilica. The average values of the selectivities obtained for adjacent pairs of *n*-alkanol homologues were 1.61 for diol-silica and 1.12 for dextran-grafted silica. The hydrophobic selectivities for *n*-alkanols of about 1.6 are typical of the hydrophilic brush-type silica-based

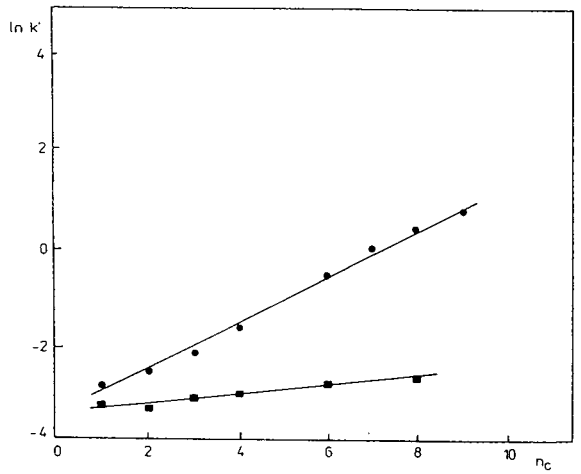

Fig. 3. Dependence of ln k' on carbon number of injected n-alkanols obtained with hydrophilic silica-based sorbents. □ = Dextran-grafted silica SG-d_7; ○ = diol-silica prepared from the same starting epoxysilica. Eluent: redistilled water.

phases for hydrophobic interaction chromatography of proteins and for aqueous SEC and the values well above 3 are typical of reversed-phase materials [20].

The preservation of the pore structure of both diol-silica and AE-dextran-grafted silicas was checked using the SEC calibration graphs for dextran standards (not shown). No significant differences between dextran-grafted, diol-bonded and bare silica gel were observed. Untypical shapes of the SEC calibration graphs were obtained for poly(ethylene oxides) in various eluents [21]. More precise measurements would be necessary to determine the degree of filling of the pore space by swollen dextran grafts.

3.3. Protein HPSEC

Dextran-grafted silica gels which show maximum hydrophilicity and minimum electrostatic interactions with proteins were packed into stainless-steel columns by the optimized slurry method. The protein SEC calibration graph (Fig. 4) obtained with the optimized dextran-grafted macroporous silica gel column is linear over a wide range of relative molecular masses (10^4–10^6) and show virtually no deviation from

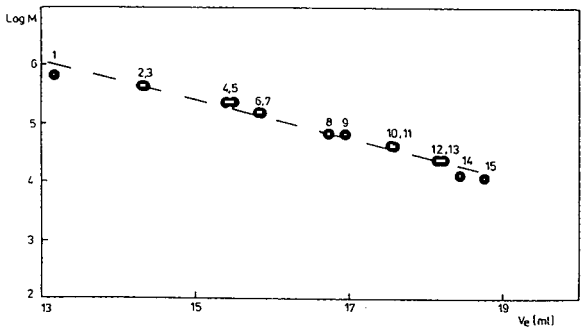

Fig. 4. SEC calibration graph for proteins obtained with a 25 × 0.8 cm I.D. column packed with SG-d_8 sorbent. 1 = TG; 2 = FR-B; 3 = FR-P; 4 = CAT-P; 5 = CAT-B; 6 = ALDO-P; 7 = ALDO-B; 8 = BSA-B; 9 = BSA-P; 10 = OVA-B; 11 = OVA-P; 12 = CHT-B; 13 = CHT-P and CHT-S; 14 = RN; 15 = CYT (abbreviations according the Table 1). Eluents, 1/15 M phosphate buffer (pH 7.0) containing 0.25 mol l^{-1} NaCl; flow-rate 2.0 ml min^{-1} detection at 289 nm.

linearity for both the acidic and basic proteins used in this study.

Fig. 5 shows an example of the SEC separation of a model mixture of proteins to demonstrate the resolving ability of such materials. It seems that the separation performance of the dextran-grafted silica columns is comparable to those obtained with commercially available silica-based stationary phases for protein HPSEC packed in columns of about the same size.

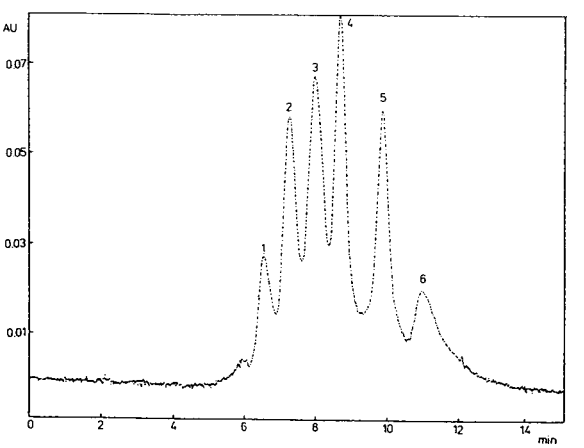

Fig. 5. HPSEC of standard protein mixture on a 50 × 0.8 cm I.D. column packed with SG-d_8 sorbent. Peaks: 1 = TG; 2 = FR-B; 3 = CAT-P; 4 = OVA-P; 5 = CYT-B; 6 = D,L-alanine. Detection at 230 nm; other conditions as in Fig. 4.

The linearity of the protein calibration graphs indicates the suitability of optimized dextran-grafted silicas for the determination of the molecular masses of proteins under appropriate operating conditions. For example, an alkaline proteinase sample obtained form a crude preparation of *Bacillus subtilis* proteinase [22] and soluble antigen from *Coxiella burnetti* propagated in chick embryo [23] were characterized. In both instances good agreement between the relative molecular masses found by polyacrylamide gel electrophoresis ($29.7 \cdot 10^3$ and $17 \cdot 10^3$, respectively) [22,23] and by HPSEC using dextran-grafted silica ($28 \cdot 10^3$ and $18 \cdot 10^3$, respectively) was observed.

4. Conclusions

An effective packing material for aqueous HPSEC was prepared by grafting dextran on to a macroporous silica support. The excellent mechanical stability of silica gel is maintained when the grafting procedure presented is applied. The electrostatic interactions of proteins with dextran-grafted silicas were minimized by combination of three effects: partial removal of silanols by reaction with γ-glycidyloxypropyltrimethoxysilane, steric shielding of residual silanols with grafted dextran macromolecules and electrostatic compensation of SiO^- groups by positively charged moieties introduced on to the dextran macromolecules prior to their immobilization. By grafting dextran on to epoxysilica, many hydroxyl groups are added to the sorbent surface. As a result, the sorbent hydrophilicity is enhanced and undesirable hydrophobic interactions with proteins are minimized. The optimized procedure for the synthesis of dextran-grafted silicas allows the preparation of sorbents showing minimum undesirable interactions with chromatographed proteins over a wide operating range of ionic strengths of the eluent. Well packed dextran-grafted silica columns with linear SEC calibration graphs for proteins have been successfully used as a medium for the HPSEC separation and characterization of proteins.

Dextran-modified solid supports may be successfully used not only in aqueous SEC but also, after additional modification, in ion-exchange [7] or affinity [9,24] chromatography of proteins.

5. Acknowledgements

We thank Dr. Ivan Novák for providing us with silica gel and Dr. Juraj Pavlinec for elemental analyses (both of the Polymer Institute of the Slovak Academy of Sciences, Bratislava, Slovak Republic), Dr. Jan-Christer Janson (Pharmacia, Uppsala, Sweden), Dr. Yoshio Kato (Toyo Soda, Shin-Nanyo, Japan), Dr. Róbert Bezák and Dr. Ladislav Welward (both of Biotika, Slovenská Lupča, Slovak Republic) for kindly providing us with some protein and dextran samples, Dr. Peter Božek (State Hospital, Bratislava, Slovak Republic) for providing us with HPLC equipment for some measurements and Mrs. Jana Tarbajovská for technical assistance.

6. References

[1] K.M. Gooding and F.E. Regnier, in K.M. Gooding and F.E. Regnier (Editors), *HPLC of Biological Macromolecules*, Marcel Dekker, New York, 1990, p. 47.
[2] P.L. Dubin, *Adv. Chromatogr.*, 31 (1992) 119.
[3] F.E. Regnier and R.Noel, *J. Chromatogr. Sci.* 14 (1976) 316.
[4] J. Köhler, *Chromatographia*, 21 (1986) 573.
[5] J. Lecourtier, R. Audebert and C. Quivoron, *J. Liq. Chromatogr.*, 1 (1978) 367.
[6] D. Mislovičová, I. Novák and M. Paštéka, *J. Chromatogr.*, 543 (1991) 9.
[7] J.-L. Tayot, M. Tardy, P. Gattel, R. Plan and M. Roumiantzeff, in R. Epton (Editor), *Hydrophobic, Ion Exchange and Affinity Methods*, Ellis Horwood, Chichester, 1978, p. 95.
[8] X. Santarelli, D. Müller and J. Jozefonvicz, *J. Chromatogr.*, 443 (1988) 55.
[9] F.L. Zhou, D. Müller and J. Jozefonvicz, *J. Chromatogr.*, 510 (1990) 71.
[10] M. Petro and D. Berek, *Chem. Listy*, 86 (1992) 816.
[11] M. Petro and D. Berek, *Chromatographia*, 37 (1993) 549.
[12] E. Pfannkoch, K.C. Lu, F.E. Regnier and H.G. Barth, *J. Chromatogr. Sci.*, 18 (1980) 430.
[13] M. Herold, *Am. Lab.*, 25, No. 4 (1993) 35.
[14] I. Novák and D. Berek, *US Pat.*, 4 382 070 (1983).
[15] P. Gemeiner and A. Breier, *Biotechnol. Bioeng.*, 24 (1982) 2573.

[16] P. Gemeiner and E. Viskupič, *J. Biochem. Biophys. Methods*, 4 (1981) 309.
[17] A.N. Glazer, R.J. DeLange and D.S. Sigman, in T.S. Work and E. Work (Editors), *Laboratory Techniques in Biochemistry and Molecular Biology, Vol. 4, Part I: Chemical Modification of Proteins*, North-Holland, Amsterdam and American Elsevier, New York, 1976, p. 77.
[18] B.V. Plapp, S. Moore and W.H. Stein, *J. Biol. Chem.*, 246 (1971) 939.
[19] J. Hermansson, *J. Chromatogr.*, 269 (1983) 71.
[20] D. Bentrop, J. Kohr and H. Engelhardt, *Chromatographia*, 32 (1991) 171.
[21] M. Petro, *Ph.D. Thesis*, Polymer Institute of Slovak Academy of Sciences, Bratislava, 1993.
[22] P. Gemeiner, V. Špánik, A. Šnajdrová, E. Stratilová, M. Horváthová, D. Hagarová and O. Markovič, *Folia Microbiol.*, 36 (1991) 283.
[23] M. Lukáčová, R. Březina, S. Schrámek and J. Pastorek, *Acta Virol.*, 33 (1989) 75.
[24] D. Mislovičová, M. Petro and D. Berek, *J. Chromatogr.*, 646 (1993) 411.

ELSEVIER

Journal of Chromatography A, 665 (1994) 47–53

JOURNAL OF CHROMATOGRAPHY A

Characterization of ethoxylated fatty alcohols using liquid chromatography with density and refractive index detection II. Quantification in liquid chromatography under critical conditions

B. Trathnigg*[,a], D. Thamer[a], X. Yan[a], B. Maier[a], H.-R. Holzbauer[b], H. Much[b]

[a]*Institute of Organic Chemistry, University of Graz, Graz, Austria*

[b]*Centre of Macromolecular Chemistry, Berlin, Germany*

Abstract

Ethoxylated fatty alcohols can be characterized by two-dimensional liquid chromatography under critical conditions (LCCC) as the first and size-exclusion chromatography as the second dimension. The effect of preferential solvation in LCCC can be eliminated by the use of two universal detectors in both dimensions, which allows a quantitative determination of all fractions as well as the amount of preferentially adsorbed solvent in LCCC.

1. Introduction

In the analysis of ethoxylated fatty alcohols (FAEs), one has to consider that these samples typically consist of different homologous series (depending on the purity of the fatty alcohol used as the starting material), and often also of polyethylene glycols (due to chain transfer to water present in the synthesis).

Hence, a complete characterization of FAEs must provide information on both the distributions of the chain length of the polyoxyethylene and the carbon number of the alkyl group.

This can be achieved using two-dimensional LC, which involves a separation of the homologous series using liquid chromatography under critical conditions (LCCC) [1–4] on a semi-preparative scale as the first dimension, and the analysis of the separated homologous series by size-exclusion chromatography (SEC) [5,6] as the second dimension.

As has been shown in Part I of this series [6], two problems have to be taken into account in the second dimension: (1) the SEC calibrations for the individual homologous series may show considerable differences, hence the individual calibrations should be used for all fractions, and (2) with universal detectors, such as the refractive index (RI) or the density detector, the response factors of FAEs will depend quite strongly on the relative lengths of the alkyl group and the polyether chain [7–9]; this dependence of the response factors on the chemical composition (and molecular mass) can be compensated using different approaches [10]. One of them is also used in this paper.

The molecular mass distribution of oligomers contained in the particular peaks produced under critical conditions can be determined with a good accuracy by the following SEC measurements;

* Corresponding author.

0021-9673/94/$07.00
SSDI 0021-9673(93)E1208-H

however, the amount of oligomers within LCCC peaks is uncertain. Since LCCC is typically performed in mixed eluents (such as methanol–water, acetonitrile–water, acetone–water etc.), preferential solvation [11–16] of the oligomers will take place, which leads to vacancy peaks, when universal (bulk property) detectors are used. If the extent of preferential solvation varies with the oligomer composition or molecular mass, the individual peaks will contain different amounts of preferentially adsorbed solvent.

As we have shown previously [16], the extent of preferential solvation of the repeating units and the end groups can be considerably different even in the cases, where this effect is generally neglected. For FAEs, the amount of solvent preferentially adsorbed by each oligomer will strongly depend on both the relative length of the hydrophobic alkyl group and the hydrophilic polyether chain. Hence, considerable errors may arise in the determination of the mass of the fractions.

In this paper, a method is described which allows an accurate determination of the amount of each particular homologous series using LCCC with dual detection in the first dimension. With SEC as the second dimension, a three-dimensional map of FAEs can be obtained.

2. Theory

2.1. Preferential solvation in LCCC

When a FAE sample is separated according to the length of the alkyl groups by LCCC for polyoxyethylene, each peak will contain a polymer homologous series [with a given end group and an unknown number of ethylene oxide (EO) units] as well as an unknown amount of preferentially adsorbed solvent.

Hence, there are three unknown variables for each peak, namely (1) the amount of the fraction, (2) the composition of the fraction and (3) the amount of preferentially adsorbed solvent.

If preferential solvation can be neglected, the amount and composition of the fraction can be determined from dual detection (density and RI), as is the case in SEC, where single mobile phases are used.

LCCC is, however, typically performed in mixed mobile phases, because critical conditions can seldom be reached in one-component mobile phases.

The determination of all parameters would require a third detection method: this could be UV detection (only for UV-absorbing samples, but not for FAEs or other aliphatic polymers) or evaporative light scattering detection [17]. There is, however, no satisfactory information available about the dependence of its response on composition and molecular mass of oligomers.

If, however, the composition of the fraction is known, one may determine the amount of fraction and preferentially adsorbed solvent with only two detectors. This information can be obtained by analyzing each fraction by SEC with dual detection in the second dimension.

2.2. Quantification in two-dimensional LC with dual detection

The area X of a peak eluting in the first dimension results from the mass m_P of polymer containing the mass fractions w_A and w_B of its components A and B, respectively, the mass m_S of preferentially adsorbed solvent, and the corresponding response factors f_A, f_B and f_S:

$$X = m_P(w_A f_A + w_B f_B) + m_S f_S \quad (1)$$

It must be mentioned that these response factors are the true ones, which are obtained by injecting the samples on the bypass. On the column the zone of "dialyzed solvent" [11] would be separated from the sample peak, thus yielding the apparent response factors [16].

If the response factors f_A and f_B and the mass fractions w_A and w_B are known, one may calculate the average response factor f_{av} of the polymer using

$$f_{av} = w_A f_A + w_B f_B \quad (2)$$

[In the case of FAEs, which consist of the end groups R–and–OH and a polyoxyethylene (PEO) chain without end groups, f_A is the

response factor of the fatty alcohol ROH, and f_B the response factor of high-molecular-mass PEO.]

Hence one may write

$$X = m_P f_{av} + m_S f_S \quad (3)$$

The mass of preferentially adsorbed solvent is given by

$$m_S = \frac{X - m_P f_{av}}{f_S} \quad (4)$$

As the same mass of preferentially adsorbed solvent must appear in both detectors, one may write

$$\frac{X_D - m_P f_{av,D}}{f_{S,D}} = \frac{X_R - m_P f_{av,R}}{f_{S,R}} \quad (5)$$

wherein the indices D and R denote the peak areas and response factors in density and RI detection, respectively. A simple rearrangement of Eq. 5 yields

$$m_P = \frac{X_D f_{S,R} - X_R f_{S,D}}{f_{av,D} f_{S,R} - f_{av,R} f_{S,D}} \quad (6)$$

from which the amount of polymer is easily obtained.

The amount of preferentially adsorbed solvent can be determined using

$$m_S = \frac{X_D f_{av,R} - X_R f_{av,D}}{f_{av,R} f_{S,D} - f_{av,D} f_{S,R}} \quad (7)$$

3. Experimental

The investigations were performed using the density detection system DDS70 (commercially available from A. Paar, Graz, Austria), which has been developed in our group. This instrument has been described in full detail in previous communications [18–20]. In SEC measurements it was combined with a Sicon LCD 201 RI detector, in LCCC with a Bischoff 8110 RI detector.

Each system was connected to a MS-DOS computer via the serial port. Data acquisition and processing was performed using the software package CHROMA [20], which has been developed for the DDS70.

In LCCC, two JASCO 880 PU pumps were used, which were equipped with Rheodyne 7125 injection valves with 50- and a 500-μl loops, respectively.

Reversed-phase LC was performed in methanol and methanol–water mixtures (from Merck, HPLC grade) on two analytical columns and a semi-preparative column filled with Spherisorb from PhaseSep (ODS2 3 μm, 100 × 4.6 mm; ODS2 5 μm, 250 × 4.6 mm; and ODS2 5 μm, 250 × 10 mm, respectively). The flow-rate was 0.5 ml/min in the analytical measurements and 2.0 ml/min in semi-preparative LCCC. An Advantec 2120 fraction collector was used in the semi-preparative separations.

SEC measurements were performed in chloroform (HPLC grade, Rathburn) at a constant flow-rate of 1.0 ml/min, which was maintained by a Gynkotek 300C HPLC pump. Samples were injected using a VICI injection valve equipped with a 100-μl loop, the concentration range was 4–8 g/l. A column set of four Phenogel columns, (2 of 500 Å + 2 of 100 Å, 30 cm each), was used for all separations.

The SEC calibrations were obtained using pure oligomers of EO (from Fluka) and SEC standards from Polymer Labs.

Samples were dissolved in the mobile phase, which was taken from the solvent reservoir using a PTFE tubing connected to a Omnifit valve. In order to minimize evaporation, the solvent bottle was sealed with a PTFE tape. Before samples were injected, the syringe was stored in a flask filled the mobile phase, and rinsed several times with the sample (in order to minimize adsorption effects).

The alkanols, polyoxyethylenes, and FAE (Brij) samples were purchased from Fluka and used without further purification.

Pure homologous series were prepared by anionic ethoxylation [21] of pure 1-alkanols using standard procedures. A monodisperse oligomer was synthesized by a modified Williamson synthesis [22–24] from 1-octylbromide and tetraethylene glycol.

4. Results and discussion

In order to evaluate the performance of this approach, we prepared several pure homologous series by ethoxylation of pure 1-alkanols and a monodisperse oligomer from 1-octylbromide and tetraethylene glycol.

These samples were analyzed by the two-dimensional LC with coupled density and RI detection.

First of all, the critical conditions for polyethylene glycol (PEG) had to be found. As can be seen from Fig. 1, all PEGs eluted at the same elution volume from an ODS2 column in methanol–water (80:20) as a mobile phase.

When samples were injected on the column, they eluted as a narrow peak, and a vacancy peak appeared, the area of which should correspond to the amount of preferentially adsorbed water. As the next step, we determined the true response factors of water, several 1-alkanols and PEG 6000 by injecting them on the bypass. The results thus obtained are shown in Table 1. Using Eqs. 6 and 7, we calculated the amounts of sample and water in each peak. The results thus obtained are given in Table 2.

As can be seen, the calculated sample masses agree very well with the injected sample size, and so do the amounts of water, whether determined from density or RI detection alone or from dual detection using Eq. 7.

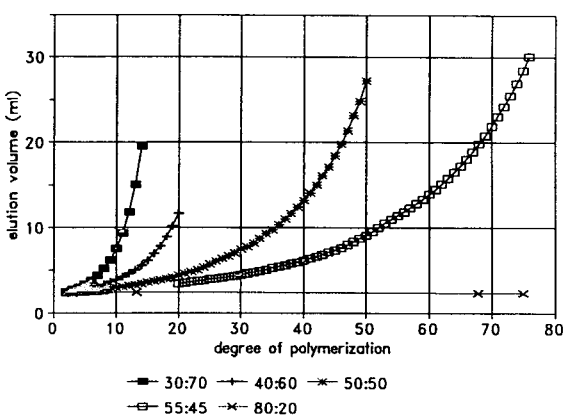

Fig. 1. Elution volumes of polyethylene glycols on ODS2 in methanol–water mixtures as a function of the degree of polymerization.

Table 1
True response factors of water, 1-alkanols and PEGs in density and RI detection, as obtained by injection on bypass

Sample	f (density)	f (RI)
Water	18.44	17.32
1-Octanol	−7.18	63.64
1-Dodecanol	−6.58	70.98
1-Tetradecanol	−6.51	73.76
PEG 6000	18.09	79.05

It should be mentioned that the determination of adsorbed water via the vacancy peak is less reliable than the determination using Eq. 7, because the system peak may also contain moisture from the air or may be influenced by adsorption in the syringe.

In Fig. 2, a chromatogram of monodisperse octyltetraethyleneglycol, as obtained by LCCC, is shown. Obviously preferential solvation occurs, as can be seen from the system peak. The small negative peak in front of the sample peak may be explained by traces of a lower oligomer (di- or trimer).

Fig. 3 shows a chromatogram of an ethoxylated 1-octanol, which contained an average of 5 EO units (determined from the EO uptake). This sample contains also a small amount of PEGs, as can be seen from the peak behind the system peak.

It is remarkable, that the peak of unreacted octanol is separated from the polymer homologous series. This could be explained by the existence of residual silanol groups on the column packing. A systematic study shall show, whether different types of octadecyl columns (silica- or polymer-based) behave in the same way. Moreover the long-term stability of the column packing will be investigated.

Fig. 4 shows a chromatogram of a sample with an average of 10 EO units, in which the amount of PEG is considerably larger, and the octanol peak has disappeared. This is quite reasonable, because with increasing conversion octanol should be consumed.

Table 2
Quantification in LCCC (ODS 2; methanol–water, 80:20)

Sample	Sample size (μg)	Sample from Eq. 6	Water (μg) vacancy peak		Water (μg) from Eq. 7
			Density	RI	
PEG 6000	197.0	193.3	82.0	79.0	78.2
1-Octanol	457.0	458.3	90.8	86.5	72.9

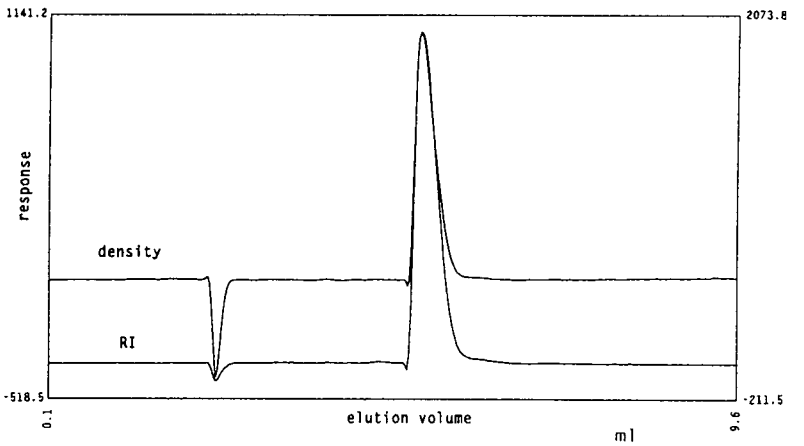

Fig. 2. Chromatogram of the monooctyltetraethylene glycol on ODS2 in methanol–water (80:20, w/w).

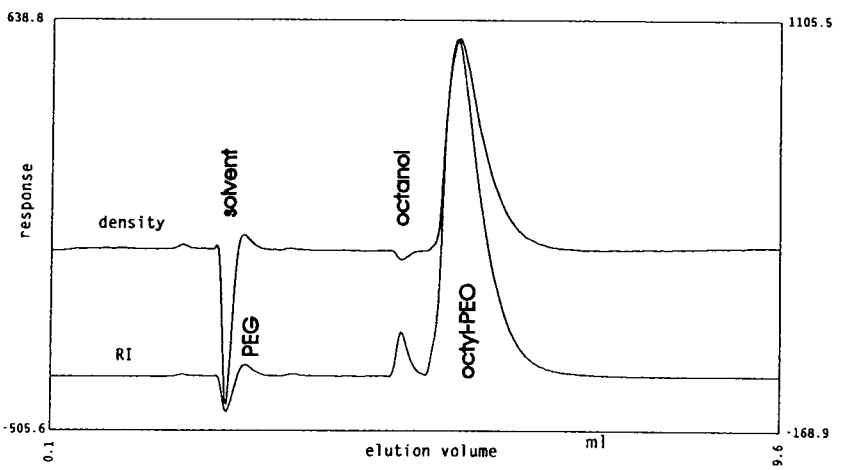

Fig. 3. Chromatogram of the ethoxylated 1-octanol with an average of 5 EO units, as obtained on ODS2 in methanol–water (80:20, w/w).

The fractions from these chromatograms were analyzed by SEC with density and RI detection, as has already been described in Part I of this series [6].

With the mass fraction of the ethylene oxide chain thus obtained we calculated the mass of polymer present in each peak in LCCC, as can be seen from Table 3.

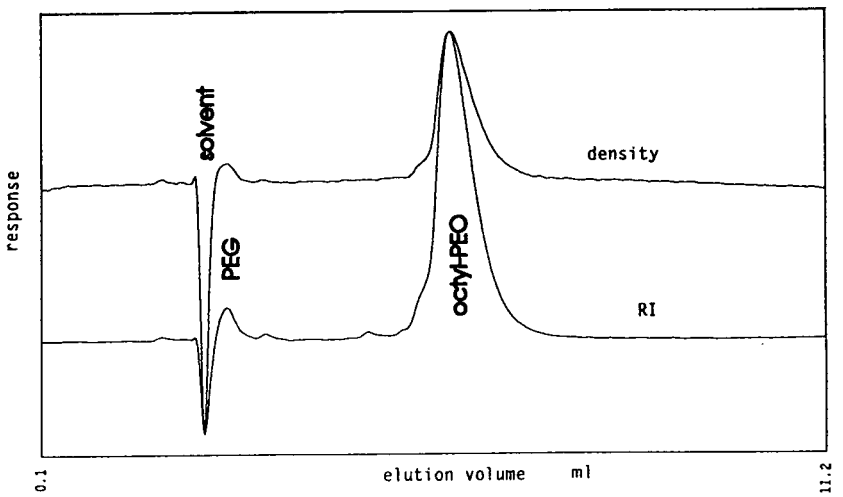

Fig. 4. Chromatogram of the ethoxylated 1-octanol with an average of 10 EO units, as obtained on ODS2 in methanol–water (80:20, w/w).

As can be seeen, the sum of the calculated masses agrees very well with the injected sample size.

5. Conclusions

Two-dimensional chromatography with LCCC as the first dimension and with SEC as the second dimension provide an excellent tool for the characterization of polymers. A quantitatively correct three-dimensional map requires, however, an accurate determination of the amount of each fraction in the first dimension. This can be achieved by using a combination of density and RI detector in both dimensions. The three important parameters for each peak in LCCC (the mass of the polymer fraction, its composition and the amount of preferentially adsorbed solvent) can be determined from the corresponding peak areas from both detectors and the average mass fractions of the components (from SEC with dual detection).

Table 3
Masses of the fractions obtained from LCCC of monooctyl-PEGs, as determined using Eq. 6

Sample	Mass (μg)		
	R_8EO_4	R_8EO_5	R_8EO_{10}
PEG	0.0	4.8	6.6
Octanol	0.0	26.0	0.0
Octyl-PEG	555.7	462.5	160.3
Sum	555.7	493.4	166.8
True sample size	549.0	489.0	176.0

6. Acknowledgement

Financial support from the Austrian Science Foundation (Project-Nr.8253 CHE) is gratefully acknowledged.

7. References

[1] B.G. Belenkii, E.S. Gankina, M.B. Tennikov and L.Z. Vilenchik, *J. Chromatogr.*, 147 (1978) 99.
[2] A.V. Gorshkov, H. Much, H. Becker, H. Pasch, V.V. Evreinov and S.G. Entelis, *J. Chromatogr.*, 523 (1990) 91.
[3] G. Schulz, H. Much, H. Krüger and C. Wehrstedt, *J. Liq. Chromatogr.*, 13 (1990) 1745.
[4] H. Pasch, H. Krüger, H. Much and U. Just, *J. Chromatogr.*, 589 (1992) 295.
[5] W. Heitz, B. Bohmer and H. Ullner, *Makromol. Chem.*, 121 (1969) 102.

[6] B. Trathnigg, D. Thamer, X. Yan, B. Maier, H.-R. Holzbauer and H. Much, *J. Chromatogr. A*, 657 (1993) 365.
[7] M. Coupkova, K. Janes, J. Sanitrak and J. Coupek, *J. Chromatogr.*, 160 (1978) 73.
[8] I. Géczy, *Tenside Deterg.*, 9 (1972) 117.
[9] I. Géczy, *Acta Chim. Acad. Sci. Hung.*, 79 (1973) 133.
[10] B. Trathnigg and X. Yan, *J. Appl. Polym. Sci., Appl. Polym. Symp.*, 52 (1993) 193.
[11] D. Berek, T. Bleha and Z. Pevna, *J. Polym. Sci., Polym. Lett. Ed.*, 14 (1976) 323.
[12] D. Berek, T. Bleha and Z. Pevna, *J. Chromatogr. Sci.*, 14 (1976) 560.
[13] I. Katime and C. Strazielle, *Makromol. Chem.*, 178 (1977) 2295.
[14] T. Spychaj, D. Lath and D. Berek, *Polymer*, 20 (1979) 437.
[15] T. Spychaj and D. Berek, *Polymer*, 20 (1979) 1109.
[16] B. Trathnigg and X. Yan, *J. Chromatogr. A*, 653 (1993) 199.
[17] Y. Mengerink, H.C.J. de Man and Sj. van der Wal, *J. Chromatogr.*, 552 (1991) 593.
[18] B. Trathnigg and Ch. Jorde, *J. Chromatogr.*, 385 (1987) 17.
[19] B. Trathnigg, Ch. Jorde and B. Maier, *Chromatogr. Anal.*, June (1989) 13.
[20] B. Trathnigg, *GIT Fachz. Lab.*, 35 (1991) 35.
[21] W. Beithan, H. Bernasch and W. Gerhardt, *Tenside Deterg.*, 19 (1982) 206.
[22] W. Gerhardt and H.-R. Holzbauer, *Tenside Deterg.*, 12 (1975) 313.
[23] W. Gerhardt and H.-R. Holzbauer, *Tenside Deterg.*, 14 (1977) 116.
[24] H.-R. Holzbauer, A. Greiner and M. Herbst, *Tenside Deterg.*, 20 (1986) 30.

ELSEVIER

Journal of Chromatography A, 665 (1994) 55–58

JOURNAL OF CHROMATOGRAPHY A

Dynamics of production of organic acids during lactic fermentation of vegetable juice

J. Karovičová, M. Drdák, J. Polonský*, A. Rajniaková

Faculty of Chemical Technology, Slovak Technical University, Radlinského 9, 812 37 Bratislava, Slovak Republic

Abstract

Strains of *Lactobacillus* were tested on prepared samples of cabbage and carrot juice mixture. The determination of phosphoric, citric, lactic, succinic and acetic acid was carried out after 40, 64, 136, 184 and 232 h of fermentation by capillary isotachophoresis. *L. plantarum* (190/86) produced the best sensoric values of fermented vegetable juices.

1. Introduction

The popularity of vegetable juices produced by lactic fermentation is growing because they represent a new type of drink and because of their high nutritive value, with a high content of vitamins and minerals [1]. They are sold either non-fermented or fermented. Because of the variety of materials used in their production, no generally used technology exists; the production method depends not only on the kind of material used, but also on the desired properties of the products [2–4]. Vegetable juices produced by lactic fermentation do not have salt or spices added, so they are suitable for dietetic use [5,6].

Enzymatic treatment of mashes can be done together with lactic fermentation, according to some workers [5,7,8]. It is stated that the best results were achieved by using *Lactobacillus plantarum* as a starting culture. From the nutritive point of view, the content of lactic acid in lactic-fermented juices is of interest [9,10].

The detection of individual acids in various food products is now carried out mostly by chromatographic methods, gas chromatography [11] and high-performance liquid chromatography [12] being the most widely used. However, the complete chromatographic separation of organic acids is not easily achieved, and the methods are time consuming and involve complex sample preparation. Organic acids in aqueous alcohols have been determined using zone electrophoresis [13]. Capillary isotachophoresis has been found suitable for the identification and determination of organic acids in foods [14–16].

In this work, we prepared a mixture of cabbage and carrot juice, fermented it and measured the organic acids produced with the application of selected microorganisms by capillary isotachophoresis.

2. Experimental

2.1. Preparation of cabbage and carrot juice samples and their fermentation

Cabbage and carrot juice were mixed in the

* Corresponding author.

0021-9673/94/$07.00
SSDI 0021-9673(93)E1053-3

proportions of 2:1, 3% of D-glucose was added and the salt concentration was adjusted to 1.5%. The juice mixture was placed in flasks and sterilized for 10 min at 121°C. L-Ascorbic acid and thiamine dichloride were added and pure cultures of lactic bacteria were inoculated. The samples were cultivated at 30°C.

2.2. Chemicals

The chemicals were of analytical-reagent grade. Standards of organic acids (here considered to include used phosphoric acid) and HCl were obtained from Lachema (Brno, Czech Republic), methylhydroxyethylcellulose (MHEC) and ε-aminocaproic acid from Serva (Heidelberg, Germany) and histidine from Sigma (St. Louis, MO, USA). Doubly distilled water was passed through a deionizer before use.

2.3. Equipment

A ZKI 01 isotachophoretic analyser (Labeco, Spišská Nová Ves, Slovak Republic) with standard columns and a conductivity detector and a TZ 4200 double-line recorder (Laboratorní Přístroje, Prague, Czech Republic) were used. An M-120 pH meter (Mikrotechnika, Prague, Czech Republic) was employed.

2.4. Electrolyte system for separation

For the identification and determination of organic acids the electrolyte system applied had the following composition: concentration of leading electrolye, 0.01 *M* HCl; counter ion, ε-aminocaproic acid, pH 4.5; additive, methylhydroxyethylcellulose (0.1%); and terminating electrolyte, $5 \cdot 10^{-5}$ *M* caproic acid–$5 \cdot 10^{-3}$ *M* histidine (pH 4–5).

2.5. Measurement procedure

Prior to isotachophoretic measurement of organic acids, samples of the fermented mixture of cabbage and carrot juice were filtered and diluted 1:25 with water. The samples were injected into the column using the four valves of the instrument. The samples of juices were analysed at a driving current of 250 μA in the preseparation column and 40 μA in the analytical column. Quantitative analysis was performed by calibration. Based on the presumed presence of the individual organic acids, standard solutions of

Table I
Organic acids in mixture of cabbage and carrot juice

Microorganism	Fermentation time (h)	Organic acid (g l^{-1})				
		Phosphoric	Citric	Lactic	Succinic	Acetic
–	Day zero	1.03	0.78	0.25	0.38	–
L. plantarum (189/86)	40	0.62	2.69	8.23	0.23	0.37
	64	–	1.39	12.90	0.71	0.36
	136	–	3.24	11.78	0.70	0.13
	184	–	1.75	11.96	0.36	0.55
	232	–	1.11	12.43	0.31	0.28
L. plantarum (190/86)	40	–	1.06	6.96	1.61	1.71
	64	–	0.80	8.48	1.49	1.76
	136	–	2.54	8.56	–	0.85
	184	–	1.23	11.28	0.89	2.08
	232	–	2.01	7.23	0.86	1.23
L. delbrückii (237/86)	40	0.59	2.22	0.59	–	–
	64	–	1.33	8.31	0.73	0.94
	136	–	1.16	7.94	0.52	0.23
	184	–	0.36	12.36	0.77	3.11
	232	–	2.01	7.23	0.86	1.23

lactic, acetic, citric, phosphoric and succinic acid of concentration 0.01 *M* were prepared.

3. Results and discussion

Samples of cabbage and carrot juice mixture were analysed on day zero before fermentation by capillary isotachophoresis and the concentrations of phosphoric, citric, lactic, succinic and acetic acid was determined. Various strains of microorganisms were applied to the prepared juice and the results of fermentation was observed after 7 days. Not only the concentrations of the individual organic acids, but also results of the determination of pH, titration acidity, decrease in reducing sugar and utilization of nitrates served for the selection of the microorganisms. On the basis of these results, we used only *Lactobacillus plantarum* (189/86), *L. plantarum* (190/86) and *L. delbrückii* (237/86) for further experiments.

Samples fermented with the selected microorganisms were analysed at set time intervals. The time intervals chosen for sampling and the results of isotachophoretic analyses were used to determine the time of maximum production of lactic acid and also of the production of acetic acid by the tested microorganism and for demonstrating its suitability for the production of fermented juices.

Isotachophoretic analyses for the determination of phosphoric, citric, lactic, succinic and acetic acid were carried out after 40, 64, 136, 184 and 232 h of fermentation. Table I gives the concentrations of organic acids in the mixture of cabbage and carrot juice on day zero and after fermentation with *L. plantarum* (189/86), *L. plantarum* (190/86) and *L. delbrückii* (237/86). The individual data are average values calculated from three measurements. Fig. 1 shows the analysis of cabbage and carrot juice mixture fermented with *L. plantarum* (189/86).

From the results for lactic acid production in Table I, it is obvious that the greatest increase, from the starting value of 0.25 g l^{-1} to 12.90 g l^{-1}, occurred in the sample with *L. plantarum* (189/86) after 64 h of fermentation. After 136 h there was a decrease and then a slight increase. Production of acetic by this microorganism increased to 0.53 g l^{-1} after 184 h of fermentation and subsequently decreased.

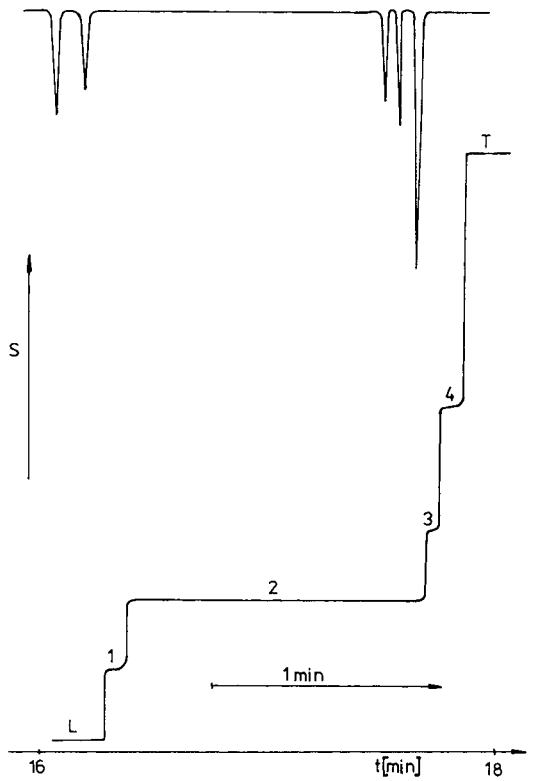

Fig. 1. Isotachophoreogram of organic acids in a sample cabbage and carrot juice mixture fermented with *L. plantarum* (189/86) for 64 h. *S* = Response of conductivity detector; L = leading electrolyte; T = terminating electrolyte; 1 = citric acid; 2 = lactic acid; 3 = succinic acid; 4 = acetic acid.

With *L. plantarum* (190/86), lactic acid production reached the maximum value of 11.28 g l^{-1} after 184 h of fermentation, then decreased. The acetic acid content also reached its maximum value of 2.08 g l^{-1} after 184 h.

L. delbrückii (237/86) gave a maximum production lactic acid of 12.37 g l^{-1} and of acetic acid of 3.11 g l^{-1} both after 184 h of fermentation.

The content of citric acid varied in the individual samples. The maximum content of 3.24

g l^{-1} occurred in the sample fermented with *L. plantarum* (189/86) for 136 h.

From the results, it is clear that *L. plantarum* (189/86) was the most suitable microorganism for lactic acid production because it produced this acid the most rapidly. However, *L. plantarum* (190/86) produced the best sensoric values of fermented vegetable juices because the concentration of acetic acid produced gave a very good taste.

For the determination of organic acids in individual fermented samples, the standard deviations, s_x [12], were as follows: phosphoric acid, 0.014–0.018; citric acid, 0.025–0.053; lactic acid, 0.016–0.042; succinic acid, 0.032–0.030; and acetic acid, 0.017–0.070 g l^{-1}. The relative standard deviations, s_r, were 0.35–1.87%.

Fig. 2 shows the changes in lactic acid content produced by fermentation with the individual microorganisms.

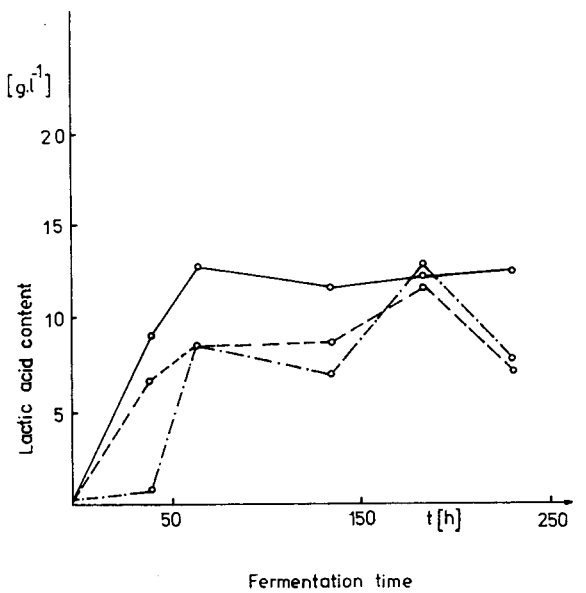

Fig. 2. Changes in lactic acid content during fermentation of cabbage and carrot juice mixture by individual microorganisms. ———, *L. plantarum* (189/86); – – – – –, *L. plantarum* (190/86); – · – · –, *L. delbrückii* (237/86).

In conclusion, the application of isotachophoresis for the determination of organic acids is very advantageous. From the results of organic acid determination, a rapid choice of suitable microorganisms for further experiments is possible. Capillary isotachophoresis was selected as a suitable method for the determination of organic acids on the basis of its useful properties (simple sample preparation, rapid determination and good reproducibility).

4. References

[1] H. Buckenhüskes, M. Schneider and W.P. Hammes, *Chem. Microbiol. Technol. Lebensm.*, 10 (1986) 42.
[2] R.E. Andersson, C.E. Eriksson, A.C. Salomonsson and O. Theander, *Lebensm.-Wiss. Technol.*, 23 (1990) 34.
[3] H.U. Liepe and M. Junker, *Ind. Gemüseverw.*, 68 (1983) 319.
[4] H. Buckenhüskes and K. Gierschner, *Flüss. Obst*, 56 (1989) 751.
[5] D. Šulc, *Flüss. Obst*, 51 (1984) 17.
[6] H.U. Liepe, personal communication, 1984.
[7] Ph. Possmann and C. Sprinz, *Confructa Stud.*, 30 (1986) 24.
[8] K. Zatelaki-Horvath and R. Andersson, *Acta Aliment.*, 15 (1986) 265.
[9] C.H. Holten, *Lactic Acid*, Verlag Chemie, Weinheim, 1971.
[10] M. Plocková and P. Březina, *Průmy. Potravin*, 12 (1984) 648.
[11] M.J. Barcelona, H.M. Liljestrand and J.J. Morgan, *Anal. Chem.*, 52 (1980) 321.
[12] N.E. Bussele and R.A. Miller, *J. Liq. Chromatogr.*, 2 (1979) 697.
[13] V. Jokl, V. Doješová and M. Matušová, *J. Chromatogr.*, 172 (1979) 239.
[14] Z. Stránsky, P. Peč, M. Kudlová, M. Mergl and J. Žabková, *Živočíšna Výroba*, 33 (1988) 211.
[15] W. Nierle, *Getreide Mehl Brot*, 42 (1988) 138.
[16] J. Karovičová, J. Polonský, M. Drdák, P. Šimko and V. Vollek, *J. Chromatogr.*, 638 (1993) 241.
[17] K. Eckschlager, I. Horsák and Z. Kodejš, *Vyhodnocovaní Analytických Výsledků a Metod*, SNTL, Prague, 1980, p. 224.

ELSEVIER

Journal of Chromatography A, 665 (1994) 59–65

JOURNAL OF CHROMATOGRAPHY A

Reversed-phase high-performance liquid chromatography of diastereomers of some phosphonodipeptides

David Sýkora*[,a], Ivan Vinš[a], Petr Hermann[b], František Kesner[b]

[a]*Tessek Ltd., Stránčická 33, 100 00 Prague 10, Czech Republic*

[b]*Faculty of Science, Department of Inorganic Chemistry, Charles University, Albertov 2030, 128 40 Prague 2, Czech Republic*

Abstract

The separation of diastereomers of four phosphonodipeptides, derivatives of 1-aminoethanephosphonic acid (AEP), was studied on different reversed-phase sorbents. The influence of the sorbent character and mobile phase composition on the retention was investigated. It was found out that the capacity factors of the *S,R* and *S,S* diastereomers were considerably different and strongly dependent on the hydrophobicity of the stationary phase. The capacity factors of both diastereomers were influenced by pH and the presence of a cation in the mobile phase in a certain pH range. All the above facts are closely connected with the dissociation constants and conformations of the phosphonodipeptides. An explanation of observed behaviour of the compounds studied is proposed.

1. Introduction

Aminophosphonic acids (**I**) and phosphonodipeptides (PDs) (**II**) differ from naturally occurring amino acids and dipeptides by the replacement of the carboxylic moiety with a phosphonic group ($-PO_3H_2$):

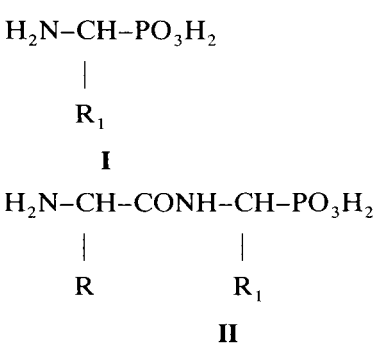

I

II

This class of compounds shows promising biological activity [1–6]. PDs containing P-terminal aminoalkylphosphonic acids have shown bacteriostatic [1,7] and herbicidal [8] effects.

PDs synthesized from optically pure amino acids can exist as four isomers, divided into two pairs. The *S,R* (L,L) and *R,S* (D,D) isomers are optically active isomers, whereas the *S,S* (L,D) and *R,R* (D,L) isomers are *meso* isomers. The members of each pair are enantiomeric and the two pairs are diastereomeric. It is well known that physico-chemical properties of diastereomers of PDs are different and, consequently, the fates of these isomers in organisms also differ considerably as well. Many of PDs have not been thoroughly studied.

The first step necessary in studying diastereomers of PDs with known absolute structure is the synthesis of the compounds of interest in a pure form. There are many methods for the preparation of PDs [9]. Unless an optically active aminoalkylphosphonic acid is used as a starting material for the reactions, a mixture of diastereomers

* Corresponding author.

0021-9673/94/$07.00
SSDI 0021-9673(93)E1183-Z

of PDs is obtained that has to be separated in the next step. For this purpose, separation methods [10] such as crystallization, precipitation or chromatography are frequently used.

The aim of this work was to verify a method for the separation of diastereomers of PDs by reversed-phase high-performance liquid chromatography (RP-HPLC) [11] and to study the influence of the stationary phase character and mobile phase composition on the chromatographic behaviour of four different diastereomers, derivatives of 1-aminoethanephosphonic acid (AEP).

2. Experimental

2.1. Chromatographic conditions

The experiments were performed on an Knauer (Bad Homburg, Germany) liquid chromatographic system consisting of a Model 64 HPLC pump, a Rheodyne (Cotati, CA, USA) Model 7125 injection valve with a 20-μl sample loop and an UV–Vis spectrophotometer (Knauer). The results were processed on a Model 700 chromatography workstation (Bio-Rad Labs., Richmond, CA, USA). CGC compact glass columns (3.3 mm × 150 mm I.D.) (Tessek, Prague, Czech Republic) were packed by the slurry method in the laboratory. The sorbents used are listed in Table 1. Samples of the phosphonodipeptides were prepared by dissolution of a mixture of the respective diastereomers in the eluent at a concentration of 0.5 mg/ml of each diastereomer. The mobile phase compositions are indicated in the text and figure captions. The flow-rate was 0.5 ml/min and detection was at 225 nm.

The capacity factors were calculated as an average from three runs; the relative standard deviation was better then 5%. As a dead volume the refractive index disturbance caused by injection of water into methanol–water (70:30) eluent was used.

2.2. Materials

The PDs were prepared as described elsewhere [12]. Four PDs were used: (1) N-(*S*)-alanyl-(*S*,*R*)-AEP (*S*-Ala-*S*,*R*-AEP), (2) N-(*S*)-methionyl-(*S*,*R*)-AEP (*S*-Met-*S*,*R*-AEP), (3) N-(*S*)-leucyl-(*S*,*R*)-AEP (*S*-Leu-*S*,*R*-AEP) and (4) N-(*S*)-phenylalanyl-(*S*,*R*)-AEP (*S*-Phe-*S*,*R*-AEP). Orthophosphoric acid and sodium hydroxide (both from Lachema, Brno, Czech Republic), ammonia solution (Odzynninki Chemizcne, Lublin, Poland), dimethylamine (DMA) and diethylamine (DEA) (both from Merck, Darmstadt, Germany) were of analytical-reagent grade. Water was redistilled and filtered through a 0.45-μm membrane filtered (Schleicher & Schüll, Dassel, Germany).

3. Results and discussion

The influence of the stationary phase on the separation of PDs by RP-HPLC was studied using silica-based sorbents with different functional groups. The mobile phase used in these experiments was 10 m*M* orthophosphoric acid adjusted with ammonia solution to pH 3–7.

The hydrophobicity of the stationary phases based on the retention of an aromatic solute (*e.g.*, toluene) increased in the order SGX Phenyl < SGX C_8 < SGX C_{18}. The hydrophobicity of PDs (assumed from the hydrophobicity of the corresponding amino acids [13]) increased in the order *S*-Ala-*S*,*R*-AEP < *S*-Met-*S*,*R*-AEP < *S*-Leu-*S*,*R*-AEP < *S*-Phe-*S*,*R*-AEP. The retention behaviour of the four PDs confirmed the main role of hydrophobic interactions in the separation, as shown in Table 2. The results confirmed that the retention of the PDs increased in the order SGX Phenyl < SGX C_8 < SGX C_{18} and also with increasing hydrophobicity of the PDs. Addition of methanol to the mobile phase led to a decrease in the capacity factors of the PDs whereas the use 2.0 *M* ammonium sulphate as the mobile phase considerably increased the capacity factors of all the PDs. It is important to stress that both diastereomers of PDs are influenced to similar extents by changes in the eluent composition.

A very good separation of diastereomers of the four PDs confirmed the published results [11] (Fig. 1). The separation of diastereomers of PDs on the reversed-phase sorbents may be explained

Table 1
Reversed-phase sorbents used for experiments

Sorbent	Matrix	Bonded group	Particle size (μm)	Pore diameter (nm)	Efficiency[c] (theoretical plates)
Tessek[a] Separon SGX Phenyl	Silica	Phenyl	7	8	6000
Tessek Separon SGX C_8	Silica	Octyl	7	8	6400
Tessek Separon SGX C_{18}	Silica	Octadecyl	7	8	6400
Tessek Separon HEMA-BIO 1000 C_{18}	Hydroxyethyl methacrylate	Octadecyl	10	30	3000
Tessek Separon EDMA 2000	Ethylene dimethacrylate	None	7	>30	700
Serva[b] Octadecyl-Si 100	Silica	Octadecyl	10	10	4800

[a] Tessek, Prague, Czech Republic.
[b] Serva, Heidelberg, Germany.
[c] The efficiency (plate number, N) was determined for cGC columns (150 × 3 mm I.D.) for toluene as the solute and methanol–water (70:30) as the eluent at a flow-rate 0.5 ml/min. The equation used for calculation was $N = (t_R/w_{1/2})^2 \cdot 5.545$, where t_R = retention time of toluene and $w_{1/2}$ = toluene peak width at half-height.

Table 2
Capacity factors (k) of *S,S* diastereomers and resolution (R_s) for *S,R* and *S,S* diastereomers of the studied PDs on SGX Phenyl, SGX C_8 and SGX C_{18} columns with different compositions of the mobile phase

Phosphonodipeptide	Mobile phase composition	pH	Capacity factor of *S,S* diastereomer (k)			Resolution (R_s)		
			SGX Phenyl	SGX C_8	SGX C_{18}	SGX Phenyl	SGX C_8	SGX C_{18}
S-Ala-*S,R*-AEP	10 m*M* H_3PO_4–MeOH (9:1)	7.0	−0.09	−0.08	−0.05	0.07	0.14	0.21
	10 m*M* H_3PO_4	7.0	−0.08	−0.03	−0.07	0.20	0.57	0.54
	10 m*M* H_3PO_4	6.0	0.04	0.12	0.19	0.49	1.05	1.15
	10 m*M* H_3PO_4	5.0	0.10	0.19	0.24	0.66	1.44	1.40
	10 m*M* H_3PO_4	4.0	0.11	0.19	0.23	0.65	1.80	1.70
	10 m*M* H_3PO_4	3.0	0.10	0.19	0.21	0.70	1.61	1.49
	2 *M* $(NH_4)_2SO_4$	5.6	0.39	0.73	0.86	2.55	3.63	2.77
S-Met-*S,R*-AEP	10 m*M* H_3PO_4–MeOH (9:1)	7.0	0.09	0.20	0.37	0.67	1.65	1.10
	10 m*M* H_3PO_4	7.0	0.19	0.76	1.79	0.90	2.94	2.83
	10 m*M* H_3PO_4	6.0	0.63	1.63	3.14	2.24	6.60	6.82
	10 m*M* H_3PO_4	5.0	0.82	1.95	3.64	3.09	7.55	9.68
	10 m*M* H_2PO_4	4.0	0.83	1.96	3.59	2.81	9.67	8.69
	10 m*M* H_3PO_4	3.0	0.81	1.95	3.45	3.40	10.20	8.68
	2 *M* $(NH_4)_2SO_4$	5.6	4.53	10.93	20.58	6.27	12.25	10.26
S-Leu-*S,R*-AEP	10 m*M* H_3PO_4–MeOH (9:1)	7.0	0.16	0.53	1.00	1.16	3.00	2.43
	10 m*M* H_3PO_4	7.0	0.33	1.95	3.97	1.35	6.92	4.72
	10 m*M* H_3PO_4	6.0	0.87	3.79	7.21	3.26	12.56	11.66
	10 m*M* H_3PO_4	5.0	1.11	4.81	8.67	4.51	15.66	14.25
	10 m*M* H_3PO_4	4.0	1.13	4.76	8.43	5.03	15.12	12.26
	10 m*M* H_3PO_4	3.0	1.15	4.73	8.43	5.60	15.02	12.21
	2 *M* $(NH_4)_2SO_4$	5.6	7.74	32.20	62.02	8.91	17.64	12.22
S-Phe-*S,R*-AEP	10 m*M* H_3PO_4–MeOH (9:1)	7.0	0.73	1.25	2.66	2.11	3.26	2.37
	10 m*M* H_3PO_4	7.0	1.30	4.44	12.69	2.19	7.83	6.29
	10 m*M* H_3PO_4	6.0	2.77	9.16	21.82	5.53	13.84	10.73
	10 m*M* H_3PO_4	5.0	3.39	11.11	24.83	6.73	15.53	15.17
	10 m*M* H_3PO_4	4.0	3.39	11.13	24.36	7.06	15.34	13.05
	10 m*M* H_3PO_4	3.0	3.35	10.73	23.06	7.32	15.40	10.31
	2 *M* $(NH_4)_2SO_4$	5.6	19.8	–	–	9.39	–	–

Adjustments of pH were made with ammonia solution. The capacity factor was calculated according the equation $k = (t_{R_2} - t_0)/t_0$, where t_{R_2} = retention time of *S,S* diastereomer and t_0 = dead time of column; and resolution $R_s = 2 \cdot (t_{R_2} - t_{R_1})/(w_{R_2} + w_{R_1})$, where t_{R_2} = retention time of *S,S* diastereomer, t_{R_1} = retention time of *S,R* diastereomer, w_{R_2} = peak width of component 2 and w_{R_1} = peak width of component 1.

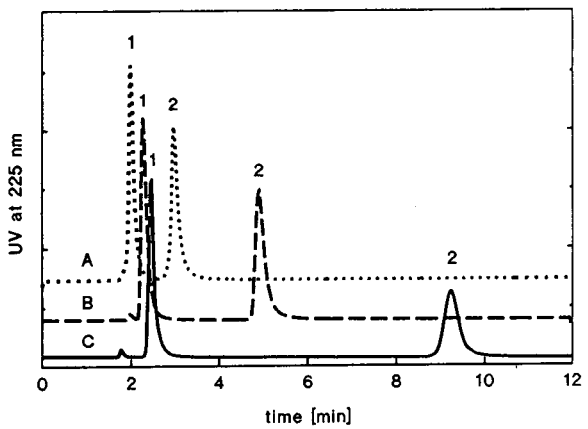

Fig. 1. Chromatograms of diastereomers of *S*-Met-*S*,*R*-AEP on cGC columns (150 × 3 mm I.D.): (C) SGX C_{18}, 7 μm (——), (B) SGX C_8, 7 μm (– – –) and (A) SGX Phenyl, 7 μm (· · · · · ·). Mobile phase 10 m*M* orthophosphoric acid adjusted with ammonia solution to pH 4.0; flow-rate, 0.5 ml/min; detection, UV at 225 nm. Peaks: 1 = *S*,*R* diastereomer; 2 = *S*,*S* diastereomer.

by their different absolute structures. The *S*,*S* diastereomer can probably fold more easily than the *S*,*R* diastereomer [14]. In the folded conformation of a zwitterion the oppositely charged $-NH_3^+$ and $-PO_3H^-$ groups are nearer in the case of *S*,*S* diastereomers, which leads to a higher stabilization of this isomer. On the basis of ref. 14, tentative structures of *S*,*R* and *S*,*S* phosphonodipeptides in aqueous solution [15] are suggested in Fig. 2.

For all the PDs tested, the *S*,*S* diastereomers were more strongly retained than the *S*,*R* diastereomers. From the proposed structure it can be seen that in the *S*,*S* diastereomer both hydrophobic side-chains are closer to each other than in the *S*,*R* diastereomer. The plane of the peptidic bond divides the molecule into two halves. The hydrophilic charged part of the *S*,*S* diastereomer is located under the plane and the two hydrophobic chains are spread above the plane. The space under and above the plane is evenly filled with charge and hydrophobic arms, respectively. This conformation is better suited for an interaction with the hydrophobic surface of a reversed-phase sorbent. In contrast, in the *S*,*R* diastereomer the hydrophobic chains are oriented oppositely to each other, and this orientation is less suitable for interactions with the sorbent.

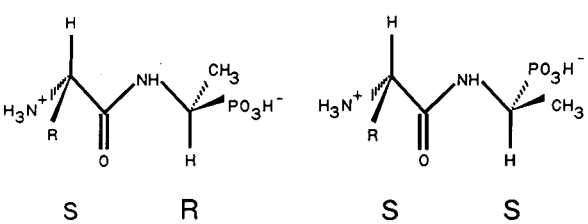

Fig. 2. Tentative structures of *S*,*R*- and *S*,*S*-phosphonodipeptides in aqueous solution.

Changes in the pH of mobile phase in the range 3–7 did not influence significantly the retention times of the *S*,*R* diastereomers, but above pH 5 a considerable decrease in the retention times of the *S*,*S* diastaereomers was observed. These dependences were very similar for all the PDs (Fig. 3). This behaviour can be explained on the basis of the dissociation constants of PDs; an example for *S*-Met-*S*,*R*-AEP [15] is presented in Table 3. As was mentioned above, the *S*,*S* diastereomers have a very stable structure if they exist in the form of neutral zwitterions, which according to the distribution diagram [15] exist in the pH range 3–5. An increase in pH above 5 leads first to the dissociation of the second proton from the phosphonic group and above pH 7 to the loss of a proton from the amino group. These processes are accompanied by a decrease in conformational

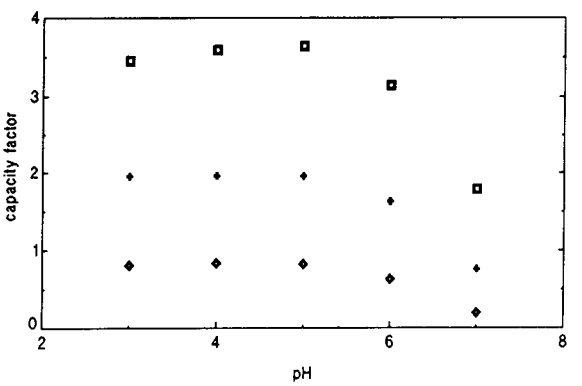

Fig. 3. Dependences of capacity factors for *S*,*S*-Met-AEP diastereomer of *S*-Met-*S*,*R*-AEP on mobile phase pH. Sorbents used: ◇ = SGX Phenyl; + = SGX C_8; □ = SGX C_{18}. Mobile phase, 10 m*M* orthophosphoric acid with pH adjusted with ammonia solution.

Table 3
pK_a values for *S*-Met-*S*,*R*-AEP

pK_a	*S*,*R*-Met-AEP	*S*,*S*-Met-AEP
p$K(NH_3^+)$	7.44	7.86
p$K(PO_3H^-)$	6.61	6.22
p$K(PO_3H_2)$	1.4	1.1

stability of the *S*,*S* diastereomer, resulting in a decrease in the capacity factors of all the *S*,*S* diastereomers studied at pH > 5. The *S*,*R* diastereomers are generally retained on reversed phases much more weakly than the *S*,*S* diastereomers even at pH 3–5, and therefore the effect of pH changes on the retention is less predictable and, as shown by the experimental results, much less pronounced.

The influence of the cation in the mobile phase on the separation and the retention times of PDs was also studied. For that purpose the pH of 10 m*M* orthophosphoric acid was adjusted in the range 3–8 with ammonia solution, sodium hydroxide, dimethylamine (DMA) and diethylamine (DEA). These dependences are very close for the three more hydrophobic PDs, and small differences can be seen only with *S*-Ala-*S*,*R*-AEP. The results obtained with *S*-Ala-*S*,*R*-AEP and *S*-Leu-*S*,*R*-AEP on SGX C_{18} are shown in Figs. 4 and 5. As expected, in the pH range 3–5 there is little influence of the cation in the mobile phase on the capacity factors of neutral zwitterions of PDs. At pH >5 the presence of DMA or DEA in the mobile phase leads to an increase in the retention times of both diastereomers of PDs in comparison with sodium hydroxide. The observed effect was stronger for DEA than for DMA. The negatively charged PDs will probably form ion pairs with hydrophobic cations at pH> 5. The retention increases in the order of increasing cation hydrophobicity, *i.e.*, ammonia solution <DMA < DEA. A decrease in the capacity factors not only for the *S*,*S* but also for the *S*,*R* diastereomers was observed for all the cations at pH 8 in comparison with pH 7. A shift of pH to 8 leads to an increase in the total negative charge of the diastereomer, which becomes *ca.* 2−, and this negative charge is seemingly not compensated for by forming of an ion pair of the diastereomer with two molecules of the ion-pairing reagent. Although the reproducibility of the capacity factors within one series of measurements was excellent, owing to the deterioration of the sorbent bonded phase after use in several different eluents the capacity factors were slightly shifted (compare corresponding data in Table 2 and Figs. 4 and 5). The observed dependences were unchanged, however.

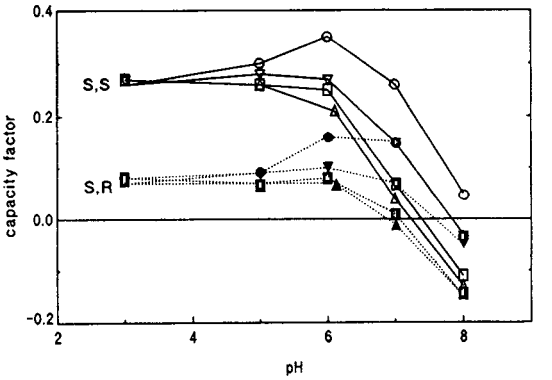

Fig. 4. Dependences of capacity factors for diastereomers of *S*-Ala-*S*,*R*-AEP on pH and eluent composition on SGX C_{18}. Mobile phase, 10 m*M* orthophosphoric acid with pH adjusted with (△, ▲) sodium hydroxide, (□, ■) ammonia solution, (▽, ▼) DMA and (○, ●) DEA.

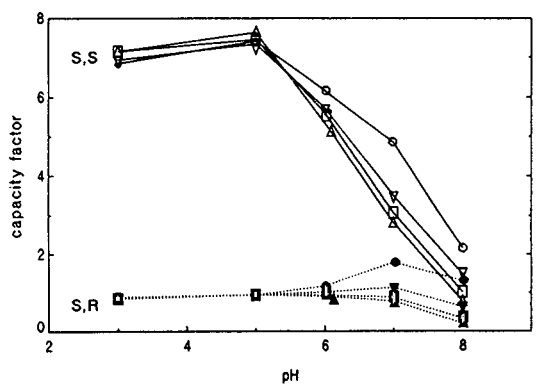

Fig. 5. Dependences of capacity factors for diastereomers of *S*-Leu-*S*,*R*-AEP on pH and eluent composition on SGX C_{18}. Mobile phase, 10 m*M* orthophosphoric acid with pH adjusted with (△, ▲) sodium hydroxide, (□, ■) ammonia solution (▽, ▼) DMA and (○, ●) DEA.

Because the differences in capacity factors were small, we checked if they are statistically significant. Using confidence intervals for a difference in means [16], we verified that the measured capacity factors at pH 7 were different for the 0.99 confidence level.

As the SGX silica-based reversed-phase sorbents are not totally end-capped, comparison was made with sorbents without silanol group activity. As a reference silica-based sorbent material Serva Octadecyl-Si 100 was used. The comparison of results obtained on SGX C_{18} and Octadecyl-Si 100 showed only one significant difference: the capacity factors for the *S,R* diastereomers in the pH range 3–7 (adjusted with ammonia solution) were nearly constant for SGX C_{18} and increased with increase in pH for Octadecyl-Si 100. The explanation may be connected with residual silanol groups on the surface of SGX C_{18}, which deliver a negative charge to the surface of the sorbent.

On the polymer-based sorbents HEMA-BIO 1000 C_{18} and EDMA 2000 the retention times achieved under the same conditions were much more smaller for the *S,S* diastereomers (*e.g.*, in 10 m*M* orthophosphoric acid, pH 7, adjusted with ammonia solution, the capacity factor for *S*-Phe-*S*-AEP was 12.7 on SGX C_{18} and 2.0 on HEMA-BIO 1000 C_{18}). These results are surprising because the capacity factors for some aromatics such as benzene and toluene are very similar for SGX C_{18} and the polymer-based sorbents HEMA-BIO 1000 C_{18} and EDMA 2000. The behaviour can probably be explained by the different structures of the sorbents: the silica-based sorbent has a more or less uniform layer of C_{18} moieties bonded on the surface, whereas on the organic polymer-based sorbents the hydrophobic groups form or are located on a net of cross-linked chains. As the differences in the retentions of the *S,R* and *S,S* diastereomers are based only on different steric orientations of hydrophobic groups, this difference is more significant in the case of silica-based RPs with a better defined interface between a non-polar stationary phase and a polar mobile phase.

4. Conclusions

Diastereomers of four PDs were successfully separated on silica-based reversed-phase sorbents and the influence of different bonded functional groups, eluent pH and cations was evaluated. The resolution of diastereomers achieved was very good. RP-HPLC was verified as a suitable method for analytical or preparative-scale separations of diastereomers of PDs. Optimization of the analysis can easily be achieved based on the observed dependences.

5. References

[1] J.G. Allen, F.R. Atherton, M.J. Hall, C.H. Hassal, S.W. Holmes, L.J. Nishet and P.S. Ringrose, *Nature (London)*, 272 (1978) 56.
[2] P. Mastalerz, L. Kupczyk-Subotkowska, Z.S. Herman and G. Laskawiec, *Naturwissenschaften*, 69 (1982) 46.
[3] R.I. Hilderbrand, J. Curley-Joseph, H.J. Lubansky and T.O. Henderson, in M. Grayson and E.J. Griffith (Editors), *Topics in Phosphorus Chemistry*, Interscience, New York 1983, pp. 297–338.
[4] V.P. Kukhar, N.M. Solodenko and V.A. Solodenko, *Ukr. Biokhim. Zh.*, 60 (1988) 95.
[5] J.S. Thayer, *Appl. Organomet. Chem.*, 3 (1989) 203.
[6] P. Kafarski and B. Lejczak, *Phosphorus Sulfur Silicon Relat. Elem.*, 63 (1991) 193.
[7] F.R. Atherton, C.H. Hassal and R.W. Lambert, *J. Med. Chem.*, 29 (1986) 29; and references cited therein.
[8] P. Wieczorek, B. Lejczak, M. Kaczanowska and P. Kafarski, *Pestic. Sci.*, 30 (1990) 43.
[9] P. Kafarski, B. Lejczak and P. Mastalerz, *Beitr. Wirkstofforschung*, 25 (1985) 1.
[10] B. Lejczak, P. Kafarski and P. Mastalerz, *J. Chromatogr.*, 324 (1985) 455.
[11] S.V. Galushko, M.Y. Belik, V.A. Solodenko, T.N. Kasheva and V.P. Kukhar, *J. Chromatogr.*, 553 (1991) 143.
[12] P. Hermann, I. Lukeš, B. Máca and M. Buděšínský, *Phosphorus Sulfur Silicon Relat. Elem.*, 79 (1993) 43.
[13] T. Sasagawa, T. Okuyama and D.C. Teller, *J. Chromatogr.*, 240 (1982) 329.
[14] V. Cucinotta, R. Purrello and E. Rizzarelli, *Comments Inorg. Chem.*, 11 (1990) 85.
[15] F. Kesner, *Diploma Thesis*, Faculty of Sciences, Charles University, Prague, 1992, p. 43.
[16] G.E.P. Box, W.G. Hunter and J.S. Hunter, *Statistics for Experimenters*, Wiley, New York, 1978, pp. 115–116.

ELSEVIER

Journal of Chromatography A, 665 (1994) 67–73

JOURNAL OF CHROMATOGRAPHY A

Chromatographic studies of the enantiomeric composition of some therapeutic compositions applied in the treatment of liver and kidney diseases

Danuta Sybilska*[,a], Joanna Kowalczyk[a], Monika Asztemborska[a], Renata J. Ochocka[b], Henryk Lamparczyk[b]

[a]*Institute of Physical Chemistry, Polish Academy of Sciences, Kasprzaka 44/52, PL-01-224 Warsaw, Poland*
[b]*Medical Academy, Faculty of Pharmacy, Gen. J. Hallera 107, PL-80-416 Gdańsk, Poland*

Abstract

A gas–liquid chromatographic system with α-cyclodextrin in formamide medium (coated on Chromosorb) was used for the separation of enantiomers of α-pinene, β-pinene, limonene and camphene in medicines applied in the therapy of liver and kidney diseases. The drugs under investigation were produced in Poland (Terpichol and Terpinex), in Germany (Rowachol and Rowatinex) and in Slovenia (Uroterp). It was found that, depending on the manufacturer, medicines possessing similar chemical compositions differ considerably from one another regarding the content of enantiomers, mainly those of α-pinene.

1. Introduction

Recently, it has been found that a large group of chiral macrocyclic compounds including cyclodextrins constitute a powerful tool for the enantiomeric separation of many compounds of various chemical natures, *i.e.*, acidic, basic and neutral, including hydrocarbons, which are very resistive to diastereoisomer formation.

There are two ways to apply cyclodextrins in gas chromatography for analytical purposes. In the early 1980s we initiated the first approach using cyclodextrins in the dissolved state (in a convenient matrix solvent) as stationary phases. This method is characterized by high enantioselectivity and a relatively low efficiency of the columns. For example, using α-cyclodextrin (α-CD) under appropriate conditions of partition gas chromatography (GC), very efficient separations of α-pinene, β-pinene and camphene into enantiomers can be achieved [1–3]. A few years later König and co-workers [4,5] and subsequently Armstrong *et al.* [6] initiated another approach, successfully using some cyclodextrin derivatives in the molten state as stationary phases in capillary columns. This important method is characterized by a relatively poor enantioselectivity but a high efficiency of the columns [7].

These two approaches are still being developed. They have their own advantages and limitations, but it would be a mistake to treat them as competitive techniques; rather, they are supplementary, and both merit attention.

This paper describes an attempt to apply inclusion processes in α-CD molecules to the study of the enantiomeric composition of ter-

* Corresponding author.

0021-9673/94/$07.00
SSDI 0021-9673(93)E0025-P

penic hydrocarbons in some medicines used in the therapy of liver and kidney diseases.

It is well known that the semi-natural mixture of several terpenes (menthol, menthone, pinenes, borneol, camphene and cineol) in olive oil has choleretic, spasmolytic and bacteriostatic properties, and it has been used as an inexpensive preparation to treat cholesterol stones in the gall bladder and the bile ducts [8–10] and in the treatment of patients with ureteric stones [11,12]. Although, the mechanism by which the terpene mixture inhibits the formation of cholesterol crystals in bile is not fully recognized, it has been found that menthol and other terpenes inhibits the lecitin–cholesterol acyltransferase activity of human plasma [13] and also (*S*)-3-hydroxy-3-methylglutaryl-CoA reductase which leads to the physiological inhibition of hepatic sterol synthesis [14].

The enzymatic mechanism of terpene action strongly suggests that the enantiomeric composition of the drug might be a very important factor determining its therapeutic properties. Many of the terpenes used for medical purposes are chiral compounds and they can exist in natural mixtures in one or two enantiomeric forms and in various proportions. Despite this fact, commercially available terpene drugs (*e.g.*, Rowachol) are usually described as a mixture of six terpenes in which even the two pinenes (α- and β-pinene) are not discriminated and the enantiomeric composition is virtually unknown [15,16].

2. Experimental

2.1. Reagents

α-CD was supplied by Chinoin (Budapest, Hungary). Chromosorb W NAW (0.18–0.25 mm) for GC was a product of Johns-Manville (Litho, USA). Commercially available drugs investigated were as follows: Terpinex and Terpichol from Herbapol (Wroclaw, Poland), Rowachol and Rowatinex from Rowa-Wagner, (Bergish, Germany) and Uroterp donated by KRKA (Novo Mesto, Slovenia). Terpene standards were as follows: (+)- and (−)-α-pinene from Aldrich (Milwaukee, WI, USA), (+)- and (−)-limonene from Merck–Schuchardt (Hohenbrunn, Germany) and (+)- and (−)-β-pinene from Fluka (Buchs, Switzerland); (+)- and (−)-camphene were prepared by ourselves [3].

2.2. Apparatus and procedure

Chromatographic studies were performed using a Hewlett-Packard (Avondale, PA, USA) Model 5890 gas chromatograph equipped with dual flame ionization detectors. The peak areas and retention times were measured by means of a Hewlett-Packard Model 3396 integrator. The compounds (0.02–0.15 μl) were injected with Hamilton microsyringes separately or as a mixture. Two types of columns were used: a packed glass column (4 m × 4 mm I.D.) containing Chromosorb W NAW (0.18–0.25 mm), coated with a formamide solution of α-CD (0.18 molal) and an HP-1 cross-linked methylsilicone fused-silica capillary column (30 m × 0.53 mm I.D.). The details for the preparation of the α-CD column have been described previously [17,18]. A constant inlet pressure (100 ± 5 kPa) and a constant argon flow-rate (40 ± 0.5 ml/min) were maintained.

The operating temperature of the α-CD column was isocratic (35°C), whereas the capillary column temperature was programmed (70°C held for 35 min, then increased from 70 to 200°C at 5°C/min and held at 200°C for 10 min).

2.3. Validation of the analytical method

In order to evaluate the repeatability of the method, an artificial mixture of (+)-α-pinene, (−)-α-pinene, (−)-β-pinene, (+)-limonene, (−)-limonene, (+)-camphene and (−)-camphene was injected. The results and the statistical evaluation are given in Table 1. The relative standard deviation (R.S.D.) in each instance is lower than 10%. The only one exception is (+)-β-pinene, and therefore, only small amount of this compound is present in the mixture. In Table 2 the separation factors (α) are presented. As can be seen, each value is higher than 1.1 and the R.S.D.s are lower than 4%. Therefore, it can be

Table 1
Repeatability of the analytical method

Run No.	Concentration (%)							
	(+)-α-Pinene	(−)-α-Pinene	(+)-β-Pinene	(−)-β-Pinene	(+)-Limonene	(−)-Limonene	(+)-Camphene	(−)-Camphene
1	14.20	13.37	1.16	12.78	15.04	11.72	15.88	15.51
2	14.87	13.25	1.13	12.30	13.35	10.73	16.60	17.77
3	14.58	13.04	1.11	12.19	15.93	12.69	14.04	15.38
4	15.21	13.26	1.78	13.24	14.39	10.94	15.03	15.80
5	14.60	13.26	1.44	12.96	14.25	10.57	16.93	17.33
6	14.97	13.12	1.52	13.02	14.75	10.60	15.12	16.80
Mean	14.74	13.22	1.36	12.75	14.62	11.21	15.60	16.43
S.D.	0.323	0.107	0.246	0.382	0.787	0.768	0.986	0.921
R.S.D. (%)	2.2	0.8	18.1	3.0	5.4	6.9	6.3	5.6

concluded that the analytical method is suitable for the determination of terpenes in therapeutic compositions. The data quoted in Tables 5 and 6 are the mean values from at least three measurements.

3. Results and discussion

3.1. Chemical composition

Terpenic mixtures are used as drugs in two different compositions. For the treatment of cholesterol stones in the gall bladder and the bile ducts, mixtures rich in menthol and pinenes are sold under the trade names Rowachol and Terpichol, whereas in compositions used for the treatment of ureteric stones (Terpinex, Rowatinex and Uroterp) the predominant compounds are pinenes and camphene. For the evaluation of the chemical composition an achiral capillary column was used.

Fig. 1 shows a typical chromatogram of a Terpichol sample. The concentrations (peak areas) found in Terpichol and Rowachol samples together with the values declared by the producer are given in Table 3. From the data in Table 3, menthol and α-pinene appear to be the predominant components of both drugs. However, in the Rowachol sample larger differences

Table 2
Statistical evaluation of enantioselectivity factors (α)

Run No.	$\alpha_{(+)/(-)}$			
	α-Pinene	β-Pinene	Limonene	Camphene
1	2.16	1.49	1.11	2.73
2	2.04	1.41	1.09	2.46
3	2.31	1.46	1.10	2.50
4	2.10	1.46	1.10	2.60
5	2.21	1.49	1.11	2.48
6	2.15	1.45	1.11	2.56
Mean	2.16	1.46	1.10	2.56
S.D.	0.085	0.027	0.007	0.089
R.S.D. (%)	3.9	1.8	0.6	3.5

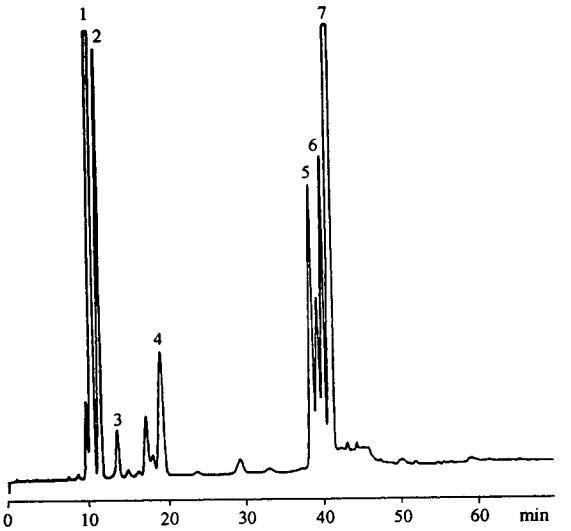

Fig. 1. Chromatogram of Terpichol obtained on an achiral capillary column. Conditions as under Experimental. Peaks: 1 = α-pinene; 2 = camphene; 3 = β-pinene; 4 = cineole; 5 = menthone; 6 = borneol; 7 = menthol.

from the declared values were found. Moreover, in the Terpichol sample undeclared limonene is also present.

Fig. 2 shows typical chromatograms of (a) Rowatinex and (b) Uroterp obtained on an achiral capillary column. In Table 4 are given the data on the chemical composition of Terpinex, Rowatinex and Uroterp obtained on the same column. The amount of limonene, eluted together with cineole, was elucidated using supplementary data from the chiral column. As can be seen, only the Rowatinex sample is in full accordance with the standard; Terpinex and Uroterp are strongly admixed with compounds not declared by the manufacturers and not identified by us (*ca.* 20%). The Uroterp sample has a high concentration of limonene and Terpinex contains large amounts of camphene and borneol. Nevertheless, α-pinene is the main constituent of the drugs used in kidney diseases.

3.2. Enantiomeric composition

The enantiomeric composition was studied using the chiral α-CD column. Fig. 3 shows chromatograms of (a) Terpichol and (b) Rowachol. Table 5 gives the enantiomeric composition of both the monoterpenic fractions obtained on the same column. It is seen that the main component, α-pinene, is mostly (81%) dextrarotatory in Terpichol whereas Rowachol contains 90% of its antipode. Similar large differences in enantiomeric composition can be observed for camphene. In Terpichol it is almost a racemic mixture consisting of 60% of the dextrarotatory component. In contrast, in Rowachol the dextrarotatory enantiomer dominates (85%). Although β-pinene is declared by the producers as a minor component, it is noteworthy that it is present as almost the

Table 3
Contents of terpenes in Terpichol and Rowachol determined on an achiral capillary column

Compound	Terpichol (%)		Rowachol (%)	
	Declared	Found	Declared	Found
α-Pinene	20.0	21.4	20.0	25.0
β-Pinene	5.0	1.0	5.0	6.5
Camphene	8.0	6.1	8.0	9.1
Cineole	3.0	3.7	3.0	2.8
Limonene	–	2.5	–	–
Menthone	9.0	6.5	9.0	7.1
Borneol	8.0	5.3	8.0	6.0
Menthol	48.0	44.7	48.0	37.0
Unidentified		8.8		12.4

Chromatographic conditions as described under Experimental.

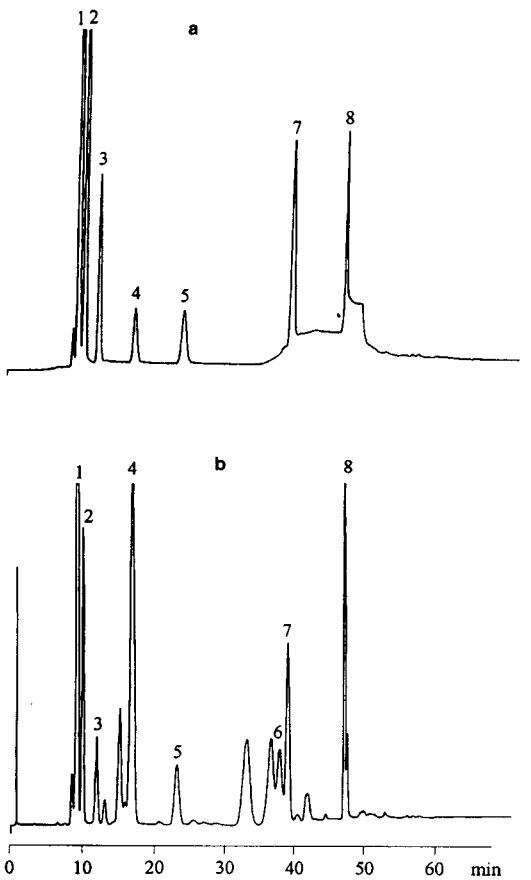

Fig. 2. Chromatograms of (a) Rowatinex and (b) Uroterp obtained on an achiral capillary column. Conditions as under Experimental. Peaks: 1 = α-pinene; 2 = camphene; 3 = β-pinene; 4 = cineole and limonene; 5 = fenchone; 6 = menthone; 7 = borneol; 8 = *trans*-anethole.

optically pure (−)-enantiomer in both preparations.

Fig. 4 shows chromatograms of (a) Terpinex, (b) Rowatinex and (c) Uroterp obtained on the chiral α-CD column. Table 6 gives the enantiomeric composition of monoterpenic fraction of the drugs. The main component (α-pinene) is mostly dextrarotatory (91%) in the Terpinex preparation and laevorotatory (89%) in Rowatinex. In contrast, Uroterp has an intermediate composition of α-pinene, consisting of 64% of the dextrarotatory isomer. Camphene exists as a nearly racemic mixture in all the drugs. Moreover, large amounts of limonene

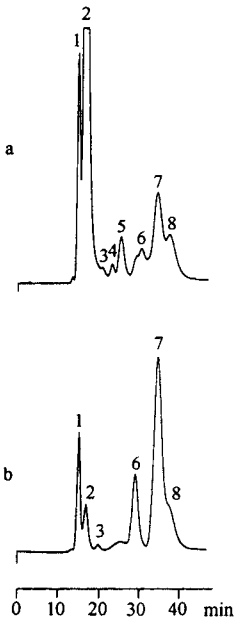

Fig. 3. Chromatograms of (a) Terpichol and (b) Rowachol obtained on a chiral α-CD column at 35°C. Peaks: 1 = (+)-camphene; 2 = (+)-α-pinene; 3 = (+)-β-pinene; 4 = (−)-limonene; 5 = (+)-limonene; 6 = (−)-β-pinene; 7 = (−)-α-pinene; 8 = (−)-camphene.

were found in Uroterp, with 70% of the (+)-enantiomer prevailing and also a trace of limonene in the Terpinex preparation with 83% of the (+)-enantiomer. Finally, it is noteworthy that β-pinene in Rowatinex and Uroterp is present as the almost optically pure (−)-enantiomer.

The results indicate large differences of the enantiomeric compositions of all the drugs considered, suggesting that the enantiomeric composition is not standardized by the manufacturers. On the other hand, biological systems are largely constructed from chiral compounds. Therefore, in such a highly chiral environment it should not be surprising that some drugs, which possess an asymmetric centre, exhibit a high degree of stereoselectivity in their interactions with macromolecules. Particularly, growing evidence of an enzymatic mechanism of terpene action on living organisms [13,14] strongly suggests enantioselectivity of this process. Moreover, clinical observation does not univocally confirm the usefulness

Table 4
Contents of terpenes in Terpinex, Rowatinex and Uroterp determined on an achiral capillary column

Compound	Terpinex (%)		Rowatinex (%)		Uroterp (%)	
	Declared	Found	Declared	Found	Declared	Found
α-Pinene	46.2	23.9	37.0	37.9	44.0	23.7
β-Pinene		1.9	9.0	9.6		2.6
Camphene	22.4	23.7	22.0	22.0	10.0	7.9
Cineole	4.5	3.7	4.0	4.0	14.0	17.6
Limonene	–		–	–	–	
Fenchone	6.0	4.6	6.0	5.0	5.1	3.3
Borneol and	15.0	9.3	15.0	13.4	14.0	8.2
isoborneol		2.6		–		4.3
trans-Anethole	6.0	4.2	6.0	5.7	12.1	9.5
Unidentified		24.0		2.0		23.0

Conditions as described under Experimental.

Table 5
Enantiomeric composition of terpenes in Terpichol and Rowachol determined on a chiral α-CD column at 35°C

Compound	Terpichol (%)	Optical purity (%)	Rowachol (%)	Optical purity (%)
(+)-α-Pinene	59.6	81	7.0	10
(−)-α-Pinene	13.6	19	60.0	90
(+)-β-Pinene	0.1	2	1.0	6
(−)-β-Pinene	4.7	98	14.8	94
(−)-Limonene	0.7	16	–	–
(+)-Limonene	3.7	84	–	–
(+)-Camphene	10.5	60	12.8	85
(−)-Camphene	7.1	40	2.2	15

Table 6
Enantiomeric composition of terpenes in Terpinex, Rowatinex and Uroterp determined on a chiral α-CD column at 35°C

Compound	Terpinex (%)	Optical purity (%)	Rowatinex (%)	Optical purity (%)	Uroterp (%)	Optical purity (%)
(+)-α-Pinene	38.3	91	6.0	11	33.3	64
(−)-α-Pinene	4.0	9	47.6	89	18.8	36
(+)-β-Pinene	1.5	50	1.0	7	–	0
(−)-β-Pinene	1.5	50	12.6	93	5.3	100
(+)-Limonene	2.9	83	–	0	13.2	70
(−)-Limonene	0.6	17	–	0	5.6	30
(+)-Camphene	25.6	55	17.7	54	7.3	46
(−)-Camphene	20.7	45	14.8	46	8.6	54

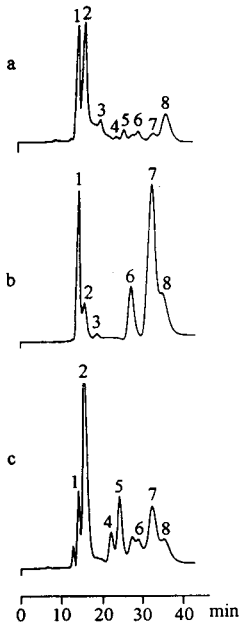

Fig. 4. Chromatograms of (a) Terpinex, (b) Rowatinex and (c) Uroterp obtained on a chiral α-CD column at 35°C. Peaks: 1 = (+)-camphene; 2 = (+)-α-pinene; 3 = (+)-β-pinene; 4 = (−)-limonene; 5 = (+)-limonene; 6 = (−)-β-pinene; 7 = (−)-α-pinene; 8 = (−)-camphene.

of terpene drugs in the treatment of cholesterol gall stones [10]. Presumably, a lack of general acceptance of these drugs by clinicians is due to the large differences in enantiomeric composition that we have observed. On the other hand, the quality and amounts of terpenes in plant species differ greatly, not only from species to species but also within species [19]. In such cases, in addition to genetic factors, both the macro- and micro-environments may be responsible for the variations in the enantiomeric compositions of terpenes. This could probably explain why the terpenic drugs produced in different countries differ so substantially.

The results presented here suggest that the difficult problem of the evaluation of terpenic drugs could be completely resolved on the basis of α-CD complexation. To achieve this goal very detailed optimization studies should be performed.

4. Acknowledgements

The authors greatly appreciate the donation of Uroterp by KRKA. This work was supported by grant 202429101 from the State Committee for Scientific Research.

5. References

[1] T. Kościelski, D. Sybilska and J. Jurczak, *J. Chromatogr.*, 280 (1983) 131.
[2] R.J. Ochocka, D. Sybilska, M. Asztemborska, J. Kowalczyk and J. Goronowicz, *J. Chromatogr.*, 543 (1991) 171.
[3] D. Sybilska, J. Kowalczyk, M. Asztemborska, T. Stankiewicz and J. Jurczak, *J. Chromatogr.*, 543 (1991) 397.
[4] W.A. König, S. Lutz and G. Wenz, *Angew. Chem., Int. Ed. Engl.*, 27 (1988) 979.
[5] W.A. König, A. Krüger, D. Icheln and T. Runge, *J. High Resolut. Chromatogr.*, 15 (1992) 184.
[6] D.W. Armstrong, W. Li and J. Pitha, *Anal. Chem.*, 62 (1990) 217.
[7] W.A. König, *Gas Chromatographic Enantiomer Separation with Modified Cyclodextrins*, Hüthig, Heidelberg, 1992, and references cited therein.
[8] W.R. Ellis, K.W. Somerville, B.H. Whitten and G.D. Bell, *Br. Med. J. Clin. Res.*, 289 (1984) 153.
[9] K.W. Somerville, W.R. Ellis, B.H. Whitten, T.W. Balfour and G.D. Bell, *Postgrad. Med. J.*, 61 (1985) 313.
[10] K. von Bergmann, A. Beck, C. Engel and O. Leiss, *Klin. Wochenschr.*, 65 (1987) 458.
[11] E. Mukamel, D. Engelstein, D. Simon and C. Servadio, *J. Urol.*, 93 (1987) 31.
[12] D. Engelstein, E. Kahan and C. Servadio, *J. Urol.*, 98 (1992) 98.
[13] R.V. Cooney, J. Nemhauser and R.J. Morin, *Lipids*, 19 (1984) 371.
[14] B. Middleton and K.P. Hui, *Biochem. Pharmacol.*, 31 (1982) 2897.
[15] B. Handelsman, G. Bonorris, J.W. Marks and L.J. Schoenfield, *Am. J. Med. Sci.*, 284 (1982) 16.
[16] I.A.D. Bouchiers, *Br. J. Med.*, 300 (1990) 592.
[17] D. Sybilska and T. Kościelski, *J. Chromatogr.*, 261 (1983) 357.
[18] D. Sybilska and J. Jurczak, *Carbohydr. Res.*, 192 (1989) 243.
[19] D. Vokou and N.S. Margaris, *Int. J. Biometeorol.*, 30 (1986) 327.

ELSEVIER

Journal of Chromatography A, 665 (1994) 75–86

JOURNAL OF CHROMATOGRAPHY A

Chiral separation of some amino alcohols by addition of helical nickel(II) chelate to the mobile phase used in reversed-phase high-performance liquid chromatography

Grzegorz Bazylak

Biochromatographic Laboratory, Human Nutrition Division, Hygienics Department, Medical University of Łodz, Jaracza 63, 90 251 Łodz, Poland

Abstract

A set of underivatized chiral primary and secondary amino alcohols, including ephedrine analogues, were separated into the respective enantiomers by reversed-phase high-performance liquid chromatography employing acetonitrile–water as the mobile phase containing newly synthesized neutral, square-planar, helically distorted nickel(II) chelate. The four chelates studied, derived from condensation of optically active tetradentate Schiff base ligands with nickel(II) acetate, were differentiated according to the alkyl substituent on the chiral centres of the parent molecule. The influence of changes in the mobile phase concentration of each chelate or acetonitrile and its flow-rate on the observed enantiomeric discrimination of solutes was investigated. Based on the three-point interaction chiral recognition model, possible structures for the associates between solutes and the chelate responsible for the enantiomeric separation were suggested. The separation efficiency obtained with the developed HPLC system was compared with the resolution of amino alcohols observed with a typical ligand-exchange HPLC system with a chiral stationary phase in the form N-2′-hydroxy-*n*-dodecyl-L-hydroxyproline and a mobile phase containing copper(II) ion. The content of pseudoephedrine enantiomers in some representative samples of its oral dosage forms (tablets, syrups, elixirs) was determined using the developed RP-HPLC method.

1. Introduction

The amino alcohol structure is present in many pharmaceuticals, *e.g.*, β-blocker and adrenergic drugs. The most pronounced differences in pharmacokinetics and bindings between enantiomers of such drugs were observed in aged Wistar rats [1]. Consequently, stereoselective liquid chromatographic methods enabling the reliable and reproducible enantiomeric determinations of amino alcohols still attract much attention. Using reversed-phase high-performance liquid chromatography (RP-HPLC) with an octadecylsilane column a variety of amino alcohols could be resolved in the form of diastereoisomers prepared by a suitable precolumn derivatization procedure [2,3] or by introducing the complexing agent, *e.g.*, esters of tartaric acid [4,5] or N-benzyloxycarbonylglycyl-L-proline [6] into the mobile phase. HPLC with a chiral stationary phase (CSP) offers some indirect [7–11] and direct [12–15] procedures for obtaining the enantioselective separation of amino alcohols. Especially with the ligand-exchange mode of HPLC (HPLEC), Yamazaki *et al.* [13,14] achieved an excellent direct separation of enantiomers of norephedrine, norpseudoephedrine and various phenolic amino alcohols on columns of octadecylsilica coated with N-*n*-dodecyl-L-hydroxyproline (DHP) and a mobile phase containing

0021-9673/94/$07.00
SSDI 0021-9673(93)E1087-G

copper(II) diacetate. However, the separation of enantiomers of aliphatic amino alcohols was not achieved with this chromatographic system. Lindner and Hirschbock [16] reported the partial resolution of noradrenaline isomers with an HPLEC system prepared by dynamically coating a reversed-phase packing with copper(II) or nickel(II) chiral complexes of (*R*,*R*)-tartaric acid mono-*n*-octylamide. In the second mode of HPLEC employing a chiral mobile phase additive (CMA) in the form of copper(II)–L-proline chelates, Lam and Malikin [17] resolved the *o*-phthalaldehyde (OPA) derivatives of series of aromatic and aliphatic amino alcohols. In view of the recently reported [18–21] selective separation of enantiomeric and diastereoisomeric alkylamines by RP-HPLC applying helically distorted nickel(II) Schiff base chelates as chiral selectors in the mobile phase, the aim of this study was to confirm the usefulness of this system for the enantioselective separation of non-derivatized amino alcohols.

2. Experimental

2.1. Chemicals

The following amino alcohols were obtained from Sigma (St. Louis, MO, USA): (*R*,*S*)-2-amino-1-(3,4-dihydroxyphenyl)ethanol (arterenol, norepinephrine, noradrenaline), (*R*,*S*)-2-amino-1-phenylethanol (phenylethanolamine, β-hydroxyphenethylamine), (*R*)- and (*R*,*S*)-2-amino-2-phenylethanol (α-phenylglycinol), (*S*)-2-amino-3-phenyl-1-propanol (L-phenylalaninol) and (1*S*,2*S*)- and (1*R*,2*R*)-pseudoephedrine.

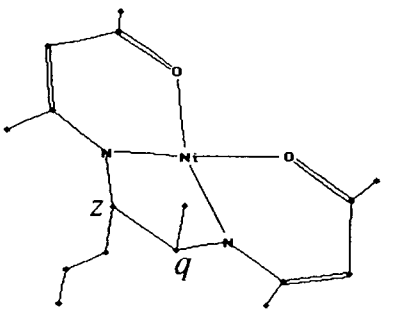

Fig. 1. Stereoscopic view of NiL[4] chelate (see Table 1) as an example of the structure of helical nickel(II) chelates used as CMA. The asymmetric carbon atoms are designated *z* and *q*. Some hydrogen atoms have been omitted for clarity.

(1*R*,2*S*)-Norephedrine was purchased from Serva (Heidelberg, Germany), (1*R*,2*S*)-ephedrine from Merck (Darmstadt, Germany) and (1*S*,2*R*)-ephedrine hydrochloride from Fluka (Buchs, Switzerland).

The four solid nickel(II) tetradentate Schiff base chelates (Fig. 1, Table 1) were synthesized, purified and characterized as described in previous reports [22–25]. (2*S*,4*R*,2′*RS*)-N-(2′-hydroxy-*n*-dodecyl)-4-hydroxyproline (HDHP) was synthesized according to the procedure described by Martens and co-workers [26,27].

2.2. Apparatus

A Pye LC3 XP chromatograph (Pye Unicam, Cambridge, UK) equipped with a multi-wavelength UV detector was applied. Separations were carried out on a Polsil ODS (ZOCh, Lublin, Poland) stainless-steel columns (25 × 0.4 cm I.D.) packed with octadecylsilica gel of particle size 7 μm.

Table 1
Nickel(II) Schiff base chelates used as the chiral mobile phase additives in HPCMA experiments

Abbreviation	Systematic name	Substituent	
		z	*q*
NiL[1]	*dl*-[4,4′-(Methylethane-1,2-diyldiimino)bis(pent-3-en-2-onato)]nickel(II)	H	CH_3
NiL[2]	*dl*-[4,4′-(1,2-Dimethylethane-1,2-diyldiimino)bis(pent-3-en-2-onato)]nickel(II)	CH_3	CH_3
NiL[3]	*dl*-[4,4′-(Butane-1,2-diyldiimino)bis(pent-3-en-2-onato)]nickel(II)	C_2H_5	H
NiL[4]	*dl*-[4,4′-(1-Methyl-2-propylethane-1,2-diyldiimino)bis(pent-3-en-2-onato)]nickel(II)	C_3H_7	CH_3

2.3. High-performance liquid chromatography with a chiral mobile phase additive (HPCMA)

For the preparation of the mobile phase, different amounts ($1 \cdot 10^{-5}$, $1 \cdot 10^{-4}$, $5 \cdot 10^{-4}$, $1 \cdot 10^{-3}$ and $1 \cdot 10^{-2}$ mol/l) of solid nickel(II) chelate (see Table 1) were carefully weighed and added to a 0.3 mol/l solution of sodium acetate, then ultrasonically degassed acetonitrile was added to the required volume (15, 20 or 25%, v/v). The pH of the final mobile phase was adjusted to 6.0 with acetate buffer. The mobile phase was then filtered and degassed under reduced pressure. The Polsil ODS column was equilibrated with 15–30 column volumes (4.20 ml) of the mobile phase prior to sample injection. The starting flow-rate was 1 ml/min. The column effluent was monitored with a UV absorbance detector operating at 254 nm. All measurements was made at 25°C. Capacity factors (k') of solutes were calculated as the means of four parallel measurements.

2.4. HPLEC measurements

The procedure for coating the column with Polsil ODS was adapted from Davankov *et al.* [28] with slight modification. The column (25 cm) was washed (flow-rate 0.5 ml/min) with 5 ml of a solution of 100 mg of HDHP in acetonitrile–water (20:80, v/v). Then 10 ml of coating mixture consisting of a concentrated solution of copper(II) acetate in acetonitrile–water (20:80, v/v) was delivered to the column. The column was equilibrated with the final mobile phase, acetonitrile–water (20:80, v/v) containing $2 \cdot 10^{-4}$ mol/l copper(II) acetate and adjusted to pH 6.0 with acetate buffer. The effluent from the column was monitored with a UV absorbance detector at 280 nm after acidification by adding 0.2 mol l^{-1} perchloric acid (1.0 ml/min) using a postcolumn mixing loop (30 cm × 0.5 mm I.D.).

2.5. Analysis of pharmaceuticals

Five products commercially available locally were used for the determination of the content of pseudoephedrine enantiomers using extraction procedures according to Peeran *et al.* [29] followed by the developed HPCMA method employing the NiL^4 chelate and the HPLEC method with HDHP chiral stationary phase.

2.6. Calculations

A standard statistical package was used for the calculation of precision and reproducibility parameters. The last-squares superimposition of nickel(II) chelates and solute enantiomers during association was made using the program PCMODEL (Serena Software, Bloomington, IN, USA).

3. Results and discussion

3.1. HPCMA measurements

Some chiral, ionized, octahedral nickel(II) complexes, mainly *n*-alkylamide derivatives, have been utilized as chiral mobile phase additives in HPLEC systems [16,30], permitting the enantioselective separation of free or dansylated amino acids. However, Lochmuller and Hagac [31] showed that also neutral, square-planar nickel(II) chelates can be used as the mobile phase dopant for the selective separation of aromatic amines using RP-HPLC systems. Such excited nickel(II) chelates are differentiated from the previously mentioned ligand-exchange chelates by the fact that during the formation of unstable associates with resolved solutes the fundamental chelate structure remains unchanged, *i.e.*, no coordination bonds between the central nickel(II) ion and the parent ligand are broken or formed. Therefore, it has been suggested [31] that specific, electrostatic, induced dipole–dipole interactions between the square-planar, coordinately unsaturated nickel(II) chelate and the polar solute acted as the principle of the observed enhanced retention. One could expect that such interactions supported by the chiral environment of nickel(II) ion in such a defined chelate structure would lead to a potential chiral selector. This approach was applied in this study in the synthesis of the series of

chiral nickel(II) complexes (Fig. 1, Table 1) with optically active, tetradentate Schiff bases.

All four chelates studied contain two chiral carbon atoms (designated *z* and *q* in Fig. 1) localized in the ethylene bridge connecting both imine nitrogen atoms. This implies the formation of only *dl* isomers of NiL^1, NiL^3, NiL^4 chelates, respectively, or *dl* and *meso* isomers of NiL^2 chelate. The *meso* isomer was separated from the *dl*-NiL^2 chelate during the purification step using a silica gel with benzene–hexane (70:30, v/v) column chromatographic system and then its content was calculated as 0.15% from the results of gas chromatographic measurements [23]. The crystal structure of all *dl*-isomers of the synthesized complexes showed [23–25] an equatorial arrangement of the tetradentate ligands around the metal centre in a slightly distorted square-planar geometry. Of the two imino ketone ligand fragments, one deviates significantly from planarity whereas the other is planar, within experimental error. The distortion and deviation from planarity increased in parallel with the bulkiness of the alkyl *z* substituent in the molecule of the nickel(II) chelate. The determination of torsion angles indicated a stable axial position of the *z* substituent in the ethylene bridge which stabilized the λ conformation of the five-membered chelate ring and the Λ configuration of chiral carbon atoms in each kind of chelate studied. This phenomenon leads to the formation of a helical structure of the chelates studied and their chirooptical properties detected by circular dichroism spectra [25,32,33]. The six-membered chelate rings, contained significantly delocalized π bonds, are not perfectly coplanar. Such coplanarity increased with decrease in the molecular volume of the *z* substituent. The partial negative or positive charge is localized on the oxygen carbonyl atoms or central nickel(II) ion, respectively. However, the surface area of the chelates is mostly non-polar, *e.g.*, for the NiL^4 chelate the non-polar saturated surface area occupied *ca.* 212 $Å^2$ of the 283 $Å^2$ of the total surface area. As suggested on the basis of adsorption isotherm data [20], the more bulky *z* substituent and the greater hydrophobicity of the chelates in the series $NiL^1 < NiL^2 < NiL^3 < NiL^4$ increased the chelate concentration on the surface of the octadecylsilane stationary phase. NMR results confirmed [23,25,34,35] that *d*-isomeric species (with an axial position of the *z* alkyl substituent) predominates in mixtures of *dl*-isomers of the nickel(II) chelates studied.

The structure of the amino alcohols studied is presented in Table 2. The amino group is attached to the primary or secondary carbon atom as in noradrenaline and, phenylethanolamine or in the remaining solutes, respectively. Only one asymmetric carbon atom exists in an α- or β-position to the phenyl ring in compounds **1**, **2** and **4** or compound **3**, respectively. Two asymmetric carbon atoms with different environments are present in solutes **5**, **6** and **7**, which implies the formation of two pairs of enantiomers. In contrast to the other solutes, in compounds **1** and **2** the amine group is adjacent to the asymmetric carbon atom.

As can be seen from Table 3, the values of the capacity factors (k') and separation factors (α) determined for amino alcohols with one chiral centre increased with increasing bulkiness of the

Table 2
Structure of amino alcohols studied, $R^3NHCH(R^1)CH(R^2)OH$

No.	Compound	R^1	R^2	R^3
1	Noradrenaline	H	$C_6H_3(OH)_2$	H
2	Phenylethanolamine	H	C_6H_5	H
3	Phenylalaninol	$CH_2C_6H_5$	H	H
4	Phenylglycinol	C_6H_5	H	H
5	Ephedrine	CH_3	C_6H_5	CH_3
6	Pseudoephedrine	CH_3	C_6H_5	CH_3
7	Norephedrine	CH_3	C_6H_5	H

Table 3
HPLC separation of *R*- and *S*-enantiomers of amino alcohols containing one asymmetric atom with mobile phases modified by NiL^{1-4} chelates

No.	Compound	NiL^1			NiL^2			NiL^3			NiL^4		
		k'_S	k'_R	α	k'_S	k'_R	α	k'_S	k'_R	α	k'_S	k'_R	α
1	Noradrenaline	6.48	6.63	1.02	7.01	7.36	1.05	7.63	8.69	1.14	8.15	10.61	1.30
2	Phenylethanolamine	7.19	7.36	1.03	7.73	8.04	1.04	8.31	9.55	1.15	9.01	12.82	1.42
3	Phenylalaninol	8.03	8.17	1.01	8.41	8.83	1.05	9.21	10.50	1.14	10.32	15.10	1.46
4	Phenylglycinol	8.43	8.51	1.02	8.72	9.24	1.06	9.75	10.81	1.14	11.31	17.19	1.52

For experimental conditions, see Fig. 2.

nickel(II) chelate employed as the chiral mobile phase additive. In all proposed chromatographic systems the most polar noradrenaline molecules were least retained (see Fig. 2). However, in spite of the type of nickel(II) chelate the *S*-enantiomers of solutes were eluted first. Contrary to the retention observed by Yamazaki *et al.* [13,14], in the HPLEC system a satisfactory separation of phenylalaninol enantiomers was achieved in the developed HPCMA mode, especially using a mobile phase containing the NiL^4 chelate. Noradrenaline isomers, containing two phenolic hydroxy groups, were also sufficiently separated ($\alpha = 1.3$) by introducing the NiL^4 chelate into the acetonitrile–water (20:80) (pH 6) mobile phase. This result is opposite to the separation of noradrenaline isomers reported by Lindner and Hirschbock [16] in the HPLEC mode.

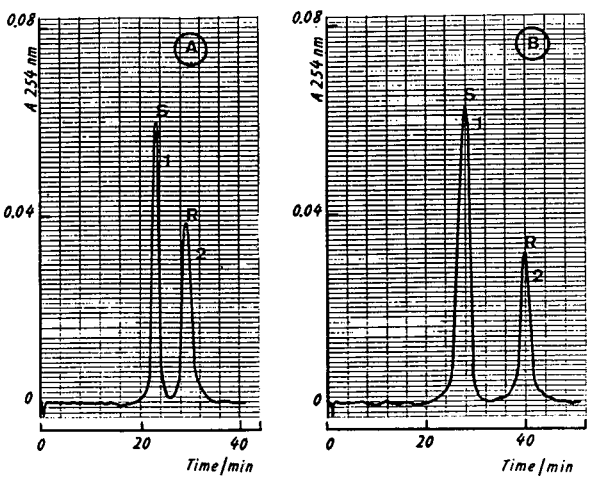

Fig. 2. Enantiomeric HPCMA separation of noradrenaline and phenylalaninol isomers of RP-HPLC with acetonitrile–water (20:80) (pH 6.0) as the mobile phase containing NiL^4 chelate ($1 \cdot 10^{-3}$ mol/l). Flow-rate, 1.2 ml/min; temperature 25°C; column, 25 × 0.4 m I.D.; column packing, Polsil ODS, 7 μm; UV detection at 254 nm. Peaks: (A) 1 = (*S*)-noradrenaline and 2 = (*R*)-noradrenaline; (B) 1 = (*S*)-phenylalaninol and 2 = (*R*)-phenylalaninol.

The observed chiral recognition of amino alcohols with one stereogenic centre can be explained using the "three-point-interaction" rule of Dalgliesh [36]. The formation of unstable associates with 1:1 stoichiometry between different square-planar nickel(II) tetradentate Schiff chelates and ammonium ion or alkylamines in polar and non-polar solutions was confirmed on the basis of reliable spectrophotometric results [25,32].

Molecular models (see Fig. 3) of the NiL^4–(*R*)-noradrenaline associate indicate that chiral recognition occurs mainly by specific attractive interactions between the negatively charged amine nitrogen atom and the positively charged, coordinated nickel(II) ion. The difference in stabilities of the enantiospecific associates is due to additional hydrogen bond formation between the hydroxyl group of the solute and the oxygen carbonyl atom in the chelate molecule. Tertiary lateral weak $\pi-\pi$ interactions between the phenolic ring of the solute and one of the six-membered chelate rings are also necessary for chiral discrimination in the developed HPCMA chromatographic system. The non-planar position of the solute in relation to the chelate ring system is

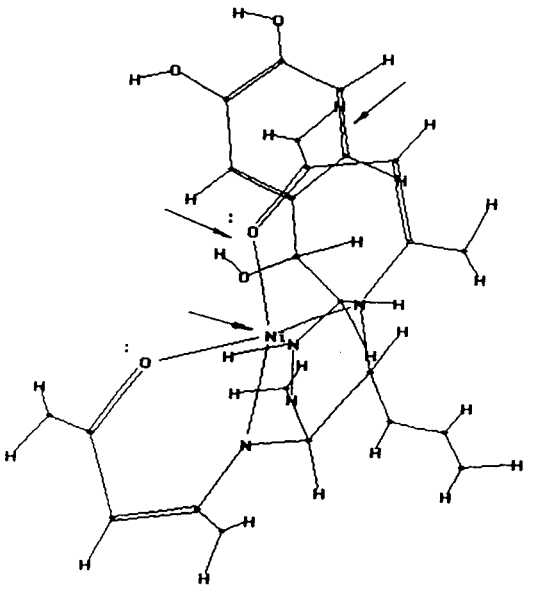

Fig. 3. Stereoscopic image of proposed structure of the NiL^4–(*R*)-noradrenaline associate formed in the developed HPCMA chromatographic system. Arrows indicate positions of the possible interaction sites.

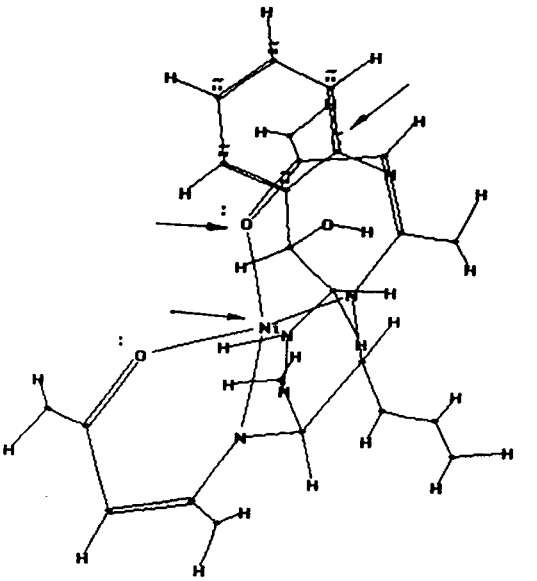

Fig. 4. Stereoscopic image of proposed structure of the NiL^4–(*S*)-phenylethanolamine associate formed in the developed HPCMA chromatographic system. Arrows indicate positions of the possible interaction sites.

forced by the antiperiplanar conformation of the *q* and *z* substituents in the chelate molecule. This should lead to a situation where an electron-deficient coordinated nickel(II) ion can be reached only by a non-hindered amine group attached or adjacent to the chiral centre of the solute. As was pointed out by Wainer *et al.* [9], the mutual relationship between the intensity of such a number of competing intermolecular interactions determines the final stereoselective associate stability, the observed retention order and the overall chromatographic enantioselectivity. Hence the recognition mechanism is changed from "three-point" like for (*R*)-noradrenaline to "two-point" as for (*S*)-phenylglycinol. The *S*-entantiomers are less retained because hydrogen bond formation at the second interaction point is two difficult (see Fig. 4). The binding affinities of the amine solutes to the coordinated nickel(II) ion increased if the amine and phenyl group were linked to the chiral carbon atom (negative inductive effect, $-I$), as is seen from the enhanced retention of phenylglycinol compared with phenylalaninol and phenylethanolamine.

The influence of the nickel(II) chelate structure on the chiral separation of amino alcohols with two stereogenic centres in the proposed HPCMA system is shown in Tables 4 and 5. Stronger retentions of all ephedrine analogues were observed for mobile phases containing the more bulky NiL^4 chelate (see Fig. 5). The norephedrine isomers, containing a primary amine group, were less retained in all instances. The best separation of the four stereoisomers was obtained with a mobile phase modified by the NiL^4 chelate (see Table 5). However, the α values for the most pronounced enantiomer pair, *R,S–S,R* of ephedrine and norephedrine or *R,R–S,S* of pseudoephedrine, were relatively low, even for the more effective selectand in the form of the NiL^4 chelate. However, it should be noted that the reported separation is more efficient than that obtained previously in an HPLEC system [13,14,16] when ephedrine isomers were not resolved. The observed retention order of

Table 4
Capacity factors, k', of isomers of amino alcohols containing two chiral centres in HPLC systems employing mobile phases modified by NiL^{1-4} chelates

No.	Compound	*R*,*S*				*S*,*R*				*S*,*S*				*R*,*R*			
		NiL^1	Nil^2	NiL^3	NiL^4	NiL^1	Nil^2	NiL^3	NiL^4	NiL^1	Nil^2	NiL^3	NiL^4	NiL^1	Nil^2	NiL^3	NiL^4
1	Ephedrine	20.7	21.0	21.3	21.6	21.4	21.8	22.4	22.7	22.8	23.1	23.7	24.8	23.8	24.3	25.7	27.3
2	Pseudoephedrine	22.3	22.8	23.6	24.1	23.7	24.1	24.7	25.8	25.6	26.7	27.3	28.4	26.1	28.9	30.1	32.3
3	Norephedrine	19.1	19.4	19.8	20.0	19.7	20.1	20.3	22.0	20.6	20.9	21.0	23.5	21.4	21.7	22.3	27.0

For experimental conditions, see Fig. 5.

Table 5
Selectivity of separation of isomers of amino alcohols containing two chiral centres in HPLC systems employing mobile phases modified by NiL^{1-4} chelates

Isomer pair	Ephedrine				Pseudoephedrine				Norephedrine			
	NiL^1	NiL^2	NiL^3	NiL^4	NiL^1	NiL^2	NiL^3	NiL^4	NiL^1	NiL^2	NiL^3	NiL^4
R,R–R,S	1.14	1.16	1.21	1.26	1.17	1.27	1.28	1.34	1.12	1.12	1.13	1.35
R,R–S,R	1.11	1.11	1.13	1.21	1.10	1.20	1.22	1.25	1.09	1.08	1.10	1.23
R,R–S,S	1.04	1.05	1.08	1.10	1.02	1.08	1.10	1.14	1.04	1.04	1.06	1.15
R,S–S,R	1.03	1.03	1.06	1.03	1.06	1.06	1.06	1.07	1.03	1.04	1.04	1.10
R,S–S,S	1.10	1.27	1.11	1.15	1.15	1.17	1.16	1.18	1.08	1.08	1.06	1.17
S,R–S,S	1.06	1.06	1.04	1.11	1.08	1.08	1.11	1.11	1.04	1.04	1.10	1.07

For experimental conditions see Fig. 5.

diastereoisomers ($RS < SR < SS < RR$) is consistent with the proposed chiral discrimination mechanism in which "three-point" associates are formed (see Fig. 6) by strongly retained *R,R*-enantiomers and nickel(II) chelates.

As shown in Fig. 7, an increasing concentration of nickel(II) chelate in the mobile phase usually slightly increased the observed values of the separation factors. The most effective are changes in concentration of the NiL^4 chelate.

Increasing the concentration of organic modifier decreased the enantiomeric separation, as illustrated in Fig. 8 for the phenylglycinol, phenylalanine, pseudoephedrine and norephedrine isomers.

Increasing the flow-rate of the mobile phase had virtually no effect on the observed enantioselectivity, as is shown in Fig. 9, probably owing to the minor effect on the values of the reduced plate height of the column as suggested by Rizzi [37] for another reversed-phase HPLC system employing chiral mobile phase additives.

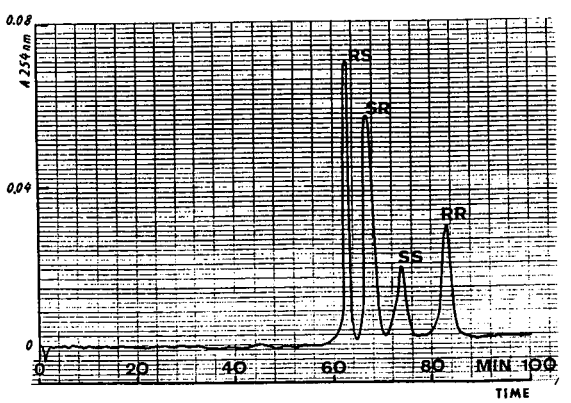

Fig. 5. Diastereomeric HPCMA separation of pseudoephedrine isomers by RP-HPLC with water–acetonitrile (20:80) (pH 6.0) as the mobile phase containing NiL^4 chelate ($1 \cdot 10^{-3}$ mol/l). For other experimental conditions, see Fig. 2.

3.2. HPLEC measurements

The results of the enantiomeric separation of amino alcohols obtained with the developed HPCMA system using helical nickel(II) chelates were compared with those for an HPLEC system

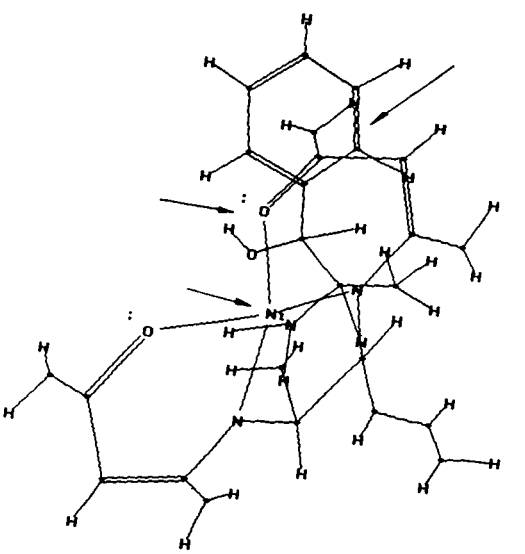

Fig. 6. Stereoscopic image of proposed structure of the NiL^4–(*R,R*)-norephedrine associate formed in the developed HPCMA chromatographic system. Arrows indicate positions of the possible interaction sites.

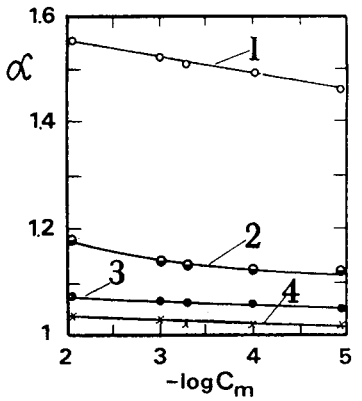

Fig. 7. Influence of the concentration of nickel(II) chelates (log C_m) in acetonitrile–water (20:8, v/v) mobile phase (pH 6) at a flow-rate of 1.3 ml/min on the separation factors (α) of phenylglycinol enantiomers: 1 = NiL^4; 2 = NiL^3; 3 = NiL^2; 4 = NiL^1.

an employing chiral stationary phase in the form of N-2′-hydroxy-*n*-dodecyl-L-hydroxyproline (HDHP) and a mobile phase containing copper(II) ions. This dynamically based chiral stationary phase was used by Busker and coworkers [26,38] for the HPLC separation of penicillamine enantiomers. Gunther [39] reviewed numerous applications of HDHP as a component of hydrocarbonaceous silica gel layers designated Chiralplate for thin-layer chromatographic enantioselective separations. The presence of an additional hydroxyl group in the alkyl side-chain of HDHP forms the second

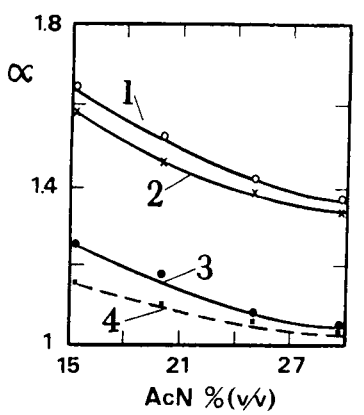

Fig. 8. Effect of acetonitrile (AcN) concentration in acetonitrile–water mobile phase (pH 6; concentration of NiL^4 chelate = $1 \cdot 10^{-3}$ mol/l; flow-rate 1.2 ml/min) on separation factors (α) of amino alcohol enantiomers: 1 = (*S*–*R*)-phenylglycinol; 2 = (*S*–*R*)-phenylalaninol; 3 = (*SS*–*RR*)-pseudoephedrine; 4 = (*RS*–*SR*)-norephedrine.

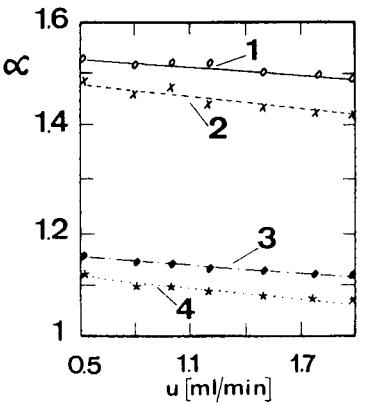

Fig. 9. Effect of flow-rate (u) of mobile phase [acetonitrile–water (20:80) (pH 6), concentration of NiL^4 chelate = $1 \cdot 10^{-3}$ mol/l) on separation factors (α) of amino alcohol enantiomers: 1 = (*S*–*R*)-phenylglycinol; 2 = (*S*–*R*)-phenylalaninol; 3 = (*SS*–*RR*)-pseudoephedrine; 4 = (*RS*–*SR*)-norephedrine.

stereogenic centre near the parent chiral hydroxyproline molecule. Both factors differentiate HDHP from N-*n*-dodecyl-L-hydroxypropline (DHP) and its N-alkyl derivatives applied previously as chiral stationary phases in the HPLC of amino acids and amino alcohol mixtures [13,14,28]. Considering the chiral recognition model developed by Davankov *et al.* [28], one would expect the hydroxyl substituent in HDHP to act as a supporting interactive site influencing the enatioselectivity of polar solute separations.

In Table 6 and Fig. 10 the observed retention of amino alcohols on the column packed with HDHP is illustrated. The *S*-enantiomers of noradrenaline and phenylglycinol were eluted first. Such a retention order of enantiomers is reversed for analogous solutes on the DHP column [14]. Phenylalaninol enantiomers were resolved using HDHP and acetonitrile–water (20:80) (pH 6) as the mobile phase containing $2 \cdot 10^{-4}$ mol l^{-1} copper(II) acetate. This result is also contrary to the previously reported retention of phenylalaninol on DHP phase using acetate buffer (pH 6) with an 8 mmol/l concentration of copper(II) acetate [14]. However, the retention orders of noradrenaline, phenylethanolamine and phenylglycinol on both the HDHP and DHP stationary phases under the applied experimental conditions were identical. Moreover, on HDHP shorter retention times of these solutes were obtained. Comparing the

Table 6
Capacity factors, k', and selectivity, α, of enantiomeric separations of amino alcohols in HPLEC experiments

No.	Compound	First-eluting	k_1' [a]	k_2' [b]	α
1	Noradrenaline	*S*	1.10	1.65	1.50
2	Phenylethanolamine	*S*	7.15	15.02	2.10
3	Phenylglycinol	*S*	10.71	18.21	1.71
4	Phenylalaninol	*S*	11.73	16.32	1.39
5	Norephedrine	*S,R*	12.30	23.34	1.89
6	Ephedrine	*S,R*	15.12	27.18	1.78
7	Pseudoephedrine	*R,R*	18.31	31.14	1.70

For experimental conditions, see Fig. 10.
[a] Capacity factor of first-eluting enantiomer.
[b] Capacity factor of second-eluting enantiomer.

results obtained on the HDHP with amino alcohol retentions achieved with the developed HPCMA system, the shorter retention and slightly greater values of the separation factors α (especially for phenylethanolamine enantiomers) are notable when the former HPLC system is applied (see Tables 4–6). Examining the retentions of ephedrine-like solutes (**5–7**) one can state that *S,R*-enantiomers were eluted first on both HDHP and DHP (see results in refs. 13 and 14). However, on HDHP the amino alcohols are less retained compared with the retentions reported on DHP [14] and with the developed HPCMA system. The selectivity of the prepared HPCMA system is greater, leading to separations of all enantiomers pairs (see Tables 5 and 6). Comparing the α values for *SR–RS* enantiomers of ephedrine calculated for the HDHP column with those obtained with the proposed HPCMA system, the former method was found to be more selective for the separation.

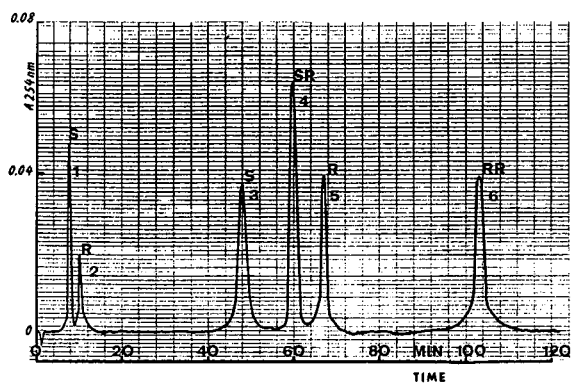

Fig. 10. Separation of noradrenaline, phenylalanine and ephedrine isomers of the HPLEC method employing an HDHP-coated Polsil ODS, 7 μl, column (25 × 0.4 cm I.D.) with acetonitrile–water (20:80) as mobile phase (pH 6.0) containing $2 \cdot 10^{-4}$ mol/l copper(II) acetate; flow-rate, 1.0 ml/min; column temperature 25°C; UV detection at 280 nm. Peaks; 1 = (*S*)-noradrenaline; 2 = (*R*)-noradrenaline; 3 = (*S*)-phenylalaninol; 4 = (*S,R*)-ephedrine; 5 = (*R*)-phenylalaninol; 6 = (*R,S*)-ephedrine.

3.3. *Analysis of pharmaceuticals*

The HPCMA separation method reported here was applied to determination of the content of pseudoephedrine enantiomers in samples of its oral dosage forms. Three different pseudoephedrine samples were analysed by both the HPCMA and HPLEC methods with four replicates. The results in Table 7 indicate that the methods have comparable repeatability and random error, as indicated by lower calculated values of the *F*-test compared with the critical value appropriate at the 0.95 probability level [40]. The methods do not differ significantly in accuracy, as verified by the values of *t* being lower than their critical value at the 0.99 probability level [40]. The correlation coefficient between the HPCMA and HPLEC results is near 0.97. However, the proposed HPCMA method offers a slightly lower relative error.

Table 7
Determination of pseudoephedrine enantiomers in pharmaceuticals

Formulation	Isomer	Method	Mean concentration[a], x (%)[b]	Sample S.D. (%)	F-Test[c,d]	t-test[c,e]
Tablet	*S,S*	HPCMA	43.1	0.181	1.90	1.10
		HPLEC	42.8	0.231		
	R,R	HPCMA	56.9	0.109	1.80	1.30
		HPLEC	57.2	0.156		
Syrup	*S,S*	HPCMA	45.1	0.123	2.10	1.80
		HPLEC	44.6	0.143		
	R,R	HPCMA	54.9	0.111	2.05	1.90
		HPLEC	55.4	0.120		
Elixir	*S,S*	HPCMA	40.1	0.125	1.10	1.05
		HPLEC	39.2	0.140		
	R,R	HPCMA	59.9	0.132	1.30	1.56
		HPLEC	60.8	0.142		

[a] Mean of four determinations.
[b] Expressed as a percentage of the claimed content.
[c] F- and t-tests were calculated for comparison of x values obtained in HPCMA and HPLEC measurements.
[d] Theoretical F ($P = 0.95$, $f_1 = f_2 = 3$) = 9.28.
[e] Theoretical t ($P = 0.99$, $f = 6$) = 3.71.

4. References

[1] A.M. Vermeulen, F.M. Belpaire, E. Moerman, F. DeSmet and M.G. Bogaert, *Chirality*, 4 (1992) 73.
[2] J. Gal, *J. Liq. Chromatogr.*, 9 (1986) 673.
[3] N. Nimura, Y. Kasahara and T. Kinoshita, *J. Chromatogr.*, 213 (1981) 327.
[4] V. Prelog, Z. Stojanak and K. Kovacevic, *Helv. Chim. Acta*, 65 (1982) 377.
[5] C. Pettersson and G. Schill, *J. Liq. Chromatogr.*, 9 (1986) 269.
[6] A. Karlsson and C. Pettersson, *Chirality*, 4 (1992) 323.
[7] W.H. Pirkle and M.H. Hyun, *J. Chromatogr.*, 322 (1985) 309.
[8] G. Gubitz, B. Pierer and W. Wendelin, *Chirality*, 4 (1992) 333.
[9] I.W. Wainer, T.D. Doyle, F.S. Fry, Jr. and Z. Hamidzadek, *J. Chromatogr.*, 355 (1986) 149.
[10] C.H. Shieh, B.L. Karger, L.R. Gelber and B. Feibush, *J. Chromatogr.*, 406 (1987) 343.
[11] L.R. Gelber, B.L. Karger, J.L. Neumeyer and B. Feibush, *J. Am. Chem. Soc.*, 106 (1984) 7729.
[12] C. Pettersson, E. Heldin and H.W. Stuurman, *J. Chromatogr. Sci.*, 28 (1990) 413.
[13] S. Yamazaki, T. Takeuchi and T. Tanimura, *J. Liq. Chromatogr.*, 12 (1989) 2239.
[14] S. Yamazaki, T. Takeuchi and T. Tanimura, *J. Chromatogr.*, 540 (1991) 169.
[15] D. Parker, *Analyst*, 117 (1992) 1313.
[16] W.F. Lindner and I. Hirschbock, *J. Liq. Chromatogr.*, 9 (1986) 551.
[17] S. Lam and G. Malikin, *J. Chromatogr.*, 368 (1986) 413.
[18] G. Bazylak, *Acta Univ. Łodz Folia Chim.*, 9 (1990) 93.
[19] G. Bazylak, *Analyst*, 117 (1992) 1429.
[20] G. Bazylak, *Analusis*, 20 (1992) 611.
[21] G. Bazylak, *Ann. Acad. Med. Łodz*, 32 (1992) 25.
[22] G. Bazylak, *Pol. J. Chem.*, 62 (1988) 331.
[23] G. Bazylak, *Pol. J. Chem.*, 66 (1992) 639.
[24] M. Bukowska-Strzyzewska, M. Maniukiewicz and G. Bazylak, *J. Crystallogr. Spectrosc. Res.*, 21 (1991) 157.
[25] G. Bazylak, *Ph.D. Thesis*, Technical University of Łodz, Łodz, 1990.
[26] E. Busker and J. Martens, *Fresenius' Z. Anal. Chem.*, 319 (1984) 907.
[27] S. Lubben, J. Martens and B. Roder, *Dtsch. Apoth.-Ztg.*, 132 (1992) 947.
[28] V.A. Davankov, A.S. Bochkov, A.A. Kurganow, P. Roumeliotis and K.K. Unger, *Chromatographia*, 13 (1980) 677.
[29] M.T. Peeran, G.S. Baravani and V.K. Bhalla, *Indian Drugs*, 25 (1988) 242.

[30] Y. Tapuchi, N. Miller and B.L. Karger, *J. Chromatogr.*, 205 (1981) 325.
[31] C.H. Lochmuller and H.H. Hangac, *J. Chromatogr. Sci.*, 20 (1982) 171.
[32] H.P. Jensen, *Acta Chem. Scand., Ser. A*, 30 (1976) 137.
[33] R. Fenton, F.S. Stephens, R.S. Vagg and P.A. Williams, *Inorg. Chim. Acta*, 201 (1992) 157.
[34] L.F. Lindoy, W.E. Moody and D. Taylor, *Inorg. Chem.*, 16 (1977) 1962.
[35] M.Y. Khuhawar, A.I. Soomro and A.G.M. Vasandami, *J. Chem. Soc. Pak.*, 12 (1990) 201.
[36] C. Dalgliesh, *J. Chem. Soc.*, 137 (1952) 3940.
[37] A.M. Rizzi, *J. Chromatogr.*, 542 (1991) 221.
[38] E. Busker, K. Gunther and J. Martens, *J. Chromatogr.*, 350 (1985) 179.
[39] K. Gunther, *J. Chromatogr.*, 448 (1988) 11.
[40] C.C. Li, *Introduction to Experimental Statistics*, McGraw-Hill, New York, 1964.

ELSEVIER

Journal of Chromatography A, 665 (1994) 87–99

JOURNAL OF CHROMATOGRAPHY A

Knowledge-based system for the automated solid-phase extraction of basic drugs from plasma coupled with their liquid chromatographic determination
Application to the biodetermination of β-receptor blocking agents

Ph. Hubert[a], P. Chiap[a], M. Moors[b], B. Bourguignon[b], D.L. Massart[b], J. Crommen*[,a]

[a]*Laboratory of Drug Analysis, Institute of Pharmacy, University of Liège, Rue Fusch 5, B-4000 Liège, Belgium*
[b]*Laboratory of Pharmaceutical and Biomedical Analysis, Pharmaceutical Institute, Free University of Brussels, Laarbeeklaan 103, B-1090 Brussels, Belgium*

Abstract

Techniques for the preparation of biological samples are often based nowadays on solid-phase extraction (SPE). The different SPE steps can be performed automatically on disposable extraction cartridges (DECs) by means of a sample processor. A knowledge-based system was developed to facilitate the development of fully automated methods for the solid-phase extraction of relatively hydrophobic basic drugs from plasma, coupled with their determination by high-performance liquid chromatography (HPLC). The DEC filled with 50 mg of cyanopropyl-bonded silica phase is first conditioned with methanol and buffer solution (pH 7.4). After sample application, the DEC sorbent is washed with the same buffer. The analytes are then desorbed with an appropriate eluent and the eluate is finally diluted with the same buffer as used in the HPLC mobile phase before injection. Under these conditions, only three variables are still to be optimized: the composition and volume of the elution solvent and the volume of buffer to be added to the eluate. On the basis of this general strategy, a decision tree providing information about suggested starting conditions and guidelines for the optimization of the three variables was developed and implemented by use of a hypermedia software. This didactic expert system was evaluated using several β-receptor blocking agents as model compounds and the operating conditions obtained for the automated SPE of these compounds are presented. A method for the determination of propranolol in plasma using the SPE conditions deduced from the knowledge-based system was validated. The absolute recovery of propranolol is *ca.* 93% and the limit of detection is 1.3 ng ml^{-1}. The mean within-day and between-day reproducibilities are 2.3 and 3.6%, respectively.

1. Introduction

When traces of drugs must be determined in complex matrices such as biological fluids, a sample handling procedure is usually needed prior to the HPLC analysis. The aims of the sample pretreatment are the release of the analyte from a conjugate or from proteins in the biological matrix, the elimination of proteins, which can clog the chromatographic column, and

* Corresponding author.

0021-9673/94/$07.00
SSDI 0021-9673(93)E0010-R

of endogenous compounds that can interfere in the assay (sample clean-up) and an increase in the concentration of the analyte to reach the detection range of the detector (trace enrichment) [1–3].

In current bioanalytical methods, solid-phase extraction (SPE) is increasingly used for sample preparation instead of traditional methods such as deproteinization or liquid–liquid extraction [3]. With the use of sample processors [4–9] such as the ASPEC (automatic sample preparation with extraction cartridges) system, the determination of drugs in plasma can be fully automated, the SPE on disposable extraction cartridges (DECs) being directly coupled with HPLC [6–8]. This is of particular interest when the number of samples is large. Most often, the use of an automated sample handling procedure leads to better results with respect to accuracy and precision than manual techniques. This holds especially true when the analyses must be performed in the low concentration range (ng ml^{-1}). However, the development of a new application is not straightforward and can be relatively time consuming [9]. For such automated systems, the lack of information about method development probably represents the main limitation.

On the basis of our expertise [8,10–16], a knowledge-based computer system for the development of automated SPE methods was elaborated. The expert system was until now restricted to the isolation of relatively hydrophobic basic drugs from plasma. The first choice for the DEC sorbent is cyanopropyl-bonded silica [10–12,14,16–19] and for the conditioning and washing steps a buffer solution of pH 7.4. After elution of the analyte with an appropriate solvent, the eluate is diluted with the same buffer as used in the HPLC mobile phase. Following this simple scheme, only three parameters are still to be optimized: the composition and volume of the elution solvent and the volume of buffer added to the eluate.

To build such an expert system, a decision tree providing information about suggested starting conditions and guidelines for the optimization of the variables mentioned above was constructed and implemented by use of hypermedia software in which the user is guided to the appropriate information through a series of questions.

For the determination in plasma of the β-adrenoreceptor antagonists chosen as model compounds in this study (Fig. 1), several methods have been proposed using either gas chromatography after derivatization [20–23] or high-performance liquid chromatography (HPLC) [18,19,24–38]. In the HPLC methods, fluorescence detection has often been preferred owing to the native fluorescence properties of most of these compounds [18,24–29,31–34,36]. UV

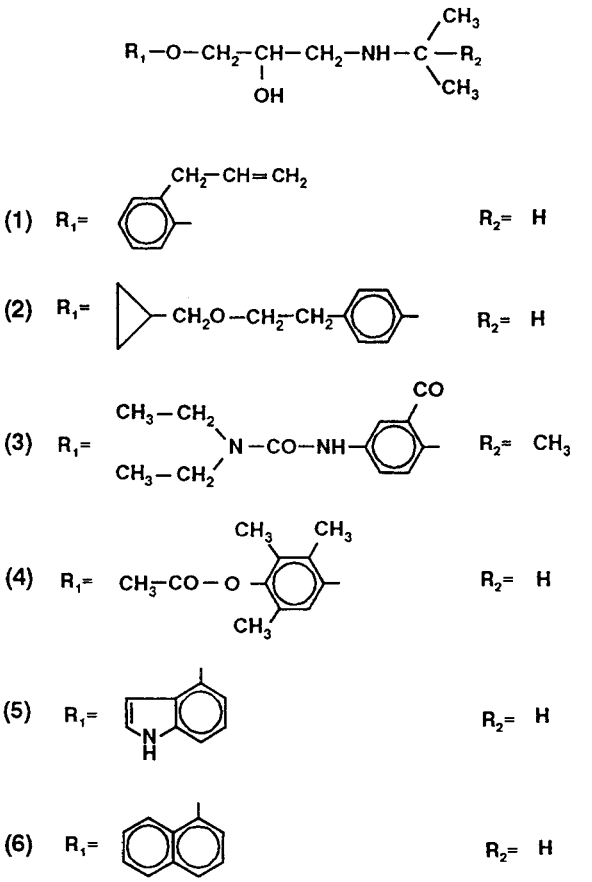

Fig. 1. Structures of the β-blocking receptor drugs investigated. 1 = Alprenolol; 2 = betaxolol; 3 = celiprolol; 4 = metipranolol; 5 = pindolol; 6 = propranolol.

[18,27,30,35,37] and amperometric [38] detection have been used in some instances.

In most bioanalytical methods mentioned above, the sample pretreatment consists of liquid–liquid extraction after alkalinization [29,31,36], followed by back-extraction into an acidic aqueous solution [24,26–28,30,32,33, 35,36]. In some instances, an additional extraction with an organic solvent after increasing the pH of the aqueous solution is performed [20–22]. Sample preparation by deproteinization has also been proposed [25]. The isolation of some β-blocking drugs by SPE, using either an Extrelut-1 column [34] or DECs packed with octadecyl- [23] or cyanopropyl-bonded silica [18], has also been considered. Finally, an HPLC method using SPE in a column-switching system has been described [38]. Except in the last instance, all sample preparation procedures were performed manually.

The principal aim of this work was to test the usefulness of the proposed knowledge-based system for the development of automated methods for the SPE of several β-receptor blocking drugs from plasma, coupled with their HPLC determination. The operating conditions obtained for automated SPE of these compounds are presented. In addition, a fully automated method for the determination of propranolol in plasma using the SPE conditions deduced from the expert system was validated with respect to recovery, linearity, precision and detectability.

2. Experimental

2.1. Apparatus

The HPLC system consisted of a Gilson (Villiers-le-Bel, France) Model 305 pump coupled to a Model F-1050 fluorescence detector from Merck–Hitachi (Darmstadt, Germany) and a Spectra 200 UV–Vis programmable wavelength detector from Spectra-Physics (San Jose, CA, USA).

A Manu-CART system, which contained a LiChroCART analytical column (250 × 4 mm I.D.) and a short LiChroCART guard column (4 × 4 mm I.D.) from Merck, was thermostated at 37 ± 0.1°C in a Julabo (Seelbach, Germany) VC 12 B water-bath.

The preparation of plasma samples was performed by use of an ASPEC system [6–8] from Gilson. This system consists of three components: a sample processor equipped with an *XYZ*-motion robotic arm, a Model 401 diluter/pipetter connected to a needle attached to the robotic arm by a transfer tube and a set of racks and accessories for disposable extraction cartridges and solvents. The SPE operations are performed on a specific rack which consists of a DEC holder, a drain cuvette and collection tubes. The DEC holder can be moved in such a way that each extraction cartridge is automatically located above the drain cuvette during the conditioning, loading and washing steps and above a collection tube during the elution step. The collected fraction is then introduced into a 0.25-ml loop of an electrically actuated injection valve for on-line HPLC analysis. The dispensing flow-rates of the different liquids used in the sampling handling procedure can be varied from 0.18 to 96.0 ml min^{-1}. The ASPEC system uses positive air pressure to push the different liquids through the DECs. The latter are covered with a special cap ensuring an air-tight fit while solvents, sample or air are dispensed through the needle.

The control of the HPLC and ASPEC systems and also the data collection were performed by use of an IBM compatible computer (CPU type 80486) equipped with two sets of Gilson software: GME-715 version 1.1. (HPLC System Controller) and GME-718 version 1.1. (Sample Manager). The hypermedia software used for the implementation of the knowledge on automated SPE was Toolbook 1.0 (Asymetrix, Bellevue, WA, USA).

2.2. Chemicals and reagents

Alprenolol hydrochloride was purchased from Sigma (Brussels, Belgium). Propranolol hydrochloride, betaxolol, pindolol, metipranolol and celiprolol hydrochloride were kindly supplied by

different pharmaceutical companies and were used as received.

Potassium dihydrogenphosphate, phosphoric acid (minimum 85%) and sodium hydroxide were of analytical-reagent grade from Merck. 2-Aminoheptane was obtained from Aldrich (Gillingham, Dorset, UK) and was doubly distilled before use [14]. Methanol and acetonitrile were of HPLC grade from Janssen (Geel, Belgium). Water was of Milli-Q quality (Millipore, Bedford, MA, USA).

Bond Elut DECs (1-ml capacity) packed with 50 mg of cyanopropylsilica (CN) with a particle size of 40 μm were used as supplied by Analytichem (Harbor City, CA, USA). When loaded with plasma the DECs were used only once, whereas they could be used several times by application of aqueous standard solutions of the analytes.

The LiChroCART analytical column was packed with Superspher 100 RP-18 (particle size 4 μm) and the LiChroCART guard column was filled with LiChrospher 100 RP-18 (particle size 5 μm) from Merck.

2.3. Chromatographic technique

The HPLC mobile phases were mixtures of 0.05 *M* phosphate buffer (pH 3.0) and acetonitrile or methanol, containing 0.5% (v/v) of 2-aminoheptane. The flow-rate was 1.2 ml min^{-1}. The nature and percentage of organic modifier in the mobile phase and the wavelengths selected for the fluorescence or UV absorbance detection of the different β-blocking drugs are given in Table 1.

The pH 3.0 phosphate buffer was prepared in a 1.0-l volumetric flask by dissolving 4.0 g of sodium hydroxide in 700 ml of water. The pH was adjusted to 3.0 with phosphoric acid (minimum 85%) and water was then added to the mark. The buffer solution was filtered through a nylon filter (0.45 μm) from Schleicher & Schüll (Dassel, Germany).

2.4. Standard solutions

Stock standard solutions of each analyte were prepared once a month in methanol at a concentration of 1.0 mg ml^{-1}. They were then stored in a refrigerator at 4°C. The methanolic solutions were first diluted with water to 10 μg ml^{-1}. The latter solutions were further diluted with water for spiking the plasma samples and with the HPLC mobile phase to measure the recoveries. New dilute solutions were prepared each day. Working standard solutions and spiked plasma samples were prepared in the concentration range 2.5–500 ng ml^{-1}.

2.5. Automatic solid-phase extraction procedure

The same operations as in a classical SPE procedure are performed automatically by use of an ASPEC system. After thawing of the plasma sample, the only manual operations are centrifu-

Table 1
Chromatographic conditions for β-blocking drugs

Analyte	Organic modifier[a] (%)	Fluorescence		UV absorbance: λ (nm)
		λ_{ex} (nm)	λ_{em} (nm)	
Alprenolol	ACN 30	230	300	–
Betaxolol	ACN 30	230	300	–
Celiprolol	ACN 25	350	480	–
Metipranolol	ACN 25	–	–	230
Pindolol	MeOH 30	255	315	–
Propranolol	ACN 30	255	340	–

[a] ACN = Acetonitrile; MeOH = methanol.

gation of the sample at 6000 rpm for 20 min and the introduction of an aliquot (*e.g.*, 2.0 ml) of the latter into a vial located in the appropriate rack of the sample processor. The automatic procedure starts by the washing of the needle and the external tubing of the injection valve with 2.0 ml of water. Between each step, the needle is rinsed with the same volume of water (flow-rate 24 ml min^{-1}) and a 10-mm air gap is generated inside the transfer tubing before the aspiration of other liquids in order to avoid cross-contamination.

The automatic sequence (see Table 2) is performed in the following way:

(i) DEC conditioning (flow-rate 6.0 ml min^{-1}; air volume 0.3 ml). At the beginning of the SPE procedure, the DEC holder is located above the drain cuvette (front position). The sorbent (cyanopropylsilica, 50 mg) is first treated with 1.0 ml of methanol; the excess of methanol is then removed with 1.0 ml of phosphate buffer (pH 7.4) in order to prepare the extraction cartridge for the application of the plasma sample.

(ii) Loading with plasma sample (flow-rate 0.18 ml min^{-1}; air volume 0.3 ml). A 1.0-ml volume of plasma sample is aspirated by the needle from the sample vial and applied on the corresponding extraction cartridge at the minimum dispensing flow-rate [8].

(iii) Washing (flow-rate 1.5 ml min^{-1}; air volume 0.6 ml). The sorbent bed is washed with 1.0 ml of phosphate buffer (pH 7.4).

(iv) Elution (flow-rate 1.5 ml min^{-1}; air volume 0.6 ml). The DEC holder is pushed by the needle above the collection tubes. The analyte is eluted from the sorbent bed with a suitable solvent. Even if another organic modifier is used in the HPLC mobile phase, methanol is selected as a starting elution solvent. The nature and volume of the latter are given in Table 3 for each compound tested. The eluate is collected in the corresponding collection tube positioned under the DEC.

(v) Dilution (flow-rate 1.5 ml min^{-1}; air volume 0.6 ml). A volume of the same buffer as used in the HPLC mobile phase (see Table III) is passed through the cartridge [14]. The DEC holder is then replaced in its front position for the following steps.

(vi) Mixing (flow-rate 1.5 ml min^{-1}). The homogenization of the final extract is performed by aspirating and dispensing it successively in the collection tube. These operations are repeated three times [15].

(vii) Injection. The total volume of the final extract or an aliquot thereof is aspirated from

Table 2
Starting scheme for the SPE of basic drugs from plasma on DEC

SPE step	Liquid	Volume (ml)	Dispensing flow-rate (ml/min)
Conditioning	Methanol	1.00	6.00
	Buffer (pH 7.4)	1.00	6.00
Sample loading	Plasma	1.00	0.18
Washing	Buffer (pH 7.4)	1.00	1.50
Elution	[a]	[a]	1.50
Buffer addition	HPLC buffer	[a]	1.50
Mixing	Plasma extract	[b]	3.00
Filling of the injection loop	Plasma extract	[b]	0.75

DEC: Bond Elut CN (50 mg; 1-ml capacity).
[a] To be optimized.
[b] Depends on the volume of the final extract. For the determination of propranolol in plasma, a 0.65-ml volume was introduced in the loop filler port of the injection valve.

Table 3
Nature and volume of the solvent used in the elution step and volume of buffer added to the organic eluate

Analyte	Elution solvent		HPLC buffer volume (μl)
	Nature[a]	Volume (μl)	
Alprenolol	MeOH + 0.3% AH	300	700
Betaxolol	MeOH + 0.3% AH	300	700
Celiprolol	MeOH + 0.2% AH	250	750
Metipranolol	MeOH	250	750
Pindolol	MeOH + 0.1% AH	300	700
Propranolol[b]	MeOH + 0.3% AH	240	410

HPLC buffer: phosphate buffer (pH 3.0).
[a] MeOH = Methanol; AH = 2-aminoheptane.
[b] Fully optimized experimental conditions.

the collection tube by the needle and introduced in the loop filler port of the injection valve. The excess is directed to waste. By automatic switching of the injection valve, 0.25 ml of the final extract is finally injected on to the analytical column of the HPLC system.

The chromatographic separation of a prepared sample is performed during the preparation of the next sample (concurrent mode).

Phosphate buffer (pH 7.4) was prepared in a 1.0-l volumetric flask by mixing 250 ml of 0.1 *M* potassium dihydrogenphosphate with 195.5 ml of 0.1 *M* sodium hydroxide and diluting to the mark with water. The pH of the buffer solution was controlled before filtration through a nylon filter (0.45 μm) from Schleicher & Schüll.

3. Results and discussion

3.1. General strategy for the development of fully automated bioanalytical methods

The general strategy summarized in Table 4 has been used successfully for developing methods in which automated SPE is coupled to HPLC for the determination of drugs in plasma [8,10–16,39].

The first step is the selection of an appropriate detection mode according to the properties of the analytes and the sensitivity and selectivity required. Fluorescence or electrochemical detection is preferred to UV detection, owing to their higher sensitivity and selectivity, when the analytes have native fluorescence or electroactive properties [40,41]. However, relatively few compounds have such properties and a derivatization step must then be introduced, making the bioanalytical procedure more complicated. For such compounds, UV detection is often a useful alternative, especially when the concentrations to be determined in the biological samples are not lower than 1 ng ml^{-1}.

Table 4
General strategy for the development of bioanalytical methods

(1) Selection of an appropriate detection mode
(2) Selection of appropriate HPLC conditions
(3) Elimination of possible memory effects
(4) Development of the SPE procedure with aqueous samples
(5) Control of method selectivity and analyte recovery with spiked plasma samples
(6) Method validation

The HPLC system is optimized by use of aqueous standard solutions of the analytes. Well documented in the literature [42–44], the selection of suitable HPLC conditions is often relatively straightforward. With basic drugs, the detrimental effects due to interactions of these compounds with the residual silanol groups on silica-based stationary phases can be avoided by use of highly deactivated modified silica [10,11,16,44] and/or by addition of a competing amine to the mobile phase [12,14,16,44]. In a bioanalytical procedure using UV detection, the retention of the analytes should be sufficiently high (capacity factors higher than 3) in order to avoid interferences with the front peak in the chromatogram, which is often relatively large in the high-sensitivity range. The use of a guard column and its frequent replacement are essential to maximize the lifetime of the analytical column [8].

At this stage of development, the presence of possible memory effects must be investigated by performing successive (at least six) direct injections of a standard solution of the analytes with the autosampler [14]. The aqueous buffer used as the dissolution medium is injected immediately afterwards. In the presence of memory effects, poor reproducibilities are often obtained on successive injections of the analytes (R.S.D.s >10%) and residual analyte peaks are generally observed on the blank chromatogram [14,45]. Such effects are due in most instances to the limited solubility of the analytes in the dissolution medium and in the rinsing and/or the washing liquids. These effects can usually be eliminated by adapting the pH of the aqueous buffer used as the dissolution medium or adding a certain percentage of organic modifier (*e.g.*, methanol) to the buffer. The use of phosphate buffer (pH 7.4) as washing liquid was found to be adequate in most instances [10,11,16,39].

After selection of suitable detection and HPLC conditions, the automated SPE procedure using DECs can also be developed by use of aqueous solutions of the analytes instead of spiked plasma samples in order to limit the consumption of DECs [11,14,39,45]. It was found that the DECs could be used several times with aqueous solutions whereas they could be employed only once after loading with plasma. By using the starting scheme presented in Table 2, very few parameters need to be optimized and the whole sample handling procedure can be developed in a relatively short time.

Subsequently, the fully automated SPE procedure coupled with HPLC determination is applied to blank and spiked plasma samples in order to confirm that method selectivity and the analyte recoveries are satisfactory. In most applications developed so far [8,10–16] according to this strategy, good results with respect to selectivity and analyte recovery have been obtained when spiked plasma samples were tested, so that no changes in the operating conditions selected by use of aqueous solutions of the analytes were necessary. However, if interfering peaks and/or a significant decrease in analyte recovery is observed with plasma samples, the SPE or HPLC parameters must be modified accordingly.

Finally, a complete validation of the bioanalytical procedure is performed.

3.2. Automated SPE procedure

Table 2 shows the different steps of a fully automated SPE procedure with DECs: the conditioning of the DEC with methanol and buffer, the application of the plasma sample, the washing step, the elution of the analytes from the cartridge, the addition to the eluate of a small volume of the same buffer as in the HPLC mobile phase, the homogenization of the extract and finally the filling of the injection loop with this extract.

The starting conditions given in Table 2 were found to be suitable in most applications [8,10–16]. The use of 50-mg DECs is particularly interesting as these cartridges can be loaded with 1 ml of plasma like the 100-mg DECs and they give rise to recoveries similar to those of the latter. However, roughly half the volumes are needed for the elution of the analytes from 50-mg DECs. The total volume of plasma extract is then reduced and the fraction of this volume that is injected into the HPLC system is proportionally larger [11,14,16,39].

The conditioning of the DECs is made in two steps. In the first step, the solvation or wetting of the sorbent is performed by passing several bed volumes of a solvent such as methanol through the DEC. Methanol is an effective solvating agent because it can interact with both the silanol groups at the silica surface and the carbon atoms of the bonded alkyl chains. In the second step, the excess of methanol is removed with a solvent similar to the sample solution to be extracted. In this respect, phosphate buffer (pH 7.4) is particularly suitable for preparing the solid phase before the application of the plasma sample.

In the sample loading step, a 1.0-ml plasma sample is applied on the solid phase. The analytes are then adsorbed on the solid phase while the proteins and other hydrophilic endogenous compounds pass through the sorbent bed. In the loading step, an important factor with respect to the analyte recovery is the dispensing flow-rate of the plasma sample on the DEC. As previously reported, while the dispensing flow-rates used in all the other steps of the SPE procedure are not critical, the use of a very low dispensing flow-rate during the application of a plasma sample is essential to obtain high analyte recoveries, especially when the analytes are strongly bound to plasma proteins [8,15,45]. Indeed, at higher dispensing flow-rates, the recoveries of the analytes decrease drastically because the residence time of the plasma sample in the DEC is reduced to such an extent that only part of the analytes is displaced from its binding to proteins and can be distributed to the solid phase. Consequently, the minimum dispensing flow-rate available (0.18 ml min^{-1}) has been systematically selected for the application of plasma in order to obtain sufficiently high recoveries (>90%). Under these conditions, the air volume introduced into the DEC after the sample application has no signifi-

cant influence, because the plasma delivery is so slow that there is virtually no residual volume of plasma at the top of the sorbent when air is dispensed [8,45].

Next, matrix components that might interfere with the analytes are washed from the DEC with a suitable solvent. In this washing step, phosphate buffer (pH 7.4) was selected because of its good clean-up efficiency: very clean chromatograms, devoid of interferences from plasma components, have been obtained in most instances [8,10–16,39]. With 50-mg cartridges, the volume of buffer used in the washing step should be limited to 1.0 ml [11,39]. On the other hand, the addition of methanol to the washing liquid gives rise to a significant decrease in the analyte recovery, especially when DECs packed with cyanopropylsilica are used in the SPE procedure [11,16].

After the elution of the analytes from the DEC with a limited volume of solvent, a volume of the same buffer as used in the HPLC mobile phase is added to the eluate in order to obtain a final extract with an eluting strength equivalent to that of the HPLC mobile phase, or lower if a concentration effect at the top of the HPLC column is wanted. It should be emphasized that when small volumes of solvent are used for the elution of the analytes, a constant volume of eluate, equivalent to the initial volume of solvent dispensed, is only obtained if the buffer to be added is also passed through the DEC [11,14,44].

The final extract is then homogenized by three successive pumping steps [15] and the total volume of this extract is generally introduced into the injection loop, the excess being directed to the waste.

Most SPE applications can be developed according this simple starting scheme. For the isolation of basic drugs from plasma, cyanopropylsilica was found to be the most suitable sorbent with respect to selectivity and analyte recovery [10–12,14,16,17–19]. Under these conditions, only three SPE parameters are still to be optimized: the composition and volume of the eluting solvent and the volume of buffer to be added to the eluate before injection [39,46].

3.3. Optimization scheme for automated solid-phase extraction

According to the starting scheme given in Table 2, 1.0 ml of plasma (or aqueous standard solution) is used in the SPE procedure and, in a first approach, the aim is to obtain the same volume for the final extract. Methanol was selected as starting elution solvent as it was found to give high recoveries in most instances [14,39]. The volumes of methanol and of HPLC buffer to be added to the eluate are then calculated in order to obtain a 1.0-ml volume of final extract with the same eluting strength as that of the HPLC mobile phase.

As can be seen in Fig. 2, once these standard SPE conditions have been settled, the first experiments are carried out and the absolute recovery of the analyte is determined. If the recovery is $\geq 90\%$, the selectivity of the auto-

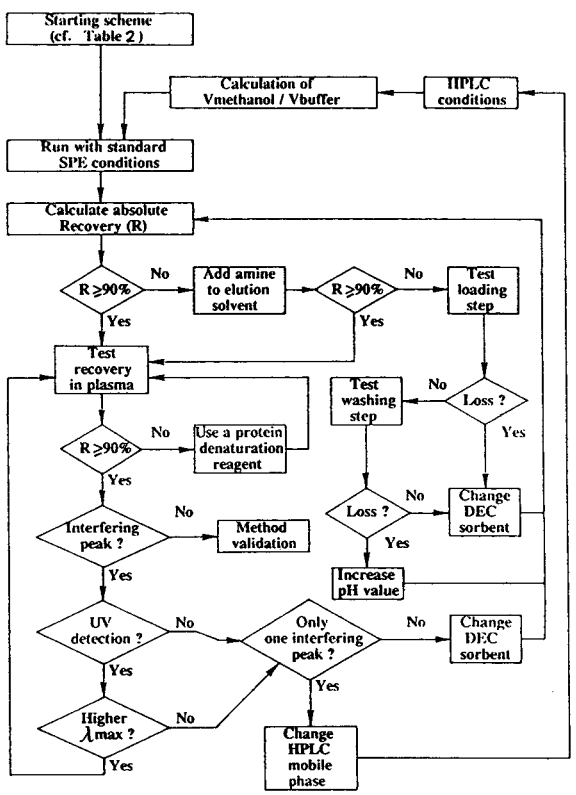

Fig. 2. Optimization scheme for automated SPE.

mated SPE procedure and the analyte recovery can be immediately evaluated with a spiked plasma sample. When the recovery obtained with the standard operating conditions and aqueous solutions of the analyte is not satisfactory (<90%), other options should be chosen.

A low recovery can be caused by several factors: the analyte may be too weakly retained on the solid phase, the analyte may be partially eluted during the washing step or the choice of methanol as elution solvent may be inappropriate. The latter possibility is the first to be investigated (*cf.*, Fig. 2). The primary interaction forces responsible for the retention of basic hydrophobic analytes on the cyanopropylsilica phase are in principle apolar Van der Waals forces, but secondary electrostatic interactions with the residual silanol groups are also very important, giving rise to very high retention and therefore low analyte recoveries in the SPE procedure. In order to minimize interactions with silanol groups, the addition to methanol of a competing amine, *e.g.*, 2-aminoheptane, as in the HPLC mobile phase, at a starting concentration of 0.1% is suggested. Table 5 shows the influence of the addition of this silanol masking agent at different concentrations on the recoveries of the different β-adrenoreceptor antagonists tested. As can be seen, a high extraction efficiency (>90%) was obtained in all instances by selecting a suitable percentage of competing amine to be added to the methanol.

If the addition of a competing amine to the eluent does not improve the recovery, possible losses in the loading and the washing steps are investigated (*cf.*, Fig. 2). Losses in the loading step may occur when the analyte is too weakly bound to the solid phase and it is then suggested that the cyanopropyl-bonded phase be replaced with the less polar phenyl or C_8 phases. When the analyte elutes partially with matrix components during the washing step, it is advisable to increase gradually the pH of the buffer used as the washing liquid. If the low recovery does not seem to be due to one of these three factors, it is concluded that the analyte is too strongly bound to the cyanopropyl-bonded phase and it is suggested that bare silica be used instead.

Once an acceptable SPE method has been developed for aqueous solutions of the analyte, the analyte recovery and the selectivity of the automated SPE method are evaluated with spiked plasma samples. If a decrease in the analyte recovery below 90% is observed with the plasma samples, this can probably be attributed to very strong binding of the analyte to plasma proteins. As shown in Fig. 2, it is then advisable to add a small volume of a concentrated acidic buffer which can displace the protein binding, so that the analyte can be more easily adsorbed on the solid phase.

Subsequently, the chromatogram of the final extract is evaluated with respect to the presence of interfering peaks. If the determination of the

Table 5
Influence of the addition of 2-aminoheptane on the recoveries of β-blocking drugs

Analyte	Recovery (%)[a]			
	MeOH	MeOH +0.1% AH	MeOH +0.2% AH	MeOH +0.3% AH
Alprenolol	79.0	82.0	91.3	95.5
Betaxolol	76.6	79.7	80.9	100.0
Celiprolol	87.0	88.5	97.0	–
Metipranolol	96.0	–	–	–
Pindolol	85.5	99.5	–	–
Propranolol	62.9	68.5	88.6	91.5

Concentration: 100 ng ml^{-1}.
[a] MeOH = Methanol; AH = 2-aminoheptane.

analyte is disturbed by interfering peaks, some options are given, such as the use of a more selective detection system or, with UV detection, the use of a higher measuring wavelength (λ_{max}). The analyst can also change the nature of the DEC sorbent or adapt the HPLC mobile phase composition in order to separate the interfering peaks from that of the analyte. In this instance, however, the whole SPE procedure must be optimized again by taking these changes into account.

Typical chromatograms obtained with plasma samples containing different β-blocking drugs are presented in Fig. 3.

3.4. Minimum volume of eluent

If a further improvement of the detectability for the analytes is wanted, an additional parameter in the development of such an automated sample preparation method is the selection of the minimum volume of solvent that still gives a satisfactory elution of the compounds [11,14,16].

In this work, this parameter was only optimized for propranolol. Fig. 4 shows that a significant decrease in the recovery of the analyte was only obtained when the volume of eluent was smaller than 0.20 ml. A volume of 0.24 ml of methanol containing 0.3% of 2-aminoheptane was finally selected for the elution of propranolol. In order to obtain a final extract with an eluting strength comparable to that of the HPLC mobile phase while minimizing dilution, 0.41 ml of pH 3.0 buffer should then be passed through the DEC [15], giving the extract a total volume of 0.65 ml (concentration factor = 1.54).

3.5. Validation of the automated method for the determination of propranolol in plasma

Absolute recovery

Table 6 gives the absolute recoveries of the analyte at six different concentrations ranging from 10 to 250 ng ml^{-1}. The mean absolute recovery for propranolol was *ca.* 93 ± 2%. This absolute recovery was calculated by comparing peak areas obtained from freshly prepared sample extracts with those found by direct injection

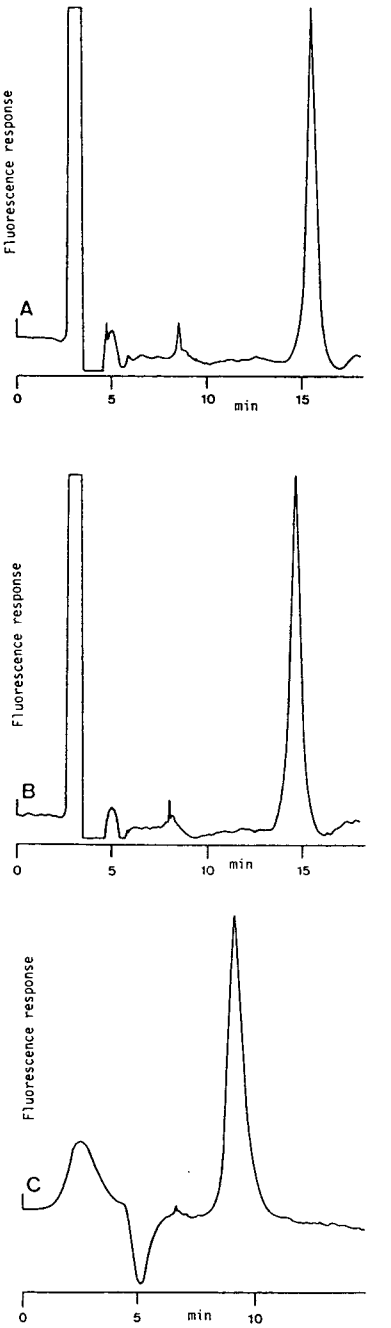

Fig. 3. Typical HPLC traces for plasma samples containing 100 ng ml^{-1} of (A) alprenolol, (B) betaxolol and (C) pindolol. Fluorescence response (arbitrary units) as a function of time (min). Extraction cartridge, Bond Elut CN (50 mg; 1-ml capacity). For SPE and chromatographic conditions, see Experimental (*cf.*, Tables 1–3).

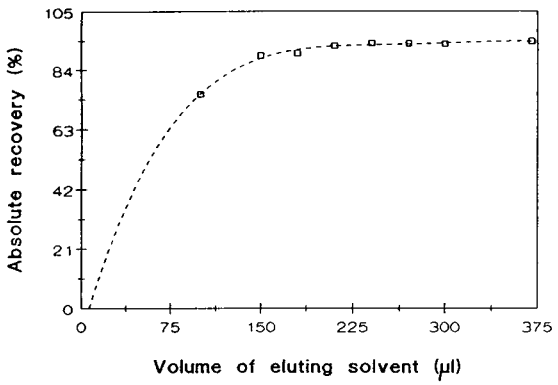

Fig. 4. Minimum volume of eluent for the elution step. Extraction cartridge, Bond Elut CN (50 mg; 1-ml capacity); eluent, methanol containing 0.3% of 2-aminoheptane; analyte concentration, 100 ng ml^{-1}. Other conditions as described under Experimental.

Table 6
Absolute recovery of propranolol using SPE on disposable extraction cartridges

Concentration (ng ml^{-1})	Recovery (%)
250	93.1
100	92.4
50	96.4
20	91.9
10	89.7
Mean	92.7
S.D.	2.5

of aqueous standard solutions at the same concentration [47], using the same autosampler.

Linearity

A calibration graph was constructed in the range 5–500 ng ml^{-1} ($n = 8$). Linear regression analysis made by plotting the analyte peak area (y) *versus* the concentration (x) in ng ml^{-1} gave the following equation:

$$y = 1465.1\ (\pm 7.8)x - 1740.4\ (\pm 1424.2)$$

$$r^2 = 0.99979$$

The linearity of the calibration graph is demonstrated by the good determination coefficient (r^2) obtained for the regression line.

Reproducibility

As shown in Table 7, the precision of the bioanalytical method was calculated by measuring the within-day and between-day reproducibilities of propranolol at four concentration levels ranging from 10 to 250 ng ml^{-1}. Mean values around 2.3% and 3.6% were obtained, respectively.

Accuracy

Accuracy was determined by analysing spiked plasma samples at four different concentrations and comparing the experimentally measured values with the nominal concentrations. The

Table 7
Precision and accuracy of the automated method for the HPLC determination of propranolol in plasma

Basis	Concentration (ng ml^{-1})	n	R.S.D.[a] (%)	R.E.M.[a] (%)
Within-day	250	5	1.6	1.2
	100	6	1.1	0.7
	50	5	2.4	2.2
	10	5	4.1	4.5
	Mean		2.3	2.2
Between-day	250	5	2.4	3.0
	100	5	2.1	2.3
	50	5	3.8	5.1
	10	5	5.9	4.2
	Mean		3.6	3.7

[a] R.S.D. = Relative standard deviation; R.E.M. = relative error of measurement.

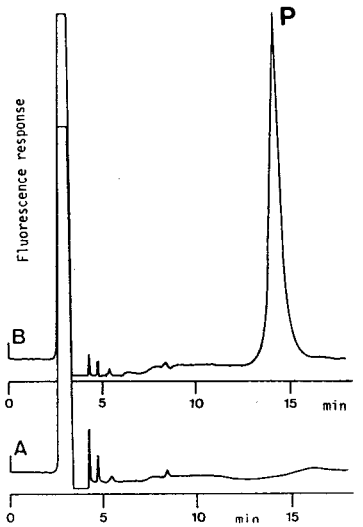

Fig. 5. Typical chromatograms of extracts from (A) blank plasma and (B) plasma spiked with 100 ng ml^{-1} of propranolol obtained by using SPE on DECs coupled with HPLC and fluorimetric detection. Fluorescence response (arbitrary units) as a function of time (min). For SPE and chromatographic conditions, see Experimental (*cf.*, Tables 1–3). Peak: P = propranolol.

accuracy of the automated method expressed as the relative error of measurement is given in Table 7. The mean values are very close to the nominal concentrations of propranolol, showing a method accuracy ranging from 0.7 to 5.1%.

Detectability

The limit of detection (LOD) and limit of quantification (LOQ) were calculated from the regression line [48] obtained with calibration graphs in the range 2.5–100 ng ml^{-1} (r^2 = 0.99986). The LOD and LOQ for propranolol were 1.3 and 4.5 ng ml^{-1}, respectively.

Selectivity

No endogenous sources of interference were observed at the retention time of the analyte. Typical chromatograms obtained with a blank plasma and with a spiked plasma containing 100 ng ml^{-1} of propranolol are presented in Fig. 5.

4. References

[1] D. Westerlund, *Chromatographia*, 24 (1987) 155.
[2] C.K. Lim, *Trends Anal. Chem.*, 7 (1988) 340.
[3] R.D. McDowall, J.C. Pearce and G.S. Murkitt, *J. Pharm. Biomed. Anal.*, 4 (1986) 3.
[4] R.D. McDowall, E. Doyle, G.S. Murkitt and V.S. Picot, *J. Pharm. Biomed. Anal.*, 7 (1989) 1087.
[5] R.D. McDowall, J.C. Pearce and G.S. Murkitt, *Trends Anal. Chem.*, 8 (1989) 134.
[6] M.C. Rouan, J. Campestrini, J.B. Lecaillon, J.P. Dubois, M. Lamontagne and P. Pichon, *J. Chromatogr.*, 456 (1988) 45.
[7] J.C. Pearce, R.D. McDowall, A. El Sayed and B. Pichon, *Int. Lab.*, November/December (1990) 34.
[8] Ph. Hubert and J. Crommen, *J. Liq. Chromatogr.*, 13 (1990) 3891.
[9] H. Lingeman, R.D. McDowall and U.A.Th. Brinkman, *Trends Anal. Chem.*, 10 (1991) 48.
[10] Ph. Hubert, P. Chiap and J. Crommen, *J. Pharm. Biomed. Anal.*, 9 (1991) 877.
[11] Ph. Hubert, P. Chiap and J. Crommen, *J. Pharm. Biomed. Anal.*, 9 (1991) 883.
[12] Ph. Hubert, P. Chiap, A. Ceccato, I. Bechet, R. Sibenaler-Dechamps, P. Maes and J. Crommen, *J. Pharm. Biomed. Anal.*, 10 (1992) 937.
[13] P. Maes, R. Sibenaler-Dechamps, C. Zimmer, M. Renson, Ph. Hubert and J. Crommen, *J. Pharm. Belg.*, 46 (1992) 198.
[14] Ph. Hubert and J. Crommen, *J. Liq. Chromatogr.*, in press.
[15] Ph. Hubert, P. Chiap, B. Evrard, L. Delattre and J. Crommen, *J. Chromatogr.*, 622 (1993) 53.
[16] Ph. Hubert, P. Chiap and J. Crommen, unpublished results.
[17] G. Musch and D.L. Massart, *J. Chromatogr.*, 432 (1988) 209.
[18] G. Musch, Y. Buelens and D.L. Massart, *J. Pharm. Biomed. Anal.*, 7 (1989) 483.
[19] M. Moors and D.L. Massart, *Trends Anal. Chem.*, 9 (1990) 46.
[20] M. Guerret, D. Lavene and J.R. Kiechel, *J. Pharm. Sci.*, 69 (1980) 1191.
[21] T.M. Ludden, D.A. Boyle, D. Gieseker, G.T. Kennedy, M.H. Crawford, L.K. Ludden and W.A. Clementi, *J. Pharm. Sci.*, 77 (1988) 779.
[22] C.R. Lee, A.C. Coste and J. Allen, *Biomed. Environ. Mass Spectrom.*, 16 (1988) 387.
[23] M.P. Quaglio, A.M. Bellini and L. Minozzi, *Il Pharmaco*, 47 (Suppl. to No. 5) (1992) 799.
[24] R.L. Nation, G.W. Peng and W.L. Chiou, *J. Chromatogr.*, 145 (1978) 429.
[25] M. Lo and S. Riegelman, *J. Chromatogr.*, 183 (1980) 213.
[26] H. Winkler, W. Ried and B. Lemmer, *J. Chromatogr.*, 228 (1982) 223.

[27] J.N. Buskin, R.A. Upton, F. Sörgel and R.L. Williams, *J. Chromatogr.*, 230 (1982) 454.
[28] V.D. Hippmann and F. Tabacs, *Arzneim.-Forsch. Drug Res.*, 33 (1983) 8.
[29] R.P. Koshakji and A.J.J. Wood, *J. Pharm. Sci.*, 75 (1986) 87.
[30] B.J. Shields, J.J. Lima, P.F. Binkley, C.V. Leier and J.J. MacKichan, *J. Chromatogr.*, 378 (1986) 163.
[31] E.C. Kwong and D.D. Shen, *J. Chromatogr.*, 414 (1987) 365.
[32] H.T. Smith, *J. Chromatogr.*, 415 (1987) 93.
[33] A. Tracqui, P. Kintz, J. Himber, A.A.J. Lugnier and P. Mangin, *Forensic Sci. Int.*, 38 (1988) 37.
[34] K.P. Devi, K.V.R. Rao, S.K. Baveja, T. Leeman and P. Daye, *J. Chromatogr.*, 434 (1988) 265.
[35] F.F.T. Ververs, H.G. Schaefer, J.P. Lefevre, L.M. Lopez and H. Derendorf, *J. Pharm. Biomed. Anal.*, 8 (1990) 535.
[36] D. Chmielowiec, D. Schuster and F. Gengo, *J. Chromatogr. Sci.*, 29 (1991) 37.
[37] W.P. Gluth and F. Sörgel, *Pharmazie*, 46 (1991) 336.
[38] M. Telting-Diaz, M.T. Kelly, C. Hua and M.R. Smyth, *J. Pharm. Biomed. Anal.*, 9 (1991) 889.
[39] Ph. Hubert, P. Chiap and J. Crommen, presented at the *3rd International Symposium on Pharmaceutical and Biomedical Analysis, Boston, MA, April 28–May 1, 1991.*
[40] G. Musch, M. De Smet and D.L. Massart, *J. Chromatogr.*, 348 (1985) 97.
[41] G. Musch and D.L. Massart, *J. Chromatogr.*, 370 (1986) 1.
[42] M. De Smet, G. Musch, A. Peeters, L. Buydens and D.L. Massart, *J. Chromatogr.*, 485 (1989) 237.
[43] G. Szepesi and K. Valko, *J. Chromatogr.*, 550 (1991) 87.
[44] G. Szepesi, *How to Use Reverse-Phase HPLC*, VCH, New York, 1992, p. 181.
[45] Ph. Hubert and J. Crommen, paper presented at the *2nd International Symposium on Pharmaceutical and Biomedical Analysis, York, April 4–7, 1990.*
[46] Ph. Hubert, P. Chiap, M. Moors, D.L. Massart and J. Crommen, presented at the *17th International Symposium on Column Liquid Chromatography, Hamburg, May 9–14, 1993.*
[47] A.R. Buick, M.V. Doig, S.C. Jeal, G.S. Land and R.D. McDowall, *J. Pharm. Biomed. Anal.*, 8 (1990) 629.
[48] J.C. Miller and J.N. Miller, *Statistics for Analytical Chemistry*, Ellis Horwood, Chichester, 1984, p. 96.

ELSEVIER

Journal of Chromatography A, 665 (1994) 101–104

JOURNAL OF CHROMATOGRAPHY A

Automatic solid-phase extraction and high-performance liquid chromatographic determination of quinidine in plasma

E. Brandšteterová*[,a], D. Romanová[b], D. Králiková[c], L. Božeková[c], M. Kriška[c]

[a]*Department of Analytical Chemistry, Slovak Technical University, Radlinského 9, 812 37 Bratislava, Slovak Republic*
[b]*Cancer Research Institute, Slovak Academy of Sciences, Bratislava, Slovak Republic*
[c]*Department of Pharmacology, Medical Faculty, Comenius University, Bratislava, Slovak Republic*

Abstract

High-performance liquid chromatography (HPLC) was used for the therapeutic drug monitoring of quinidine in clinical samples. Solid-phase extraction (SPE) was studied in both off-line and on-line modes. SPE was performed in an automatic on-line mode using a fully automated Prospekt system. Extraction recoveries were in the range 97.1–99.4% for 1–2 μg/ml quinidine concentrations. For HPLC separation an Ultrasep RP-8 reversed-phase column was applied with acetonitrile–water (9:1) containing 0.3% triethylamine (pH 2.5) as the mobile phase. The Prospekt system is recommended for the routine monitoring of quinidine in plasma samples. Concentrations were in therapeutic range (1.2–3.6 μg/ml).

1. Introduction

Quinidine is widely used in the therapy of atrial fibrillation and certain other cardiac arrhythmias. It is generally regarded as a myocardial depressant drug as it lowers excitability, conduction velocity and contractibility. The quinidine preparations given to patients contain small amounts of dihydroquinidine, which has cardiac effects similar to those of quinidine [1].

Several different assay methods for quinidine have been described. Such as fluorescence measurements, which are non-specific. Certain high-performance liquid chromatographic (HPLC) procedures have been published for quinidine determination in therapeutic concentrations in plasma (2–5 μg/ml).

Liquid extraction with benzene has been applied for the simultaneous determination of quinidine and caffeine with theobromine as an internal standard. The detection limit was 0.5 μg/ml with UV detection (254 nm) [2]. A cyano-bonded column has been tested for the HPLC determination of quinidine in serum and urine [3]. Both UV and fluorescence detection were compared.

Quinidine and quinine have been determined in sheep plasma samples following extraction with hexane–ethyl acetate (9:1). The main pharmacokinetic parameters were calculated [4]. Standard extraction procedures have been published for a general method and the analysis of pharmaceutical dosage forms by HPLC using a μBondapak C_{18} column with binary solvent system has been reported [5].

An HPLC method for some indole and quinoline alkaloids including quinidine and quinine used a LiChrosorb RP-8 Select B column and UV detection (275 nm) [6]. HPLC with fluorescence detection has been recommended

* Corresponding author.

0021-9673/94/$07.00
SSDI 0021-9673(93)E1273-3

for the determination of quinidine and quinine in plasma and blood following simple liquid–liquid extraction; cinchonine was applied as an internal standard. The extraction recoveries were 79.3% for quinidine and 82.9% for quinine [7].

Extraction with methanol–dichlormethane (15:95) has been applied to the HPLC separation and determination of quinidine in serum with UV detection at 210 nm [8]. The calibration graph was linear in the range 1–5 μg/ml.

The aim of this work was to develop a rapid and simple method for the automated on-line SPE–HPLC determination of quinidine in plasma samples for the therapeutic concentration monitoring of patients treated with quinidine as an active antiarrhythmics. This method could permit analysis without a separate plasma preseparation and direct injection of clinical samples is possible.

2. Experimental

2.1. Apparatus

HPLC experiments were carried out on an LKB (Bromma, Sweden) modular HPLC system and a Knauer (Bad Homburg, Germany) isocratic HPLC system. For automatic sample preparation, the Prospekt SPE system (SunChrom Friedrichsdorf, Germany) combined with a solvent delivery unit (SDU) and a Marathon autosampler was tested. SPE Bakerbond cartridges (C_{18}, 10 × 3 mm I.D.) (J.T. Baker, Gross-Gerau, Germany) were used for on-line SPE of clinical samples. The mobile phase was acetonitrile–water (15:85) containing 0.3% of triethylamine (pH 2.5) at a flow-rate of 0.6 ml/min. Phosphoric acid was used to adjust the pH to 2.5. Separations were carried out with an Ultrasep C_8 column (Bischoff, Leonberg, Germany).

2.2. Chemicals

Standards of quinidine and quinine were obtained from Slovakofarma (Hlohovec, Slovak Republic) and methanol, acetonitrile, triethylamine and phosphoric acid were supplied by Lachema (Brno, Czech Republic).

2.3. Procedure

In the on-line SPE mode, the cartridge was washed with methanol and with water, each for 2 min (2 ml/min). After loading a clinical sample (100 μl), the proteins were removed by washing with water for 2 min (1 ml/min) and the drugs were eluted into the chromatographic column with the mobile phase for 1 min (0.6 ml/min).

3. Results and discussion

According to the literature, the recommended content of acetonitrile in the mobile phase is 4–20% (v/v). Triethylamine is an important component of the mobile phase as it improves the peak shape, resolution and selectivity. It was found that its concentration did not change the retention time significantly. 0.3% of triethylamine was sufficient and with 15% acetonitrile yielded a resolution $R_{ij} = 1.4$ and a selectivity coefficient of 1.25.

Automatic on-line SPE is a very effective preseparation technique and coupling the preseparation cartridge with the analytical column gives the possibility of direct injection of clinical samples. This procedure was realized using the Prospekt system, which is a fully automated on-line sample clean-up and injection system that combines the constant quality assurance advantages of a disposable cartridge system with the automated aspects of precolumn technology [9]. Samples are automatically loaded on disposable cartridges, purged with one or more liquids for sample clean-up and directly eluted to the HPLC column (Fig. 1). Within the Prospekt system all samples undergo exactly the same procedure including the time span between extraction and chromatographic separation. The whole system is controlled by the Prospekt unit to change solvents, flow-rates and number of steps. 99 programmes give the possibility of changing the parameters for different types of analyses. A

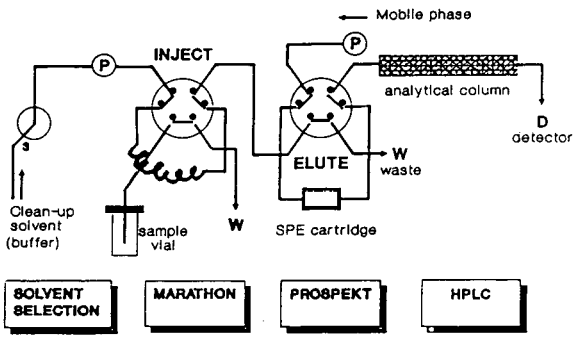

Fig. 1. Switching diagram for elution and analysis.

schematic diagram of the SPE–HPLC system is shown in Fig. 2.

A chromatogram obtained by automatic SPE–HPLC analysis of a serum sample (after treatment with quinidine) with the quinine as an internal standard, using the Bischoff C_8 column and the Prospekt system with Bakerbond cartridges, is illustrated in Fig. 3. Both compounds and dihydroquinidine were well separated. No interferences from serum sample are revealed in chromatogram.

The detection limit for quinidine was 25 ng/ml and the extraction recoveries were 97.1–99.4% for 1–2 μg/ml quinidine concentrations.

The method has been applied in hospital laboratories for routine monitoring. The overall procedure is efficient as the system begins the analysis of a new sample before that of the previous sample is completed. The results of some practical clinical analyses are given in

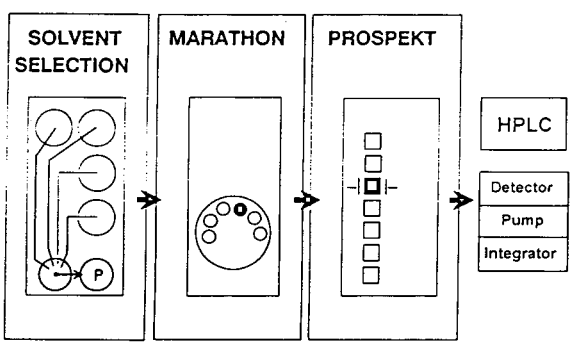

Fig. 2. Fully automated sample preparation system.

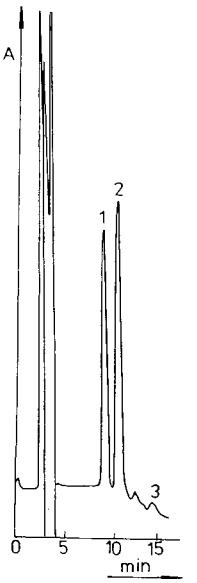

Fig. 3. SPE–HPLC of a clinical sample. Column, Bischoff Ultrasep C_8; Mobile phase, acetonitrile–water (15:85) containing 0.3% triethylamine (pH 2.5); flow-rate, 0.6 ml/min; detection, UV at 250 nm. Peaks: 1 = quinidine; 2 = quinine; 3 = dihydroquinidine.

Table 1. All the quinidine concentrations were within the therapeutic range.

4. Acknowledgements

We thank SunChrom (Spark Deutschland), (Friedrichsdorf, Germany) for providing the Prospekt system and Donau Trading (Zürich, Switzerland and Bratislava, Slovakia) for the Bischoff Ultrasep C_8 column. Bakerbond car-

Table I
Quinidine concentrations in clinical samples

Patient No.	Quinidine (μg/ml)	Within-batch R.S.D. (%) ($n = 5$)
1	3.4	1.4
2	3.3	1.8
3	3.6	2.1
4	1.2	1.2
5	2.3	1.9

tridges were supplied by J.T. Baker (Gross-Gerau, Germany).

5. References

[1] *Drug Monitoring Data*, American Association for Clinical Chemistry, Washington, DC, 1980.
[2] L.N. Ace and B. Chandhuri, *Anal. Lett.*, 20 (1987) 1483.
[3] J.J. McKichan and B. Shields, *Ther. Drug Monit.*, 9 (1987) 104.
[4] G.W. Mikaly, K.M. Hyman and R.A. Smallwood, *J. Chromatogr.*, 415 (1987) 177.
[5] A.S. Sidhu, J.M. Kennedy and S. Deeble, *J. Chromatogr.*, 391 (1987) 233.
[6] A.L. Hermans, T. Van der Leer and R. Verpoorte, *J. Chromatogr.*, 479 (1989) 39.
[7] M.D. Edstein, E. Prasitthipayoung and A. Sabchareon, *Ther. Drug Monit.*, 12 (1990) 493.
[8] G.L. Hoger, D.C. Clawson and A. Brookshier, *J. Chromatogr.*, 572 (1991) 159.
[9] *Prospekt, Technical Specifications*, Spark Holland, Emmen.

ELSEVIER

Journal of Chromatography A, 665 (1994) 105–109

JOURNAL OF CHROMATOGRAPHY A

Short Communication

Application of high-performance liquid chromatography to the analysis of the complex volatile mixture of blackcurrant buds (*Ribes nigrum* L.)

J. Píry*, A. Príbela

Department of Saccharides and Food Preservation, Faculty of Chemical Technology, Slovak Technical University, Radlinského 9, 812 37 Bratislava, Slovak Republic

Abstract

The essential oil of blackcurrant buds was fractionated into hydrocarbons and oxygenated compounds and the two fractions were submitted to reversed-phase high-performance liquid chromatographic (HPLC) column. Volatile carbonyls belong among the most important compounds for the blackcurrant flavour and were therefore analysed in detail. The carbonyls were converted into 2,4-dinitrophenylhydrazones and the mixture of 2,4-dinitrophenylhydrazones was separated into derivatives of keto acids and monocarbonyl and dicarbonyl compounds. Each fraction was submitted to HPLC. The results of the HPLC separations are discussed.

1. Introduction

The most important part of the blackcurrant shrub for flavour isolation is the dormant buds. The essential oil of blackcurrant buds gives off a strong terpenic flavour overwhelmed by a catty note [1]. Although the hydrocarbon fraction represents the major part of the oil, it does not explain the blackcurrant odour. The oxygenated compounds represent the most odorous volatile components and exhibit the characteristic blackcurrant odour [2,3]. The volatile compounds in blackcurrant buds have been investigated [3–6] using gas chromatography, mass spectrometry and infrared spectrometry. The application of high-performance liquid chromatography (HPLC) in aroma research is still in a stage of development. In the literature emphasis is put on the potential of this method for the separation of aroma concentrates. An effective HPLC method has been used for prefractionation of monoterpene and sesquiterpene hydrocarbons from the oxygenated compounds [4,7]. Liquid chromatography can be applied to subdivide an aroma concentrate into fractions in order to judge them sensorially.

This study was undertaken in order to increase the knowledge of essential oil analysis and blackcurrant bud volatiles. The objectives were to separate the volatile mixture into hydrocarbons and oxygenated compounds and to precipitate the volatile components with a carbonyl group.

* Corresponding author.

0021-9673/94/$07.00
SSDI 0021-9673(93)E0037-U

The results of HPLC separations of hydrocarbons, oxygenated compounds and carbonyls are described. The derivatives of carbonyl compounds have been separated previously only using thin-layer chromatography [8].

2. Experimental

Dormant buds (*Ribes nigrum* L., variety Eva) were harvested from cuttings during February 1993. The variety is descended form a crossing of Silvergieter's Zwarte × Holland Black. The buds were stored at −21°C before use. All reagents used (HPLC grade) were obtained from Lachema (Brno, Czech Republic), except for methanol and pentane (HPLC grade), which were obtained form Merck (Darmstadt, Germany).

2.1. Analysis of blackcurrant bud essential oil

Dormant buds (100 g) were mixed with 500 ml of distilled water and comminuted in a blender for 3 min. The volatile components were steam distilled in a Likens–Nickerson extractor (constructed by Mr. Greif of this department) for 45 min with pentane (100 ml) as solvent. The pentane extract was dried over anhydrous Na_2SO_4. The solution was filtered and the pentane was evaporated on a water-bath at 40°C under atmospheric pressure through a Vigreux column (Kavalier, Sázava and Sáz, Czech Republic) to 0.5 ml. The concentrate was fractionated in a jacketed column at 11°C on a 5 g of silica gel (0.2–0.5 mm) (Merck) hydrated to 15% (w/w). The hydrocarbons were eluted with 50 ml of pentane and the oxygenated fraction was eluted with 40 ml of diethyl ether. The eluates were dried over anhydrous Na_2SO_4 and concentrated to 0.4 ml for HPLC analysis. A HPP 4001 high-pressure pump equipped with a LCD 2563 UV–Vis detector and a TZ 4620 line recorder (Laboratorní přístroje, Prague, Czech Republic) were used. Separations were performed using a Separon SGX C_{18} reversed-phase column (150 mm × 3 mm I.D.), particle diameter 5 μm (Tessek, Prague, Czech Republic). The operating conditions were as follows: mobile phase, methanol–water [4:1 (v/v) for the hydrocarbon fraction and 1:1 (v/v) for the oxygenated fraction], sensitivity, 8; UV detection at 254 nm; injection volume, 0.5 μl (LCI-30 injector; Laboratornmí přístroje).

2.2. Analysis of the carbonyls of blackcurrant bud volatiles

Dormant buds (250 g) were mixed with 1000 ml of distilled water and comminuted in a blender for 4 min. The volatile components were steam distilled in a distillation apparatus at atmospheric pressure. The ultimate volume of a distillation product was 200 ml.

Approximately 25 ml of a 1% solution of 2,4-dinitrophenylhydrazine in 7.5% hydrochloric acid were added to the distillation product. The suspension was heated at 100°C for 5 min and then cooled to room temperature. After standing overnight, the suspension with precipitated 2,4-dinitrophenylhydrazones (2,4-DNPHs) was filtered and the excess of reagent removed by washing with 7.5% hydrochloric acid until the effluent becomes colourless. The residual HCl was then removed by washing with water. Precipitated 2,4-DNPHs were dissolved in 100 ml of chloroform.

The chloroform solution of 2,4-DNPHs was extracted by shaking five times with 10 ml of 10% sodium carbonate solution to remove the 2,4-DNPHs of keto acids. After adjustment of the pH to 3 with 85% phosphoric acid, the 2,4-DNPHs of keto acids were extracted by shaking five times with 10 ml of chloroform. The chloroform extract was dried over anhydrous Na_2SO_4 and concentrated on a water-bath of 0.5 ml.

The chloroform solution of 2,4-DNPHs was dried over anhydrous Na_2SO_4 and heated at 62°C to remove the solvent. The dry residue was extracted by shaking five times with 10 ml of *n*-hexane to dissolve the mono-2,4-DNPHs. The hexane extract was concentrated on a water-bath to 0.5 ml.

The dry residue was dissolved in 50 ml of chloroform. The chloroform solution of bis-2,4-

DNPHs was concentrated on a water-bath to 0.5 ml.

Each fraction was submitted to HPLC analysis. The conditions were the same as for the analysis of the blackcurrant bud essential oil except that the mobile phase was methanol–water (4:1, v/v) for each fraction and UV detection was carried out at 365 nm.

3. Results and discussion

Steam distillation–extraction of the buds allows the recovery of 0.4–0.6 ml of essential oil per 100 g of buds.

In the literature emphasis is put on the potential of HPLC for the separation of aroma concentrates. However, HPLC analysis of a total essential oil usually does not give a complete separation of all of the components present, the peaks of the hydrocarbon constituents often overlapping with those of oxygen-containing compounds. Prefractionation of a naturally occurring mixture of essential oils by column chromatography is effective in separating hydrocarbons from oxygenated compounds and leads to a better HPLC separation. For this reason the blackcurrant bud essential oil mixture was fractionated into hydrocarbons and oxygenated compounds by column chromatography on silica gel by elution with pentane and diethyl ether.

The HPLC traces for the hydrocarbons and oxygenated compounds are shown in Figs. 1 and 2. In a reversed-phase HPLC column, increasing numbers of carbon atoms cause an increase in retention time, but an increase in the number of carbon–carbon double bonds cause a decrease in retention time [9]. As a consequence of using a reversed-phase HPLC column, the sesquiterpenes and sesquiterpenoids have longer retention times than monoterpenes and monoterpenoids and this provides a basis for peak identification. Injection of pure α-pinene, β-pinene, α-terpinene, 3-carene, *m*-cymene, *p*-cymene (Aldrich, Steinheim, Germany), β-caryophyllene and α-humulene (Sigma, St. Louis, MO, USA) resulted in a chromatographic profile of monoterpenes in the time period from

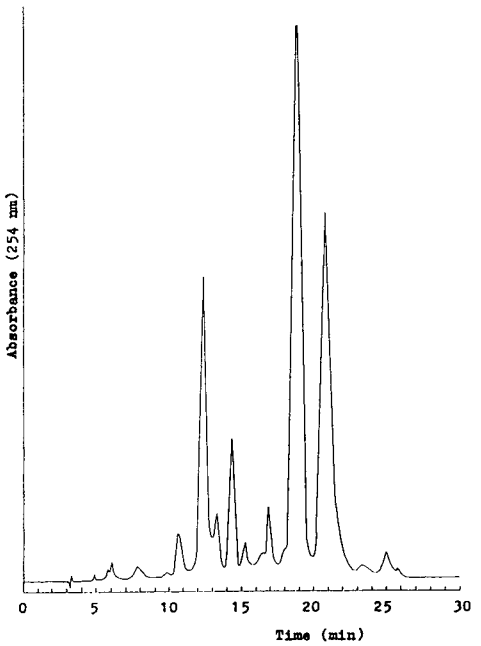

Fig. 1. HPLC separation of volatile hydrocarbons of blackcurrant buds. Reversed-phase HPLC column, 150 mm × 3 mm I.D., Separon SGX C_{18}; mobile phase, methanol–water (4:1, v/v); flow-rate, 0.3 ml/min; UV detection at 254 nm.

4 to 18 mins and that of sequiterpenes from 18 to 26 mins (Fig. 1).

The most important compounds for the aroma of blackcurrant bud oil are present in the polar fraction. These polar volatiles contain the most odorous compounds and exhibit the characteristic blackcurrant odour. Volatile carbonyls, present in a very small amounts, belong among the most important compounds for the blackcurrant flavour. For this reason, the carbonyls were analysed in detail. The carbonyl compounds were converted into 2,4-DNPHs. The mixture of 2,4-DNPHs obtained from blackcurrant bud volatiles is a complicated mixture consisting of the derivatives of saturated and unsaturated aliphatic aldehydes and ketones, terpenoids and aromatic-type carbonyl compounds. Before analysis by HPLC it is advisable to separate the mixture into classes containing one type of carbonyl compound. The mixture of 2,4-DNPHs was separated into derivatives of keto acids and monocarbonyl and dicarbonyl compounds. Each

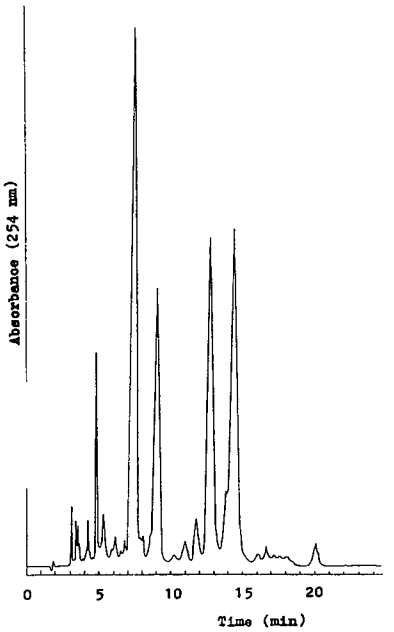

Fig. 2. HPLC separation of volatile oxygenated compounds of blackcurrant buds. Conditions as in Fig. 1 except mobile phase, methanol–water (1:1, v/v).

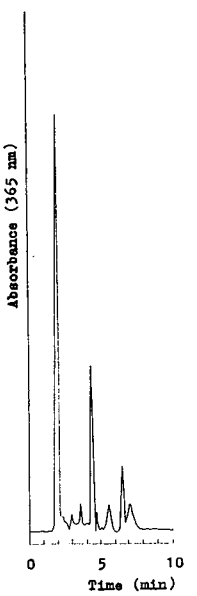

Fig. 3. HPLC separation of 2,4-DNPHs of keto acids. Conditions as in Fig. 1 except UV detection at 365 nm.

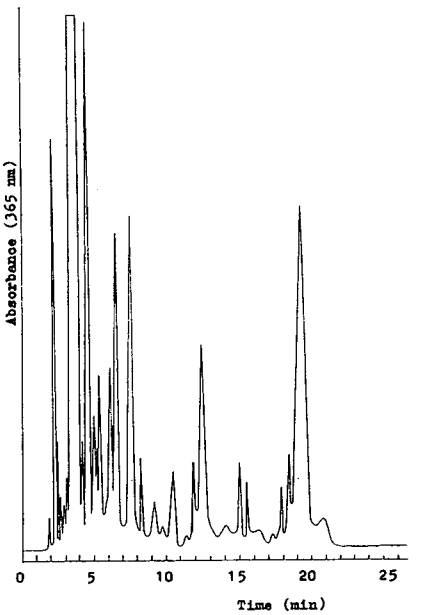

Fig. 4. HPLC separation of 2,4-DNPHs of monocarbonyl compounds. Conditions as in Fig. 1 except UV detection at 365 nm.

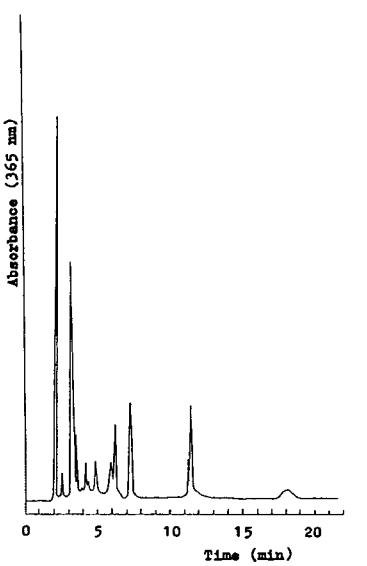

Fig. 5. HPLC separation of 2,4-DNPHs of dicarbonyl compounds. Conditions as in Fig. 1 except UV detection at 365 nm.

fraction was submitted to HPLC (Figs. 3, 4 and 5). As can be seen, monocarbonyl compounds represent the major part of the carbonyl volatiles. It will be necessary to use, after regeneration, gas chromatography–mass spectrometry for identification of the carbonyl compounds.

4. Conclusions

Reversed-phase HPLC appears to be useful for the analysis of essential oils and 2,4-DNPHs. As is shown in Figs. 1–5, HPLC was suitable for testing the essential oils and the fingerprint method. The low temperatures at which separation takes place is an advantage over gas chromatography, and is especially important when dealing with thermolabile compounds such as many occur in essential oils.

5. References

[1] J. Rigaud, P. Etiévant, R. Henry and A. Latrasse, *Sci. Aliments*, 6 (1986) 213.
[2] A. Latrasse, J. Rigaud and J. Sarris, *Sci. Aliments*, 2 (1982) 145.
[3] J.L. Le Quéré and A. Latrasse, *J. Agric. Food Chem.*, 38 (1990) 3.
[4] M. F. Kerslake and R.C. Menary, *Perfum. Flavor.*, 9 (1985) 13.
[5] M.F. Kerslake, A.G. Latrasse and J.L. Le Quéré, *J. Sci. Food Agric.*, 47 (1989) 43.
[6] J.L. Le Quéré and A. Latrasse, *Sci. Aliments*, 6 (1986) 47.
[7] B.B. Jones, B.C. Clark and G.A. Iacobucci, *J. Chromatogr.*, 178 (1979) 575.
[8] J.H. Dhont, C. Vinkenborg, H. Compaan, F.J. Ritter, R.P. Labodie, A. Verweij and R.A. de Zeeuw, *J. Chromatogr.*, 130 (1977) 205.
[9] M.H. Gordon and R.E. Griffith, *Food Chem.*, 43 (1992) 71.

ELSEVIER

Journal of Chromatography A, 665 (1994) 111–116

JOURNAL OF CHROMATOGRAPHY A

Evaluation of shape selectivity of liquid crystals in capillary gas chromatography

J. Krupčík[a], M. Valachovičová[a], G. Kraus*[,b]

[a]Department of Analytical Chemistry, Faculty of Chemical Technology, Slovak Technical University, Radlinského 9, 812 37 Bratislava, Slovak Republic

[b]Department of Chemistry, Martin Luther University Halle–Wittenberg, Weinbergweg 16, D-06120 Halle/Saale, Germany

Abstract

The shape selectivity of 4-octoxyphenyl 4-pentoxybenzoate as a liquid crystal stationary phase was monitored in the separations of *o*-, *m*- and *p*-xylene and *cis*- and *trans*-1,2-dimethylcyclohexane and -decalin in the temperature range 54–83°C with both increasing and decreasing column temperatures in 5°C steps. Retention indices were used to study the dependence of retention on temperature. The influence of temperature on the shape selectivity of the liquid crystal stationary phase was measured as the dependence of log α on $1/T$. The use of saturated cyclic compounds for measuring the shape-selective properties of a liquid crystal stationary phase is superior to the use of xylenes as they are less polar than xylenes and their selectivity factors are more sensitive to selectivity changes.

1. Introduction

The exceptional separating properties of liquid crystals as stationary phases in gas chromatography (GC) were first described in the 1960s [1,2], and the GC separation of various samples on liquid crystal stationary phases has been reviewed [3,4]. The use of liquid crystals as stationary phases in capillary GC is extremely advantageous because in this technique the "shape selectivity" of the stationary phase is combined with the high efficiency of the capillary column [3,4]. The shape selectivity of these stationary phases is usually determined with respect to samples whose molecules differ in shape whereas the other factors that determine the retention of sample molecules are very similar; *m*- and *p*-xylene are usually used to test the liquid crystal shape selectivity [3,4]. However, the polarities of *m*- and *p*-xylene differ, which can substantially influence their retention on polar liquid crystal stationary phases. It is clear that for the determination of shape selectivity non-polar solutes differing in shape should be used.

The aim of this work was to evaluate the shape selectivity of a glass capillary column coated with a 4-octoxyphenyl 4-pentoxybenzoate liquid crystal stationary phase for separating *o*-, *m*- and *p*-xylene and stereoisomers of 1,2-dimethylcyclohexane and decalin.

2. Experimental

GC was performed with a Fractovap 2350 gas chromatograph (Carlo Erba, Milan, Italy) equipped with an all-glass inlet split injection port and using flame ionization detection (FID). Hydrogen was used as the carrier gas at a flow-

* Corresponding author.

0021-9673/94/$07.00
SSDI 0021-9673(93)E1272-2

rate of 40 cm/min. Signals were registered with an HP 9366 integrator and via Peak 96 were sent to an IBM-compatible PC where they were evaluated with HP CHEM software (all products were purchased from Hewlett-Packard, Waldbronn, Germany). For computer reconstruction of chromatograms unpublished software was used [5].

A capillary column was prepared from soft glass using a published procedure [6]. The column was 30 m × 0.30 mm I.D., with a 0.12-μm stationary phase film thickness. 4-Octoxyphenyl 4-pentoxybenzoate was used as a liquid crystal stationary phase, exhibiting transition temperatures of Cr-53-N-85-Is (crystalline nematic isotropic).

The shape selectivity of the prepared capillary column was measured for the separation of mixtures of C_7–C_{12} *n*-alkanes, *o*-, *m*- and *p*-xylene and *cis*- and *trans*-1,2-dimethylcyclohexane and -decalin. The shapes of these molecules are shown in Fig. 1. The gas hold-up time was measured using methane.

3. Results and discussion

The shape selectivity of 4-octoxyphenyl 4-pentoxybenzoate was measured from the data obtained by separating a test sample isothermally at the temperatures of its transition state with both increasing (54→83°C) and decreasing (83→54°C) temperatures in 5°C increments. In Fig. 2, the chromatogram obtained in the separation of a test sample at 83°C is shown. The shape selectivity of the liquid crystal is very high, as *m*- and *p*-xylene are separated very well. However, some problems occurred with the separation of *p*- and *o*-xylene. *Cis*- and *trans*-1,2-dimethylcyclohexane and -decalin were separated without any overlapping problems.

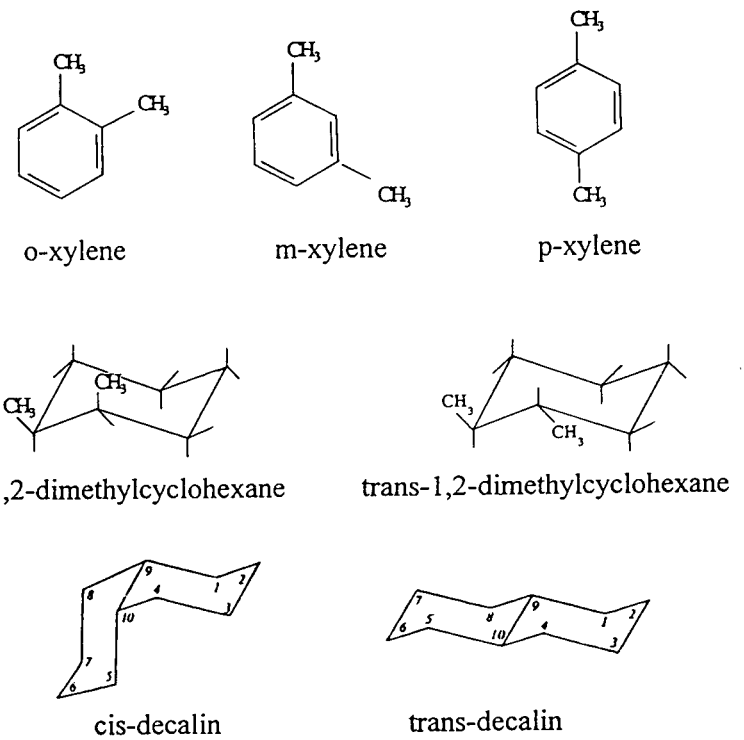

Fig. 1. Molecular shapes of the isomers tested.

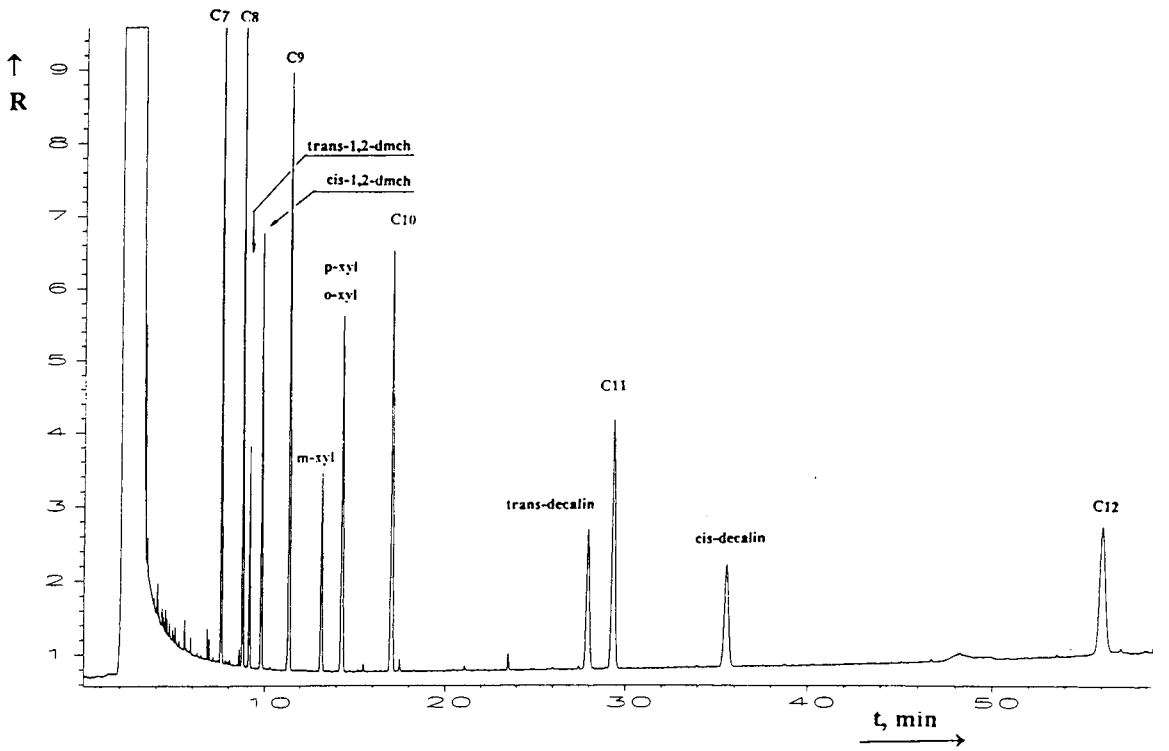

Fig. 2. Separation of a test sample at 83°C. C_8–C_{12} = *n*-alkanes; 1,2-dmch = 1,2-dimethylcyclohexane; xyl = xylene.

Retention indices (I) were used to monitor the dependence of retention on temperature (Figs. 3 and 4). Retention indices were measured with a repeatability of ±1 index units. Their reproducibility was not measured as this depends on, *inter alia*, the film thickness of the stationary phase. Regression analysis of the dependences shown in Figs. 3 and 4 showed that the retention at any chosen temperature in the interval 54–83°C varies substantially depending on the temperature change mode. The most pronounced difference was found for *cis*- and *trans*-decalin, as follows also from comparison of the slopes of lines for these compounds in Figs. 3 and 4. The dependence of the polarity of the liquid crystal stationary phase on temperature in the range considered is less pronounced than the temperature dependence of the shape selectivity as the difference in the slopes of the corresponding lines for the xylenes is smaller than that for the decalins in Figs. 3 and 4.

The temperature dependence of the shape selectivity of the liquid crystal stationary phase was further monitored by determining the selectivity factor (α) using the dependence of log α on $1/T$, as shown in Fig. 5. The semi-logarithmic dependence of the shape selectivity factor (log α) on $1/T$ was derived from the equation used for the calculation of partial molar free energies of solution [7]:

$$\Delta G = \Delta H - T\Delta S \quad (1)$$

and the equation used for the calculation of the difference in the partial molar free energies for solutes i and j from chromatographic data [8]:

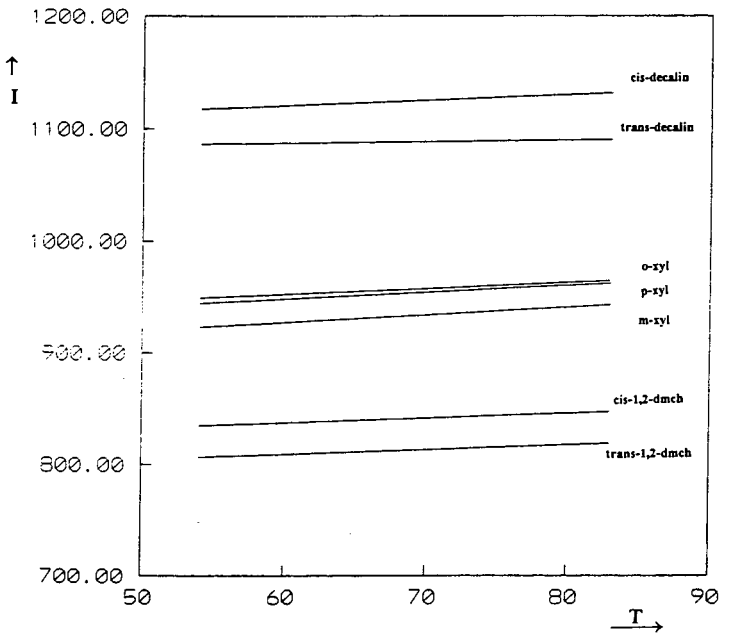

Fig. 3. Dependence of retention indices (I) on temperature (T) in the temperature-increasing mode (54→83°C). Abbreviations as in Fig. 2.

$$\Delta(\Delta G_{j,i}) = -RT \ln \alpha \quad (2)$$

After rearrangement of these equations we obtain

$$\ln \alpha = -\frac{\Delta(\Delta H_{j,i})}{RT} + \frac{\Delta(\Delta S_{j,i})}{R} \quad (3)$$

where R is the gas constant and $\Delta(\Delta H_{j,i})$ and $\Delta(\Delta S_{j,i})$ are the enthalpy and entropy differences of solutes i and j differing in shape, respectively.

An increase in the temperature of the liquid crystal stationary phase diminishes its shape selectivity as a result of the decrease in the degree of molecular ordering of liquid crystals with temperature.

From Eq. 3 and Fig. 5, it follows that the dependence of the shape selectivity of the stationary phase on temperature can easily be studied using the enthalpic $\Delta(\Delta H_{j,i}/R)$ term. For example, for the lines shown in Fig. 5, the following slopes $[\Delta(\Delta H_{j,i})/R)]$ were found by regression analysis: −2.93 for *cis*- and *trans*-1,2-dimethylcyclohexane; −2.73 for *p*- and *m*-xylene; −2.11 for *o*- and *p*-xylene; and −3.34 for *cis*- and *trans*-decalin. From these data, it follows that *cis*- and *trans*-1,2-dimethylcyclohexane and -decalin are better solutes for measuring the stationary phase shape selectivity than xylenes, as their slopes $\Delta(\Delta H_{j,i})/R$ are substantially higher.

4. Conclusions

The shape selectivity of a liquid crystal stationary phase can be successfully monitored using either *o*-, *m*- and *p*-xylene or *cis*- and *trans*-1,2-dimethylcyclohexane and -decalin. The use of cyclic compounds for measuring the shape-selective properties of a liquid crystal stationary phase is superior to the use of xylenes as saturated cyclic compounds are less polar than xylenes and their shape selectivity factors are more sensitive to stationary phase shape-selectivity changes.

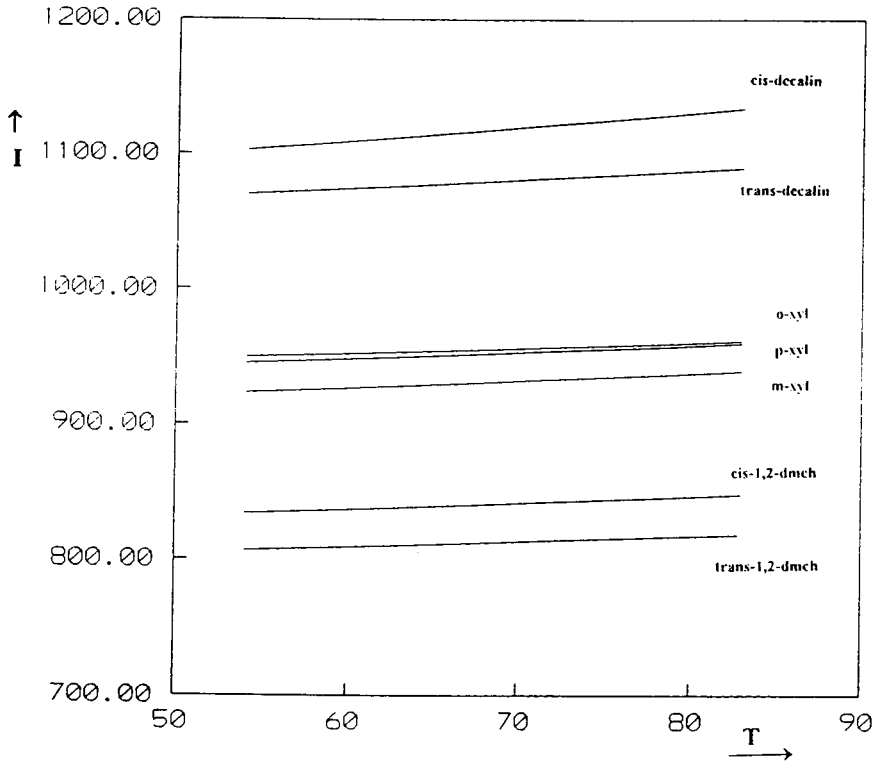

Fig. 4. Dependence of retention indices (I) on temperature (T) in the temperature-decreasing mode (83→54°C). Abbreviations as in Fig. 2.

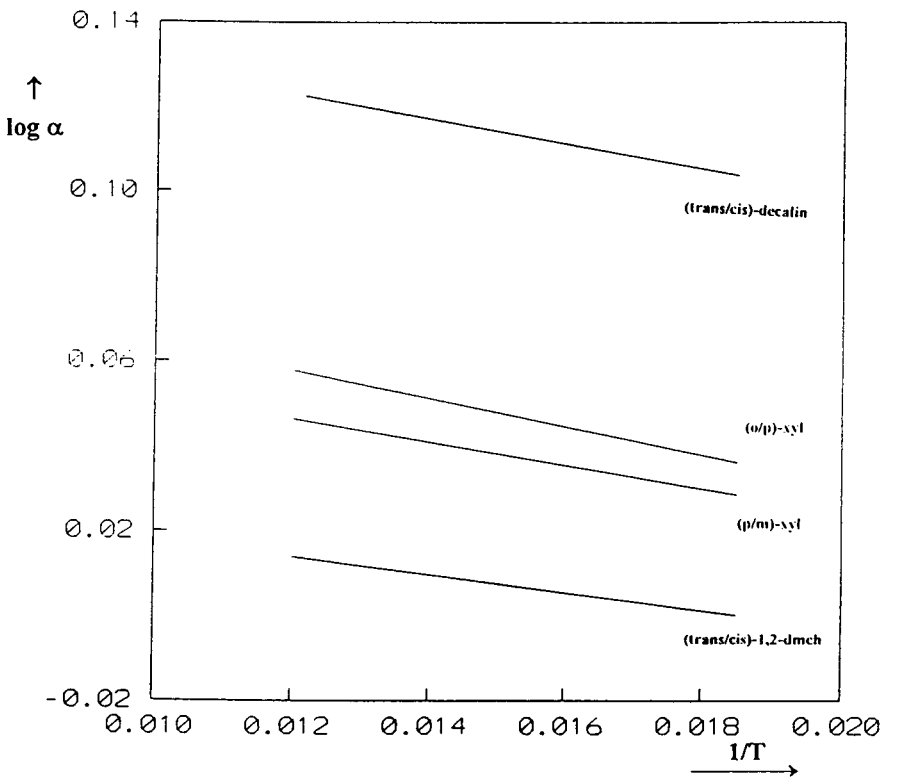

Fig. 5. Dependence of log α on $1/T$ in the temperature-increasing mode (54→83°C). Abbreviations as in Fig. 2.

5. References

[1] H. Kelker, *Fresenius' Z. Anal. Chem.*, 198 (1963) 254.
[2] H. Kelker, *Ber. Bunsenges. Phys. Chem.*, 67 (1963) 698.
[3] T.G. Andronikashvili, L.G. Arustamova, N.T. Sultanov and K.G. Markarjan, *Zhidkije Kristally w Kapillarnoj Chromatografii (Liquid Crystals in Capillary Chromatography)*, Mecniereba, Tiflis, 1982 (in Russian).
[4] J. Mazur and Z. Witkiewicz, *LC·GC Int.*, 3, No. 5 (1990) 38–49.
[5] J. Hrouzek, Department of Analytical Chemistry, Faculty of Chemical Technology, Slovak Techical University, Bratislava, unpublished software.
[6] J. Krupčík, M. Kristín, M. Valachovičová and Š. Janiga, *J. Chromatogr.*, 126 (1976) 147.
[7] J.R. Conder and C.L. Young, *Physicochemical Measurements by Gas Chromatography*, Wiley, New York, 1979, p. 154.
[8] N.K. de Vries, B. Coussens, R.J. Meier and G. Heemels, *J. High Resolut. Chromatogr.*, 15 (1992) 499.

ELSEVIER

Journal of Chromatography A, 665 (1994) 117–123

JOURNAL OF CHROMATOGRAPHY A

Sequence distribution of styrene–butadiene copolymers by ozonolysis, high-performance liquid chromatographic and gas chromatographic–mass spectrometric techniques

M.E. Pattuelli*, A. Montalti, G.T. Viola, A. Zazzetta

Enichem Elastomeri, Via Baiona 107/111, 48100 Ravenna, Italy

Abstract

The sequence distribution of styrene units in various styrene–butadiene copolymers (SBR) was investigated by liquid chromatographic (LC) and gas chromatographic–mass spectrometric (GC–MS) measurements on their ozonolysis products. Ozonolysis was performed in methylene chloride followed by reductive degradation with lithium aluminium hydride. LC was found to be a very effective technique for the characterization and quantitative evaluation of the sequence distribution of random and tapered block copolymers because of its high detection efficiency of short and long sequences. LiChrospher C_{18} reversed-phase columns, a ternary gradient system and an evaporative light-scattering detector were used. Peaks corresponding to various low-molecular-mass species were identified by GC–MS and assigned to 1,4Bde–$(Sty)_m$–1,4Bde or 1,4Bde–$(Sty)_m$–$(1,2Bde)_n$–1,4Bde sequences of the original copolymers (Bde = butadiene, Sty = styrene).

1. Introduction

The sequence distribution of styrene units has been recognized as a dominant factor governing the mechanical and viscoelastic properties of styrene–isoprene and styrene–butadiene elastomers. There have been several reports concerning the structural investigation of random and tapered forms of these copolymers. Ozone degradation has been used to provide quantitative information about the distribution of styrene units in these copolymers [1–4]; a combination was proposed of ozonolysis and high-resolution gel-permeation chromatographic (GPC) measurements, followed by NMR analysis for molecular characterization of the collected fractions.

Montaudo and co-workers [5–9] demonstrated that mass spectrometry (MS) is a powerful and rapid method suitable for the detection of a series of oligomers formed in the partial ozonolysis. Their results yielded detailed information on the distribution of monomers for several condensation and addition copolymers.

In this paper, we propose a method for the quantitative evaluation of the distribution of styrene units in various styrene–butadiene rubbers by HPLC of the ozonolysis products. HPLC has been shown to be a very effective technique suitable for the detection of a series of oligomers because of its high detection efficiency for either short [3] or long sequences. GC–MS chemical ionization (CI) and desorption chemical ionization (DCI) were successfully used to identify the separated products.

* Corresponding author.

0021-9673/94/$07.00
SSDI 0021-9673(93)E1099-L

2. Experimental

2.1. Materials and ozonolysis

The chemical used were commercial and experimental products and were appropriately purified before use. The compositions of the samples are given in Table 1. All samples were ozonolysed following a procedure described by Tanaka and co-workers [1–4].

2.2. HPLC

The separation of the ozonolysis products was performed by HPLC using a Gilson (Biolabo, Milan, Italy) liquid chromatograph with a double-pumping system (Models 305 and 306). The LC measurements were conducted by using a LiChrospher C_{18} 5 μm analytical column (Bracco, Milan, Italy). The solvent flow-rate was 1 ml/min. Samples were injected via a 10-μl loop injector. Rainin Dynamax UV1 UV (Biolabo) and CONOW DDL21 light-scattering (Eurosep, Cergy, France) detectors were used. A linear mobile phase gradient from methanol–water to tetrahydrofuran (HPLC grade; Carlo Erba, Milan, Italy) was used. Preparative separations were performed with a high-resolution column (Rainin Microsorb C_{18} 5 μm; Biolabo). The solvent flow-rate was 10 ml/min. A total of 500 μl of the THF sample solution was injected. The LC effluent peaks were trapped in glass vials, dried and analysed by MS.

2.3. GC–MS

GC–MS analyses were performed with a Hewlett-Packard Model 5890 gas chromatograph combined with a Hewlett-Packard Model 5971A quadrupole mass spectrometer equipped with a CI ion source.

GC separations were accomplished on an HP1 silica capillary column (Hewlett-Packard). The transfer line was held at 280°C. The oven temperature programme was initial temperature 60°C, increased at 20°C/min to 320°C. Helium was used as the carrier gas. The mass spectrometer was scanned from m/z 10 to 650. Isobutane was used as the CI reagent gas.

2.4. DCI

Experiments were performed using a Finnigan TSQ 700 triple-stage quadrupole mass spectrometer. The ion source was kept at 60°C. A rhenium wire (standard from Finnigan) was used. The wire heating current was programmed from 0 to 1 A at 40–80 mA/s (about 40–80°C/s, up to about 1000°C). The CI reagent gas mainly used was isobutane at a pressure of 0.5 mbar. The resolution was unitary.

3. Results and discussion

It is known that the double bonds of 1,4- and 1,2-units in styrene–butadiene copolymers (SBR) were completely decomposed under the ozonolysis conditions used here [1–4]. The resulting products are represented by the following general formula:

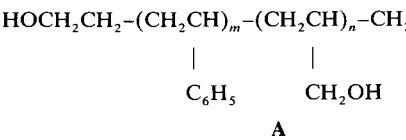

A

Table 1
Compositions of SBR samples

Sample	Styrene (mol %)	1,2-Butadiene (mol %)	1,4-Butadiene (mol %)
(a) Experimental SBR	17.4	16.5	66.1
(b) SBR 1721	17.3	8.5	74.2
(c) Solprene 1205	11.4	9.1	79.5

The sequence distribution of styrene units can be determined by HPLC measurements of **A**.

3.1. Random SBR by anionic polymerization

A model SBR prepared with potassium *tert.*-amylate (KTA) as a modifier was analysed by the ozonolysis–HPLC method, as shown in Fig. 1.

By MS measurements of the collected fractions, the peaks were assigned to the products derived from the 1,4Bde–$(Sty)_m$–1,4Bde ($n = 0$ and $m = 1,2,3$, etc., in formula **A**) and 1,4Bde–$(1,2Bde)_n$–$(Sty)_m$–1,4Bde ($n = 1$ and $m = 1,2,3$, etc., in formula **A**) sequences respectively (Sty = styrene; Bde = butadiene), which are represented by Sm and SmV (Table 2). As shown in Fig. 1, LC analysis was able to separate the two sequences and the relative diastereomers for lower oligomers, as confirmed by NMR analysis [3].

This kind of efficiency was decreased in the long sequences ($n > 4$), where the two families were co-eluted. Good resolution was found for styrene sequences of up to 21 monomeric units.

In order to carry out a quantitative analysis of the styrene sequence distribution, both the UV and evaporative light-scattering detection (ELSD) traces were analysed. A UV detection system has been used previously in GPC, where the molar absorptivity per styrene unit at 254 nm

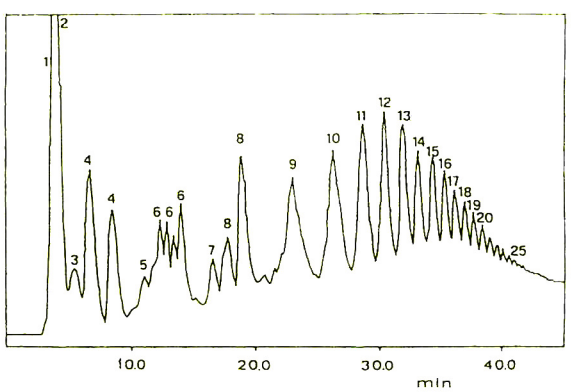

Fig. 1. HPLC separation of the ozonolysis products from sample (a) (Table 1). Structural identification of the collected fractions is reported in Table 2.

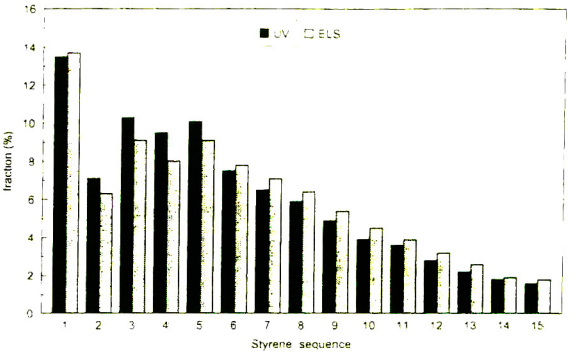

Fig. 2. Sequence distribution of styrene units in sample (a) (Table 1) with UV and ELS detection.

was independent of the sequence length [2]. During ternary gradient elution in HPLC, a considerable drift of the baseline was observed owing to the continuous change in solvent composition; this could be a problem for the accurate quantitative evaluation of the separated oligomers. The choice of ELSD, with a response virtually independent of the gradient, was useful in order to test the UV detection efficiency when the gradient was applied. Further, ELSD was used to control the extent of the ozonolysis reaction in order to exclude the presence of possible dienic sequences not or partially

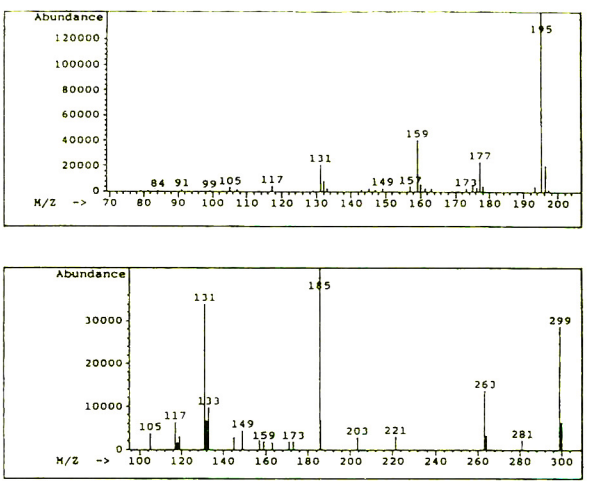

Fig. 3. GC–MS (CI) mass spectra of fractions S1 and S2.

ozonolysed. Fig. 2 shows the good agreement between the sequence distribution of styrene units obtained from the UV and ELSD traces.

In Fig. 3 the GC–MS spectra of the early separated HPLC peaks are reported. The molecular ion $[MH]^+$ and fragment ion $[MH - 18]^+$ are observed, indicating that these are OH-terminated oligomers.

DCI mass spectra of the higher LC cuts are shown in Fig. 4. Only molecular ion regions are displayed, but fragment ions were essentially absent, even for the higher molecular mass oligomers.

3.2. Random SBR by emulsion polymerization

The LC trace of SBR 1721 is shown in Fig. 5. Here only the peaks denoted S1, S1V, S2, S2V, S3 were present. The sequence distribution was determined from the integrated intensity of the UV peaks. In Fig. 6 is reported the sequence distribution of styrene units and the theoretical

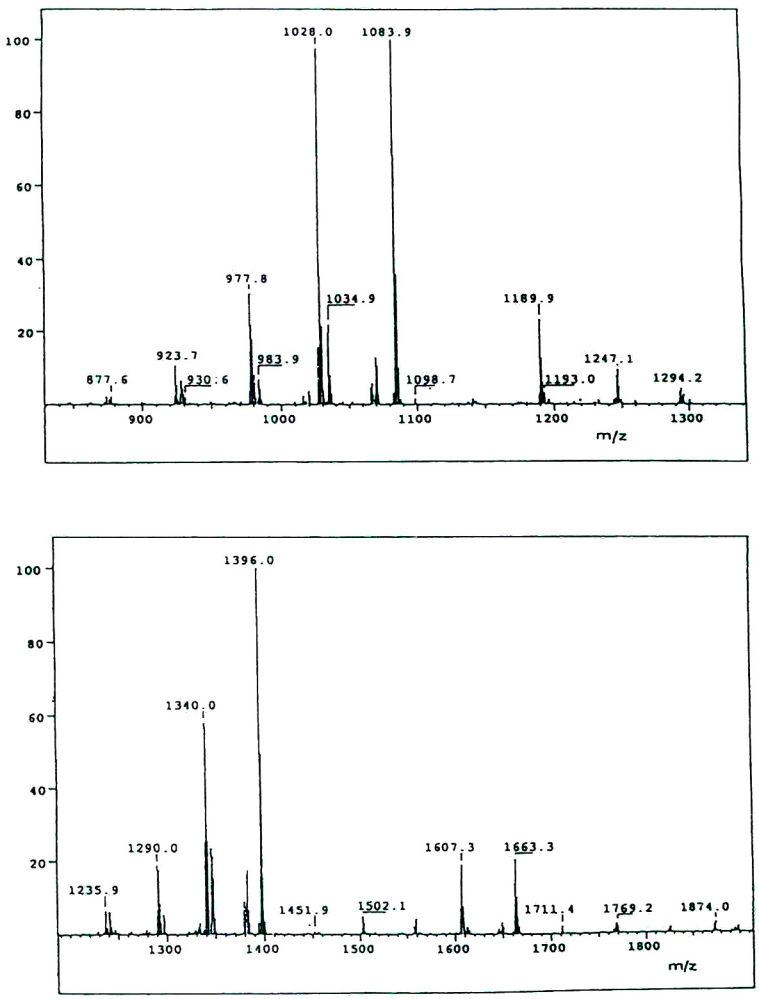

Fig. 4. Positive-ion DCI mass spectra of fractions S9 and S12.

Table 2
Identification of the ozonolysis products from sample (a) (Table 1) by HPLC and MS analysis

HPLC peak No.	Nominal mass[a]	$HOCH_2CH_2(Sty)_m-(1,2Bde)_n-CH_2CH_2OH$		
		m	*n*	Designation
1	252	1	1	S1V
2	194	1		S1
3	352	2	1	S2V
4	298	2		S2
4	298	2		S2
5	460	3	1	S3V
6	402	3		S3
6	402	3		S3
6	402	3		S3
7	564	4	1	S4V
8	506	4		S4
8	506	4		S4
9	610	5		S5
10	714	6		S6
11	818	7		S7
12	922	8		S8
13	1026	9		S9
14	1130	10		S10
15	1234	11		S11
16	1338	12		S12
17	1442	13		S13
18	1546	14		S14
19	1650	15		S15
20	1754	16		S16
21	1858	17		S17
22	1962	18		S18
23	2066	19		S19
24	2170	20		S20
25	2274	21		S21

[a] Nominal mass spectrometric molecular weight (C = 12; H = 1; O = 16).

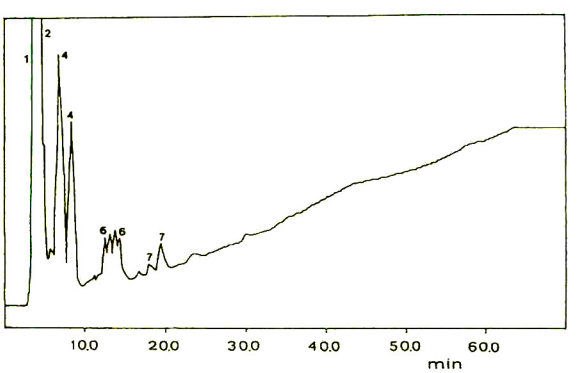

Fig. 5. HPLC separation of the ozonolysis products from sample (b) (Table 1). For peak numbers, see Table 2.

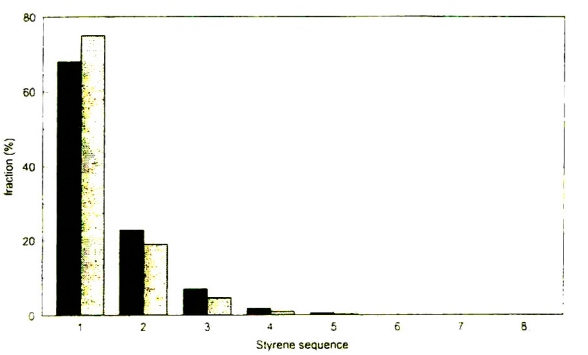

Fig. 6. Sequence distribution of styrene units in sample (b) (Table 1): experimental and theoretical. Solid bars = UV detection; dotted bars = statistical.

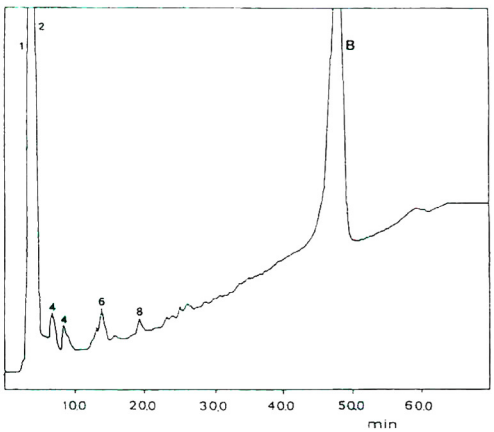

Fig. 7. HPLC separation of the ozonolysis products from sample (c) (Table 1). For peak numbers, see Table 2; B = long styrene sequences.

distribution that follows an exponential function, assuming a statistical copolymerization.

3.3. Partially blocked SBR by anionic polymerization

Fig. 7 shows the ozonolysis–HPLC trace of sample (c) (tapered copolymer), Solprene 1205. The peaks were assigned by using the relationship shown in Table 2. The broad peak observed at 40–45 min in Fig. 7 was assigned to the long styrene sequences; the average sequence length was estimated by GPC to be 90–100. The relative intensity of the block sequence peak was found to be 20% according to the GPC measurements [2]. Fig. 8 reports the sequence distribution of styrene units obtained from the relative intensity of the LC peaks.

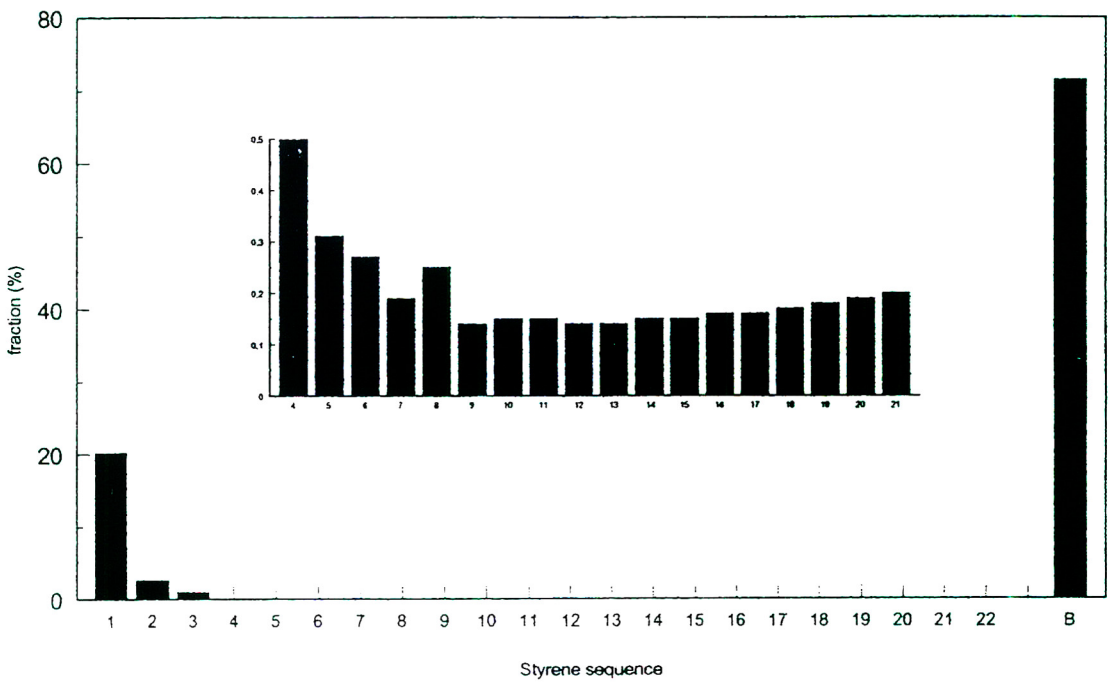

Fig. 8. Sequence distribution of styrene units in sample (c) (Table 1).

4. References

[1] Y. Tanaka, H. Sato, Y. Nakafutami and Y. Kashiwazaki, *Macromolecules*, 16 (1983) 1925.
[2] Y. Tanaka, H. Sato and J. Adachi, *Rubber Chem. Technol.*, 59 (1986) 16.
[3] Y. Tanaka, Y. Nakafutami, Y. Kashiwazaki, J. Adachi and K. Tadokoro, *Rubber Chem. Technol.*, 60 (1987) 207.
[4] Y. Tanaka, K. Nunogaki and J. Adachi, *Rubber Chem. Technol.*, 61 (1987) 36.
[5] G. Montaudo, E. Scamporrino and D. Vitalini, *Macromolecules*, 22 (1989) 623.
[6] G. Montaudo, E. Scamporrino and D. Vitalini, *Macromolecules*, 22 (1989) 627.
[7] G. Montaudo, E. Scamporrino and D. Vitalini, *Macromolecules*, 24 (1991) 376.
[8] G. Montaudo, *Macromolecules*, 24 (1991) 5829.
[9] G. Montaudo, E. Scamporrino, D. Vitalini and R. Rapisardi, *J. Polym. Science, Part A, Polym. Chem.*, 30 (1992) 525.

ELSEVIER

Journal of Chromatography A, 665 (1994) 125–132

JOURNAL OF CHROMATOGRAPHY A

Determination of toxaphene in soil by electron-capture negative-ion mass spectrometry and capillary column gas chromatography

Francis I. Onuska*,[a], Ken A. Terry[a], Alan Seech[b], Michael Antonic[b]

[a]*National Water Research Institute, Research and Applications Branch, 867 Lakeshore Road, Burlington, Ontario L7R 4A6, Canada*

[b]*Grace-Dearborn Environmental Engineering Group, 3451 Erindale Station Road, Mississauga, Ontario L5A 3T5, Canada*

Abstract

Although toxaphene is now limited in use, interest in its analysis continues because of its persistence and widespread atmospheric transport in the environment and its presence in many dump-sites all over the world. Top soil samples collected from a dump site were analyzed for toxaphene residues. Analyses were performed by wall-coated open tubular column gas chromatography in tandem with electron-capture negative-ion mass spectrometry. Since the concentrations of toxaphene residues were at mg/kg levels, the application of a mass spectrometer as a substance-selective detector has been applied. Advantages of this mode of real-time acquisition in continuous repetitive scanning of mass spectra has significant advantages in comparison to the selected-ion monitoring technique. An average R.S.D. of 10 % and recoveries of 90 to 109% were obtained. Levels down to 50 μg/kg are obtainable.

1. Introduction

Toxaphene presence in world-wide ecosystem requires establishing its unambiguous identification and quantitation in routine analytical laboratories. Interest in its quantitation continues because of its persistence especially in many dump-sites located in the United States, Russia, Egypt, Sudan, Ethiopia and Tanzania and other cotton producing countries [1].

Toxaphene is known to be toxic to various species of fish. Toxic effects in fish include decreased viability of ova of brook trout (*Salvelinus santinalis*) that have been exposed to toxaphene at ng/kg levels [2]. Evidence of long-range airborne transport of toxaphene has been documented by Bidleman and Olney [3].

The selection of analytical techniques for the measurement of toxaphene residues has received an every increasing attention because of its complex composition and wide-spread occurrence in various compartments of our ecosystem [1] especially it is used on cotton crops. Toxaphene represents a complex mixture of at least 700 polychlorinated bornane congeners with an average elemental composition of $C_{10}H_{10}Cl_8$. Due to its complex nature, the quantitation of toxaphene is difficult. Under gas chromatograph-

* Corresponding author.

0021-9673/94/$07.00
SSDI 0021-9673(93)E1181-X

ic conditions employing electron-capture detection (ECD), the toxaphene congeners often overlap each other, as well, organochlorine pesticides (OCs) interfere with quantitation, and there is no individual pure toxaphene congener commercially available for use as a primary standard.

In our previous report [4], we described the performance of gas chromatography–electron impact MS–selected-ion monitoring (SIM) and MS–SIM solid-probe programmable temperature techniques. The latter, especially provides a significant improvement of samples throughput, since the total *toxaphene residue* concentration is obtained in less than 5 min per sample. However, this methodology requires a ^{37}Cl-labelled toxaphene and preferably high-resolution mass spectrometer, since at low resolution results may be affected by interferences of other pesticides.

Current US EPA methodology (SW-846) [5] consists of electron impact mass spectrometry and high-resolution gas chromatography (HRGC)–ECD method (8270 and 8280), both of which are greatly affected by interferences such as polychlorinated biphenyls (PCBs) and chlordane [3]. Jannson and Wideqvist [6] and Swackhamer *et al.* [7] published an electron-capture negative ion HRGC–MS–SIM method that is selective for toxaphene in fish and milk samples.

The application of a mass spectrometer as a substance-selective detector in HRGC–MS is well recognized. The most widely used data acquisition technique is the continuous repetitive scanning of mass spectra. Each integer mass between the starting and ending masses is measured and recorded. The final mass spectrum illustrates a widely used data reduction process. Each point on the ordinate is the normalized sum of all the ion abundances in a single mass spectrum and each point on the abscissa represents a spectrum number of the electron-capture negative chemical ionization (EC-NCI) profile. This plot is referred as total ion current (TIC) profile. Since concentrations of toxaphene in samples were at mg/kg range, it was possible to perform both confirmation and quantitation of toxaphene in one run.

In our work, the electron capture negative ion HRGC–MS is extended to soil samples, which therefore suggests its applicability to other solid wastes. It is the purpose of this paper to present some of the concepts involved in the application of ECNCI HRGC–MS of the computer-controlled mass spectrometer as a substance-selective detector.

2. Experimental

2.1. Chemicals

Toxaphene and TCB reference standards were obtained from the US EPA Repository (Research Triangle Park, NS, USA). All solvents used for extraction and cleanup were purchased from Burdick & Jackson (Muskegon, MI, USA).

2.2. Extraction

Extraction was accomplished according to standard methods using Polytron extractor [8]. The soil sample (1 g) was extracted with 50 ml CH_2Cl_2–acetone (1:1, v/v) in a 250-ml stainless-steel beaker. The sonicator was adjusted to pulsed operation and output control was set to full power and duty cycle to 50%. The sample was sonicated for 3 min. The beaker was lowered and the probe washed down into the beaker with CH_2Cl_2–acetone (10 ml). The extraction was repeated twice with fresh solvents. Combined extracts were dried through a Na_2SO_4 column. After filtration, 10 ml of isooctane was added to the filtrate, and the filtrate was evaporated on a rotary evaporator to 2–3 ml volume at 40°C.

2.3. Cleanup

A Florisil column was prepared by placing a charge of activated Florisil in a chromatographic column (30 × 1 cm I.D.) over a 1-cm layer of anhydrous Na_2SO_4 [2]. An amount of 5 g of 120–150 μm Florisil previously activated at 130°C for 16 h was added and topped with 1.5 cm layer of anhydrous Na_2SO_4. Each column was prewashed with 20 ml of *n*-hexane. When the solvent reached the top of the Na_2SO_4 layer,

the concentrate from the extraction step was quantitatively transferred onto the column and allowed to drain onto the bed of Florisil. The column walls were washed with a 10-ml portion of the 50 ml *n*-hexane–diethyl ether (94:6, v/v). When the solvent reached the top of the Florisil the remaining part of the eluent (40 ml) was gradually added to the column. The eluate was collected for further analysis. It contained aldrin, benzene hexachloride (BHC), chlordanes, DDD, heptachlor, DDE and DDT isomers, lindane, methoxychlor, mirex, PCBs and toxaphene. More polar compounds such as endosulfan, endrin, dieldrin and phthalates were removed from the column with 50 ml of hexane–diethyl ether (80:20) solution. The extract was filtered and concentrated just to dryness on a rotary evaporator. The Florisil column effluent was treated with 5 ml of cold sulfuric–fuming nitric acid (1:1) for 15 min at room temperature to remove DDT and its metabolities [8]. PCBs were removed from most of the pesticides by silica gel column chromatography [9].

About 20 g of silica gel (*e.g.* E. Merck silica gel 60) was placed in a 100-ml beaker and activated at 130°C for 16 h. Then, it was transferred to a 100-ml glass stoppered bottle. The silica gel column was prepared by plugging chromatographic column (30 × 1 cm I.D.) with glass wool, filling it with a 1 cm layer of anhydrous Na_2SO_4, 5 g of activated silica gel and topping it with a second 1 cm layer of anhydrous Na_2SO_4. The column was prewashed with 20 ml *n*-hexane. The sample extract was added to the column and rinsed with 5 ml *n*-hexane–diethyl ether (94:6). The remaining 35 ml of the solution was added and the effluent collected in a 125-ml round-bottom flask. This fraction contained the PCBs, hexachlorobenzene (HCB), aldrin, heptachlor, mirex and the *p,p'*-DDE. The second fraction eluate consisting of 40 ml *n*-hexane–diethyl ether (75:25) contained a small amount of *p,p'*-DDE, BHC isomers, DDT, chlordanes, nonachlor, heptachlor epoxide, methoxychlor and toxaphene. The eluate volumes were reduced on the Rotovap and the resulting residues adjusted to 1 ml with isooctane prior to their quantitation using HRGC–EC-NCI MS.

2.4. Gas chromatography–mass spectrometry

Mass spectra were measured with a Hewlett-Packard Engine 5989A GC–MS System and HP 5890 Series II gas chromatograph equipped with programmable split/splitless electronic pressure programming, which provides accurate and precise control of column head pressure, resulting in good retention time reproducibility. The inlet pressure can be constant, programmed, or set to maintain a desired column flow-rate. The oven contained a 25 m × 0.25 mm I.D. DB-5 wall-coated open tubular (WCOT) column [film thickness (d_f) – 0.25 μm]. Helium was used as the carrier gas at the linear velocity of 40 cm/s at 80°C. The initial temperature was held at 80°C for 1 min followed by a temperature programming rate of 20°C/min to 200°C, afterwards at 4°C/min to 280°C.

The flow of methane reagent gas for chemical ionization was introduced via reagent gas flow controller and was optimized by employing the procedure for EC-NCI recommended by the manufacturer. The ion source pressure in EC-NCI mode was maintained at *ca.* 0.4 Torr (1 Torr = 133.3 Pa). The injector port and transfer line temperatures were maintained at 200 and 250°C, respectively. The ion source temperature was held at 150°C.

2.5. Quantitation

To quantitate ions by means of the mass chromatography, complete mass spectra from *m/z* 100 to 500 were scanned. The EC-NCI mass spectra are less complex than electron impact and chemical ionization spectra and exhibit only masses due to losses of Cl and HCl from the molecular ion. In the EC-NCI mass spectra, the most abundant ions were M^- of hexachloro bornanes and bornenes and the $[M - Cl]^-$ ions from hepta to decachloro congeners.

After running the total ion chromatogram (TIC) of a standard solution containing toxaphene the specific ions of chlorinated congener peaks were evaluated for impurities or contamination and compared with a real sample from a specific dump site. Only non-contaminated chro-

Table 1
Quantitation ions used for toxaphene in electron-capture negative-ion mass spectrometry

Congener group	M_r	Ion monitored	Quantitation ion
Hexachlorobornenes	340	M^-	342
Hexachlorobornanes	342	M^-	342
Heptachlorobornenes	374	$[M-Cl]^-$	343
Heptachlorobornanes	376	$[M-Cl]^-$	343
Octachlorobornenes	408	$[M-Cl]^-$	377
Octachlorobornanes	410	$[M-Cl]^-$	377
Nonachlorobornenes	442	$[M-Cl]^-$	413
Nonachlorobornanes	444	$[M-Cl]^-$	413
Decachlorobornenes	476	$[M-Cl]^-$	449
Decachlorobornanes	478	$[M-Cl]^-$	449

Mass chromatograms are shown in Figs. 1 and 2.

matographic peaks were selected for quantitation. Selected ions for monitoring toxaphene congeners are given in Table 1. Quantitation was performed relative to the internal standard 2,3,5,3′,4′-pentachloro biphenyl.

3. Results and discussion

The simplest type of process which leads to a negative ion mass spectrum under chemical ionization conditions occurs when the reagent gas acts simply as a buffer gas in producing a high yield of thermal electrons. These give rise to an electron capture mass spectrum of toxaphene moieties that possess a positive electron affinity, and this is the counterpart to the charge transfer mass spectrum in positive chemical ionization mode of operation.

The total ion chromatogram (TIC) shown in trace A (Fig. 1) of toxaphene standard scanned from m/z 200 to 500, illustrates complexity of the mixture of chlorinated bornanes and bornenes. It can be assumed that many chlorinated pesticides may overlap with toxaphene peaks and will obstruct determination of toxaphene.

The solid probe mass spectrum of the toxaphene standard shown in trace B (Fig. 1) indicates which ions should be selected for determination of toxaphene taking into account isotopic distribution of chlorine pattern and a correct abundances of different chlorine contributions according to the degree of chlorination. The specific ions selected for determination of toxaphene peaks are given in Table 1. The most abundant ions from a given isotopic cluster in Fig. 1B were selected to be the quantitation ions.

Fig. 2 shows the toxaphene mass chromatograms from the soil extract that can be used for the unambiguous determination of toxaphene and even for the homologue specific determination of its homologue specific patterns according to the chlorination of bornane/bornene moieties. A similar mass chromatogram (EC-NCI) can easily be obtained by pulling out individual masses from the TIC for the chlordane contamination which should be checked by monitoring masses at m/z values 237, 239; 264, 266; 300, 302; 334, and 336. Our samples were not contaminated with chlordane.

The use of EC-NCI HRGC–MS has provided information of the qualitative reliability, sensitivity, high selectivity and quantitative accuracy during analysis. There is no significant evidence for any contribution to chromatographic TIC trace by chemical degradation.

Improved injection techniques permit electronic pressure programming. This means that column flow-rate can be maintained at a constant rate during temperature programming run, or it can be programmed as an additional parameter to achieve the required quick sample transfer onto WCOT column, better separation and shorter run times. We applied pressure programming

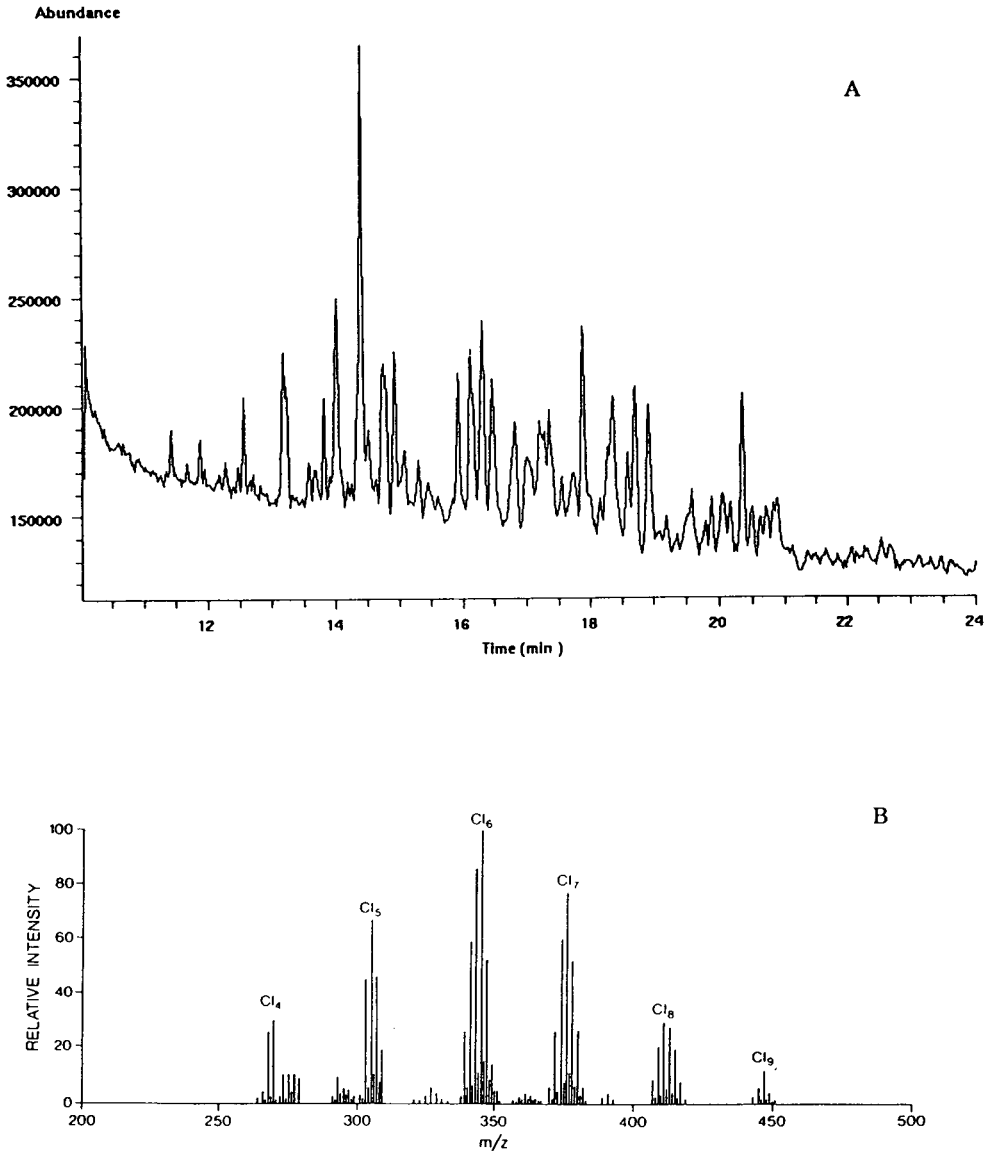

Fig. 1. (A) The total ion chromatogram of toxaphene (100 μg/kg) scanned from m/z 200 to 500 (conditions are given in the text). (B) Methane electron-capture negative-ion mass spectrum of toxaphene obtained via solid-probe inlet.

with splitless injection using a single taper deactivated linear at 200°C to reduce possible decomposition of toxaphene labile components. The chromatograms indicated remarkable stability and no sign of decomposition with an excellent retention time stability. The initial program ramp from 80 p.s.i. (1 p.s.i. = 6894.76 Pa) was followed by a single downward ramp. We concluded that this type of injection is mandatory for obtaining correct quantitative results. Considering the possibility of dehydrochlorination or reductive dechlorination in a variety of biological systems, reduction would appear the less likely in this instance, since the soil was exposed to air

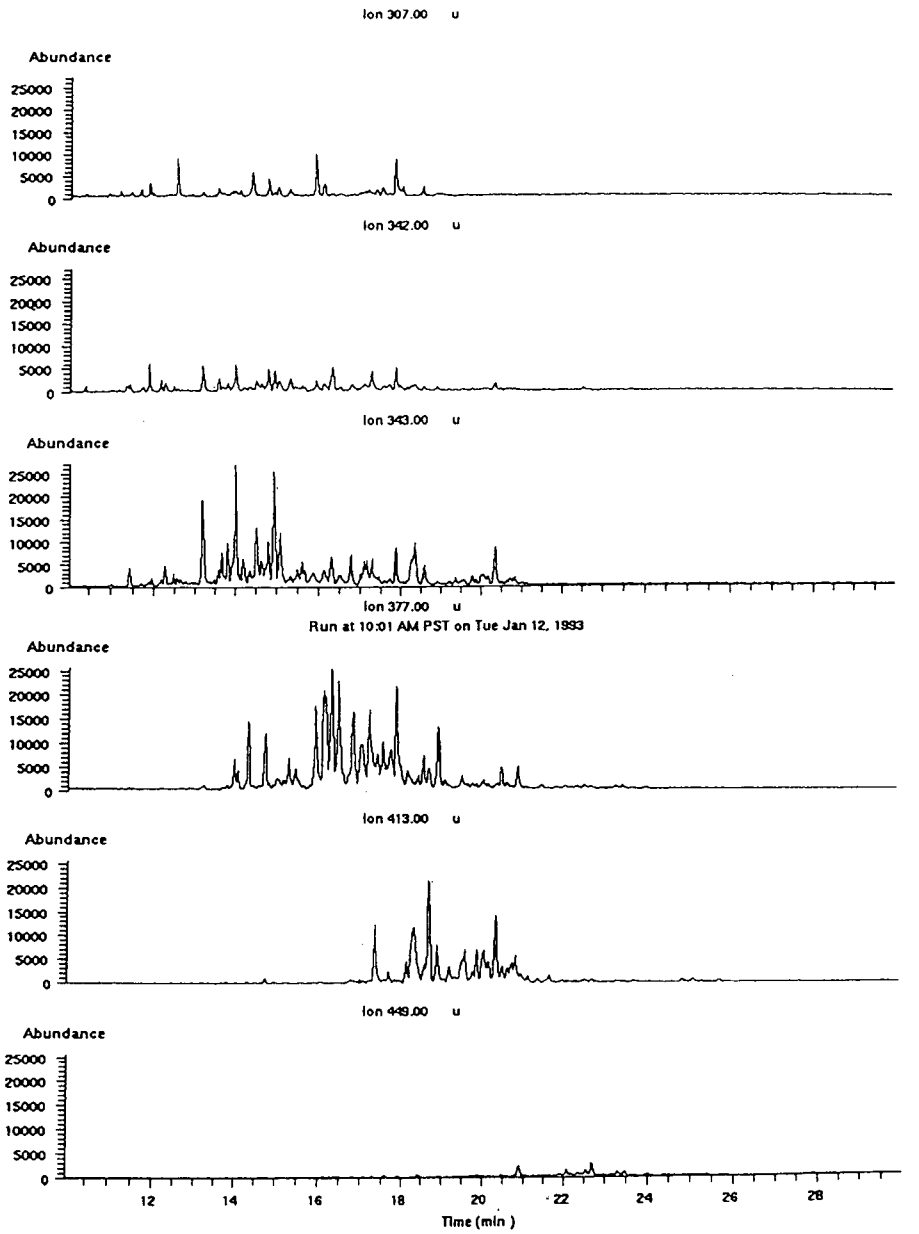

Fig. 2. Toxaphene mass chromatograms obtained from the TIC using specific masses selected from the solid-probe mass spectrum.

during the long period. However, no direct evidence was obtained on biodegradation since neither the components undergoing degradation nor metabolites were identified.

The ions monitored for toxaphene are the $[M - Cl^{\bullet}]^{-}$ ions resulting from $C_{10}H_{12}Cl_x$ through $C_{10}H_8Cl_{10}$ compositions (bornanes and overlapping contributions from ions resulting

from bornenes. Internal standard, 2,4,5,3′,4′-pentachlorobiphenyl having retention time of 14.38 min was monitored at m/z 326 for quantitation.

Table 2 provides results of analyses of selected soil samples for toxaphene. It can be seen even at different levels of the toxaphene concentration in soil samples between 800 and 1200 μg/g, that relative distribution among chlorine homologue classes did not differ significantly. A simple comparison between different levels provides an interesting observation. Differences in variation for hexachlorinated homologues are lower than 10%, and for heptachlorinated congeners less than 3%. Greater variations are observed for nona- and decachlorinated congeners (23.6 and 16%, respectively).

A similar laboratory experiment involving long-term exposure of soil samples containing approximately 25 μg/g toxaphene underwent 123 day treatments employing unique anaerobic dechlorination processes developed at Grace-Dearborn Environmental Engineering Group. Different treatment shows different kinetics of degradation as it can be seen in Fig. 3. A summary of these data indicates a modest degradation of toxaphene during this period.

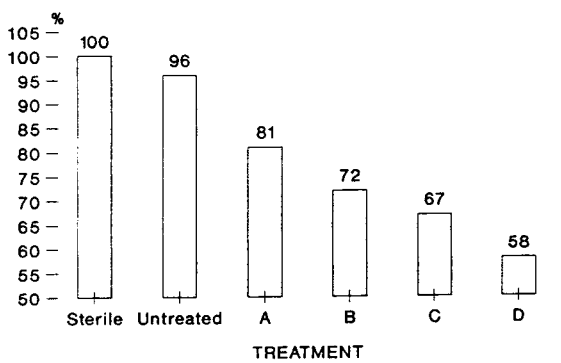

Fig. 3. A controlled experiment data showing biodegradation of toxaphene. Test duration 123 days.

4. Conclusions

The presented results demonstrate the feasibility of performing multicomponent quantitative analyses of toxaphene at the mg/kg–μg/kg level using a 1-g sample of soil by electron-capture negative-ion mass spectrometry after separation of toxaphene congeners by HRGC. The application of a mass spectrometer as a substance-selective detector shows advantages of the continuous repetitive scanning of mass spec-

Table 2
Quantitation of toxaphene in soil samples in mg/kg

Sample	Total tox.	6chloro-	7chloro-	8chloro-	9chloro-	10chloro-
1	716	171.8	250.6	229.1	57.3	7.2
2	908	217.9	317.8	290.5	72.6	9.2
3	842	168.4	269.4	286.3	88.4	9.5
4	728	174.7	254.8	232.9	58.2	7.4
5	891	222.7	311.8	294.0	58.0	4.5
6	1159	283.9	441.4	376.7	81.1	5.9
7	1070	235.4	342.4	353.1	117.7	21.4
8	821	180.6	262.7	270.9	90.3	16.5
9	1181	253.9	395.6	389.7	124.0	17.8
10	1233	272.3	419.2	394.6	135.6	11.3
11	668	147.0	233.8	217.1	66.8	3.3
12	940	188.0	300.8	319.8	94.0	37.6
13	772	154.4	254.8	254.9	84.8	23.1
14	1098	241.6	384.3	373.3	87.8	11.0
15	1950	448.5	702.0	624.0	146.2	29.3
16	1095	240.9	383.3	372.3	87.6	10.9

tra over selected ion monitoring. The EC-NCI mass spectra of toxaphene clearly indicates impurities that can be detected and corrected for and in SIM may provide false-positive data.

5. References

[1] *Proceedings of the Workshop on the Analytical and Environmental Chemistry of Toxaphene*, Department of Indian and Northern Affairs, Atmospheric Environmental Service and Department of Fisheries and Oceans, Burlington, 1993.

[2] D.B. Sargeant, and F.I. Onuska, in B.K. Afghan and A.S.Y. Chau (Editors), *Analysis of Organics in the Aquatic Environment*, CRC Press, Boca Raton, FL, 1989.

[3] T.F. Bidleman and C.E. Olney, *Nature*, 257 (1975) 475.

[4] F.I. Onuska, K.A. Terry, *J. Chromatogr.*, 471 (1989) 161.

[5] *Test Methods for Evaluating Solid Waste (SW-846)*, Vol. 1B, US Environmental Protection Agency, Washington, DC, 1986.

[6] B. Jansson and U. Wideqvist, *J. Environ. Anal. Chem.*, 13 (1983) 309.

[7] D.L. Swackhamer, M.J. Charles and R.A. Hites, *Anal. Chem.*, 59 (1987) 913.

[8] A.K. Klein and D.J. Link, *J. Assoc. Off. Anal. Chem.*, 53 (1970) 524.

[9] S. Jensen, L. Reutergardh and B. Jansson, *Manual of Methods in Aquatic Environmental Research, Part 9, Fisheries Technical Paper No. 212*, UN Food and Agriculture Organization, Rome, 1983, p. 21.

ELSEVIER

Journal of Chromatography A, 665 (1994) 133–138

JOURNAL OF CHROMATOGRAPHY A

Purge-and-trap injection capillary gas chromatographic determination of volatile aromatic hydrocarbons in river sediment

P. Kuráň, R. Kubinec, I. Ostrovský, L. Soják*

Chemical Institute, Faculty of Natural Sciences, Comenius University, Mlynská Dolina CH-2, 84215 Bratislava, Slovak Republic

Abstract

Dynamic headspace and purge-and-trap with methanolic extraction techniques for the simple and rapid determination of trace amounts of volatile aromatic hydrocarbons in river sediments were compared. The purge-and-trap technique with metanolic extraction using an external standard method gives a better representativeness of the analysed sample, a twofold higher precision and twofold lower detection limits. When the internal standard method is applied, the precision of both methods increases 3–4 times and the detection limits decrease 4–5 times.

1. Introduction

Water and sediment are two matrices closely related to each other in a water column. The determination of organic pollutants in water and sediment samples has been intensively studied during last two decades [1]. Many methods for the determination of organic compounds in ground and surface waters have been described but their direct application to the determination of volatile organic compounds (VOCs) in inland water sediments is infrequent. The water column consists of two phases, the aqueous phase and suspended solids, which complicate their sampling and analysis. It is necessary to take into account factors such as the particle size distribution of the sediment, the content of organic carbon and the considerable composition variability of various types of sediments. In the determination of VOCs, the loss of volatile components during sampling and sample handling and the representativeness of the collected sample should be considered. Available techniques for the determination of volatiles allow results of varying quality, and require validation of the applied methods [2].

Proper sampling is a necessary condition for obtaining reliable analytical results. The sediments represent dynamic systems and therefore the results of every sediment analysis are related to the time of sampling.

The treatment of the collected sediment is usually a critical stage of analysis. It is time consuming and represents the greatest source of errors in environmental analysis [3,4].

The most frequent techniques used for the determination of volatiles are headspace methods [5,6] and purge-and-trap methods [7,8,9] that can be employed in various arrangements. For the static headspace method, the analyte

* Corresponding author.

0021-9673/94/$07.00
SSDI 0021-9673(93)E1200-J

concentrations are not changed after achieving equilibrium. This equilibrium is only disturbed during sampling before injection. The technique is simple and undemanding with regard to instrumentation, but its disadvantage is the relatively low sensitivity. In the dynamic headspace method, the gaseous phase over the sample is permanently purged with carrier gas, which carries the analytes to the trapping medium. This technique enables lower detection limits to be achieved [1]. It is possible to determine the solutes with a lower vapour pressure and the possibility of contamination from the septum is removed. The quality of a representative sample can be improved by modifying these techniques with extraction of volatiles from sediment with a suitable solvent. When methanol is used as the solvent, the microbial degradation of the contaminants is suppressed by its toxic effects. The possibility of the loss of very volatile compounds and the possibility of contamination of the extract are solved by minimizing the free space over the solvent [2,7].

The dependence of the accuracy of analytical results on the solid matrix type can differ. In the analysis of VOCs in solid matrices [5,10] this dependence was not observed and for this reason it is possible to employ a simple external standardization method. However, in the determination of gasoline constituents in different soil types, such a dependence of the results obtained on the matrix type was found [2].

The purpose of this work was to compare dynamic headspace and purge-and-trap injection with metanolic extraction (PTI/MeOH) techniques for the determination of trace amounts of volatile aromatic hydrocarbons at the ppm level in river sediments from the point of view of reliability of the results (precision, reproducibility and recovery).

2. Experimental

2.1. Purge-and-trap unit

The PTI device (Chrompack, Middelburg, Netherlands) was used as an automatic stripping and preconcentration system. This unit is designed for the isolation and preconcentration of volatiles from liquid matrices. This device allows the simultaneous connection of one capillary column to two parallel detectors.

The PTI unit consisted of a 5-ml stripping vessel, a water condenser cooled with ethanol, a fused-silica capillary column (30 cm × 0.53 mm I.D.; film thickness 2.65 μm) coated with an immobilized methylsilicone stationary phase (SE-54) and an oven that heats the trapping capillary tube.

2.2. Gas chromatograph

A CP 9000 gas chromatograph (Chrompack) was used. The separation was carried out using a fused-silica capillary column (25 m × 0.32 mm I.D.; film thickness 0.52 μm) with SE-54 as the stationary phase. The column was connected to a flame ionization detector by means of a metal coupling and a 30 cm length of capillary of 0.32 mm I.D.

The oven temperature was maintained at 40°C for 7 min, then programmed at 10°C/min to 240°C. After reaching the final temperature, the analysis was completed. Nitrogen (99.999% purity) (MG Tatragas, Bratislava, Slovak Republic) was used as the carrier gas.

2.3. Reagents and standards

Drinking water was used for dilution of the methanolic extract.

A standard mixture of volatile aromatic hydrocarbons (benzene, 3.5 mg/kg; toluene, 3.5 mg/kg; ethylbenzene, 6.9 mg/kg; *m*-xylene, 6.9 mg/kg; *o*-xylene, 6.9 mg/kg) was prepared from analytical-reagent grade chemicals (Lachema, Brno, Czech Republic) by dilution with methanol.

2.4. Dynamic headspace method

A 1-g amount of the wet sediment was spiked with 4 μl of the standard mixture of volatile aromatic hydrocarbons. The sample was heated in a water-bath (70°C) and purged with nitrogen

(99.999%) at 30 ml/min. The volatiles were trapped in the SE-54 (2.65 μm) fused-silica capillary column (30 cm × 0.53 mm I.D.) cooled to −100°C. After 10 min the capillary was heated to 220°C. Subsequently, the volatiles were desorbed into the SE-54 (0.52 μm) analytical capillary column (25 m × 0.32 mm I.D.).

2.5. Purge-and-trap with methanolic extraction method

A 1-g amount of the wet sediment was spiked with 4 μl of the standard mixture, then 1 ml of methanol was added and the mixture was shaken for 2 min in a closed vessel. A 100-μl volume of the extract was transferred into 5 ml of drinking water, which was immediately purged at 30°C for 10 min. The other analytical parameters were the same as for the dynamic headspace method.

3. Results and discussion

The possibilities of using the Chrompack purge-and-trap injector, designed for the determination of volatiles in waters, in the determination of volatile aromatic hydrocarbons in sediments using the dynamic headspace and the PTI/MeOH techniques were studied. As model compounds benzene, toluene, ethylbenzene, *m*-xylene and *o*-xylene were used with the aim of finding the optimum experimental conditions for their simple and rapid determination at the ppm level.

3.1. Influence of spiking procedure on response

The influence of the location of adding pollutant to the sediment on the response and reproducibility was studied. A considerable difference in the results obtained by the dynamic headspace and PTI/MeOH methods was observed when the surface and the bottom layer of the sediment were spiked with the standard mixture. The differences in the responses of the peak areas of the analytes from seven successive analyses for these two extreme positions of pollutant addition are documented in Table 1. It can be seen that the peak areas of aromatics in the dynamic headspace method are approximately double for sediment spiked in the surface layer. This result is related to the better contact of the purge gas with analytes spiked on the surface. In the PTI/MeOH method this effect, despite a *ca.* tenfold lower response, is considerably suppressed and the peak areas of aromatics are on average about 20–30% higher (with the exception of benzene). The relative standard deviations confirm the elimination of this effect because they are virtually independent of the position of pollutant addition.

This experiment basically simulates heteroge-

Table 1
Peak areas of standard aromatic hydrocarbons and their relative standard deviations for the different procedures of sediment spiking for dynamic headspace (under 70°C) and PTI/MeOH (under 30°C) techniques

Aromatic hydrocarbon	x_p				R.S.D. (%)			
	Dynamic headspace		PTI/MeOH		Dynamic headspace		PTI/MeOH	
	1	2	1	2	1	2	1	2
Benzene	15 451	47 666	2133	4225	85.0	35.3	41.8	21.1
Toluene	17 892	44 509	6044	8435	88.1	26.2	36.7	11.1
Ethylbenzene	47 708	100 905	5202	7178	92.1	27.3	29.4	19.9
m-Xylene	50 998	105 929	5533	7513	89.4	26.9	26.9	19.7
o-Xylene	56 673	115 116	6074	7889	83.4	26.1	22.0	18.2

x_p = average peak area ($n = 7$); R.S.D. = relative standard deviation; 1 = bottom layer spiked with standard; 2 = surface spiked with standard.

Table 2
R.S.D.s and detection limits (DL) for standard aromatic hydrocarbons added to the sediment using the external standard method with the dynamic headspace (under 70°C) and PTI/MeOH (under 30°C) techniques

Aromatic hydrocarbon	Dynamic headspace			PTI/MeOH		
	x_p	R.S.D. (%)	DL (mg/kg)	x_p	R.S.D. (%)	DL (mg/kg)
Benzene	31 558	70.1	7.4	3457	36.4	3.8
Toluene	31 201	61.6	6.5	7427	28.6	3.0
Ethylbenzene	74 307	60.2	12.5	6190	28.3	5.0
m-Xylene	78 464	59.0	12.3	6523	26.9	5.6
o-Xylene	85 894	56.6	11.7	6953	24.4	5.1
Average	–	61.5	10.1	–	28.9	4.5

x_p = average peak area ($n = 14$); R.S.D. = relative standard deviation.

neous sediments and indicates the parameter that influences the results of the analysis.

3.2. External and internal standardization methods

A comparison of the precisions and detection limits for the external and internal standardization methods without taking into account the influence of the spiking procedure is presented in Tables 2 and 3.

In a real analysis of a sediment, especially a heterogeneous one, it is not possible to predict the position of a pollutant in the sediment. The final result in the dynamic headspace technique will contain an error depending on the pollutant position. This is why it is necessary to evaluate results obtained for both extreme positions as one set, and hence it is possible to approach the closest to the real situation.

The values in Table 2 indicate that in the PTI/MeOH method the precision of peak areas is approximately twice that for the dynamic headspace method (average R.S.D. 28.9% *vs.* 61.5%), which indicates the elimination of the effect of the pollutant position. The detection limits, calculated on the basis of average peak areas of aromatics and their standard deviation for 99% probability (the coefficient of the Student distribution for 13 degrees of freedom is $t = 3.01$), are *ca.* 50% lower for the PTI/MeOH technique (4.5 *vs.* 10.1 mg/kg).

Table 3
R.S.D.s and detection limits (DL) for standard aromatic hydrocarbons added to the sediment using the internal standard method with the dynamic headspace (under 70°C) and PTI/MeOH (under 30°C) techniques

Aromatic hydrocarbon	Dynamic headspace			PTI/MeOH		
	x_p	R.S.D. (%)	DL (mg/kg)	x_p	R.S.D. (%)	DL (mg/kg)
Benzene	42.86	39.1	4.1	54.66	14.0	1.5
Toluene	41.89	18.8	2.0	123.08	20.8	2.2
Ethylbenzene	100.00	–	–	100.00	–	–
m-Xylene	107.08	3.2	0.7	106.07	3.3	0.7
o-Xylene	120.40	7.7	1.6	114.13	7.0	1.5
Average	–	17.2	2.1	–	11.2	1.5

x_p = average peak area ($n = 14$); R.S.D. = relative standard deviation.

Table 4
Recoveries of standard aromatic hydrocarbons from sediment using the dynamic headspace (under 70°C) and PTI/MeOH (under 30°C) techniques

Aromatic hydrocarbon	Dynamic headspace			PTI/MeOH		
	x_p	R.S.D. (%)	Recovery (%)	x_p	R.S.D. (%)	Recovery (%)
Benzene	145 163	45.7	21.7	16 694	16.8	20.7
Toluene	140 690	24.4	22.2	19 745	20.4	37.6
Ethylbenzene	263 725	14.8	28.2	22 359	15.8	27.6
m-Xylene	269 175	14.2	29.1	22 224	15.6	29.4
o-Xylene	264 792	11.3	32.3	21 066	15.5	33.0
Average	–	22.1	26.7	–	16.8	29.7

x_p = average peak area ($n = 7$); R.S.D. = relative standard deviation.

Despite the increased precision of the analysis by using the PTI/MeOH method, the relative standard deviations were still relatively high (see Table 2). Therefore, the possibilities of increasing the precision of the method by using ethylbenzene as an internal standard were studied. Both methods were again compared. The average peak areas of particular aromatics with the corresponding relative standard deviations and detection limits are given in Table 3. They were recalculated with respect to the area of ethylbenzene as an internal standard (=100). In this case the precision of the PTI/MeOH method was on average 11.2% and for the dynamic headspace method 17.2%; the detection limits were 1.5 mg/kg on average for the PTI/MeOH method and 2.1 mg/kg for the dynamic headspace method. The precision of both methods in comparison with results obtained from the external standard method increased approximately 3–4 times and simultaneously the detection limits were decreased approximately 4–5 times. It is concluded that the results obtained by the two techniques are comparable.

3.3. Recoveries of volatile aromatics from sediment

The recoveries of aromatics from sediment are given in Table 4. They are relatively low for both

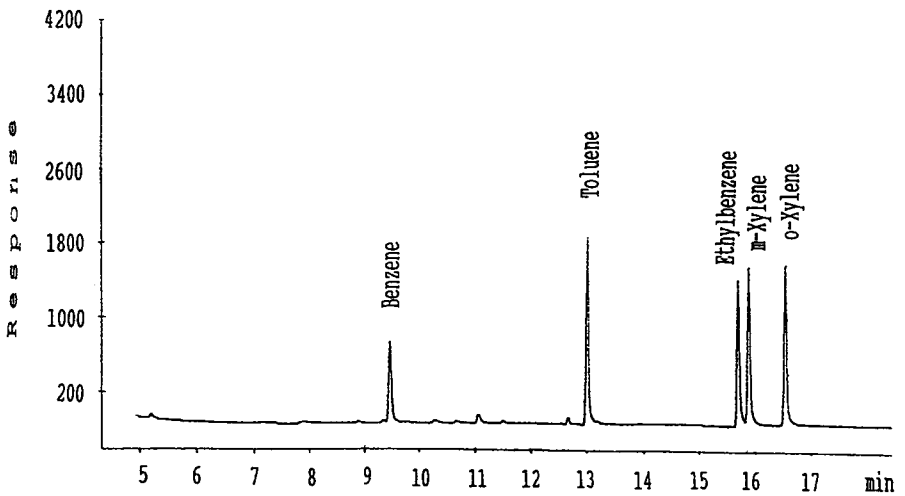

Fig. 1. Chromatogram of the standard mixture of volatile aromatic hydrocarbons in a sediment analysed by the PTI/MeOH method.

the dynamic headspace and PTI/MeOH techniques (on average 26.7% and 29.7%, respectively). The low recoveries are related to the short purging times in both methods in order to decrease time and economics of the analyses. The recovery of aromatics increases moderately with decreasing volatility. This finding is contradictory to results presented in the literature [1], where it was stated that the recovery decreases with increasing boiling point. The problem of the recovery increase and detection limit decrease will be studied further.

The results obtained were employed for the determination of volatile hydrocarbons in sediments and sludges by means of the PTI/MeOH technique. A chromatogram of the standard mixture is shown in Fig. 1.

4. Conclusions

Dynamic headspace and PTI/MeOH techniques for the determination of volatile aromatic hydrocarbons in river sediment from the point of view of precision, sensitivity, representativeness of the analysed sample and recovery were compared. The PTI/MeOH method with an external standard gives a better representativeness of the analysed portion and a twofold higher precision and twofold lower detection limits. When the internal standard method is applied, the precision of both methods increases 3–4 times and the detection limits decrease 4–5 times. The results obtained for the two techniques with the internal standard method are comparable. The disadvantage of both methods is the low recovery of aromatics from sediment.

5. References

[1] A.P. Bianchi, M.S. Varney and J. Philips, *J. Chromatogr.*, 542 (1991) 413.
[2] J.L. Parr, G. Walters and M. Hoffman, in P.T. Kostecki and E.J. Calabrese (Editors), *Hydrocarbon Contaminated Soils and Groundwater*, Vol. 1, Lewis, MI, 1991, p. 105.
[3] R.E. Majors, *LC · GC*, 4 (1992) 10.
[4] C.L.P. Thomas, *LC · GC*, 6 (1992) 9.
[5] A. Venema, *J. High Resolut. Chromatogr.*, 13 (1990) 537.
[6] M. Tóth and H.R. Buser, *J. Chromatogr.*, 598 (1992) 303.
[7] J.V. Hinshaw, *LC · GC*, 3 (1990) 22.
[8] R.P. Eganhouse, T.F. Dorsey and C.S. Phinney and A.M. Westcott, *J. Chromatogr.*, 628 (1993) 81.
[9] S.A. Rounds and J.F. Pankow, *J. Chromatogr.*, 629 (1993) 321.
[10] A. Hagman, *Ph.D. Thesis*, University of Stockholm, Stockholm, 1988, p. 7.

ELSEVIER

Journal of Chromatography A, 665 (1994) 139–153

JOURNAL OF CHROMATOGRAPHY A

Method for the group separation of non-*ortho*-, mono-*ortho*- and multi-*ortho*-substituted polychlorinated biphenyls and polychlorinated dibenzo-*p*-dioxins/polychlorinated dibenzofurans using activated carbon chromatography

Anton Kočan*, Ján Petrík, Jana Chovancová, Beata Drobná

Institute of Preventive and Clinical Medicine, Limbová 14, 833 01 Bratislava, Slovak Republic

Abstract

A cheap, efficient and reliable method for the separation of mono-*ortho*-/non-*ortho*-substituted polychlorinated biphenyls (PCBs), multi-*ortho*-PCBs and polychlorinated dibenzo-*p*-dioxins/polychlorinated dibenzofurans (PCDDs/PCDFs) from one another and from other interferents was developed. A mixture of activated carbon AX-21 (50 mg) and Celite 545 as a carbon support (1:19) packed in a diposable tube was used. The compounds were gradually eluted with cyclohexane–dichloromethane–methanol (2:2:1) and toluene (a coplanar PCB fraction). PCDDs and PCDFs were regained by extraction of the inverted AX-21–Celite column with a small volume of toluene in a special miniaturized extraction apparatus. Recoveries from the column for PCBs and PCDDs/PCDFs varied from 63% to 100%. The method was used successfully for the fractionation of PCB technical formulations (Delor 103 and 105), municipal waste incinerator fly ash and biological samples (human adipose tissue, butter, egg and fish samples). The method is suitable for both mass spectrometric and electron-capture detection.

1. Introduction

The toxicity of polychlorinated dibenzo-*p*-dioxins (PCDDs) and polychlorinated dibenzofurans (PCDFs), mainly the most toxic 2,3,7,8-tetrachlorodibenzo-*p*-dioxin (TCDD), has been relatively closely investigated [1]. Recent studies [2] have also shown that polychlorinated biphenyl (PCB) congeners which are biochemically active [arylhydrocarbon hydroxylase (AHH) and ethoxyresorufin O-deethylase (EROD) induction] have planar or almost planar molecular structures, *i.e.*, have chlorine substitution of the aromatic rings in both *para* positions and in two or more of the four *meta* positions. In addition, the analyses carried out following extensive human exposure to PCBs in Fukuoka (Japan) [3] and Taiwan [4] have showed that technical PCB mixtures such as Aroclors [5], Delors [6] and Kanechlors [7], in addition to several tens of PCB congeners, also contain substantially more toxic PCDFs as by-products. However, it has been found that some PCB congeners present in technical PCB mixtures [7] and environmental samples [8–10] also exhibit extremely high toxicity comparable to those of 2,3,7,8-substituted PCDDs and PCDFs [11].

There are at least three environmentally occurring coplanar non-*ortho*-substituted PCBs, namely 3,3′,4,4′-tetra- (IUPAC No. 77 according

* Corresponding author.

0021-9673/94/$07.00
SSDI 0021-9673(93)E1163-T

to Ballschmiter and Zell [12]), 3,3',4,4',5-penta- (No. 126), and 3,3',4,4',5,5'-hexachlorobiphenyl (No. 169), with proposed TEFs (2,3,7,8-TCDD toxic equivalency factors) of 0.01, 0.1, and 0.05, respectively [13], and at least eight coplanar mono-*ortho*-PCBs, namely 2,3',4,4',5-penta- (No. 118), 2,3,3',4,4'-penta- (No. 105), 2',3,4,4',5-penta- (No. 123), 2,3,4,4',5-penta- (No. 114), 2,3,3',4,4',5-hexa- (No. 156), 2,3,3',4,4',5'-hexa- (No. 157), 2,3',4,4',5,5'-hexa- (No. 167) and 2,3,3',4,4',5,5'-heptachlorobiphenyl (No. 189) with proposed TEFs of 0.001 [13], fulfilling the above-mentioned structural conditions. As these TCDD-like PCB congeners have been found in environmental and biological samples mostly at substantially higher levels than 2,3,7,8-substituted PCDDs and PCDFs, their contribution to the total TEQ (2,3,7,8-TCDD toxic equivalent) dominates those of the PCDDs and PCDFs [7,10,14–20].

For these reasons, it is important to determine, in addition to the "classical" PCBs (Nos. 28, 52, 101, 138, 153 and 180) and the 2,3,7,8-substituted PCDDs and PCDFs, also the non-*ortho*- and mono-*ortho*-PCBs.

As even high-resolution gas chromatographic (HRGC)–mass spectrometric (MS) with selected-ion monitoring (SIM) peaks of the non-*ortho*- and mono-*ortho*-PCBs may be overlapped with those of multi-*ortho*-PCBs [6,21] and other interfering co-extracted compounds, *e.g.*, DDE and DDT, and in addition environmental levels of multi-*ortho*-PCBs, mono-*ortho*-PCBs, non-*ortho*-PCBs and PCDDs/PCDFs are very different, it may be useful to divide precleaned or raw sample extracts into at least two fractions containing non-/mono-*ortho*-PCBs and PCDDs/PCDFs. Carbon chromatography gives an opportunity for realising this demand.

Smith *et al.* [22] developed a very successful method (which has been used in many variations [8,16,23,24]) for PCDD/PCDF determination based on cleaning up extracts of biological samples using potassium and caesium silicate, silica gel and H_2SO_4–silica and active carbon AX-21 (50 mg) dispersed on glass fibres [25]. There are many papers dealing with the testing of the efficiency of various types of active carbon (*e.g.*, Norit, Darco, AX-21, PX-21, Carbopack C, Supelco SP-1, Altech SK-4, Wako, Carbosphere, Baker, Separcol R-CARB cartridges) and the suitability of various supports (*e.g.*, polyurethane foam, sand, glass fibres, Chromosorb, Celite, silica gel, polystyrene–divinylbenzene copolymers) [17,24–36].

After the non-*ortho*- and mono-*ortho*-PCBs had become compounds of interest because of their toxicity, the ability of activated carbon to retain these pollutants has started to be utilized [9,10,15–17,19,20,23,31–41]. HPLC on porous graphitic columns has also provided satisfactory results in the field [18,42–44]. Various types of semi-automated apparatus that include an active carbon column with reverse elution have been introduced [40,45–47]. On a Carbopack C column, it is even possible to separate non-*ortho*- from mono-*ortho*-PCBs [35].

From our point of view, some of the above methods have drawbacks, such as high elution solvent consumption, expensive sorbents, low recoveries, uncertain reproducibility, low adsorption capacity, insufficient separation of compounds of interest, a need for more complex devices (HPLC, automation) and excessive background electron-capture detection (ECD) noise.

In this paper, we describe a cheap, reliable, highly reproducible, robust and efficient method based on the carbon chromatography that permits the separation of two groups of toxic chloroaromatic pollutants, namely coplanar PCBs (non-*ortho*- and mono-*ortho*-) and PCDDs/PCDFs, from each other and from interfering compounds, including di- to tetra-*ortho*-substituted PCBs.

2. Experimental

2.1. Reagents and standards

Solvents. *n*-Hexane, cyclohexane, dichloromethane, methanol, toluene (all of pesticide quality were obtained from Labscan, Dublin, Ireland) and *n*-heptane (for residue analysis) from Merck (Darmstadt, Germany).

Adsorbents. Super-A Activated Carbon AX-

21, lot No. 88049 (Anderson Development, Adrian, USA), Celite 545, 0.020–0.045 mm (Serva, Heidelberg, Germany), Florisil, 0.150–0.250 mm (Fluka, Buchs, Switzerland), silica gel 60, 0.063–0.200 mm (Merck) and ICN alumina B Super 1 (ICN Biomedicals, Eschwege, Germany) were used.

Other materials. Sodium sulphate, anhydrous granulated for residue analysis (Merck), sulphuric acid, GR, 95–97% (Merck), potassium hydroxide, GR (Merck), silver nitrate, GR (Medika, Bratislava, Slovak Republic), glasswool, silane treated (Chromatography Research Supplies, Addison, USA) and nitrogen, 99.99% (Linde-Technoplyn, Bratislava, Slovak Republic), purified by molecular sieve 5A and charcoal traps, were used.

Standards. *n*-Heptane solutions of di-*ortho*-PCBs [Nos. 28 (2,4,4′-trichlorobiphenyl, *i.e.*, mono-*ortho*-PCB congener), 52, 101, 138, 153 and 180 (400 ng ml^{-1} each), 10 $\mu g\ ml^{-1}$ solutions were purchased from Labor Dr. Ehrenstorfer, Augsburg, Germany], mono-*ortho*-PCBs [Nos. 105, 114, 118, 123, 156, 157, 167 and 189 (200 ng ml^{-1} each), 35 $\mu g\ ml^{-1}$ solutions were purchased from Amchro, Sulzbach/Taunus, Germany], non-*ortho*-PCBs [Nos. 77, 126 and 169 (400 ng ml^{-1} each), 35 $\mu g\ ml^{-1}$ solutions were purchased from Amchro] $^{13}C_{12}$-labelled PCBs [Nos. 77, 126, 169, 105 and 118 (100 ng ml^{-1} each), 40 $\mu g\ ml^{-1}$ solutions were purchased from Cambridge Isotope Labs., Woburn, MA, USA], PCDDs/PCDFs [1,2,4-TrCDD, 2,3,7,8-TCDD, 2,3,7,8-TCDF, 1,2,3,7,8-PeCDD, 1,2,3,4,7,8-HxCDD, OCDD, and OCDF (TrCDD = trichlorodibenzo-*p*-dioxin; TCDF = tetrachlorodibenzofuran; HxCDD = hexachlorodibenzo-*p*-dioxin; OCDF = octachlorodibenzofuran; TCDD = tetrachlorodibenzo-*p*-dioxin; PeCDD = pentachlorodibenzo-*p*-dioxin; OCDD = octachlorodibenzo-*p*-dioxin) (400 ng ml^{-1} each), solids were either purchased from Cambridge Isotope Labs. or were kindly donated by Dr. K. Olie, University of Amsterdam], $^{13}C_{12}$-labelled 2,3,7,8-substituted PCDDs and PCDFs (50 ng ml^{-1} TCDDs/TCDFs, 100 ng ml^{-1} PeCDDs/pentachlorodibenzofurans (PeCDFs), 150 ng ml^{-1} HxCDDs/hexachlorodibenzofurans (HxCDFs), 200 ng ml^{-1} heptachlorodibenzo-*p*-dioxins (HpCDDs)/heptachlorodibenzofurans (HpCDFs) and 300 ng ml^{-1} OCDD/OCDF), and some organochlorine pesticides [hexachlorobenzene (HCB), γ-benzene hexachloride (γ-HCH), *p,p′*-DDE and *p,p′*-DDT (1600, 400, 1600 and 400 ng ml^{-1}, respectively), solids were purchased from Supelco, Bellefonte, PA USA] were used as model compounds for the development of the separation method.

2.2. Samples

For the evaluation of the carbon separation method, the following samples were used.

PCB technical formulations. These were Delor 103, a technical PCB mixture corresponding to Aroclor 1242 (Chemko, Strážske, Slovak Republic), Delor 105, a technical PCB mixture corresponding to Aroclor 1254 (Chemko).

Fly ash. Fly ash from a municipal waste incinerator (MWI) in Bratislava (Slovak Republic) (10 g) was treated with 5% HCl, centrifuged, filtered through a Büchner funnel, dried at 50°C (maximum) and Soxhlet extracted with toluene for 24 h and either the residues were applied to an AX-21–Celite column or the toluene extract was cleaned up using a modified silica column and an ICN alumina B Super 1 column and the residues were then applied to the AX-21–Celite column [48,49].

Biological samples. The samples used were butter fat (pooled sample from eight Slovak producers), fish oil (pharmacy, Bratislava), oil from a cod liver tin (imported from Germany), shark fat (an *n*-hexane–acetone extract of shark meat purchased at a supermarket, Bratislava), catfish fat (an *n*-hexane–acetone extract of catfish meat purchased at a supermarket, Bratislava), egg fat (an egg obtained from a family farm, Sobotište, Slovak Republic; the yolk was mixed with anhydrous Na_2SO_4, a column was packed with the mixture and the fat was extracted with diethyl ether) and human fat (adipose tissue from an autopsy, Bratislava, extracted in the same way as the egg yolk). The

majority of lipids from the fat samples, if 1 g was taken for analysis, was removed with a Florisil column [60 g of Florisil activated at 600°C for 4 h and then overnight at 130°C, prewashed with 150 ml of *n*-hexane and analytes eluted with 300 ml of diethyl ether–*n*-hexane (3:50)]. A disposable column packed with 0.5 g of Florisil, 1 g of 44% H_2SO_4–silica, 0.5 g of Florisil and 1 g of anhydrous Na_2SO_4 was used for removing lipids from about 50-mg fat samples.

2.3. Carbon chromatography

Preparation of AX-21–Celite mixture. Activated carbon AX-21 (4 g) was thoroughly mixed with Celite 545 (76 g) to produce a 1:19 mixture. The mixture was purified using Soxhlet extraction with toluene for 8 h, dried in a vacuum oven at 100°C, then activated in a GC oven at 200°C under a nitrogen atmosphere for at least 8 h and stored in a desiccator.

Preparation of AX-21–Celite column. A disposable glass tube (30 cm × 10 mm O.D. × 8 mm I.D.) rinsed with acetone and *n*-hexane, including its outer surface [from this point the bottom part (11–12 cm) of the tube must not come into contact with hands or other contaminating surfaces], was perfectly sealed with a dense 1-cm silanized glass-wool plug which was shifted about 0.5–0.75 cm into the column. The tube was gradually packed with 0.1 g of Celite 545 and 1 g of the activated AX-21–Celite mixture, *i.e.*, the column contained 50 mg of AX-21 (the packing portions were always shaken with a vibration device). Carbon particles retained on the inner tube wall were rinsed off with a gentle stream of toluene (10 ml) from a pipette. After the carbon particles had settled, 0.1 g of Celite was poured into the toluene layer. As soon as the toluene had almost soaked into the column packing, the wall was rinsed with 3 ml of toluene in the same way as above. Finally, another 0.1-g portion of Celite was added and the column wall was again rinsed with 3 ml of toluene. The ready-to-use column is illustrated in Figure 1.

After the toluene rinse, the column was prerinsed with 5 ml of cyclohexane–dichloromethane–methanol (2:2:1) and finally with 5 ml of *n*-hexane. Then a sample extract (raw or precleaned) in 1 ml of *n*-hexane could be applied to the column. The sample container was then rinsed out with 3 × 0.5 ml of *n*-hexane.

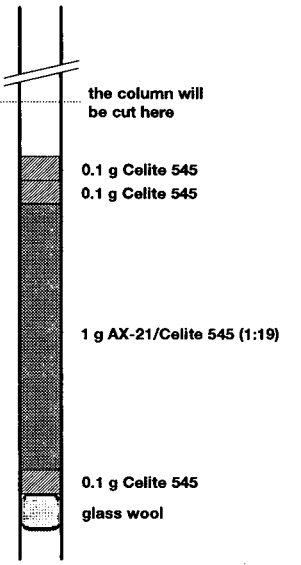

Fig. 1. Cross-section of the ready-to-use AX-21–Celite column. See text for description of adsorbent and column preparation.

Elution. Based on the elution profiles obtained, we decided on fractions as follows:

Fraction 1a: 4 ml of cyclohexane–dichloromethane–methanol (2:2:1), contains none of the model compounds (except approximately one third of *p,p'*-DDE and one quarter of *p,p'*-DDT);

Fraction 1b: 7 ml of cyclohexane–dichloromethane–methanol (2:2:1), contains multi-*ortho*-PCBs (no No. 28), γ-HCH, *p,p'*-DDT and *p,p'*-DDE;

Fraction 1c: 24 ml of cyclohexane–dichloromethane–methanol (2:2:1), contains none of the model compounds;

Fraction 2a: 2 ml of toluene, contains none of the model compounds;

Fraction 2b: 10 ml of toluene, contains the mono-*ortho*-PCBs, and the non-*ortho*-PCBs.

The column after air-drying overnight was carefully cut at about 1–1.5 cm above the packing and this empty space was filled with a dense plug of glass-wool. This shortened column (10–

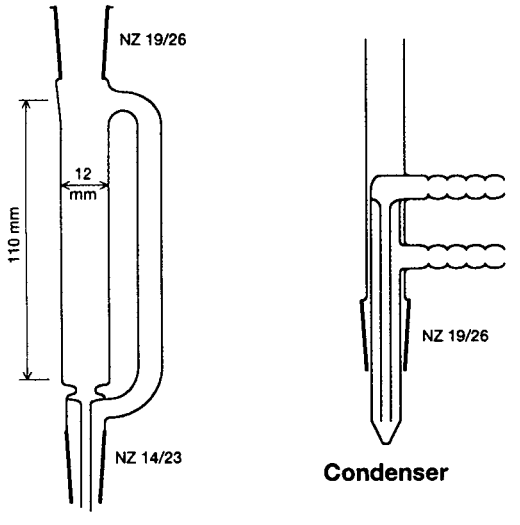

Fig. 2. Parts of the extraction apparatus (a conical-bottomed flask is not illustrated).

11 cm long) was placed in an inverted position in a miniature Soxhlet-like extractor heated by a sand-bath (see Figs. 2 and 3). The empty space at the top of the column (0.5–0.75 cm) should always be filled with dripping toluene to ensure a column flow. Tri- to octachlorinated dibenzo-*p*-dioxins and dibenzofurans were extracted for 3 h with 10 ml of toluene (fraction 3).

2.4. GC–ECD and GC–MS

GC–ECD. For most elution and recovery studies an HP 5890 gas chromatograph (Hewlett-Packard, Palo Alto, CA, USA) equipped with a ^{63}Ni electron-capture detector operated at 320°C with nitrogen at 60 ml min^{-1} as make-up gas was used. A 60 m × 0.25 mm I.D. DB-5 fused-silica capillary column (J & W Scientific, Folsom, CA, USA) at 210 kPa helium column head pressure connected with a splitless injector at 280°C (purge time 1 min) was held at 110°C for 1.5 min, then programmed to 200°C at 30°C min^{-1} and from 200°C to 315°C at 2.5°C min^{-1}, and held at the final temperature until elution of peaks had ceased. The peaks were integrated by an Apex 2.0 chromatographic computer integrator.

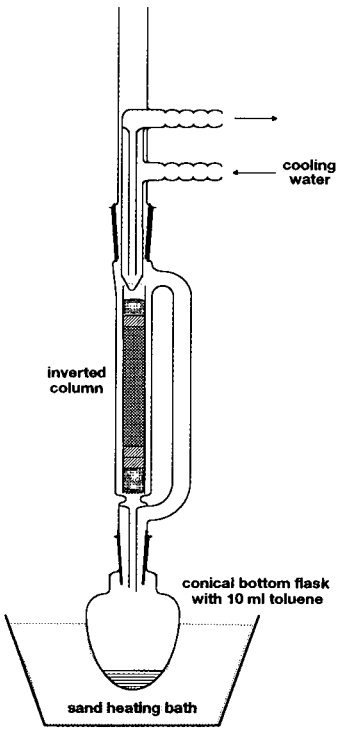

Fig. 3. Schematic diagram of the extraction of PCDDs and PCDFs retained on the AX-21–Celite column.

GC–MS I. An HP 5840A gas chromatograph (Hewlett-Packard) with a 60 m × 0.25 mm I.D. DB-5MS fused-silica capillary column (J & W Scientific) combined through a direct interface with an HP 5985A mass spectrometer in the selected-ion monitoring mode (GC–MS-SIM) was used for the detection of non-, mono- and multi-*ortho*-PCBs and organochlorine pesticides. Two or three *m/z* values corresponding to the most abundant ions from molecular clusters of PCBs and HCB ($[M]^+$, $[M+2]^+$ and/or $[M+4]^+$) were monitored. For *p,p'*-DDE, *p,p'*-DDT and γ-HCH, ions at *m/z* 246.00 and 248.00, *m/z* 235.00 and 237.00 and *m/z* 180.95 and 218.95, respectively, were used. The GC–MS conditions were as follows: column temperature, initially 110°C for 1 min, then program at 30°C min^{-1} to 200°C and at 2.5°C min^{-1} to 305°C; splitless injection port temperature, 280°C; purge time, 1 min; injection volume, 2 μl; carrier gas, helium;

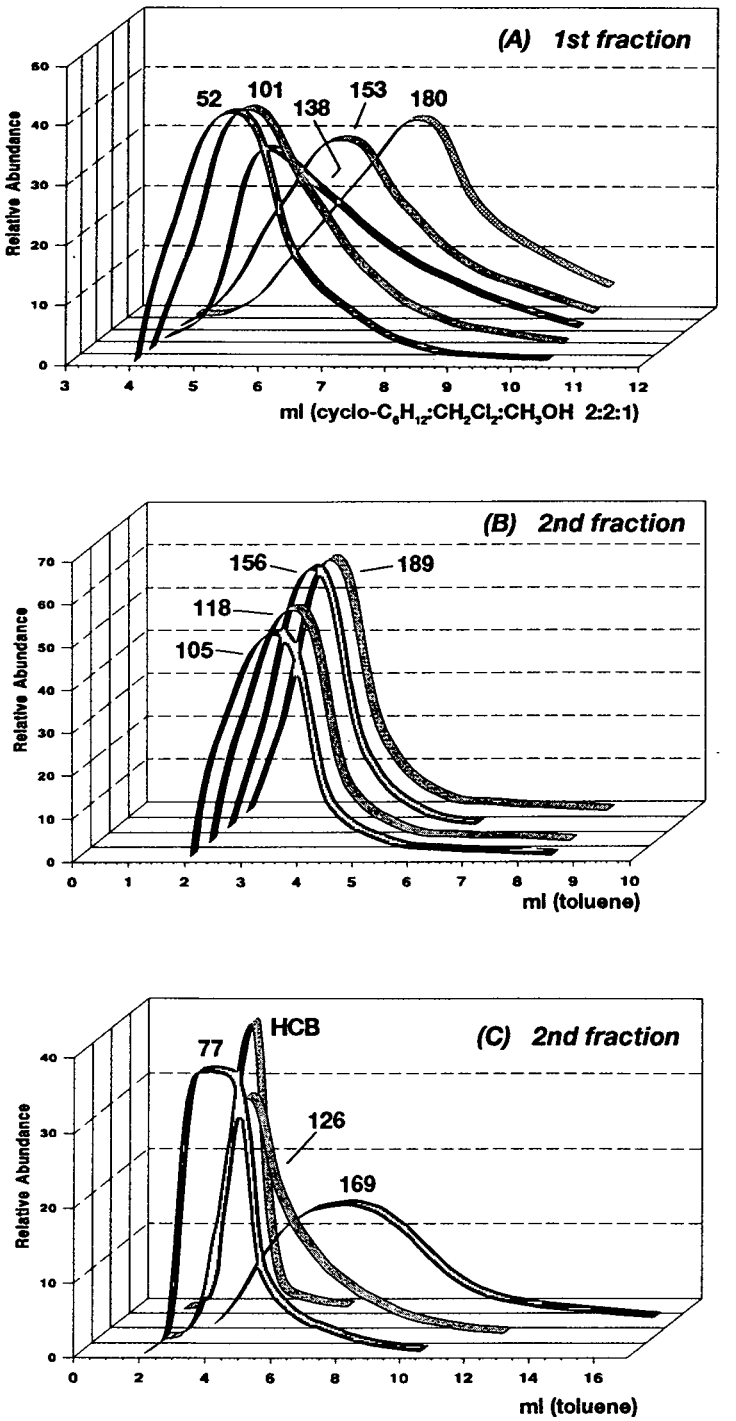

Fig. 4. Elution profiles of (A) di-*ortho*-substituted PCBs, (B) mono-*ortho*-PCBs and (C) non-*ortho*-PCBs + HCB on the AX-21–Celite column. Elution conditions as described in the text; 1-ml subfractions were collected and analysed by HRGC–ECD.

column head pressure, 190 kPa; direct interface temperature, 275°C and ionization energy, 70 eV.

GC–MS II. An HP 5890 Series II gas chromatograph (Hewlett-Packard) with a 30 m × 0.25 mm I.D. SP-2331 fused-silica capillary column (Supelco) combined through a direct interface with an HP 5970B mass-selective detector (Hewlett-Packard) in the SIM mode was used for PCDD and PCDF detection. Two or three m/z values corresponding to the most abundant ions from molecular clusters of PCDDs and PCDFs ($[M]^+$, $[M+2]^+$ and/or $[M+4]^+$) were monitored. The GC–MS conditions were as follows: column temperature, initially 120°C for 1 min, then programmed at 25°C min^{-1} to 200°C, at 1°C min^{-1} to 230°C and at 10°C min^{-1} to 260°C; splitless injection port temperature, 280°C; purge time, 1.5 min; carrier gas, helium; column head pressure, 70 kPa; direct interface temperature, 260°C; and ionization energy, 70 eV.

3. Results and discussion

Activated carbon AX-21 was chosen because of its sufficient adsorption capacity, activity stability, low price and its commonly reported use [8,16,20,22,23,25,26,28,31,36,37,41,46,50]. Celite 545 as a physical support for the activated carbon, when packed in a gravity column, fulfils the conditions stipulated for inertness, purity, perfect immobilization of the carbon and acceptable column flow. To achieve a sufficient adsorption capacity, up to 50 mg of AX-21 was mixed with 950 mg of Celite 545, *i.e.*, at a ratio of 1:19 (5%, w/w). However, this amount of activated carbon necessitates a high elution volume of toluene so that the adsorbed PCDDs and PCDFs (especially OCDD and OCDF) can be eluted even from the inverted AX-21–Celite column. Moreover, the fractions 1a, 1b, 1c, 2a and 2b bring lead to lower chlorinated dioxins and dibenzofurans being transported through

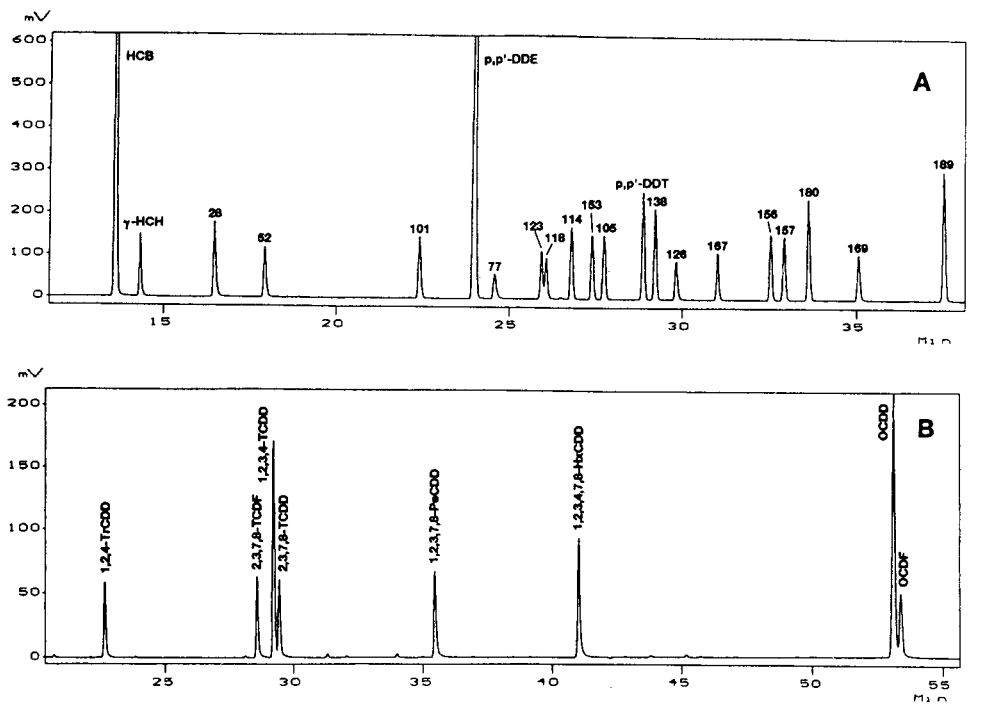

Fig. 5. HRGC–ECD (DB-5, 60 m) of (A) six "classical" PCB congeners (Nos. 28, 52, 101, 138, 153 and 180), three non-*ortho*-substituted PCBs (Nos. 77, 126 and 169), eight mono-*ortho*-PCBs (Nos. 123, 118, 114, 105, 167, 156, 157 and 189) and some organochlorine pesticides (HCB, γ-HCH, *p,p'*-DDE, and *p,p'*-DDT) and (B) some PCDDs and PCDFs used for carbon chromatographic method development. HRGC–ECD conditions as described in the text.

almost the whole of the column packing (2,3,7,8-TCDD traces begin to appear in the 16th ml of toluene). This means that TCDDs will be on the top of the inverted column and for their elution a larger volume of toluene should be applied. To decrease the elution volume as much as possible we made an original miniaturized "Soxhlet-like" extractor, the dimensions of which are adjusted to the inverted AX-21–Celite column (see Figs. 2 and 3).

A mixture of cyclohexane, dichloromethane and methanol (2:2:1, v/v/v) as an eluting solvent was selected because of its capability to elute non-planar molecules of non-polar, intermediate polar and polar compounds from carbon adsorbents. The elution curves of HCB and of the most important di-, mono- and non-*ortho*-substituted PCBs on the AX-21–Celite column are shown in Fig. 4. The curves were constructed from the abundance values of some of the

Table 1
Average recoveries of some congeners of PCDDs, PCDFs, di-*ortho*-, mono-*ortho*-, and non-*ortho*-PCBs, HCB, γ-HCH, *p,p'*-DDE and *p,p'*-DDT from the AX-21–Celite column

Compound	Amount added (ng)	Recovery (%)[a]			Standard deviation (%)
		Fraction 1b	Fraction 2b	Fraction 3	
PCB-28	20	–[b]	22	–	4.8
PCB-52	20	88	–	–	15.2
PCB-101	20	98	–	–	16.8
PCB-138	20	99	–	–	20.2
PCB-153	20	97	–	–	18.5
PCB-180	20	98	–	–	15.2
PCB-77	10	–	82	–	5.3
PCB-126	10	–	91	–	4.0
PCB-169	10	–	77	21	$4.4_{fr\ 2b}/4.0_{fr\ 3}$
PCB-123	10	–	84	–	4.8
PCB-118	10	–	82	–	5.3
PCB-114	10	–	80	–	5.8
PCB-105	10	–	84	–	4.0
PCB-167	10	–	88	–	4.4
PCB-156	10	–	90	–	7.3
PCB-157	10	–	86	–	6.2
PCB-189	10	–	100	–	5.8
HCB	80	–	40	–	16.0
γ-HCH	20	77	–	–	10.2
p,p'-DDE	80	62	–	–	12.2
p,p'-DDT	20	76	–	–	18.5
1,2,4-TrCDD	5	–	–	63	9.0
2,3,7,8-TCDF	5	–	–	71	7.3
1,2,3,4-TCDD	10	–	–	74	10.2
2,3,7,8-TCDD	5	–	–	75	11.6
1,2,3,7,8-PeCDD	5	–	–	85	12.9
1,2,3,4,7,8-HxCDD	5	–	–	85	11.5
OCDD	5	–	–	64	12.9
OCDF	2.5	–	–	64	9.0

[a] 4 ml of cyclohexane–dichloromethane–methanol 2:2:1 (fraction 1a), 7 ml of the same mixture (1b), 24 ml of the same mixture (1c), 2ml of toluene (2a), 10 ml of toluene (2b), "Soxhlet-like" extraction (fraction 3) and other chromatographic conditions are described in the text. Average of six determinations.

[b] Dashes indicate that the compounds were not detected or were present in negligible concentrations.

compounds, as are separated in Fig. 5, determined by HRGC–ECD in captured 1-ml carbon column subfractions.

After the elution volumes for the individual groups of the compounds had been determined according to the elution curves (see Figure 4), recovery tests ($n = 6$) were performed. A mixture of standards (see Fig. 5) was used for the tests. Average recoveries and standard deviations for fractions 1b, 2b and 3 are presented in Table 1. When the recoveries are <80%, the losses are probably caused by irreversible adsorption (PCDDs and PCDFs), during solvent evaporation (No. 28, HCB, γ-HCH) or by eluting in other fractions (*p,p'*-DDE and *p,p'*-DDT in fraction 1a, No. 28 in fraction 1c and No. 169 in fraction 3). The recovery of No. 169 can be improved by increasing the elution volume of fraction 2b from 10 ml to 16–18 ml of toluene, provided that PCDD/PCDF losses are of little importance, *e.g.*, the PCDDs and PCDFs are not going to be determined.

In our laboratory we also currently use a gravity column packed with 3 g of ICN alumina B Super 1, which is able to separate PCBs and PCDDs/PCDFs between the following two fractions: (A) PCBs Nos. 28, 52, 101, 138, 153, 180, 123, 118, 114, 167, 156, 157, 189 and partly (about 30–50%) 105 (2% CH_2Cl_2 in *n*-hexane, 25 ml); and (B) di- to octaCDD/CDF, No. 77, 126, 169 and the remainder of No. 105 (50% CH_2Cl_2 in *n*-hexane, 30 ml).

The efficiency of the method was tested using various real samples such as technical PCB mixtures (Delor 103 and Delor 105), MWI fly ash, fish, butter, egg and human adipose tissue. We observed that the presence of higher lipid amounts (>0.2 g) applied on the 1-g AX-21–Celite column resulted in decreased retention of the analytes, *e.g.*, some of mono-*ortho*-PCBs

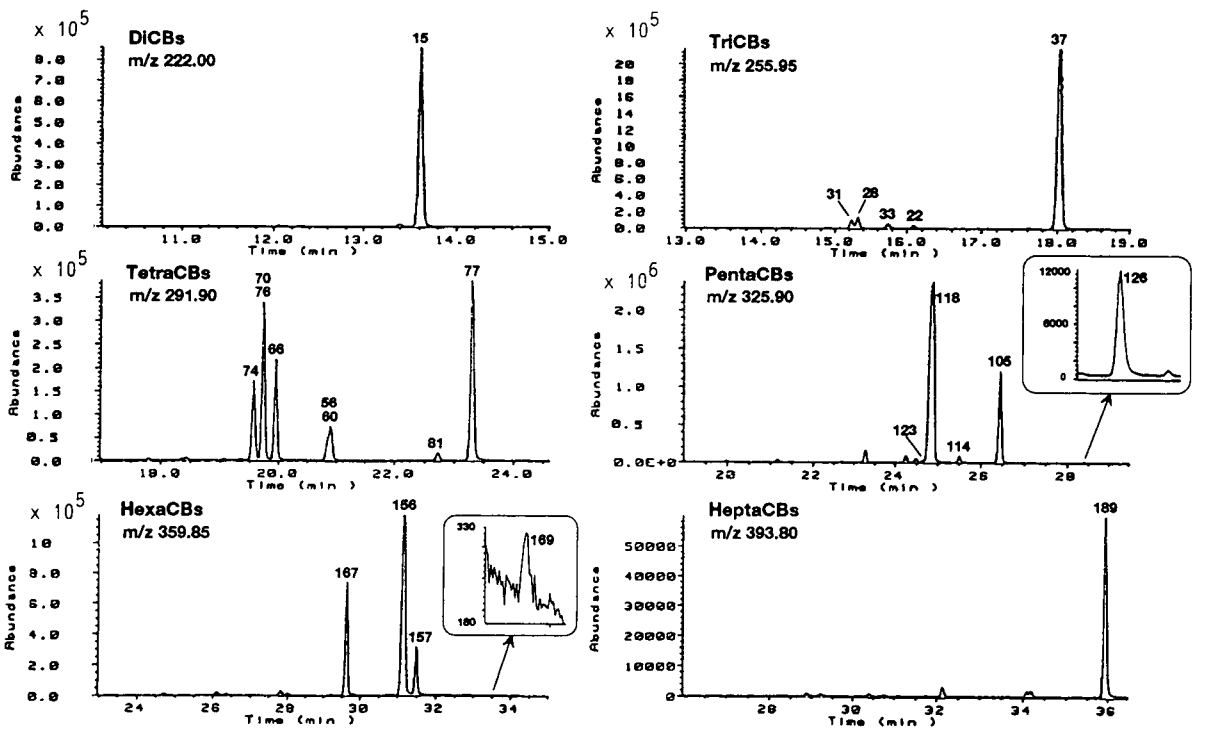

Fig. 6. HRGC–MS-SIM (DB-5MS, 60 m) of mono-*ortho*- and non-*ortho*-substituted di- to heptachlorobiphenyl congeners present in the fraction 2b from the AX-21–Celite column, *i.e.*, in 10 ml of toluene after 4 ml of cyclohexane–dichloromethane–methanol (2:2:1) (fraction 1a), 7 ml of the same eluting solvent (fraction 1b), 24 ml of the same eluting solvent (fraction 1c) and 2 ml of toluene (fraction 2a). Sample fractionated: 1 mg of Delor 105 (for details, see the text).

partly eluted in fraction 1c. For this reason it is necessary to remove the lipids as much as possible either by chemical treatment (decomposition with sulphuric acid or alkali metal hydroxides) or by chromatography (Florisil, gel permeation). Florisil chromatography is less suitable because a more polar eluting solvent (*e.g.*, 6% diethyl ether in *n*-hexane) must be used in order that the coplanar PCBs can elute, with the consequence that part of the lipids (triglycerols of unsaturated fatty acids present mainly in vegetable and fish oil) elute together with the PCBs.

Mass fragmentograms of non-/mono-*ortho*-PCBs separated by the carbon column from a 1-mg sample of Delor 105 are presented in Fig. 6. Tetra- to hexaCDFs were determined in fraction 3. Levels of the compounds mentioned above are given in Table 2. The TEQs calculated from non-*ortho*- and mono-*ortho*-PCBs found in Delor 103 and Delor 105 are substantially higher than those from PCDDs/PCDFs (62 *versus* 2.7

Table 2
Levels of HCB, mono-*ortho*- and non-*ortho*-substituted PCBs, PCDDs and PCDFs in PCB technical mixtures of Slovak provenance (Delor 103 and Delor 105)[a] and a fly ash sample from a municipal waste incinerator in Bratislava

Compound	Concentration[b]		
	Delor 103 ($\mu g\,g^{-1}$)	Delor 105 ($\mu g\,g^{-1}$)	MWI flyash (ng g^{-1})
HCB	2.6	4.2	59 000
PCB-77	5 270	1 020	0.74
-126	32	56	1.1
-169	N.D.	N.D.	0.26
-81	355	75	0.15
PCB-118	3 300	14 700	0.82
-114	160	270	0.11
-105	1 600	4 800	0.63
-167	85	4 300	0.24
-156	190	8 700	0.51
-157	15	1 700	0.27
-189	29	350	0.32
2378-TCDF	2.0	2.2	
Other TCDFs	57	10	
12378- + 12348-PeCDF	1.1	0.69	
23478-PeCDF	4.8	0.54	
Other PeCDFs	14	3.4	
123478- + 123479-HxCDF	N.D.	0.27	
Other HxCDFs	N.D.	N.D.	
PCDDs, total	N.D.	N.D.	247
PCDFs, total	79	17	128
PCDDs + PCDFs	79	17	375
I-TEQ[c]	2.7	0.55	5.2
TEQ[d]	62	51	0.13

[a] The AX-21–Celite column was used for the group separation; PCB-77, 126, 169, 105 and 118, PCDDs and PCDFs were quantified by spiking $^{13}C_{12}$-surrogates; concentrations of remaining PCB congeners and HCB were calculated using MS-SIM responses of their standards and the recoveries as are given in Table 1.

[b] N.D. = Not detected (<0.05 $\mu g\,g^{-1}$ for PCDFs and 0.3 $\mu g\,g^{-1}$ for PCBs).

[c] Toxic equivalents were calculated from 2,3,7,8-substituted PCDDs and PCDFs (values are not given) using international toxic equivalency factors according to NATO/CCMS [51].

[d] Toxic equivalents calculated from mono-*ortho*- and non-*ortho*-PCBs using toxic equivalency factors according to ref. 13.

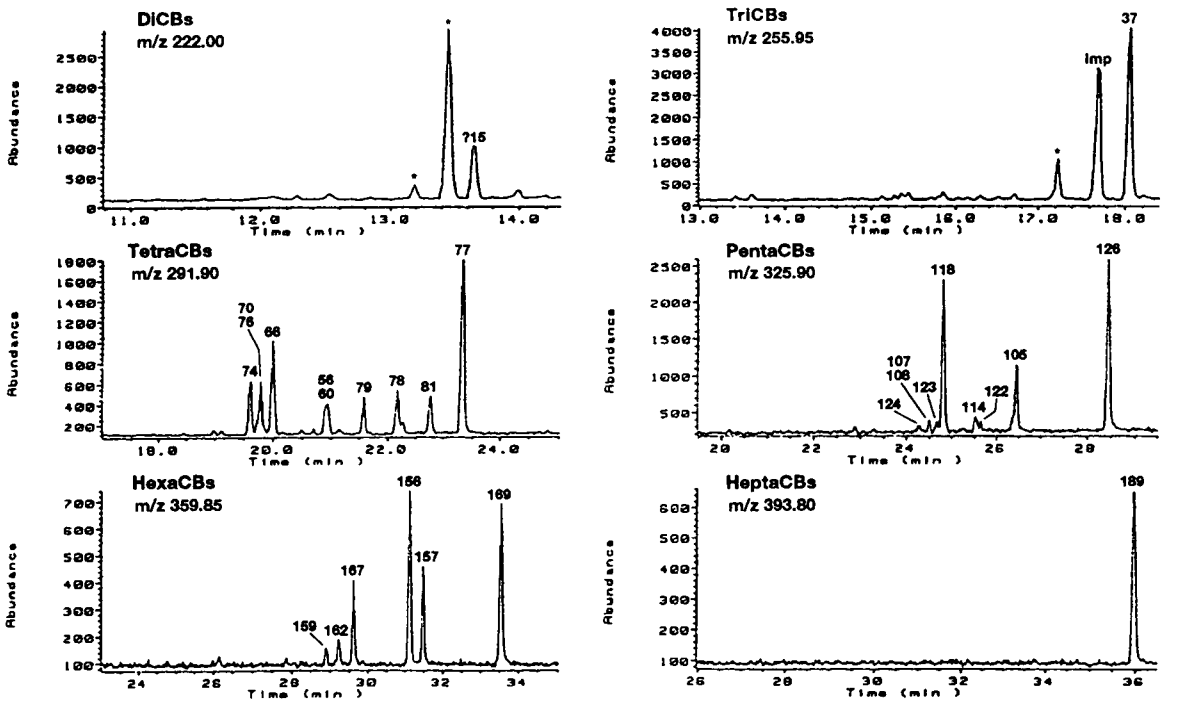

Fig. 7. HRGC–MS-SIM (DB-5MS, 60 m) of mono-*ortho*- and non-*ortho*-substituted di- to heptachlorobiphenyl congeners present in fraction 2b from the AX-21–Celite column. Sample fractionated: 10 g of fly ash from a municipal waste incinerator (for details, see the text). Asterisks indicate unidentified PCB congeners.

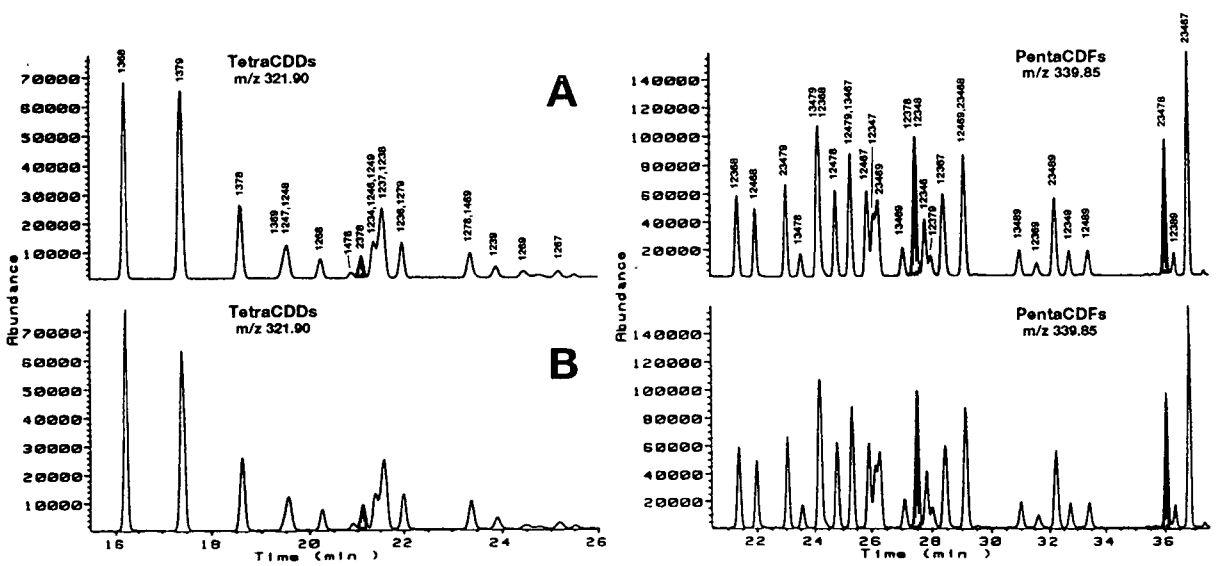

Fig. 8. Comparison of HRGC–MS-SIM (SP 2331, 30 m) of tetraCDDs and pentaCDFs found in the fractions 2b of a toluene extract of MWI fly ash (10 g) after (A) "classical" clean-up using an H_2SO_4–KOH–$AgNO_3$–silica column and a basic alumina column (upper traces) and (B) no clean-up (lower traces).

ppm and 51 *versus* 0.55 ppm, respectively). In accordance with results published by Kannan *et al.* [32], we observed that about 99.5% of No. 110 co-eluting with No. 77 on a DB-5 column is removed in the first fractions on our AX-21–Celite column. However, the remainder of No. 110 in environmental samples can still interfere when ECD is used.

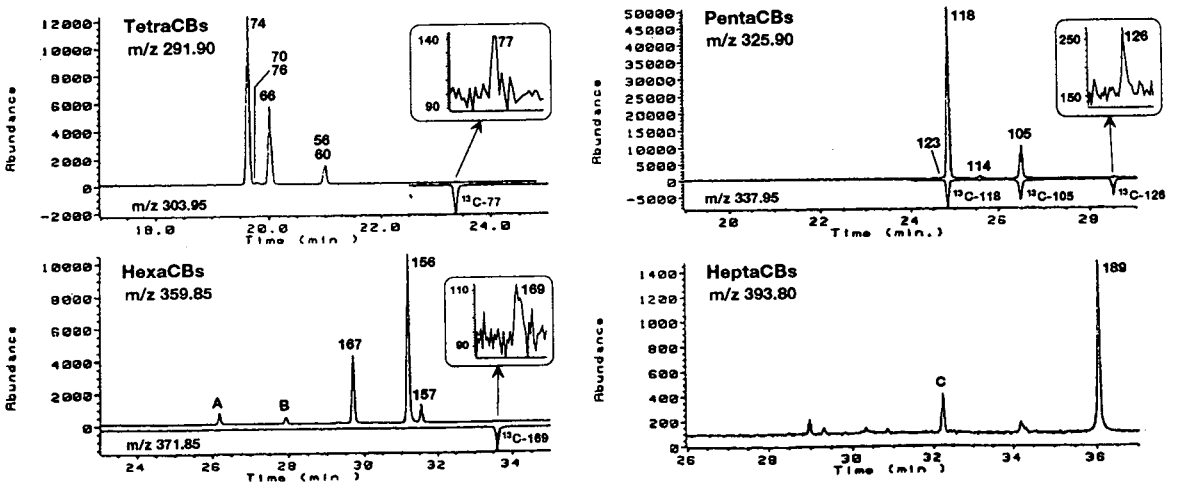

Fig. 9. HRGC–MS-SIM (DB-5MS, 60 m) of mono-*ortho*- and non-*ortho*-substituted tetra- to heptachlorobiphenyl congeners present in the AX-21–Celite fraction 2b. Peaks oriented negatively (abundance is adjusted) belong to $^{13}C_{12}$-surrogates. Sample fractionated: 1 g of fat from human adipose tissue cleaned up on a Florisil column (for details, see the text).

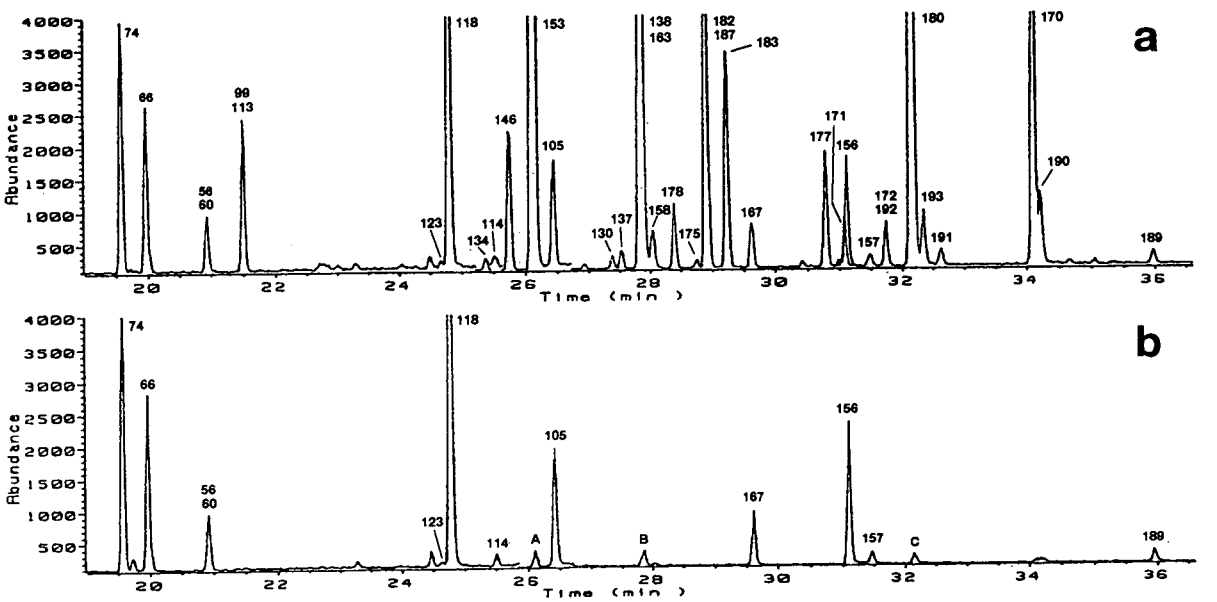

Fig. 10. Summed HRGC–MS-SIM (DB-5MS, 60 m) of tetra- to heptaCBs found in (a) a human fat sample cleaned-up on an H_2SO_4–silica column and (b) the AX-21–Celite fraction 2b of the sample in (a) (for details, see the text). The peaks labelled A, B and C represent negligible remainders of PCB congeners Nos. 153, 138 and 180, respectively.

Mass fragmentograms of di- to heptaCBs present in the AX-21–Celite column fraction 2b of an MWI fly ash sample extract are shown in Fig. 7. Although the raw extract was applied directly to the carbon column, the mass fragmentographic patterns of non-/mono-*ortho*-PCBs and PCDDs/PCDFs were congruent with those for the same fly ash sample extracted parallelly, cleaned up using the "classical" procedure to remove precursors of PCDDs and PCDFs such as polychlorinated phenoxyphenols and diphenyl ethers (an H_2SO_4–KOH–$AgNO_3$–silica column and a basic Al_2O_3 column) and also fractionated on the carbon column (Fig. 8). However, no statistic evaluation was made. It is noteworthy that in the fly ash sample the concentrations of Nos. 77, 126 and 169 congeners were higher than those of the individual mono-*ortho*-PCBs. Mono-*ortho*-PCB, non-*ortho*-PCB and PCDD/PCDF concentrations are given in Table 2. In this instance the TEQ value calculated from the PCDDs and PCDFs is higher than the total TEQ from non-*ortho*- + mono-*ortho*-PCBs (5.2 *versus* 0.13 ppb).

Mass fragmentograms of tetra- to heptaCBs detected in fraction 2b (1 g of human fat analysed; fat removed using the Florisil column) are shown in Fig. 9.

The capability of the AX-21–Celite column to remove multi-*ortho*-PCBs and other interferents present in a human adipose tissue sample (50 mg) is illustrated by comparison of the summed mass fragmentograms of tetra- to octaCBs present in a human fat sample after the H_2SO_4–silica clean-up + AX-21–Celite fractionation and after AX-21–Celite fractionation only, as shown in Fig. 10. Fig. 11 shows the results of HRGC–ECD of the above-mentioned samples.

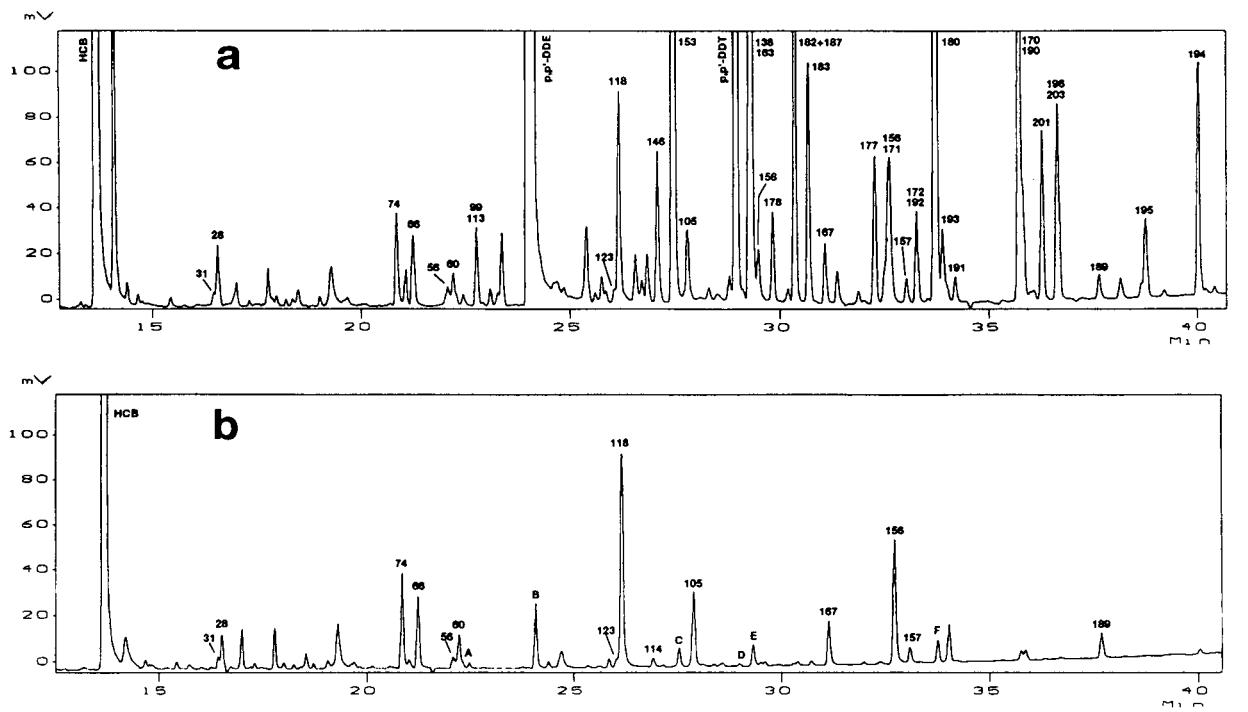

Fig. 11. HRGC–ECD chromatograms (DB-5, 60 m) of (a) a human fat sample cleaned up on an H_2SO_4–silica column and (b) the AX-21–Celite fraction 2b of the sample in (a) (for details, see the text). The peaks labelled A, B, C, D, E and F represent negligible remainders of No. 101, *p,p'*-DDE, No. 153, *p,p'*-DDT, No. 138 and No. 180, respectively.

The method presented was also successfully verified using egg, butter and fish (shark and catfish meat, fish oil and cod liver).

4. Acknowledgements

This work was supported by the Ministry of Health of the Slovak Republic. We thank Dr. P. Schmid of the Swiss Federal Institute of Technology and University of Zürich, Switzerland, for his kind gift of AX-21 activated carbon at an early stage of this study. The skilled technical assistance of Mrs. Jarmila Paulíková and Mr. Roman Vadovič is gratefully acknowledged.

5. References

[1] *Environmental Health Criteria 88: Polychlorinated Dibenzo-p-dioxins and Dibenzofurans*, World Health Organization, Geneva, 1989.
[2] P. de Voogt, D.E. Wells, Reutergårdh and U.A.Th. Brinkman, *Int. J. Environ. Anal. Chem.*, 40 (1990) 1.
[3] J. Nagayama, M. Kuratsune and Y. Masuda, *Bull. Environ. Contam. Toxicol.*, 15 (1976) 9.
[4] P.H. Chen, J.M. Gaw, C.K. Wong and C.J. Chen, *Bull. Environ. Contam. Toxicol.*, 25 (1980) 325.
[5] G.W. Bowes, M.J. Mulvihill, B.R.T. Simoneit, A.L. Burlingame and R.W. Risebrough, in F. Cattabeni, A. Cavallaro and G. Galli (Editors), *Dioxin—Toxicological and Chemical Aspects*, SP Medical and Scientific Books, New York, 1978, Ch. 8, p. 79.
[6] A. Kočan, J. Petrík and I. Holoubet, in T. Damstra, L.S. Birnbaum, M.J. Charles, J.C. Corton, R. Deriksen, W.F. Greenlee and G.W. Lucier (Editors), *DIOXIN'91, Proceedings of the 11th International Symposium on Chlorinated Dioxins and Related Compounds, Research Triangle Park, NC, September 23–27, 1991*, University of North Carolina, Chapel Hill, 1991, p. 332.
[7] S. Tanabe, N. Kannan, T. Wakimoto, R. Tatsukawa, T. Okamoto and Y. Masuda, *Toxicol. Environ. Chem.*, 24 (1989) 215.
[8] T.R. Schwartz, D.E. Tillitt, K.P. Feltz and P.H. Peterman, *Chemosphere*, 26 (1993) 1443.
[9] C.-S. Hong, B. Bush and J. Xiao, *Ecotoxicol. Environ. Saf.*, 23 (1992) 118.
[10] É. Dewailly, J.P. Weber, S. Gingras and C. Laliberté, *Bull. Environ. Contam. Toxicol.*, 47 (1991) 491.
[11] S. Safe, *Environ. Carcin. Ecotoxicol. Rev.*, C9 (1991) 261.
[12] K. Ballschmiter and M. Zell, *Fresenius'Z. Anal. Chem.*, 302 (1980) 20.
[13] S. Safe, *Chemosphere*, 25 (1992) 61.
[14] L.M. Smith, T.R. Schwartz and K. Feltz, *Chemosphere*, 21 (1990) 1063.
[15] J. Tarhanen, J. Koistinen, J. Paasivirta, P.J. Vuorinen, J. Koivusaari, I. Nuuja, N. Kannan and R. Tatsukawa, *Chemosphere*, 18 (1989) 1067.
[16] D.G. Patterson, Jr., C.R. Lapeza, Jr., E.R. Barnhart, D.F. Groce and V.W. Burse, *Chemosphere*, 19 (1989) 127.
[17] Ch.-S. Hong and B. Bush, *Chemosphere*, 21 (1990) 173.
[18] L.G.M.Th. Tuinstra, J.A. van Rhijn, A.H. Roos, W.A. Traag, R.J. van Mazijk and P.J.W. Kolkman, *J. High Resolut. Chromatogr.*, 13 (1990) 797.
[19] D.T. Williams and G.L. LeBel, *Chemosphere*, 22 (1991) 1019.
[20] W.M. Jarman, S.A. Burns, R.R. Chang, R.D. Stephens, R.J. Norstrom, M. Simon and J. Linthicum, *Environ. Toxicol. Chem.*, 12 (1993) 105.
[21] J. Krupčík, A. Kočan, J. Petrík, P.A. Leclercq and K. Ballschmiter, *Chromatographia*, 35 (1993) 410.
[22] L.M. Smith, D.L. Stalling and J.L. Johnson, *Anal. Chem.*, 56 (1984) 1830.
[23] H. Beck, A. Dross and W. Mathar, *Chemosphere*, 19 (1989) 1805.
[24] M. Nygren, M. Hansson, M. Sjöström, C. Rappe, P. Kahn, M. Gochfeld, H. Velez, T. Gent-Guenther and W.P. Wilson, *Chemosphere*, 17 (1988) 1663.
[25] L.M. Smith, *Anal. Chem.*, 53 (1981) 2152.
[26] J.N. Huckins, D.L. Stalling and W.A. Smith, *J. Assoc. Off. Anal. Chem.*, 61 (1978) 32.
[27] L.J. Babiak and A.S.Y. Chau, *J. Assoc. Off. Anal. Chem.*, 62 (1979) 1174.
[28] P.H. Cramer, R.E. Ayling, K.R. Thornburg, J.S. Stanley, J.C. Remmers, J.J. Breen and J. Schwemberger, *Chemosphere*, 20 (1990) 821.
[29] K. Norén, A. Lundén, J. Sjövall and A. Bergman, *Chemosphere*, 20 (1990) 935.
[30] A.K.D. Liem, A.P.J.M. de Jong, J.A. Marsman, A.C. den Boer, G.S. Groenemeijer, R.S. den Hartog, G.A.L. de Korte, R. Hoogerbrugge, P.R. Koostra and H.A. van't Klooster, *Chemosphere*, 20 (1990) 843.
[31] D.W. Kuehl, B.C. Butterworth, J. Líbal and P. Marquis, *Chemosphere*, 22 (1991) 849.
[32] N. Kannan, G. Petrick, D. Schulz, J. Duinker, J. Boon, E. van Arnhem and S. Jansen, *Chemosphere*, 23 (1991) 1055.
[33] L. Zupaičič-Kralj, J. Jan and J. Marsel, *Chemosphere*, 23 (1991) 841.
[34] E. Storr-Hansen and T. Cederberg, *Chemosphere*, 24 (1992) 1181.
[35] S.S. Atuma and Ö. Andersson, *Chemosphere*, 27 (1993) 1.

[36] P. Schmid, M.E. Suter-Hofmann and Ch. Schlatter, *Chemosphere*, 18 (1989) 1741.
[37] J.N. Huckins, D.L. Stalling and J.D. Petty, *J. Assoc. Off. Anal. Chem.*, 63 (1980) 750.
[38] S. Tanabe, N. Kannan, T. Wakimoto and R. Tatsukawa, *Int. J. Environ. Anal. Chem.*, 29 (1987) 199.
[39] M. Athanasiadou, S. Jensen and E. Klasson Wehler, *Chemosphere*, 23 (1991) 957.
[40] W.E. Turner, S.G. Isaacs and D.G. Patterson, Jr., *Chemosphere*, 25 (1992) 805.
[41] R. Lazar, R.C. Edwards, C.D. Metcalfe, T. Metcalfe, F.A.P.C. Gobas and G.D. Haffer, *Chemosphere*, 25 (1992) 493.
[42] C.S. Creaser and A. Al-Haddad, *Anal. Chem.*, 61 (1989) 1300.
[43] J. de Boer, C.J.N. Stronck, F. van der Valk, P.G. Wester and M.J.M. Daudt, *Chemosphere*, 25 (1992) 1227.
[44] C.-S. Hong, B. Bush, J. Xiao and E.F. Fitzgerald, *Chemosphere*, 24 (1992) 465.
[45] C.R. Lapeza, Jr., D.G. Patterson, Jr., and J.A. Liddle, *Anal. Chem.*, 58 (1986) 713.
[46] C.A. Ford, D.C.G. Muir, R.J. Norstrom, M. Simon and M.J. Mulvihill, *Chemosphere*, 26 (1993) 1981.
[47] R.R. Chang, W.M. Jarman, C.C. King, C.C. Esperanza and R.D. Stephens, *Chemosphere*, 20 (1990) 881.
[48] A. Kočan, J. Petrík, J. Chovancová, L. Neubauerová, and M. Bezačinský, *Chemosphere*, 23 (1991) 1473.
[49] A. Kočan, A. Zemek, and M. Popl, *Collect. Czech. Chem. Commun.*, 56 (1991) 1221.
[50] *Method 1613: Tetra- through Octa- Chlorinated Dioxins and Furans by Isotope Dilution HRGC/HRMS (Revision A)*, US Environmental Protection Agency, Alexandria, VA, 1990.
[51] D.G. Barnes (Editor), *Pilot Study on International Information Exchange on Dioxins and Related Compounds: International Toxicity Equivalency Factors (I-TEF) Method of Risk Assessment for Complex Mixtures of Dioxins and Related Compounds*, Report No. 176, North Atlantic Treaty Organization/Committee on the Challenges of Modern Society, US Environmental Protection Agency, Washington, DC, 1988.

ELSEVIER

Journal of Chromatography A, 665 (1994) 155–162

JOURNAL OF CHROMATOGRAPHY A

Applications of gas chromatography–mass spectrometry in clinical chemistry

Helmut Gleispach*, Hans-Jörg Leis, Werner Windischhofer

University Children's Hospital, Auenbruggerplatz, A-8036 Graz, Austria

Abstract

Two applications of gas chromatography–mass spectrometry in clinical chemistry, are described, namely the identification and determination of compounds present in biological fluids. For the first application, the biological substances are derivatized to stable forms for gas chromatography and to give appropriate spectra in the mass spectrometer operated in the scanning mode. This method is used for the diagnosis of organic acidurias, different enzyme deficiencies causing congenital adrenal hyperplasia and other disturbances of steroid metabolism, for differentiation between adrenal carcinoma or adenoma, etc. The second application is the use of the mass spectrometer as a very sensitive and selective gas chromatographic detector. This, in combination with stable isotope dilution methods, is the most accurate analytical method in clinical chemistry. The substances are derivatized to forms suitable for gas chromatography and to give a few specific and intense fragment ions in the mass spectrometer operated in selected-ion monitoring mode. Substances that can be detected in this way include steroids, vitamins, prostaglandins, carbohydrates, drugs and pesticides.

1. Introduction

Gas chromatography–mass spectrometry (GC–MS) was, in earlier times, a method that needed very skilled laboratory staff and was therefore used only in some specialized centres. More recently GC–MS has become easier to handle and the instruments smaller and it is now widely used in clinical chemistry. The development of very sensitive desktop instruments enables the user to measure, in the electron impact (EI) or chemical ionization (CI) mode, positive and negative ions in the scan mode or with selected-ion monitoring (SIM). This has greatly widened the applications of GC–MS. MS has some great advantages over other GC detectors. Different metabolites in a chromatogram are identified by other GC detectors only from the retention time previously detected with standards. Using GC–MS, the substances are identified on the basis of their spectra and a computerized library search. Moreover, substances can be localized by specific ion chromatograms [1]. In this way, it became possible to install computer programs carrying out the diagnosis with respect to retention times and spectra of the key metabolites of a certain syndrome. This is especially useful in the diagnosis of inborn errors of amino acid metabolism, where the interpretation of a urinary chromatogram would be laborious. Quantification can be achieved using GC–MS and stable isotope dilution (SID) techniques [2]. Substances labelled with stable isotopes have nearly the same chemical and physical properties as their natural analogues but can be detected by MS in the presence of the natural analogues

* Corresponding author.

0021-9673/94/$07.00
SSDI 0021-9673(93)E1219-P

from the difference in molecular mass. The labelled analogue is added in a constant amount to the sample immediately after collection. After the entire preparation steps, the substances are converted into derivatives giving a few specific and prominent fragment ions in the MS ion source. The mass spectrometer is operated in the SIM mode in order to obtain the highest possible sensitivity. The labelled compound is measured simultaneously with the natural analogue. All loss is compensated for by the calculation based on the comparison of the peak area of a specific ion of the labelled substance with that of the corresponding ion of the natural metabolite. SID–GC–MS is the most sensitive and accurate analytical method in clinical chemistry [3] and can be applied to all biological substances that are thermally stable enough for GC.

2. Experimental

2.1. Materials

N,N-Bis(trimethylsilyl)trifluoroacetamide (BSTFA), heptafluorobutyric anhydride (HFBA), acetonitrile and pyridine were obtained from Pierce (Rockford, IL, USA), pentafluorobenzyl bromide (PFB-Br) from ICT (Vienna, Austria), [^{18}O]water and platinum dioxide from Ventron (Karlsruhe, Germany), Silicar CC4 was from Mallinckrodt (St. Louis, MO, USA), *tert.*-butyldimethylsilyl (tBDMS) chloride from Fluka (Buchs, Switzerland) and β-glucuronidase–aryl sulphatase from Serva (Heidelberg, Germany). All other reagents and solvents of analytical-reagent grade were purchased from Merck (Darmstadt, Germany).

2.2. Gas chromatography

Analysis was performed on a Fisons GC 8000 gas chromatograph coupled to a Trio 1000 quadrupole mass spectrometer (Fisons Instruments, Manchester, UK). The gas chromatograph was equipped with a DB-5 capillary column (15 m × 0.25 mm I.D., 0.25-μm film thickness) (Fisons Instruments). Helium was used as the carrier gas. The splitless Grob injector was kept at 290°C. The temperature programme of the column was adapted to the different classes of substances so that minimum retention times and optimum separations were achieved.

2.3. Mass spectrometry

EI and CI mass spectra were recorded with one scan per second; the mass range was adapted to the particular needs of the substance classes. In the SIM mode the sampling time was set at 100 or 200 ms per mass. Positive-and negative-ion CI mass spectra were measured with methane as reagent or moderating gas and an electron energy of 70 eV. The GC–MS transfer line was kept at 310°C and the ion source temperature was 220°C.

2.4. Derivatization

For silylation, 50 μl of BSTFA–pyridine (1:2, v/v) were added to the dried sample, after heating at 75°C for 30 min the reagent was removed by evaporation under a stream of nitrogen and the residue was dissolved in 50 μl of hexane [4].

Pentafluorobenzyl (PFB) esters were prepared by reaction with 50 μl of PFB-Br solution in acetonitrile (7%, w/w) and 10 μl of diisopropylethylamine for 15 min at room temperature [5].

To prepare heptafluorobutyrates, 100 μl of HFBA–benzene–triethylamine (10:200:1, v/v/v) were added to the dried sample and reacted at 75°C for 30 min., 200 μl of benzene were added and the mixture was washed with 1% ammonia solution and then with water. The organic phase was dried under nitrogen and dissolved in hexane or dichloromethane [6].

2.5. Urine analysis for steroids

The steroids excreted in the urine as glucuronides and sulphates were hydrolysed enzymatically with β-glucuronidase–aryl sulphatase at pH 5 and 37°C for 30 h. The pH was adjusted to 6 and the sample brought on to an Extrelut 20 column. The steroids were eluted with 40 ml of

dichloromethane. The eluate was evaporated to dryness and the residue dissolved in 5 ml of benzene. A preseparation was performed on 4 g of alumina washing with 30 ml of benzene and eluting with 20 ml of benzene–ethanol (8:2). The extract was dried and than silylated [7].

2.6. Urine analysis for organic acids

The analysis of the pattern of organic acids in urine is very useful for the diagnosis of inborn errors of amino acid metabolism [9,10]. However, the preparation of the urine is a major problem. Many substances with very different polarities, such as sugars, amino acids, phosphoric acid, urea, steroids and bile acids, are present in the urine and the polarities of the different organic acids differ widely. Various methods for the separation of the organic acids from other urinary compounds have been described [11], but in our experience part of the organic acids is lost in these preseparation steps. We therefore used the following procedure: deuterated methylmalonic acid, deuterated N-acetylaspartic acid and tricarballylic acid were added as internal standards to a part of the fresh urine corresponding to 1 μmol of creatinine. After freeze-drying, the residue was silylated and a part was injected on to the GC column. The temperature programme was 1 min at 40°C, then increased at 5°C/min to 180°C and at 30°C/min to 310°C.

3. Results and discussion

The use of GC–MS for the elucidation of the pattern of metabolites is demonstrated on the analysis of urine from a patient with congenital adrenal hyperplasia (CAH) and a patient with an inborn error of amino acid metabolism, namely propionic acidaemia. GC–MS for the determination of substances by use of SID–GC–MS is shown for the measurement of the urinary excretion of N-acetylaspartic acid from a patient with Canavan's disease.

3.1. Identification of urinary steroids

The analysis of the urinary steroid pattern was used for the diagnosis of different enzyme deficiencies in adrenal cortisol production.

Patient 1. Fig. 1 shows the results obtained form a 3-month-old girl suspect to have CAH. In the total ion chromatogram four prominent peaks were obtained. The two peaks at m/z 360 and 270 are significant fragments of 17-oxo-

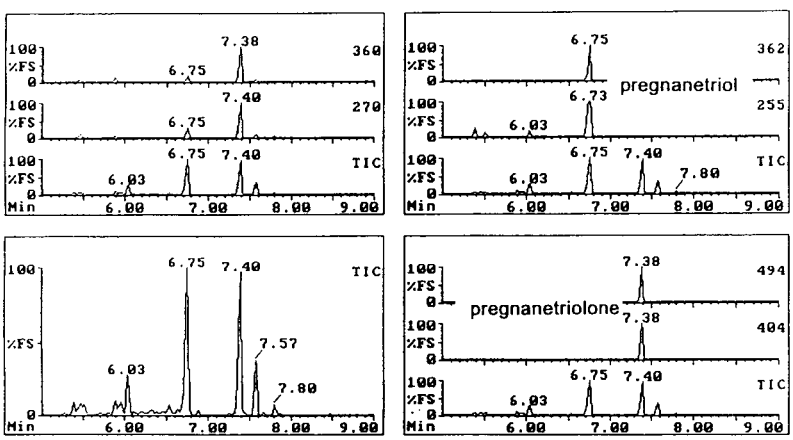

Fig. 1. Urine extract form a girl with congenital adrenal hyperplasia. The total ion chromatogram (TIC) and specific ion chromatograms together with the TIC are shown together but with four different windows. The ions at m/z 360 and 270 are usually indicative of androsterone and etiocholanolone; in this extract both steroids are absent and the two peaks result from unspecific fragments of pregnanetriol and pregnanetriolone, as the retention times correspond to those of the ions at m/z 362 and 255 characteristic of pregnanetriol and m/z 494 and 404 specific for pregnanetriolone.

steroids, but in this urine extract the two intense peaks in these ion chromatograms were identified as ions of key metabolites of a 21-hydroxylase deficiency, namely pregnane-3,17,20-triol and pregnane-3,17,20-triol-11-one. This is demonstrated through the ion chromatograms with m/z 362 and 255 corresponding to pregnanetriol and m/z 494 and 404 resulting from pregnanetriolone and identification from the spectra and a library search. The peak with retention time (t_R) 6.03 min was identified as pregnane-3,20-diol and that with $t_R = 7.57$ min as pregn-5-ene-3,17,20,21-tetraol-11-one. Substantial amounts of 17-oxosteroids were not detectable in this urine extract. The absence of this group of urinary steroids may be due to a multiple adrenal enzyme deficiency. The ability to reveal the presence or absence of metabolites from the mass chromatograms makes the interpretation of a chromatogram easy to understand even by untrained workers. Additionally, based on the spectra, unusual steroids can be identified.

Patient 2. An extremely tall girl was suspected of cortisol overproduction. The urinary steroid chromatogram showed a very high peak which was identified as dehydroepiandrosterone (DHEA). This metabolite is indicative of an adrenal carcinoma [8] and surgical intervention showed the tumour, which could be removed. In this instance the use of GC–MS was crucial as surgical intervention was recommented based only on the presence of a high excretion of DHEA, which was identified from the retention time and spectrum.

3.2. Evaluation of the organic acid pattern in urine

The evaluation of the often very complex chromatograms is done by a computer program. Three organic acids, key metabolites of the disease, are selected for each of the most common organo acidurias. These metabolites are detected in a time window through two specific fragments. Some organo acidurias are listed in Table 1 together with three key metabolites, their two specific fragment ions and the relative retention times (t_R). Fig. 2 shows the result of the use of such a computer program for a patient with a severe form of propionic acidaemia. In this instance most of the compounds present in the urine remain invisible in the total ion chromatogram (TIC), suppressed by the extremely high amounts of lactic acid, 3-hydroxypropionic acid and 3-hydroxybutyric acid. The printout shows in four windows the TIC and the mass chromatograms of the three main organic acids, lactic acid [time window (tw) 7–9 min, m/z 190 and 219], 3-hydroxypropionic acid (tw 10–12 min, m/z 177 and 219) and 3-hydroxybutyric acid (tw 10–12 min, m/z 191 and 117). These three substances are rapidly identified from the spectra and a library search (Fig. 3) and the disease can be diagnosed. A good correlation is obtained for the library search irrespective from the fact that the amount of 3-hydroxypropionic acid was too high for the dynamic range of the multiplier.

Quantification of the more important metabolites can be achieved with the aid of a computer by correlation of the peak areas of specific masses of the substance of interest with those of the internal standards, which are m/z 221 for [$^2H_3$]methylmalonic acid, m/z 307 for [$^2H_3$]-N-acetylaspartic acid and m/z 377 for tricarballylic acid. The computer program used allows the rapid identification of the key metabolites also in complex chromatograms and helps to provide confidence in the presence or absence of expected substances and hence to avoid a wrong diagnosis.

3.3. Determination of metabolites by SID–GC–MS

Substances labelled with stable isotopes such as deuterium or oxygen-18 (^{18}O) show nearly the same chemical and physical behaviour as their natural analogues but can be detected simultaneously with the natural products by MS. Substances labelled with stable isotopes are therefore ideal internal standards for GC–MS procedures. They are added in a constant amount to the biological sample immediately after collection and follow the whole preseparation and derivatization process. Quantification is per-

Table 1
Organic acidurias, key metabolites, specific fragments and relative retention times

Disease	Specific metabolite	m/z	m/z	t_R
Propionic acidaemia	3-Hydroxy-propionic acid	219	177	115
	Lactic acid	219	190	106
	3-Hydroxy-butyric acid	191	117	116
Methylmalonic acidaemia	Methylmalonic acid	247	218	122
	3-Hydroxy-propionic acid	219	177	115
	3-Hydroxy-isovaleric	205	131	121
Malonic aciduria	Malonic acid	233	133	121
	Methylmalonic acid	247	218	122
	Succinic acid	247	172	131
Isovaleric acidaemia	3-Hydroxy-isovaleric acid	205	131	121
	3-Hydroxy-isovalerylglycine	261	176	152
	4-Hydroxyl-isovaleric acid	204	247	126
Methylglutaconic acidaemia	3-Methylglutaconic acid E	273	198	148
	3-Methylglutaric acid	204	69	143
	3-Hydroxy-isovaleric acid	205	131	121
3-Hydroxy-3-methylglutaryl-CoA lyase deficiency	3-Hydroxy-3-methylglutaric acid	363	273	161
	3'-Methylglutaric acid	204	69	143
	3-Hydroxy-isovaleric acid	205	131	121
Glutaric acid type 1	Glutaric acid	261	158	140
	3-Hydroxy-glutaric acid	259	217	158
	Glutaconic acid	259	217	145
Glutaric acid type 2	Glutaric acid	261	158	140
	Ethylmalonic acid	261	217	129
	Adipic acid	275	111	151
Fumarase deficiency	Fumaric acid	245	147	135
	Succinic acid	247	172	132
	Lactic acid	219	190	106
Canavan's disease	N-Acetylaspartic acid	304	158	167
Quantification with	$[^2H_3]$-N-Acetylaspartic acid	307	161	167

formed by comparing the peak area of a specific fragment of the labelled compound with that of the corresponding fragment of the natural analogue. The substances can be measured in the EI, CI or negative-ion chemical ionization (NICI) mode, but multiple ion detection (MID) has to be used for exact quantification. All loss occurring during the preparation of the sample is compensated for in this way. This method is therefore the most accurate method in clinical chemistry. Measuring in the NICI mode is often also the most sensitive quantification procedure. Some substances measured in our laboratory in the NICI mode are listed in Table 2 together with detection limits and relative standard deviations (R.S.D.s).

The results of the analysis of the urinary excretion of N-acetylaspartic acid by a patient with Canavan's disease are given as an example of quantification in the EI mode. Canavan's disease is a form of leukodystrophy inherited as an autosomal recessive disorder combined with spongy degeneration of the brain. The aspartoacylase deficiency [12,13] causes a highly increased level of urinary N-acetyl-L-aspartic acid, which is used for diagnosis. A 200 n*M* concentration of $[^2H_3]$-N-acetylaspartic acid [14] was added to an amount of urine corresponding to 1

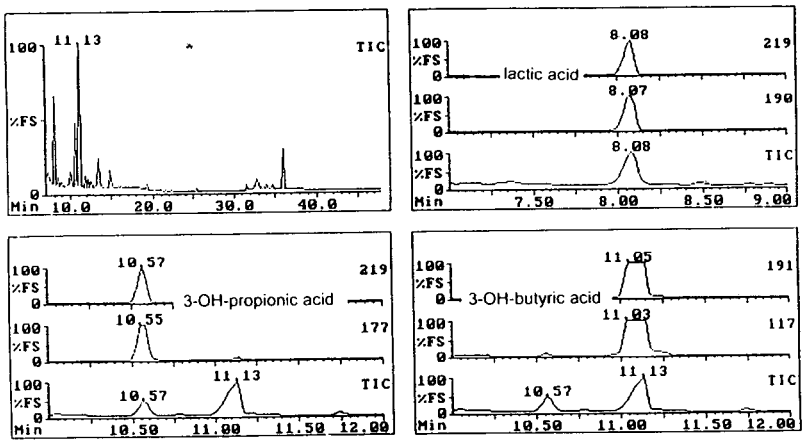

Fig. 2. Analysis of freeze-dried urine from a patient with propionic acidaemia after silylation. One window shows the TIC of the whole run and the others show the ion chromatograms of two specific ions of three key metabolites of the disease together with the TIC in the corresponding time window (tw), namely lactic acid (tw = 7–9 min, m/z 219 and 190), 3-hydroxypropionic acid (tw = 10–12 min, m/z 219 and 177) and 3-hydroxybutyric acid (tw = 10–12, m/z 191 and 117).

μM creatinine, than it was freeze-dried, silylated and injected splitless on to the GC column. The temperature program was 1 min at 80°C, then increased at 30°C/min at 330°C, where it was maintained for 10 min. The chromatogram in Fig. 4 was obtained in the EI mode scanning form m/z 40 to 500 with one scan per second. The spectrum on the left was obtained in the same way from N-acetylaspartic acid, whereas that on the right was obtained from the peak resulting from natural and [$^2H_3$]-N-acetylaspartic acid present in the sample. The fragments of the natural substance can be readily observed beside the fragments of the triply labeled compound. The influence of the kinetic isotope effect is demonstrated by the differences in the retention times of the labelled and unlabelled analogues. Deuteration shortens the retention times slightly, thus the retention time of the labelled N-acetylaspartic acid TMS derivative was 9.18 min (m/z 307 and 161) compared with 9.20 min for the natural analogue (m/z 304 and 158). Quanti-

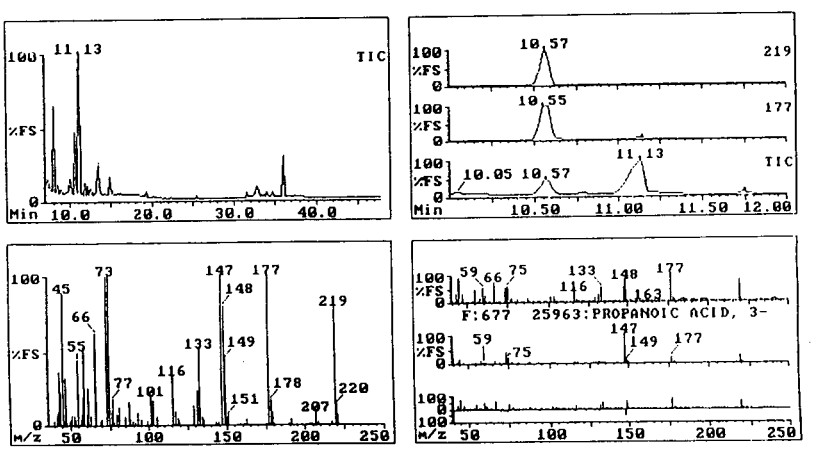

Fig. 3. Analysis of freeze-dried urine from a patient with propionic acidaemia after silylation. The four windows show the TIC, the ion chromatograms of m/z 219 and 177 in the time window 10–12 min characteristic of 3-hydroxypropionic acid, the spectrum of the peak with a retention time of 10.55 min and the results of the library search.

Table 2
Detection limits and variability for SID–GC–NICI-MS determination different compounds

Substance	Ref.	Detection limit (pg/per sample)	R.S.D. (%)[a]	
			Intra-assay	Inter-assay
Prostaglandins (PGs)	15			
$PGF_{2\alpha}$		5	1.1	2.4
PGE_2		20	2.2	2.3
PGE_1		40	1.3	2.3
6-Keto-$PGF_{1\alpha}$		30	1.4	2.0
Thromboxanes (TX_s)	15′			
TXB_2		20	2.0	2.2
2,3-dinor TXB_2		10	1.1	2.9
Hydroxy fatty acids	16			
5-HETE[b]		40	2.8	3.9
12-HETE		40	2.8	4.0
15-HETE		15	2.7	3.9
12-HHT[b]		10	2.9	3.9
Drugs				
Diclofenac	17	10	0.34	4.04
Terbutaline	18	100	0.95	1.35
Orciprenaline	18	100	2.14	2.04
Captopril	19	500	1.15	2.13
Ketotifen	20		2.3	4.5

[a] $n = 10$.
[b] HETE = Hydroxy-eicosa-tetraenoic acid; HHT = hydroxy-heptadeca-trienoic acid.

fication was carried out by another GC run where the mass spectrometer was again operated in the EI mode but with MID. For the [$^2H_3$]-N-acetylasparate and ion at m/z 307 was recorded for quantification and that at m/z 161 for identification. For the natural analogue the ion for

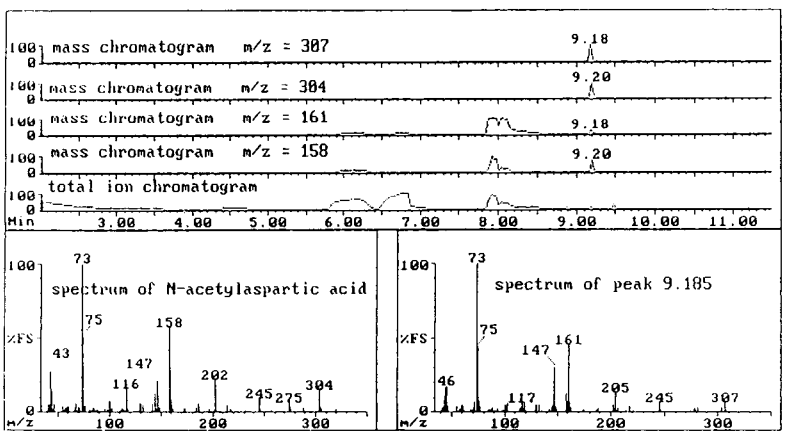

Fig. 4. Analysis of freeze-dried urine form a patient with Canavan's disease after silylation. The three windows show the TIC together with the ion chromatograms of m/z 304 and 158 indicative of natural N-acetylaspartic acid and m/z 307 and 161 corresponding to the trideuterated analogue. One window shows the spectrum of natural N-acetylaspartic acid and one that of the peak with a retention time of 9.185 min.

quantification was that at m/z 304 and the ion at m/z 158 was used for confirmation. An excretion of 75 μM of N-acetylaspartic acid per mM of creatinine was found. The level in healthy persons is *ca.* 3 μM per mM creatinine, so the diagnosis of Canavan's disease was confirmed by the fifteenfold elevated excretion of N-acetylaspartic acid. This is a good example demonstrating the use of GC–MS in both modes for the identification of a key metabolite and quantification by SID measurement.

4. Acknowledgements

This work was sponsored by the Fonds zur Förderung der wissenschaftlichen Forschung (Vienna, Austria, project number P-9337 MED). The authors thank Fisons Instruments for supplying the Trio 1000 GC–MS equipment.

5. References

[1] R.L. Foltz, in A.P. De Leenheer, R.R. Roncucci and C. Van Peteghem (Editors), *Quantitative Mass Spectrometry in Life Sciences II (Proceedings of the 2nd Symposium, Ghent, June 13–16, 1978)*, Elsevier, Amsterdam, 1978, p. 39.

[2] S.P. Markey, A.J. Lewy and R.W. Colburn, in A.P. De Leenheer, R.R. Roncucci and C. Van Peteghem (Editors), *Quantitative Mass Spectrometry in Life Sciences II (Proceedings of the 2nd) Symposium, Ghent, June 13–16, 1977)*, Elsevier, Amsterdam, 1978, p. 17.

[3] M.G. Rinsler and F.L. Mitchell, *Z. Klin. Chem. Klin. Biochem.*, 12 (1974) 558.

[4] H. Gleispach, *J. Chromatogr.*, 91 (1974) 407.

[5] R.C. Murphy and R.C. Strife, *J. Chromatogr.*, 305 (1984) 3.

[6] H. Ehrsson, T. Walle and H. Brotell, *Acat. Pharm. Suec.*, 8 (1971) 319.

[7] H. Gleispach, *Z. Klin. Chem. Klin. Biochem.*, 11 (1973) 482.

[8] H. Gleispach, J.J. Alcaniz Cerando, B. Barcelo Lucerga, L. Salto Hernandez and J. Glatzl, *Pädiatr. Grenzgeb.*, 13 (1974) 265.

[9] P.T. Ozand and G.G. Gascon, *J. Child. Neurol.*, 6 (1991) 196.

[10] P.T. Ozand and G.G. Gascon, *J. Child. Neurol.*, 6 (1991) 288.

[11] G. Hoffmann, S. Aramaki, E. Blum-Hoffmann, W.L. Nyhan and L. Sweetman, *Clin. Chem.*, 35 (1989) 587.

[12] R. Matalon, K. Michals, D. Sebesta, M. Deanching, P. Gashkoff and J. Casanova, *Am. J. Med. Genet.*, 29 (1988) 463.

[13] P.T. Ozand, G.G. Gascon and M. Dhalla, *Am. J. Med. Genet.*, 35 (1990) 266.

[14] H.J. Leis, P.T. Ozand, A.A. Odaib and H. Gleispach, *J. Chromatogr.*, 578 (1992) 116.

[15] H.J. Leis, E. Hohenester, H. Gleispach, E. Malle and B. Mayer, *Biomed. Environ. Mass Spectrom.*, 14 (1987) 617.

[16] H.J. Leis, E. Malle, B. Mayer, G.M. Kostner, H. Esterbauer and H. Gleispach, *Anal. Biochem.*, 162 (1987) 337.

[17] H.J. Leis, H. Gleispach, E. Malle and V. Nitsche, *Biomed. Environ. Mass Spectrom.*, 17 (1988) 307.

[18] H.J. Leis, H. Gleispach, V. Nitsche and E. Malle, *Biomed. Environ. Mass Spectrom.*, 19 (1990) 382.

[19] H.J. Leis, M. Leis and W. Welz, *J. Chromatogr.*, 529 (1990) 299.

[20] H.J. Leis and E. Malle, *Biol. Mass Spectrom.*, 20 (1991) 467.

ELSEVIER

Journal of Chromatography A, 665 (1994) 163–168

JOURNAL OF CHROMATOGRAPHY A

Separation of C_{11}–C_{14} branched-chain alcohols by high-resolution gas chromatography on a modified β-cyclodextrin stationary phase

J. Krupčík*,[a], I. Špánik[a], P. Sandra[b]

[a]*Department of Analytical Chemistry, Faculty of Chemical Technology, Slovak Technical University, Radlinského 9, 812 37 Bratislava, Slovak Republic*

[b]*Department of Organic Chemistry, University of Ghent, Krijgslaan 281, S-4, B-9000 Ghent, Belgium*

Abstract

The separation of C_{11}–C_{14} branched-chain alcohols and their acetyl derivatives by gas chromatography on a fused-silica capillary column coated with heptakis (6-O-*tert.*-butyldimethylsilyl-2,3-di-O-diacetyl)-β-cyclodextrin dissolved in OV-1701 (1:1) was studied. It is demonstrated that the separation of positional isomers of these alcohols and their acetyl derivatives on this stationary phase is poorer than that on Carbowax 20M. Enantiomers of the alcohols were resolved on this stationary phase at temperatures below 110°C, whereas enantiomers of their acetyl derivatives were not resolved under similar conditions.

1. Introduction

Cyclodextrins (CDs) and their derivatives are used for the separation of both geometric and enantiomeric isomers. The separation of the former depends on the inclusion effects, whereas the separation of the latter on modified CDs can be successful also for molecules with diameters that are substantially larger than the diameters of the CD cavities and therefore inclusion in a cavity is excluded. Fused-silica capillary columns coated with several alkyl and/or acyl α-, β- and γ-CD derivatives are suitable for the enantiomeric separation of a wide variety of volatile compounds of different molecular size and functionality [1]. It has become increasingly evident that not inclusion but reversible diastereomeric association in the outer sphere of the CD cavity, possibly supported by conformational changes ("induced fit"), is responsible for chiral recognition [2].

The aim of this work was to study the separation of positional and enantiomeric isomers of C_{11}–C_{14} branched-chain alcohols (obtained by hydroformylation of C_{10}–C_{13} *n*-alkenes) by gas chromatography (GC) on a fused-silica capillary column coated with a 1:1 mixture of OV-1701 and heptakis (6-O-*tert.*-butyldimethylsilyl-2,3-di-O-diacetyl)-β-CD.

2. Experimental

GC was performed with a Hewlett-Packard (HP) Model 5890 gas chromatograph equipped with flame ionization detector and a split–split-

* Corresponding author.

0021-9673/94/$07.00
SSDI 0021-9673(93)E1206-F

less injection port. Separations were performed on a 25 m × 0.33 mm I.D. fused-silica capillary column coated with a 0.125-μm film of the mixed stationary phase of OV-1701 and heptakis (6-O-*tert.* - butyldimethylsilyl-2,3-di-O-diacetyl)-β-CD (1:1). The GC oven was operated at various temperatures for isothermal experiments from 80 to 140°C in 10°C increments. The chromatograms were registered by an HP 3396 integrator and using Peak 96 software were sent to a PC where they were evaluated with HP Chem software (all products from Hewlett-Packard, Waldbronn, Germany).

The alcohol samples were prepared by hydroformylation of C_{10}–C_{13} *n*-alkenes using a procedure described previously [4]. A summary of the alcohols expected in the hydroformylation products of C_{10}–C_{13} *n*-alkenes and their labelling as used in this paper is given in Table 1.

It is convenient formally to consider the CH_2OH group as the functional group of alcohols in the hydroformylation products. In this way all alcohols obtained by the hydroformylation of *n*-alkenes (except for 1-ols) can be regarded as analogous to secondary alcohols. For instance, 2-butyl-nonanol:

$$CH_3-(CH_2)_3-\underset{\displaystyle CH_2OH}{\underset{|}{CH}}-(CH_2)_6-CH_3$$

is structurally similar to 5-dodecanol, and we label it as 12–5 to indicate the number of the carbon atoms in the *n*-alkyl chain by the first number and the position of the CH_2OH group in this chain by the second number.

Acetyl derivatives of the alcohols were prepared by acetylation with an excess of acetyl chloride as described [4].

3. Results and discussion

3.1. Separation of positional isomers

The separation of the alcohols listed in Table 1 by GC on a fused-silica capillary column coated with the mixture of OV-1701 and heptakis (6-O-*tert.*-butyldimethylsilyl-2,3-di-O-diacetyl)-β-CD (1:1) at 120°C is shown in Fig. 1 and the separation of the acetyl derivatives of these alcohols under similar conditions in Fig. 2. From a comparison of these figures, it can be concluded that the separation of alcohols is influenced mainly by hydrogen bonds. The influence of dispersive interactions of the alkyl chain on the separation of isomers of branched-chain alcohols is less pronounced. For acetyl derivatives of alcohols, where the hydrogen atom in the hydroxyl group is replaced by an acetyl group, acetyl derivatives of alcohols cannot interact with the stationary phase with hydrogen bonds. Therefore, the contribution of the shape of the alkyl chain interaction with the stationary phase to the retention substantially influences

Table 1
List and labels of alcohols obtained by hydroformylation of C_{10}–C_{13} *n*-alkenes

Alcohol	Label	Alcohol	Label
1-Undecanol	10–1	2-Methyl-1-dodecanol	12–2
2-Methyl-1-decanol	10–2	2-Ethyl-1-undecanol	12–3
2-Ethyl-1-nonanol	10–3	2-Propyl-1-decanol	12–4
2-Propyl-1-octanol	10–4	2-Butyl-1-nonanol	12–5
2-Butyl-1-heptanol	10–5	2-Pentyl-1-octanol	12–6
1-Dodecanol	11–0	1-Tetradecanol	13–1
2-Methyl-1-undecanol	11–2	2-Methyl-1-tridecanol	13–2
2-Ethyl-1-decanol	11–3	2-Ethyl-1-dodecanol	13–3
2-Propyl-1-nonanol	11–4	2-Propyl-1-undecanol	13–4
2-Butyl-1-octanol	11–5	2-Butyl-1-decanol	13–5
2-Pentyl-1-heptanol	11–6	2-Pentyl-1-nonanol	13–6
1-Tridecanol	12–1	2-Hexyl-1-octanol	13–7

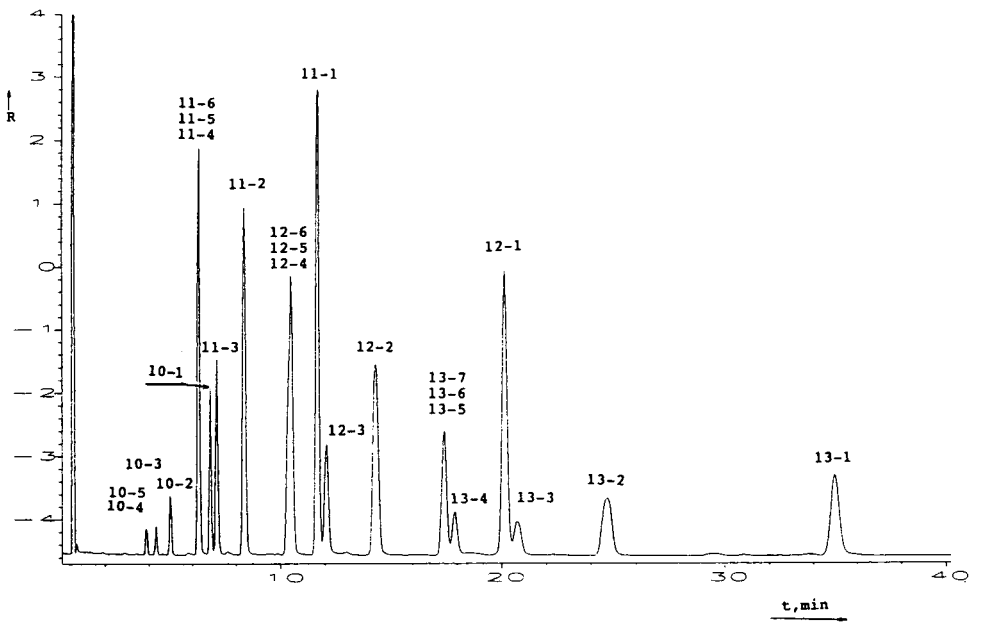

Fig. 1. Separation of alcohols at 120°C. For identification of peaks, see Table 1.

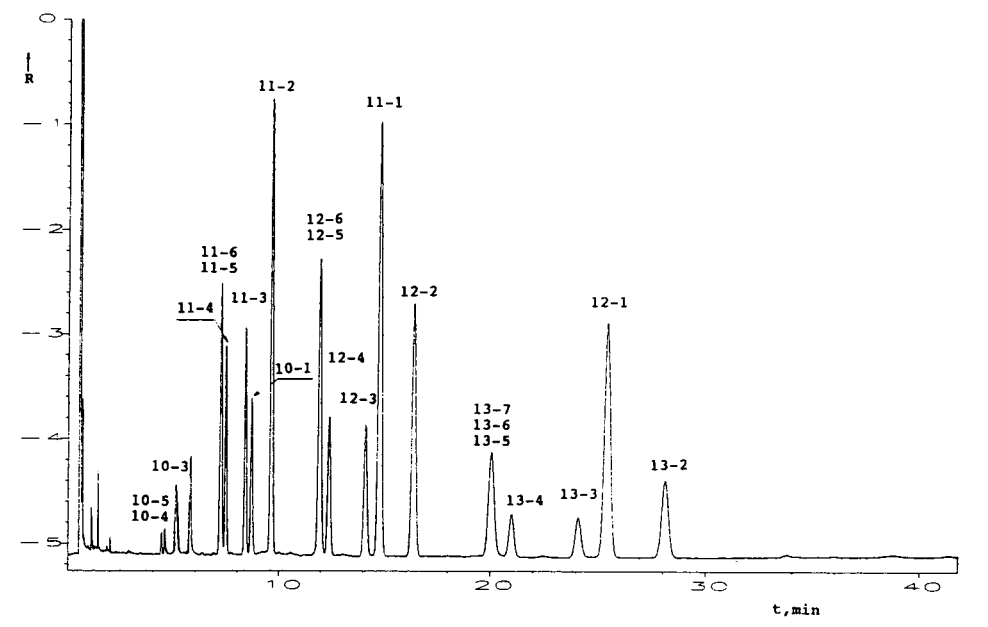

Fig. 2. Separation of acetyl derivatives of alcohols at 120°C. For identification of peaks see Table 1.

the separation. This is the reason why the resolution of positional isomers of acetyl derivatives (Fig. 2) is better than that of alcohols (Fig. 1).

Comparison of Figs. 1 and 2 with the chromatograms obtained for alcohols and their acetyl derivatives on a capillary column coated with Carbowax 20M [4] shows that Carbowax 20M is more suitable for the separation of positional isomers of branched-chain alcohols and their acetyl derivatives. Fig. 1 shows no separation of positional isomers of –4 and –5 compounds, whereas on Carbowax 20M they were fully resolved [4]. Fig. 2 shows no separation of positional isomers of –5 and –6 compounds, whereas on Carbowax 20M they were resolved [4].

The identification of branched-chain alcohols in the hydroformylation products was described previously [4]. In this work, the dependence of log t'_R on carbon atom number (n) in the alkyl chain was used for the tentative identification of sample constituents, as demonstrated in Fig. 3 for acetyl derivatives of the alcohols at 110°C. Straight lines were found for 1-, 2-, 3-, 4- and 5-positional isomers; with the 5-isomer, however, the isomers 6- or 6- + 7-isomers are also eluted.

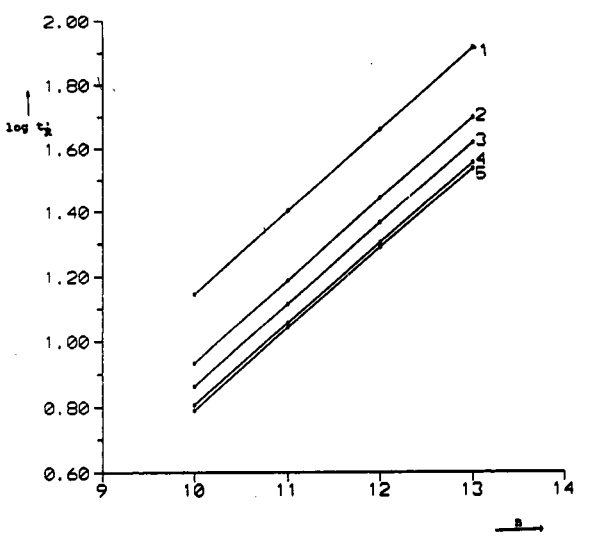

Fig. 3. Dependence of log t'_R on number of carbon atoms in the n-alkyl chain (n) for acetyl derivatives of alcohols at 110°C.

Separations of branched-chain undecanols and dodecanols and their corresponding acetyl derivatives at 100°C are shown in Figs. 4 and 5. Comparison of Figs. 4 and 5 with Figs. 1 and 2 shows a very small influence of temperature on the separation of the positional isomers for both alcohols and their acetyl derivatives.

3.2. Separation of enantiomeric isomers

In contrast to the small influence of temperature on the separation of the positional isomers of alcohols and their acetyl derivatives, a decrease in temperature significantly improved the separation of enantiomeric alcohols, as follows from a comparison of Figs. 1 and 4 (split peaks 10–3, 10–2, 11–4 and 11–2 in Fig. 4). From Figs. 2 and 5, virtually no influence of a decrease in temperature on the separation of the acetyl derivatives is observed. Further improvement in the separation of enantiomeric pairs is shown in Fig. 6, where branched-chain alcohols are separated at 90°C.

4. Conclusions

The separation of C_{11}–C_{14} branched-chain alcohols and their acetyl derivatives on a fused-silica capillary column coated with heptakis (6-O-*tert.*-butyldimethylsilyl-2,3-di-O-diacetyl)-β-CD dissolved in OV-1701 (1:1) leads to following conclusions. (i) Acetyl derivatives of positional isomers of branched-chain alcohols are better separated than the parent alcohols at given experimental conditions. (ii) The separation of positional isomers of both branched-chain alcohols and their acetyl derivatives on this chiral column is poorer than that on Carbowax 20M, which indicates that there is no inclusion of solutes on this type of modified cyclodextrin. (iii) The successful separation of enantiomeric pairs of several C_{11}–C_{14} branched-chain alcohols was achieved at 90°C. (iv) No enantiomeric separation of acetyl derivatives of C_{11}–C_{14} branched-chain alcohols was achieved at 70–120°C.

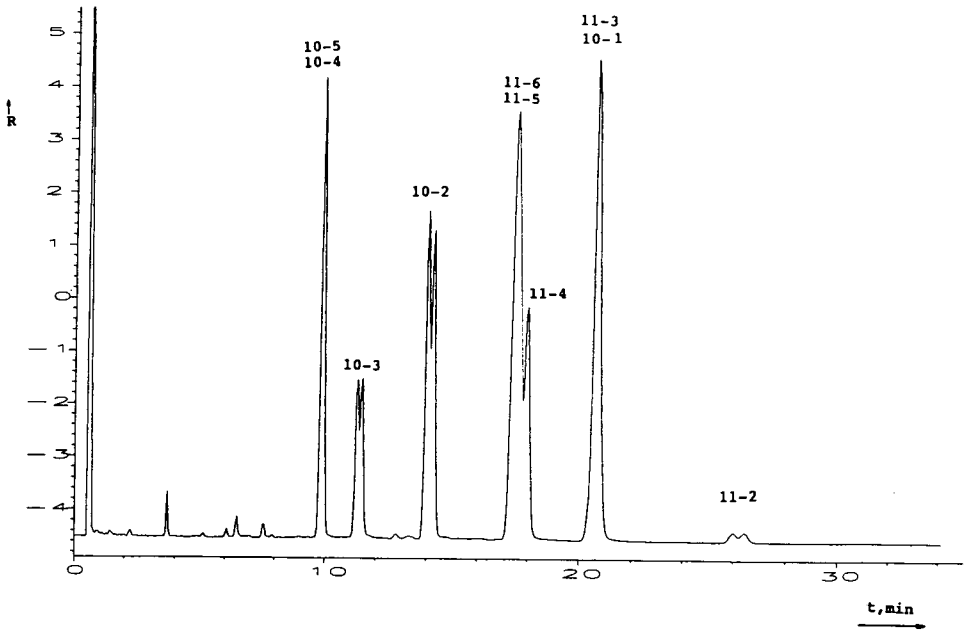

Fig. 4. Separation of branched-chain undecanols and dodecanols at 100°C. For identification of peaks, see Table 1.

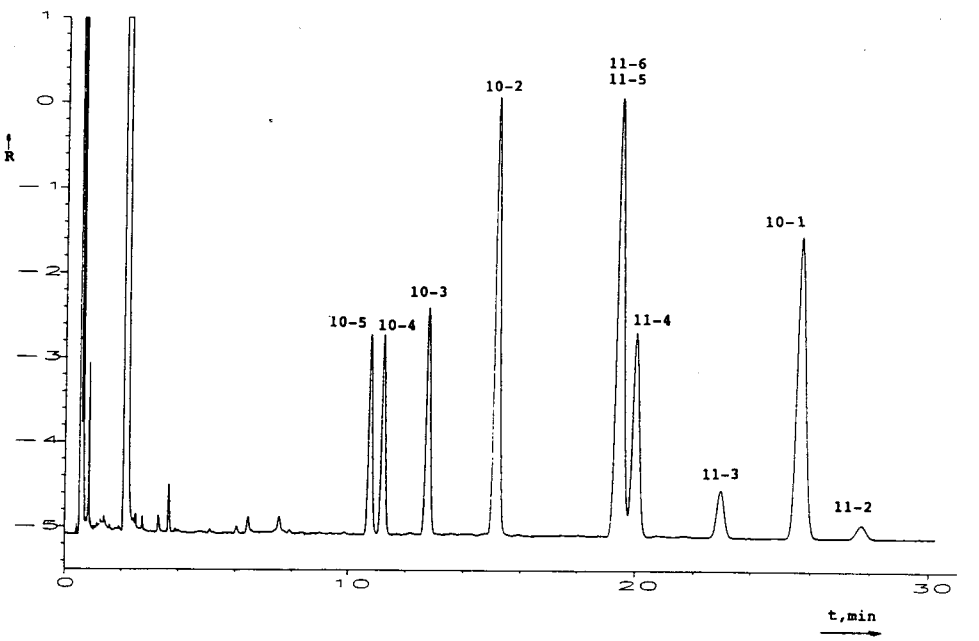

Fig. 5. Separation of acetyl derivatives of branched-chain undecanols and dodecanols at 100°C. For identification of peaks, see Table 1.

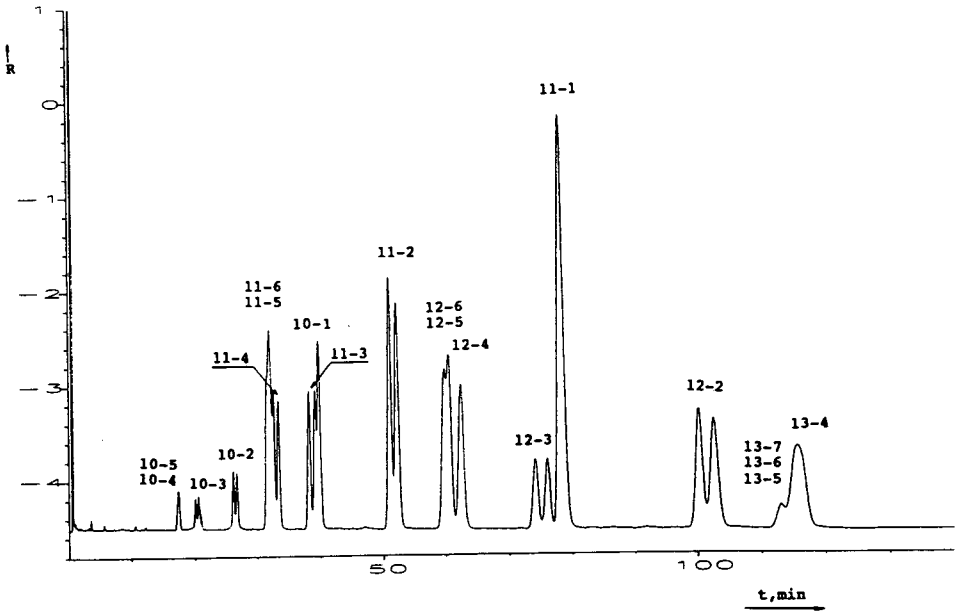

Fig. 6. Separation of C_{11}–C_{14} branched-chain alcohols at 90°C. For identification of peaks, see Table 1.

5. Acknowledgements

The authors thank the European Community for a Tempus Project Grant (JEP-0379-90/2) and the Slovak Ministry of Education for Grant No. 1/990927/92.

6. References

[1] W.A. König, *Gas Chromatographic Enantiomer Separation with Modified Cyclodextrins*, Hüthig, Heidelberg, 1992.

[2] W.A. König, B. Geherke, D. Icheln, P. Evers, Y. Donecke and W. Wang, *J. High Resolut. Chromatogr.*, 15 (1992) 367.

[3] W. Buda, C. Jaques, A. Venema and P. Sandra, in P. Sandra (Editor), *Fifteenth International Symposium on Capillary Chromatography*, Vol. I, Hüthig, Heidelberg, 1993, p. 230.

[4] J. Krupčík and D. Repka, *Collect. Czech. Chem. Commun.*, 50 (1985) 1808.

ELSEVIER

Journal of Chromatography A, 665 (1994) 169–173

JOURNAL OF CHROMATOGRAPHY A

Identification of the isomers from mono- and dinitration of phenyl- and diphenylacetic acids by gas chromatography with Fourier transform infrared and mass spectrometric detection

L. Soják*[,a], A. Perjéssy[a], R. Kubinec[a], A.G. Giumanini[b], P. Strazzolini[b]

[a]*Institute of Chemistry and Department of Organic Chemistry, Faculty of Natural Sciences, Comenius University, Mlynská dolina, 842 15 Bratislava, Slovak Republic*

[b]*Department of Chemical Sciences and Technologies, University of Udine, I-33100 Udine, Italy*

Abstract

The problem of the identification of the isomers from mono- and dinitration of diphenylacetic acid prior to their individual separation was investigated by studying the corresponding methyl esters by capillary gas chromatography with Fourier transform infrared detection with the aid of data obtained by gas chromatography–mass spectrometry (GC–MS) in the positive-ion mode. The isomer assignments were essentially made by extrapolation of the observations of the IR stretching vibrations of both the nitro group and the benzene ring in the methyl esters of mononitrophenylacetic acid isomers. Heteronuclear nitro substitution of diphenylacetic acid was confirmed by GC–MS. The occurrence of products of dinitration on the same benzene ring, if any, was below the observable limits in the mixtures studied.

1. Introduction

In the course of synthetic work [1] aimed at the preparation of the mono- and dinitrophenylacetic and diphenylacetic acids, we encountered the problem of the identification of the isomers produced in both the mono- and the dinitration procedures. Most of the likely isomers not only are commercially unavailable, but also are not known in the literature or their syntheses are cumbersome. No chromatographic or spectral data for most of these compounds have been published. A simple and rapid procedure for their identification was extremely desirable. The investigated dinitration mixtures presented the problems of identification of the position and attachment of the nitro groups to one or two benzene rings. Mass spectrometry alone is generally unable to distinguish between ring-substituted isomers [2], especially between *meta* and *para* isomers.

This paper describes the investigation of this problem by combining the high separation power of capillary gas chromatography (cGC) with the highly informative detection of the eluates by both Fourier transform infrared (FT-IR) spectrometry and electron impact ionization mass spectrometry (MS).

* Corresponding author.

0021-9673/94/$07.00
SSDI 0021-9673(93)E1121-F

2. Experimental

2.1. Materials

The chemicals used were of 99% purity from Aldrich (Milwaukee, WI, USA).

Nitro compound mixtures came from different reaction batches; they were usually obtained by direct nitration of phenylacetic and diphenylacetic acid or their methyl esters under different experimental conditions [1]. 2-Nitrodiphenylacetic acid and its methyl ester was also nitrated according to procedures leading mainly to either 2,2′- or 2,4′-dinitro products. The authentic original substrate 2,2′-dinitrodiphenylacetic acid was obtained by crystallization from the mononitration reaction mixture of 2-nitrophenylacetic acid. 4,4′-Dinitrodiphenylacetic acid was obtained from the dinitration of diphenylacetic acid with pure HNO_3. Free nitro and dinitro acid mixtures were methylated with dry ethereal diazomethane to obtain the corresponding methyl esters before admission to the injection port of the GC apparatus.

2.2. GC–FT-IR and GC–MS measurements

GC separations were carried out on a capillary column (50 m × 320 μm I.D. coated with OV-1 as stationary phase (0.33 μm film thickness). The capillary column was prepared as described previously [3]. The carrier gas was helium at an inlet pressure 0.15 MPa. The column temperature was programmed with an isothermal period at 150°C for 2 min, then increased at 10°C min^{-1} to 300°C with an isothermal period at 300°C for 5 min. For detection of the separated peaks, flame ionization (FID), FT-IR and MS detection were applied.

A Finnigan (Bremen, Germany) Model 1020 mass spectrometer equipped with an automated data collection system was used to record electron impact positive-ion mass spectra at 70-eV electron energy. The separated GC peaks were monitored by MS many times during the elution to ensure homogeneity of the eluted material. Peaks from reactions under different conditions were compared for identity by both GC and MS. Whenever possible, mass spectra of GC peaks were compared with those of authentic specimens that were recorded both via the GC system and via the direct inlet port.

A Hewlett-Packard (Palo Alto, CA, USA) Model 5890 Series II gas chromatograph with an HP Model 5965 A IR detector was used to obtain FT-IR spectra.

3. Results and discussion

As the identification of isomeric products obtained by nitration of phenyl- and diphenylacetic acid has not previously been investigated by using FT-IR spectrometry, we present below more detailed information about the spectral and structural assignment. To simplify the identification of products of dinitration we first studied the products of the mononitration of phenylacetic acid (**I**).

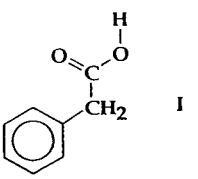

I

The chromatogram of the mixture of mononitrophenylacetic methyl esters is shown in Fig. 1. The peak identifications and the FT-IR data measured for the methyl esters of the products of mononitration of phenylacetic acid (**I**) are given in Table 1.

As the GC–FT-IR system employed could not be used for the identification the region of CH out-of-plane wagging vibrations of the benzene ring (900–650 cm^{-1}), we applied the well resolved absorption bands belonging mainly to the stretching vibrations of both the NO_2 group and the benzene ring. The *ortho*, *meta* and *para* isomers from the mononitration of phenylacetic acid can be assigned on the basis of the FT-IR spectra of their methyl esters as follows. The carbonyl stretching frequency [ν(C = O)] of the $COOCH_3$ group hardly undergoes any changes

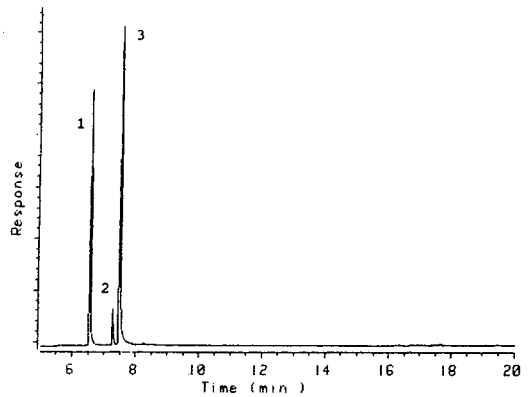

Fig. 1. Chromatogram of the mixture of mononitrophenylacetic acid methyl esters. Peak identifications as in Table 1.

on passing from isomer to isomer. Nearly the same is true regarding the symmetrical stretching frequency of the NO_2 group [$\nu_s(NO_2)$]. However, the structurally sensitive IR property of the mononitrated molecule is the asymmetric stretching vibration of the nitro group [$\nu_{as}(NO_2)$] [4,5].

For the *para*-substituted isomer (with respect to the electron-releasing property of the $-CH_2COOCH_3$ moiety), the lowest value is observed for $\nu_{as}(NO_2)$, which is caused by the efficient conjugation of the NO_2 group with the aromatic π-electron system. For the *ortho*-substituted compound a higher frequency band of $\nu_{as}(NO_2)$ was found because of deconjugation due the steric effect between the NO_2 group and the $-CH_2COOCH_3$ chain of the molecule. For the *meta* isomer the conjugation between the NO_2 group and the aromatic ring should be weakened and consequently the $\nu_{as}(NO_2)$ absorption appeared at the highest frequency (1548 cm^{-1}), which is 12 cm^{-1} higher than the $\nu_{as}(NO_2)$ absorption of the well conjugated *para* isomer. In addition, for the *para*-substituted derivative an additional sharp absorption band was observed at *ca.* 1600 cm^{-1}, which belongs to the stretching vibration mode of the aromatic ring [ν(arom.)] and usually characterizes the *para* position of the substituent group.

The second step in the study of the dinitration was to investigate the products of mononitration of diphenylacetic acid (**II**).

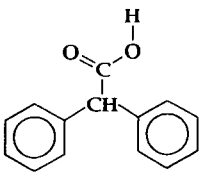

II

The chromatogram of the products from the nitration of diphenylacetic acid methyl esters is shown in Fig. 2. The peak identifications and the FT-IR data measured for these isomers are given in Table 2. The FT-IR spectral behaviour of the mononitro derivatives of the methyl esters of diphenylacetic acid in the region of the NO_2 stretching vibration frequencies is close to that of the mononitro derivatives of the methyl ester of phenylacetic acid. However, for all the nitrated methyl esters of diphenylacetic acid we observed a shift of 7 cm^{-1} to lower frequencies in the bands belonging to the $\nu(C=O)$ of the ester moiety, which is caused by the electron-donating effect of the additional benzene ring.

On the basis of the above empirical investigations, we were able to identify the six isomeric products obtained by the dinitration of diphenylacetic acid.

Table I
GC and FT-IR data for methyl esters of the products of the mononitration of phenylacetic acid (**I**)

GC peak No. (Fig. 1)	Retention time (min)	Position of NO_2 group on benzene ring	$\nu(C=O)$ (cm^{-1})	$\nu_{as}(NO_2)$ (cm^{-1})	$\nu_s(NO_2)$ (cm^{-1})	ν(arom.) (cm^{-1})
1	6.57	*ortho*	1764	1544	1353	–
2	7.27	*meta*	1763	1548	1354	–
3	7.52	*para*	1763	1536	1350	1602

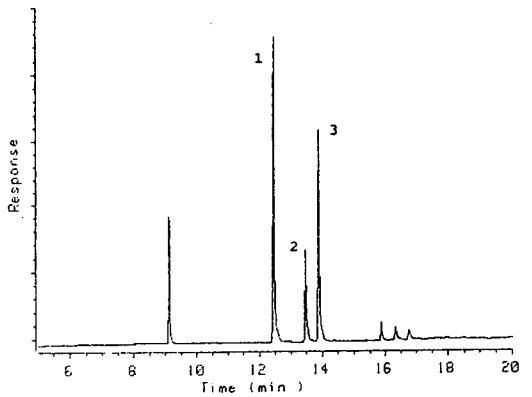

Fig. 2. chromatogram of methyl esters of products from the nitration of diphenylacetic acid. Peak identifications as in Table 2.

MS was used to confirm that the main products of the dinitration of diphenylacetic acid are heteronuclear dinitro derivatives. The common feature of mono- and dinitro derivatives of diphenylacetic acid (**II**) was the presence of the ion at m/z 167, which was found to correspond to $C_{12}H_9N$ by high-resolution MS and is believed to have the structure of the carbazole parent ion. For the mononitro derivatives this ion was accompanied by its protonated species $C_{12}H_{10}N^+$. By and large, the molecular ion is always absent in mononitro derivatives and in all dinitro derivatives containing at least one nitro group in the *ortho* position. Owing to steric effects, the parent ions and their fragments are more exposed by extensive cleavage: the mass spectra of *ortho* derivatives were substantially more complex than those not having nitro groups in this location. The presence of the carbomethoxy group was always evidenced by the ion at m/z 59 and most often by an ion obtained by the loss of 59 u from the parent ion.

When we performed the nitration of 2-nitrodiphenylacetic acid, the GC profile showed only minor amounts of two products, the mass spectra of which could be reconciled with those of some dinitro derivatives, which could only be homonuclearly dinitrated products containing at least one nitro group in the ortho position. These spectra showed peaks in the upper mass region which were not present in any of the heteronuclearly dinitrated products.

The chromatogram of the dinitration products of diphenylacetic acid methyl esters is shown in Fig. 3. The peak identifications and the FT-IR data measured for the methyl esters of the products of heteronuclear dinitration of diphenylacetic acid and their assignments are given in Table 3. As both the *para*, *para* and *ortho*, *ortho* isomers (*i.e.*, the methyl esters of 4,4′- and 2,2′-dinitrodiphenylacetic acid) were

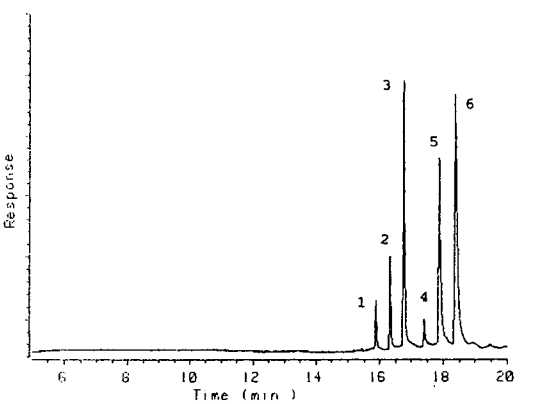

Fig. 3. Chromatogram of methyl esters of the dinitration products of diphenylacetic acid. Peak identifications as in Table 3.

Table 2
GC and FT-IR data for methyl esters of the products of the mononitration of diphenylacetic acid (**II**)

GC peak No. (Fig. 2)	Retention time (min)	Position of NO_2 group on benzene ring	ν(C=O) (cm^{-1})	$\nu_{as}(NO_2)$ (cm^{-1})	$\nu_s(NO_2)$ (cm^{-1})	ν(arom.) (cm^{-1})
1	12.45	*ortho*	1756	1543	1355	–
2	13.46	*meta*	1757	1547	1353	–
3	13.88	*para*	1757	1537	1350	1600

Table 3
GC and FT-IR data for methyl esters of the products of the heteronuclear dinitration of diphenylacetic acid (**II**)

GC peak No. (Fig. 3)	Retention time (min)	Position of NO_2 groups on benzene rings	ν(C=O) (cm^{-1})	$\nu_{as}(NO_2)$ (cm^{-1})	$\nu_s(NO_2)$ (cm^{-1})	ν(arom.) (cm^{-1})
1	15.87	*ortho,ortho*	1757	1545	1353	*ca.* 1605
2	16.32	*ortho,meta*	1758	1546	1354	–
3	16.75	*ortho,para*	1758	1543	1351	1603
4	17.36	*meta,meta*	1759	1548	1352	–
5	17.85	*meta,para*	1759	1547	1351	1604
6	18.35	*para,para*	1758	1543	1349	1600

also isolated and identified as pure compounds, their spectral data were used as reference values for the assignment of further isomers. In the FT-IR spectra of all isomers containing at least one *para*-substituted benzene ring the previously discussed ν(arom.) band was observed at *ca.* 1600 cm^{-1} as the characteristic feature of *para* substitution. This phenomenon was used to distinguish the isomers belonging to the three GC peaks from others. With *ortho,ortho* substitution there is an exception: the additional ν(arom.) band at *ca.* 1605 cm^{-1} is also present in the spectra owing the *ortho* effect of both NO_2 groups. To distinguish the isomers containing *meta*-substituted nuclei, again the criterion of the upward shift of the $\nu_{as}(NO_2)$ absorption caused by the deconjugation effect was employed.

It follows from the comparison of retentions in Figs. 2 and 3 and from the corresponding FT-IR spectra that the last three small peaks at retention times of 15.86, 16.31 and 16.75 min in the nitration products of diphenylacetic acid in Fig. 2 are identical with peaks 1, 2 and 3, respectively in Fig. 3, *i.e.*, *ortho,ortho-*, *ortho,meta-* and *ortho,para*-dinitro derivatives, respectively, of diphenylacetic acid.

4. Conclusions

This work has shown conclusively that the combination of GC with FT-IR and MS detection allows the successful identification of all the isomers from the nitration and dinitration of mono- and diphenylacetic acid. It is possible that the essential features of this method could be applied to the identification of nitration mixtures from similar substrates.

5. Acknowledgements

This work was carried out with partial support from funds for inter-university cooperation between Comenius University, Bratislava (Slovakia), and the University of Udine (Italy). The Italian National Research Council provided a research grant to A.G.G. (93.03024.CT03).

6. References

[1] A.G. Giumanini, P. Strazzolini, G. Verardo and M. Poiana, in preparation.
[2] L.A. Burlingame (Editor), *Topics in Organic Mass Spectrometry*, Wiley-Interscience, New York, 1970.
[3] P. Farkaš, L. Soják, M. Kováč and J. Janák, *J. Chromatogr.*, 471 (1989) 251.
[4] O. Exner, Š. Kováč and E. Solčániová, *Collect. Czech. Chem. Commun.*, 37 (1972) 2156.
[5] A. Perjéssy, D. Rasala, P. Tomasik and R. Gawinecki, *Collect. Czech. Chem. Commun.*, 50 (1985) 2443.

ELSEVIER

Journal of Chromatography A, 665 (1994) 175–184

JOURNAL OF CHROMATOGRAPHY A

Relationship between structure and chromatographic behaviour of secondary alcohols and their derivatives separated by high-resolution gas chromatography with a modified β-cyclodextrin stationary phase☆

J. Krupčík*,[a], E. Benická[a], P. Májek[a], I. Skačáni[a], P. Sandra[b]

[a]Department of Analytical Chemistry, Faculty of Chemical Technology, Slovak Technical University, Radlinského 9, 812 37 Bratislava, Slovak Republic

[b]Department of Organic Chemistry, University of Ghent, Krijgslaan 281, S-4, B-9000 Ghent, Belgium

Abstract

Low-boiling secondary alcohols (2-butanol, 2-pentanol and 2- and 3-hexanol) and their methyl, pentyl, acetyl and trifluoroacetyl derivatives were separated by gas chromatography on a fused-silica capillary column coated with a mixture of OV-1701 and heptakis (6-O-*tert.*-butyldimethylsilyl-2,3-di-O-acetyl)-β-cyclodextrin (1:1). The retention of these solutes was studied by determining their separation factors (α) and this temperature dependences. The retention of enantiomers was correlated with optical activity and structural data obtained by theoretical calculations. It was demonstrated that the separation of enantiomers on a modified cyclodextrin stationary phase is governed *inter alia* by total molecule asymmetries.

1. Introduction

Fused-silica capillary columns coated with several alkyl and/or acyl α-, β- and γ-cyclodextrin (CD) derivatives are suitable for the enantiomeric separation of a wide variety of volatile compounds of different molecular size and functionality [1]. The gas chromatographic (GC) separation of more than 250 optical isomers has been demonstrated on capillary columns coated with diluted permethylated or perpentylated α-, β- and γ-CDs or heptakis(2,6-di-O-methyl-3-O-acetyl)-β-CD in OV-1701 stationary phase [2]. Schmalzing *et al.* [3] described a method for preparing capillary columns with a chemically bonded permethylated-β-CD stationary phase through polysiloxane linkages on which more than 100 enantiomers including hydrocarbons, alkyl halides, O-isopropyl-N-trifluoroamino acids, ketones, lactones, ethers, underivatized alcohols and diols were successfully separated. Most alcohols have a separation factor $\alpha = 1.04$ that is not dependent on the molecular mass (*e.g.*, pentanol and α-terpineol), but differences were found between similar compounds (*e.g.*, $\alpha = 1.06$ for 4-methyl-2-pentanol and $\alpha = 1.02$ for 4-methyl-3-pentanol). This clearly shows that the shape of the guest molecule plays an important role in chiral recognition expressed as a "shape selectivity" [3].

König and co-workers [4–8] and Li and Arm-

* Corresponding author.

☆ Part of this paper was presented at the *15th International Symposium on Capillary Chromatography, Riva del Garda, May 24–27, 1993.*

0021-9673/94/$07.00
SSDI 0021-9673(93)E1207-G

strong [9] showed that α-, β- and γ-CDs modified with higher alkyl (*e.g.*, penthyl) and/or acetyl groups are liquids suitable as stationary phases in capillary GC with fused-silica capillaries. Li and Armstrong [9] separated more than 150 pairs of enantiomers by GC on capillaries coated with hexakis(2,6-di-O-pentyl-3-O-trifluoroacetyl)-α-CD (DP-TFA-α-CD), heptakis (2,6-di-O-pentyl-3-O-trifluoroacetyl)-β-CD (DP-TMA-β-CD) or octakis(2,6-di-O-pentyl-3-O-trifluoroacetyl)-γ-CD (DP-TFA-γ-CD). Excellent resolutions of secondary alcohols, diols, amino alcohols, α-halocarboxylic acid esters, halohydrocarbons, glycidyl analogues, lactones, bicyclic compounds and pyran and furan derivatives were obtained on columns coated with DP-TFA-γ-CD. (*R*)- and (*S*)-2-chloropropionic acid methyl esters showed an α value of 2.69 on DP-TFA-β-CD, which is unusually large for a GC separation of enantiomers [9].

However, there is a lack of a systematic study on the interaction mechanisms between the "host" CD derivatives and the "guest" enantiomeric solutes. The applications selected to illustrate the enantioselectivity of a CD derivative are the result of trial and error [10].

The host–guest interaction via inclusion complex formation could be an explanation for the chiral resolution obtained with macrocyclic CD derivatives [11]. The CD macrocycle moreover recognizes the chiral host through an induced fit [11]. König *et al.* [11] stated that there are facts opposing inclusion complexes, as the enantiomers of substances that are too large to fit into the macrocyclic cavity can be successfully separated. This indicates that the enantioselective interaction could take place at the outer surface of a molecule [11].

The separation of enantiomers occurs through reversible diastereomer association between the solutes and the chiral environment. However, various kinds of binding interaction may also be involved [12]. The successful enantiomer separation of totally unfunctionalized saturated hydrocarbons on peralkyl derivatives of β- and γ-CD [11,12] demonstrates that Van der Waals interactions are sufficient for chiral recognition.

Armstrong *et al.* [13] observed enantioselective peak reversals for some enantiomeric compounds separated by GC under similar conditions on columns coated with derivatized α-, β- and γ-CD. Peak reversals have been observed between α- and β-CD and between β- and γ-CD, but not between α- and γ-CD, which is evidence that CD are "size-selective" phases.

König *et al.* [11] showed a reversal of the elution order of α-pinene, β-pinene and limonene enantiomers on columns coated with heptakis(6-O-methyl-2,3-di-O-pentyl)-β-CD and octakis(6-O-methyl-2,3-di-O-pentyl)-γ-CD, respectively. On the β-CD derivative all (−)-enantiomers eluted before the (+)-enantiomers, whereas on the γ-CD derivative the elution order was reversed [12]. On γ-CD derivative all the (+)-enantiomers studied by König *et al.* [11] were eluted before corresponding the (−)-derivatives.

König *et al.* [14] found that by GC analysis of terpineols on a capillary column coated with heptakis(2,6-di-O-methyl-3-O-pentyl)-β-CD the retention orders of enantiomeric pairs differing only in stereo configuration, *e.g.*, (+)-terpinen-4-ol eluted before the (−)-enantiomer, whereas (−)-α-terpineol eluted before the (+)-enantiomer. This clearly shows that in addition to other factors, stereo configuration can have a dominant influence on chiral interactions.

From systematic studies of the enantioselectivity of α-, β- and γ-CD derivatives having identical substitution patterns towards certain chiral substrates, it has become increasingly evident that not only inclusion, possibly supported by conformational changes, but also association in the outer sphere of the cyclodextrin cavity are responsible for chiral recognition [15]. The meaning of inclusion of solutes in a CD cavity is, however, often misunderstood. Inclusion in many instances does not mean that the whole molecule is located in the CD cavity. The accommodation of part of the molecule (alkyl or functional group) is also often considered as inclusion.

The investigation of the temperature dependence of separation factors also indicated that conformational parameters play an important role. Separation factors not only dramatically

decrease with increasing column temperature but may result in a reversal of elution order [16]. Reversal of the elution order is, according to Watanabe *et al.* [17], an indication of two different and temperature-dependent modes of diastereomeric host–gest interactions (molecules of the enantiomers with the molecules of the enantiomeric selective stationary phase). This may occur with members of a homologous series too [18].

The aim of this work was to study the separation of low-boiling secondary alcohols (2-butanol, 2-pentanol and 2- and 3-hexanols) and their methyl, acetyl and trifluoroacetyl derivatives by high-resolution (HR) GC on a fused-silica capillary column coated with a mixture of OV-1701 and heptakis(6-O-*tert.*-butyldimethylsilyl-2,3-di-O-acetyl)-β-CD (1:1). For the derivatization of secondary alcohols similar reactions were used to those generally used for the preparation of modified cyclodextrin stationary phases in HRGC. The separation factors (α) and their temperature dependences were correlated with optical activities of the solutes and data obtained by the theoretical calculations.

2. Experimental

2.1. Gas chromatography

GC was performed with a Hewlett-Packard Model 5890 gas chromatograph equipped with a flame ionization detector and a split–splitless injector. Separations were performed on a 25 m × 0.30 mm I.D. fused-silica capillary column coated with a 0.125-μm film of the mixed stationary phase OV-1701 and heptakis(6-O-*tert.*-butyldimetylsilyl-2,3-di-O-acetyl)-β-CD (1:1) [19]. The GC oven was operated at various temperatures for isothermal experiments from 30 to 70°C in 10°C increments. Several experiments were performed at 15, 20 and 25°C. A volume of 0.05 or 0.1 μl of individual samples with concentrations of 10 mg/ml in diethyl ether was injected, except for 2-butanol trifluoroacetate, which was dissolved in methanol. Hydrogen was used as the carrier gas at an inlet pressure of 200 kPa. The split flow was 100 ml/min and the septum flow 3 ml/min. Nitrogen was used as the make-up gas at a flow-rate of 30 ml/min.

Chromatograms were registered by a HP 3396 integrator and using Peak 96 software were sent to a PC where they were evaluated with HPChem software (all products from Hewlett-Packard, Waldbronn, Germany).

2.2. Analytes

2-Butanol and 2-pentanol were obtained from Merck (Darmstadt, Germany). 2-Hexanol was prepared by hydration of 1-hexene [20].

Acetyl derivatives of the secondary alcohols were prepared by reaction with acetyl chloride or acetic anhydride [21]. Trifluoroacetyl derivatives of the secondary alcohols were prepared by reaction with trifluoroacetic anhydride [22]. Methyl and pentyl ethers of the secondary alcohols were prepared by alkylation with corresponding alkyl iodide [23,24]. A list of the compounds used and their abbreviations is given in Table 1.

Table 1
Abbreviations of analytes used

Compound	Abbreviation
2-Butanol	2-BuOH
2-Pentanol	2-PeOH
2-Hexanol	2-HexOH
3-Hexanol	3-HexOH
2-Butyl acetate	2-BuOCOCH$_3$
2-Pentyl acetate	2-PeOCOCH$_3$
2-Hexyl acetate	2-HexOCOCH$_3$
3-Hexyl acetate	3-HexOCOCH$_3$
2-Butyl trifluoroacetate	2-BuOCOCF$_3$
2-Pentyl trifluoroacetate	2-PeOCOCF$_3$
2-Hexyl trifluoroacetate	2-HexOCOCF$_3$
3-Hexyl trifluoroacetate	3-HexOCOCF$_3$
Methyl 2-butyl ether	Me-2-BuEt
Methyl 2-pentyl ether	Me-2-PeEt
Methyl 2-hexyl ether	Me-2-HexEt
Pentyl 2-butyl ether	Pe-2-BuEt
Pentyl 2-pentyl ether	Pe-2-PeEt
Pentyl 2-hexyl ether	Pe-2-HexEt
Pentyl 3-hexyl ether	Pe-3-HexEt

2.3. Reagents

Diethyl ether, methanol, acetyl chloride and trifluoroacetic anhydride were obtained from Merck (Darmstadt, Germany).

2.4. Theoretical calculations

Conformations corresponding to energy minima of hydroxy, methoxy, pentoxy, acetyl and trifluoroacetyl derivatives of 2-butane, 2-

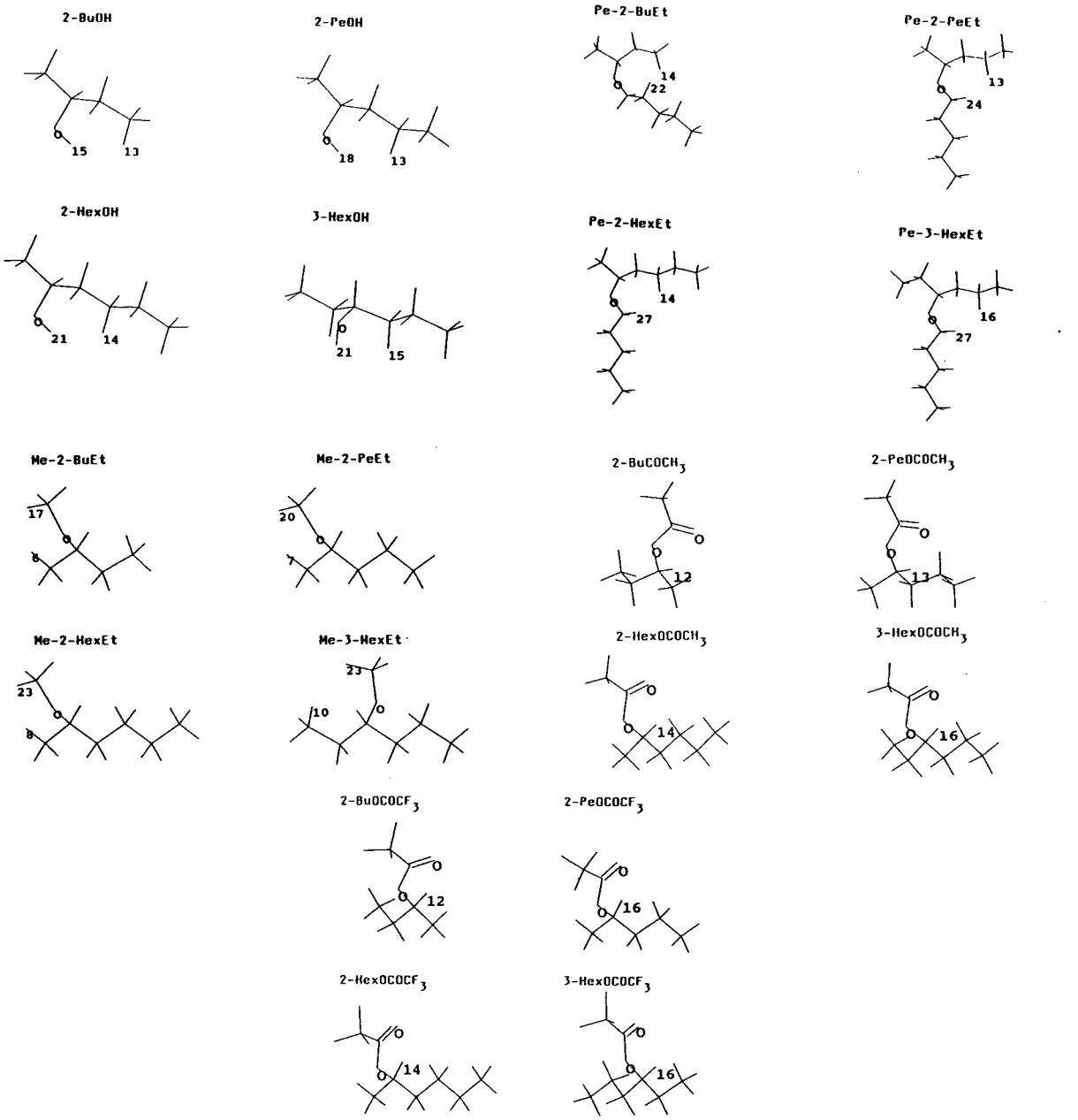

Fig. 1. Stick models of the optimized structures found for the considered molecules by the AM1 method. For illustration oxygen atoms are labelled and atoms with critical intra-atomic distances are numbered.

pentane and 2- and 3-hexane were calculated with HyperChem (trademark of Autodesk Inc.) for Windows Version 2.0. In searching for the optimum conformation of the considered derivatives on the semi-empirical level the AM1 method [25] was used.

Structures of the solutes expressed by conformations of molecules corresponding to energy minima in the gas phase found by AM1 are shown in Fig. 1. Some data that characterize the electronic structure (net charges and dipole moments) of the compounds in optimized conformations are given in Table 2. In the last two columns of Table 2 critical distances (lengths in Å) are given for atoms that substantially influence free rotation along the C–C bond.

The optimum conformation of permethylated-β-CD and heptakis(6-O-*tert.*-butyldimethylsilyl-2,3-di-O-acetyl)-β-CD shown in Fig. 2 was found by the molecular mechanics calculation MM+ method [26] in the gas phase.

The starting geometries of the considered molecules were designed by the molecular editor which is built in the HyperChem software. The RHF gradient optimization of the model built structure was performed and a value of 0.02 kcal/Å · mol was used as a convergence criterion for the RMS gradient method. The standard parameterization MM+ [26] was used for potentials in the molecular mechanics calculations and the same value of RMS gradient was chosen for the convergence. The energy minima are, however, very flat and often separated by a small rotation energy barrier (several kCal/mol) and consequently local minima can be found with non-expected conformations, as we have found for 2-butylacetate and 2-butyltrifluoroacetate. To avoid this discrepancy different starting structures were designed for all studied compounds. All calculations were performed on a 50-MHz IBM PC/486 computer.

3. Results and discussion

The separation of 2-butanol, 2-pentanol and 2- and 3-hexanols by GC on a fused-silica capillary column coated with the mixture of OV-1701 and

Table 2
Net changes, dipole moments and critical intra-atomic distances found by the AM1 method for molecules of the considered compounds with optimized conformations

Compound	Net charge (e)	Dipole moment (D)	Critical distance	
			Atoms	Length (Å)
2-BuOH	$29.1 \cdot 10^{-3}$	1.64	H13–H15	2.15
2-PeOH	$29.4 \cdot 10^{-3}$	1.66	H13–H18	2.14
2-HexOH	$29.6 \cdot 10^{-3}$	1.67	H14–H21	2.13
3-HexOH	$23.7 \cdot 10^{-3}$	1.53	H15–H21	2.12
2-BuOCOCH$_3$	$35.8 \cdot 10^{-3}$	1.80	O7–H12	2.32
2-PeOCOCH$_3$	$30.8 \cdot 10^{-3}$	1.76	O9–H13	2.23
2-HexOCOCH$_3$	$29.9 \cdot 10^{-3}$	1.74	O10–H14	2.21
3-HexOCOCH$_3$	$31.3 \cdot 10^{-3}$	1.79	O10–H16	2.23
2-BuOCOCF$_3$	$38.7 \cdot 10^{-3}$	3.12	O7–H12	2.38
2-PeOCOCF$_3$	$36.0 \cdot 10^{-3}$	3.15	O9–H16	2.29
2-HexOOCF$_3$	$35.0 \cdot 10^{-3}$	3.11	O10–H14	2.27
2-HexOCOCF$_3$	$35.3 \cdot 10^{-3}$	3.11	O10–H16	2.29
Me-2-BuEt	$25.6 \cdot 10^{-3}$	1.30	H6–H17	2.20
Me-2-PeEt	$26.0 \cdot 10^{-3}$	1.28	H7–H20	2.20
Me-2-HexEt	$26.1 \cdot 10^{-3}$	1.28	H8–H23	2.20
Me-3-HexEt	$26.4 \cdot 10^{-3}$	1.30	H10–H23	2.43
Pe-2-BuEt	$32.2 \cdot 10^{-3}$	1.39	H14–H17	2.28
Pe-2-PeEt	$31.2 \cdot 10^{-3}$	1.24	H13–H23	2.27
Pe-2-HexEt	$31.4 \cdot 10^{-3}$	1.25	H14–H27	2.26
Pe-3-HexEt	$30.4 \cdot 10^{-3}$	1.19	H16–H27	2.29

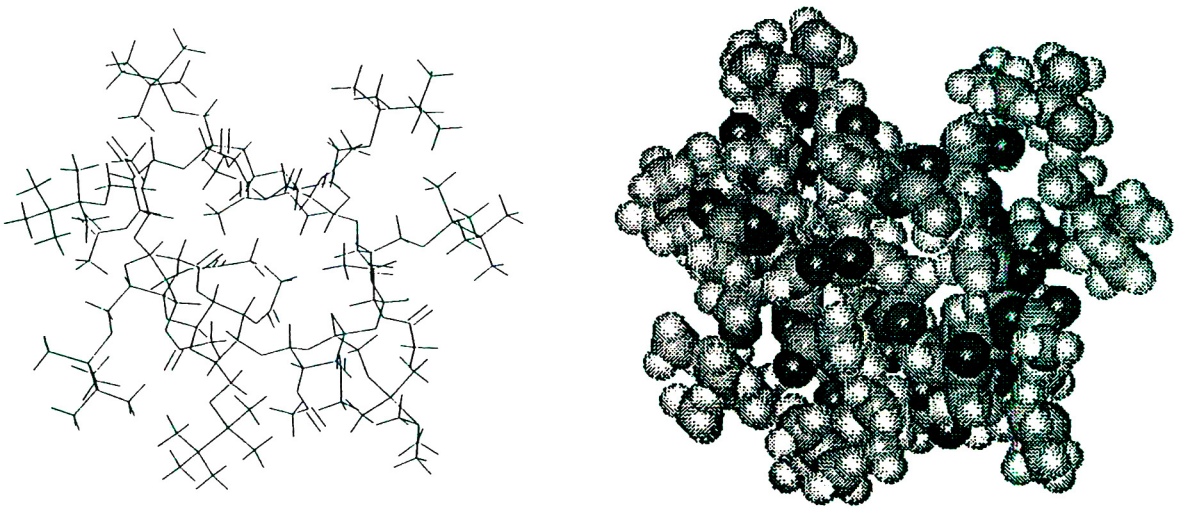

Fig. 2. Stick and spherical models of optimized structure of heptakis(6-O-*tert.*-butyldimethylsilyl-2,3-di-O-acetyl)-β-CD as found by the MM+ method.

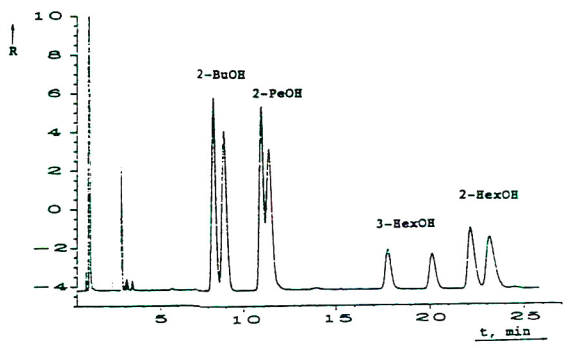

Fig. 3. Separation of enantiomers of 2-butanol, 2-pentanol and 2- and 3-hexanols by capillary GC with heptakis(6-O-*tert.*-butyldimethylsilyl-2,3-di-O-acetyl)-β-CD at 40°C.

heptakis(6-O-*tert.*-butyldimethylsilyl-2,3-di-O-acetyl)-β-CD is shown in Fig. 3. A reasonable separation of the enantiomers of 2-butanol and 2-hexanol, an excellent separation of the 3-hexanols and a relatively poor separation of the 2-pentanols is observed. In Table 3, published data for the optical rotation of some secondary alcohols are given. It follows from Table 3 that the chirality of the alcohols decreases with increase in molecular mass and (*R*)-enantiomers turn the polarized light to left (−) and (*S*)-enantiomers to the right (+). Since the optical rotation is a molecular property, a decrease of optical rotation with molecular mass is expected [29]. It is further evident that the separation of alcohols in

Table 3
Optical rotations of some secondary alcohols (from ref. 30)

Compound	Temperature (°C)	[α]	Note
(*R*)-(−)-2-Butanol	20	−13	Neat
(*S*)-(+)-2-Butanol	20	+13	Neat
(*R*)-(−)-2-Pentanol	20	−13	Neat
(*S*)-(+)-2-Pentanol	20	+13	Neat
(*R*)-(−)-2-Hexanol	24	−11	Neat
(*S*)-(+)-2-Hexanol	24	+11	Neat
(*R*)-(−)-3-Hexanol[a]	20	−7.2	Neat
(*S*)-(+)-3-Hexanol[a]	20	+6.8	In chloroform

[a] From ref. 31.

Fig. 3 does not fully correlate with the data in Table 3 as for 2-pentanols and 3-hexanols. The discrepancies in these correlations can be explained by the specific interactions of different shapes of alcohol molecules (see Fig. 1) with a modified cyclodextrin stationary phase. The enantiomers of the alcohols with an ethyl group linked to an optically active carbon atom (2 butanol and 3-hexanol) show a specific molecular shape (a six-membered ring, which hinders free rotation). This asymmetry is, however, enlarged with the interaction of the considered compounds with the modified CD stationary phase and these enantiomers are separated much better in Fig. 3 than those with a longer alkyl chain (2-pentanol and 2-hexanol).

In Table 4 a cyclodextrin derivative exhibits a lower optical activity than the corresponding native compound. As the diastereometric complexes are responsible for the chiral recognition of secondary alcohols, and cyclodextrins turn the light to the right (+), the retention of (*R*)-(−)-enantiomers is higher than that of (*S*)-(+)-enantiomers, which has already been confirmed by analysis of pure enantiomers [27]. As the relationship between the optical properties both solutes and CDs and the separation of solute enantiomers on CDs is very complex and includes *inter alia* the type of interaction, position of interaction and separation temperature, we shall discuss them separately [28].

The enantiomeric resolution of secondary butyl chloride, butyl bromide and butyl iodide, which according to Venema *et al.* [29] can be explained by correlation of retention with the molecular volumes, can also be explained by correlation of the retention with the molecule polarizabilities. This parameter, connected with both the molecular volumes and optical activities for the considered alkyl halides, increases with increase in the relative atomic mass of the halide [*e.g.*, $M_r(I) > M_r(Br) > M_r(Cl)$].

The structures of methyl 2-alkyl ethers do not differ substantially and the separation of their enantiomers is also comparable (Fig. 4). Substitution of hydrogen atoms in the OH groups for cyclodextrin derivatives leads to permethylated cyclodextrins which show lower optical activity than exhibited by the native cyclodextrins (Table 4). This could be a reason why diastereomeric complexes between a given cyclodextrin stationary phase and methyl 2-alkyl ethers are weaker than those with secondary alcohols. The separation in Fig. 4 is not as good as that in Fig. 3. The

Table 4
Optical rotations of α-, β- and γ-cyclodextrins and some of their derivatives [11]

Cyclodextrin derivative	$[\alpha]_D^{22}$ [a]
α-Cyclodextrin	153.0[b]
β-Cyclodextrin	162.0[b]
γ-Cyclodextrin	176.1[b]
Hexakis(6-O-*tert.*-butyldimethylsilyl-2,3-di-O-pentyl)-α-cyclodextrin	68.0
Heptakis(6-O-*tert.*-butyldimethylsilyl-2,3-di-O-pentyl)-β-cyclodextrin	65.2
Octakis(6-O-*tert.*-butyldimethylsilyl-2,3-di-O-pentyl)-γ-cyclodextrin	74.4 ($c = 0.7$)
Hexakis(2,3-di-O-pentyl)-α-cyclodextrin	41.7
Heptakis(2,3-di-O-pentyl)-β-cyclodextrin	108.9
Octakis(2,3-di-O-pentyl)-γ-cyclodextrin	104.6 ($c = 0.7$)
Hexakis(6-O-acetyl-2,3-di-O-pentyl)-α-cyclodextrin	40.8 ($c = 0.8$)
Heptakis (6-O-acetyl-2,3-di-O-pentyl)-β-cyclodextrin	81.1
Hexakis(6-O-butyryl-2,3-di-O-pentyl)-α-cyclodextrin	71.5
Heptakis(6-O-butyryl-2,3-di-O-pentyl-β-cyclodextrin	83.5 ($c = 0.2$)
Octakis(6-O-methyl-2,3-di-O-pentyl)-γ-cyclodextrin	80.9 ($c = 0.7$)

[a] Solvent for optical rotation measurements was chloroform ($c = 1$ unless stated otherwise). Solvent for optical rotation measurements of underivatized CDs was water.
[b] From ref. 30.

substitution of hydrogen atoms in OH groups of secondary alcohols containing the pentyl group leads to pentyl 2-alkyl ethers, which were not separated on the capillary column in the temperature range 30–80°C. Possible reasons why these compounds are not separated are discussed elsewhere [28].

The separations of 2-pentyl and 2-hexyl acetate enantiomers are comparable (Fig. 5). However, the separation of 3-hexyl acetate enantiomers is poorer and 2-butyl acetate enantiomers do not separate under the given conditions. These results correlate with the structures shown in Fig. 1. The enantiomers of 2-butyl acetate were partially resolved at 15 and 100°C, probably with reversal of retention order. The reversal of the retention of 2-butyl acetate enantiomers with temperature is currently under study and will be reported elsewhere [28].

The structures of 2-alkyl trifluoroacetates were similar (see Fig. 1) and the separation of these compounds was also similar (Fig. 6).

The energy of diastereomeric interactions can be found from the differences in the interaction energies of (*R*)-(−)- and (*S*)-(+)-enantiomers with the cyclodextrin stationary phase. This difference can be found from the semi-logarithmic dependence of the selectivity factor ($\ln \alpha$) on the reciprocal of absolute temperature ($1/T$).

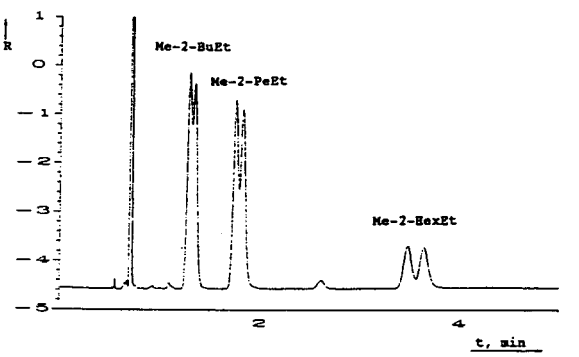

Fig. 4. Separation of enantiomers of methyl 2-butyl, methyl 2-pentyl and methyl 2-hexyl ethers by capillary GC with heptakis(6 - O - *tert.* - butyldimethylsilyl - 2,3 - di - O - acetyl)-β-CD at 40°C.

Linear equations for these dependences are given in Table 5. The correlation coefficients in Table 5 show acceptable linearity. The data for 2-butyl acetate are not included as only poor resolution was obtained in the range 15–100°C.

The slopes of the dependences are characteristic of the homologous series and characterize the differences between the diastereomeric interactions of enantiomeric pairs with the stationary phase. The relationships between the slopes and intercepts of the dependences in Table 5 are under study and will be published elsewhere [28].

Table 5
Semi-logarithmic dependence of separation factor (α) of the considered compounds on temperature ($1/T$)

Compound	Equation	Correlation coefficient
2-BuOH	$\ln \alpha = (92.6/T) - 0.221$	0.9939
2-PeOH	$\ln \alpha = (72.3/T) - 0.190$	0.9998
2-HexOH	$\ln \alpha = (52.8/T) - 0.124$	0.9925
3-HexOH	$\ln \alpha = (210.3/T) - 0.546$	0.9995
2-PeOCOCH$_3$ [a]	$\ln \alpha = (258.7/T) - 0.750$	0.9989
2-HexOCOCH$_3$ [a]	$\ln \alpha = (236.5/T) - 0.705$	0.9951
3-HexOCOCH$_3$ [a]	$\ln \alpha = (188.1/T) - 0.563$	0.9960
2-BuOCOCF$_3$	$\ln \alpha = (194.7/T) - 0.476$	0.9964
2-PeOCOCF$_3$	$\ln \alpha = (202.2/T) - 0.500$	0.9989
2-HexOCOCF$_3$	$\ln \alpha = (201.7/T) - 0.499$	0.9994
Me-2-BuEt[b]	$\ln \alpha = (124.5/T) - 0.344$	–
Me-2-PeEt[b]	$\ln \alpha = (152.8/T) - 0.447$	–
Me-2-HexEt[b]	$\ln \alpha = (171.7/T) - 0.511$	–

[a] Calculated from measurements obtained at 30, 40 and 50°C.
[b] Calculated from measurements obtained at 30 and 40°C.

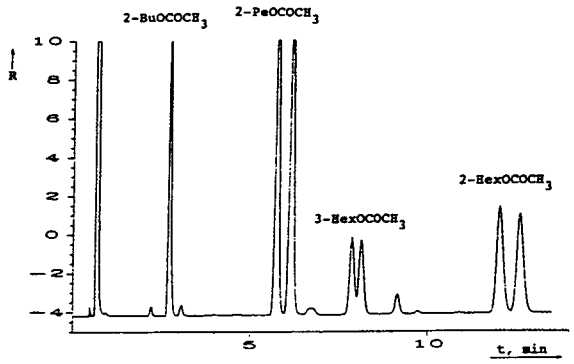

Fig. 5. Separation of enantiomers of 2-butyl, 2-pentyl and 2- and 3-hexyl acetates by capillary GC with heptakis(6-O-*tert.*-butyldimethylsilyl-2,3-di-O-acetyl)-β-CD at 40°C.

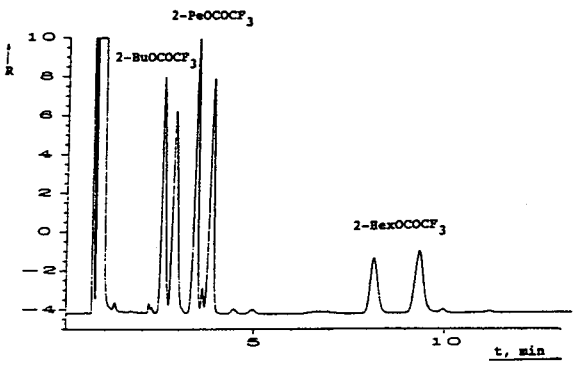

Fig. 6. Separation of enantiomers of 2-butyl, 2-pentyl and 2- and 3-hexyl trifluoroacetates by capillary GC with heptakis (6-O-*tert.*-butyldimethylsilyl-2,3-di-O-acetyl)-β-CD at 40°C.

4. Acknowledgements

The authors thank the European Community for a Tempus Project Grant (JEP-0379-90/2) and the Slovak Ministry of Education for Grant No. 1/990927/92.

5. References

[1] W.A. König, *Gas-Chromatographic Enantiomer Separation with Modified Cyclodextrins*, Hüthig, Heidelberg, 1992.
[2] W. Keim, A. Köhnes, W. Melzow and H. Römer, *J. High Resolut. Chromatogr.*, 14 (1991) 507.
[3] D. Schmalzing, M. Jung, S. Mayer, J. Rickert and V. Schurig, *J. High Resolut. Chromatogr.*, 15 (1992) 723.
[4] W.A. König, S. Lutz, P. Mischnik-Lublecke, B. Brassat and G. Wenz, *J. Chromatogr.*, 447 (1988) 193.
[5] W.A. König, S. Lutz, G. Wenz and E. von der Berg, *J. High Resolut. Chromatogr. Chromatogr. Commun.*, 11 (1988) 506.
[6] W.A. König, S. Lutz and G. Wenz, *Angew. Chem.*, 27 (1988) 979.
[7] W.A. König, S. Lutz, C. Colbergg, N. Schmidt, G. Wenz, E. von der Berg. A. Mosandl, C. Gunther and A. Kusterman, *J. High Resolut. Chromatogr. Chromatogr. Commun.*, 11 (1988) 621.
[8] W.A. König, S. Lutz, M.Hagen, R. Krebber, G. Wenz, K. Baldenius, J. Ehlers and H.T. Diek, *J. High Resolut. Chromatogr.*, 12 (1988) 35.
[9] W.-Y. Li and D.W. Armstrong, *J. Chromatogr.*, 509 (1990) 303.
[10] P. Sandra, *J. High Resolut. Chromatogr.*, 13 (1990) 665.
[11] W.A. König, D. Icheln, T. Runge, I. Pforr and A. Krebs, *J. High Resolut. Chromatogr.* 13 (1990) 702.
[12] V. Schurig, M. Jung, D. Schmalzing, M. Schleimer, J. Duvekot, J.C. Buyten, J.A. Peene and P. Musche, *J. High Resolut. Chromatogr.*, 13 (1990) 470.
[13] A.W. Armstrong, W.-Y. Li and J. Pitha, *Anal. Chem.*, 62 (1990) 214.
[14] W.A. König, N. Gehrcke, D. Icheln, P. Evers, J. Donecke and W. Wang, *J. High Resolut. Chromatogr.*, 15 (1992) 367.
[15] W.A. König, D. Icheln, P. Evers, T. Runge, M. Richters and J. Pietruszka, in P. Sandra (Editor), *13th International Symposium on Capillary Chromatography*, Vol. I, Hüthig, Heidelberg, 1991, p. 234.
[16] W.A. König, D. Icheln and I. Hardt, *J. High Resolut. Chromatogr.*, 14 (1991) 694.
[17] K. Watabe, R. Charles and E. Gil-Av, *Angew. Chem.*, 101 (1989) 194; *Angew. Chem., Int. Ed. Engl.*, 28 (1989) 192.
[18] A. Mosandl, K. Rettinger, K. Fischer, H.G. Schmarr and B. Mass, *J. High Resolut. Chromatogr.*, 13 (1990) 382.
[19] K. Janques, W.M. Buda, M. Pottie, J. Van der Eycken, M. Vandewalle, A. Venema and P. Sandra, in P. Sandra (Editor), *15th International Symposium on Capillary Chromatography*, Vol. I, Hüthig, Heidelberg, 1993, p. 319.
[20] B.T. Brooks and J. Humprey, *J. Am. Chem. Soc.*, 40 (1918) 822.
[21] R. Altschul, *J. Am. Chem. Soc.*, 68 (1946) 2609.
[22] E.J. Bourne, M. Stacey, J.C. Tatlow and R. Woral, *J. Chem. Soc.*, (1958) 3268.
[23] A.W. Smith and C.E. Boord, *J. Am. Chem. Soc.*, 48 (1926) 1515.
[24] F. Nerdel, E. Henkel, R. Kayser and G. Kannebbley, *J. Prakt. Chem.*, 3 (1956) 153.
[25] M.J.S. Dewar, E.G. Zoebish, E.F. Hely, J.J.P. Stewart, *J. Am. Chem. Soc.*, 107 (1977) 8127.
[26] N.L. Allinger, *J. Am. Chem. Soc.* 98 (1977) 8127.

[27] I.D. Smith and C.F. Simpson, *J. High Resolut. Chromatogr.*, 15 (1992) 800.
[28] J. Krupčík, P. Májek, P. Sandra and A. Venema, *J. High Resolut. Chromatogr.*, submitted for publication.
[29] A. Venema, H.H. Hendriks and R.V. Geest, *J. High Resolut. Chromatogr.*, 14 (1991) 676.
[30] *Aldrich Catalogue Handbook of Fine Chemicals 1992–1993*, Aldrich Chemie, Steinheim, 1992–93, p. 364.
[31] R.C. Weast (Editor), *CRC Handbook of Chemistry and Physics*, CRC Press, Boca Raton, FL, 65th ed., 1984–85, p. C-330.

ELSEVIER

Journal of Chromatography A, 665 (1994) 185–190

JOURNAL OF CHROMATOGRAPHY A

Detection and assay of secondary metabolites of *Penicillium vermiculatum* DANG

B. Proksa*, J. Adamcová, J. Fuska

Department of Biochemical Technology, Faculty of Chemistry, Slovak Technical University, 812 37 Bratislava, Slovak Republic

Abstract

Thin-layer chromatography on silica gel plates with detection at 254 and 365 nm, spraying with vanillin–sulphuric acid, ethanol ammonia, aqueous iron(III) chloride or ethanolic potassium hydroxide is suggested for rapid detection of (−)-vermiculin, (−)-vermiculinic and vermiculic acids, (−)-vermistatin, (−)-mitorubrinol, vermilutin, (±)-dehydroaltenusin, (+)-vermixocin A, (−)-vermixocin B, funiculosic acid and 2-methylsorbic acid, metabolites of *Penicillium vermiculatum* DANG. High-performance liquid chromatography on a Separon SGX C_{18} compact glass column eluted with methanol–water (pH 3) mixtures with detection at various wavelengths was used for assaying these compounds in cultivation media and extracts during their processing.

1. Introduction

Recently, vermiculin, a sixteen-membered macrodiolide, was isolated from the cultivation medium of *Penicillium vermiculatum* DANG in our laboratory [1]. Because this diolide showed promising pharmacological, especially antimicrobial, cytotoxic and immunoregulatory, activities, greater amounts of this compound were required for further biological evaluation. In the course of a detailed study of the microbial-producing strain and elaboration of pilot-plant technology for vermiculin preparation, we isolated further metabolities of *P. vermiculatum*: the phthalidopyranone (−)-vermistatin [2], the azaphilone (−)-mitorubrinol [3], the xanthone vermilutin [4], the lactone (±)-dehydroaltenusin [5], the 5*H*,7*H*-dibenzo[*c*,*f*][1,5]dioxocine derivatives (+)-vermixocin A and B [6], the phthalaldehydic funiculosic acid [3] and aliphatic 2-methylsorbic acid [7]. We also identified vermiculinic and vermiculic acid, intermediates in vermiculin biosynthesis [8].

P. vermiculatum is the imperfect (conidial) state of *Talaromyces flavus* (Klöcker) Stolk and Samson, the commonly occurring soil fungus, producing secondary metabolites other than those mentioned above [9–11]. Mycotoxins of *T. flavus* and of other microbial strains have been examined by thin-layer chromatography (TLC) [12] and high-performance liquid chromatography (HPLC) [13]. As only the determination of vermiculin [14,15] and mitorubrinol [15] has been published so far, we developed a method for the identification and determination of all known metabolites of *P. vermiculatum*.

2. Experimental

2.1. Apparatus

The HPLC equipment (Laboratory Instruments, Prague, Czech Republic) consisted of an

* Corresponding author.

0021-9673/94/$07.00
SSDI 0021-9673(93)E1162-S

HPP 5001 pump, an LCI 30 injector with a 3-μl loop, an LCD 2040 variable-wavelength UV detector and a CI-105 integrator.

The columns were glass cartridges (compact glass column) (150 × 3 mm I.D.) packed with Separon SGX C_{18}, 7 μm (Tessek, Prague, Czech Republic).

Silufol UV-254 plates (10 × 10 cm) (Kavalier, Votice, Czech Republic) were used for TLC.

UV spectra were recorded with a Specord 40 M spectrophotometer (Zeiss, Jena, Germany).

2.2. Chemicals and reagents

All the metabolites were isolated and purified in our laboratory. They were identified by physico-chemical (m.p., optical rotation) and spectral (UV, IR, MS and NMR) data.

All chemicals were of analytical-reagent grade (Lachema Brno, Czech Republic).

Vanillin–sulphuric acid reagent (D_3) was prepared by dissolving vanillin (0.5 g) in concentrated sulphuric acid (5 ml) and diluting to 100 ml with ethanol. After spraying, TLC plates were heated at 105°C for 5 min.

Aqueous Iron(III) chloride reagent (D_4) was prepared by dissolving $FeCl_3 \cdot 6H_2O$ (1.0 g) in 100 ml of water.

Ethanolic ammonia solution (D_5) was prepared by dissolving ammonia solution (5 ml) in and diluting to 100 ml with ethanol.

Ethanolic potassium hydroxide solution (D_6) was prepared by dissolving KOH (5 g) in 100 ml of ethanol. After spraying, the plates were heated at 105°C for 5 min.

2.3. Determination of vermiculin in a technical-grade product

A solution of vermiculin (5.0 mg in 25.0 ml of acetonitrile) was injected on to the column. The mobile phase was methanol–water (35:65) (pH 3, adjusted with phosphoric acid) at a flow-rate of 0.3 ml/min and the detection wavelength was 230 nm.

2.4. Determination of organic acids in cultivation medium of P. vermiculatum

A 20.0-g amount of medium acidified with 1 *M* hydrochloric acid (1 ml) was extracted with chloroform (three times, 15 ml each), the combined organic extracts were re-extracted with 0.1 *M* sodium hydrogecarbonate solution (twice, 15 ml each), the combined aqueous solutions were diluted to 50.0 ml with water and aliquots of the solution was injected on to the chromatographic column. The mobile phase was methanol–water (50:50) (pH 3) at a flow-rate of 0.6 ml/min and the detection wavelength was 240 nm. The efficiency of organic acid extraction was established with a sample spiked with 2-methylsorbic, vermiculinic and vermiculic acid (75 μg/ml each) and was 96.5%, 99.2% and 98.2%, respectively.

2.5. Determination of vermixocin A in cultivation medium containing whey

A 20.0-g amount of medium was extracted with ethyl acetate (3 times, 15 ml each), the combined extracts were evaporated to dryness, the residue was dissolved in methanol and the solution was diluted to 25.0 ml with methanol. The mobile phase was methanol–water (55:45) at a flow-rate of 0.6 ml/min and the detection wavelength was 230 nm.

3. Results and discussion

So far, we have isolated and structurally characterized (−)-vermiculin, (−)-vermistatin, (−)-mitorubrinol, vermilutin, (±)-dehydroaltenusin, vermixocins, funiculosic acid and 2-methylsorbic acid (Fig. 1) in cultivation media of *P. vermiculatum*.

A combination of TLC R_F values with specific colours developed after spraying with appropriate reagents was used for the rapid detection of these metabolites (Table 1). Vermiculin and its precursors, vermiculinic acid and vermiculic acid gave brown spots only with vanillin reagent and ethanolic potassium hydroxide after heating for 5

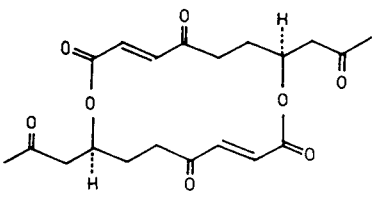

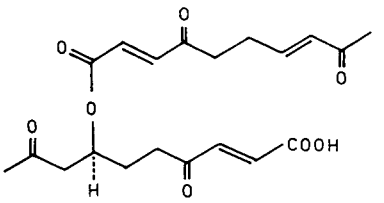

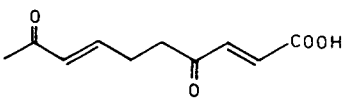

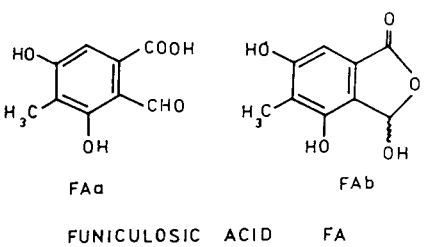

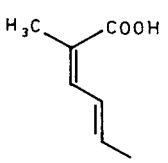

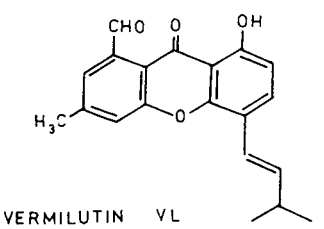

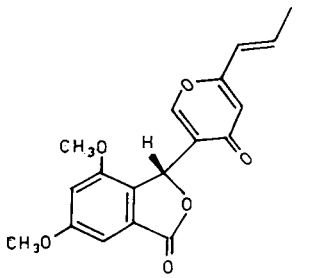

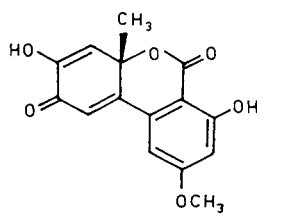

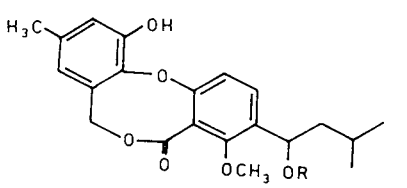

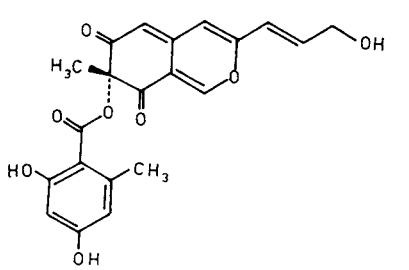

Fig. 1. Metabolites of *Penicillium vermiculatum* DANG.

Table 1
TLC data for *P. vermiculatum* metabolites

Compound	R_F in system[a]			Detection[b]					
	S_1	S_2	S_3	D_1	D_2	D_3	D_4	D_5	D_6
Vermilutin	0.99	0.97	0.99	+	+	G	Y	–	R
Dehydroaltenusin	0.94	0.46	0.73	+	+	R	O	B	B
Vermixocin B	0.94	0.48	0.78	+	–	G	–	–	–
Vermistatin	0.91	0.33	0.56	+	+	–	–	–	Y
Vermilutin	0.88	0.26	0.36	+	–	B	–	–	B
Vermiculinic acid	0.80	0.15	0.27	+	–	B	–	–	B
Methylsorbic acid	0.79	0.60	0.71	+	+	V	–	–	B
Vermixocin A	0.68	0.23	0.37	+	–	G	–	–	–
Vermiculic acid	0.63	0.09	0.20	+	–	B	–	–	B
Funiculosic acid	0.44	0.13	0.17	+	+	–	V	–	Y
Mitorubrinol	0.41	0.08	0.10	+	+	B	Y	R	R

[a] S_1 = chloroform–methanol (9:1); S_2 = benzene–methanol (9:1); S_3 = chloroform–2-propanol (19:1).
[b] D_1 = 254 nm; D_2 = 365 nm; D_3 = vanillin–sulphuric acid; D_4 = iron(III) chloride; D_5 = ethanolic ammonia; D_6 = ethanolic potassium hydroxide. Colours: B = brown; G = green; O = orange; R = red; V = violet; Y = yellow.

min. The red colour of mitorubrinol with ammonia is a specific reaction of azaphilones [16]. A remarkable observation was the green colour of biogenetically related vermixocins and the xanthone vermilutin with vanillin reagent. Vermilutin, dehydroaltenusin, funiculosic acid and mitorubrinol gave also characteristic coloured

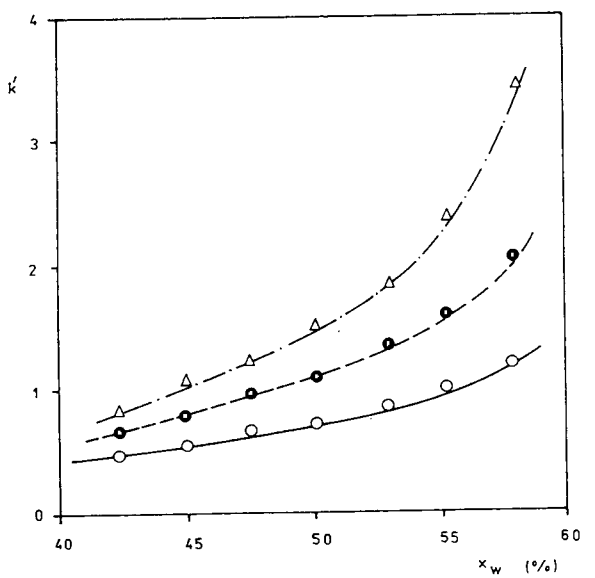

Fig. 2. Plot of capacity factor (k') and volume percentage of water in the mobile phase (x_w). ○ = Vermiculic acid; ◘ = vermiculin; △ = vermiculinic acid. Column, 150 × 3 mm I.D., Separon SGX C_{18} (7 μm); mobile phase, methanol–water (pH 3); flow-rate, 0.4 ml/min.

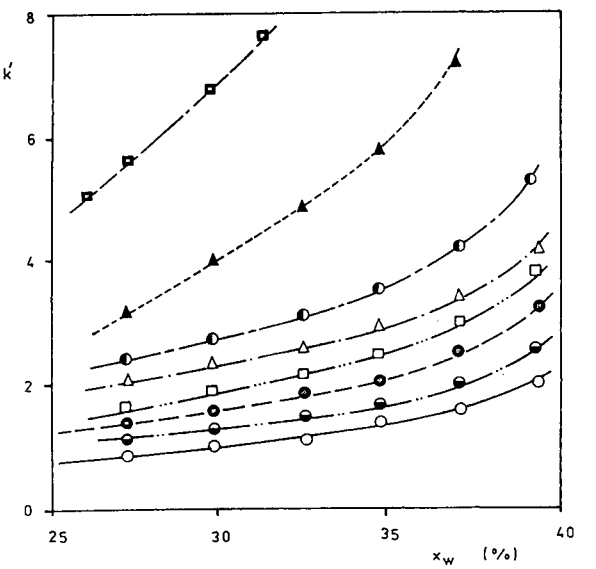

Fig. 3. Plot of capacity factor (k') and volume percentage of water in the mobile phase, x_w. ○ = Dehydroaltenusin; ◒ = funiculosic acid; ◘ = vermilutin; □ = mitorubrinol; △ = methylsorbic acid; ◐ = vermistatin; ▲ = vermixocin A; ■ = vermixocin B. Column, 150 × 3 mm I.D., Separon SGX C_{18} (7 μm); mobile phase, methanol–water (pH 3); flow-rate, 0.4 ml/min.

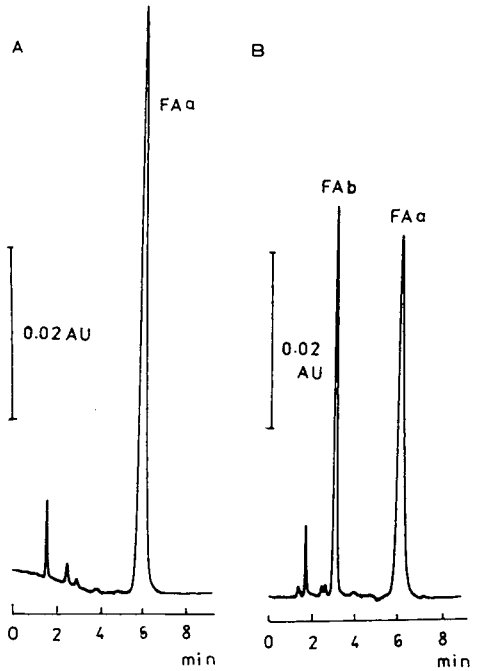

Fig. 4. Chromatograms of funiculosic acid: (A) fresh solution; (B) solution refluxed for 1 h at pH 2. FAa = phthaladehydic form; FAb = phthalidic form. Column, 150 × 3 mm I.D., Separon SGX C_{18} (7 μm); mobile phase, methanol–water (55:45) (pH 3); flow-rate, 0.5 ml/min; detection wavelength, 230 nm.

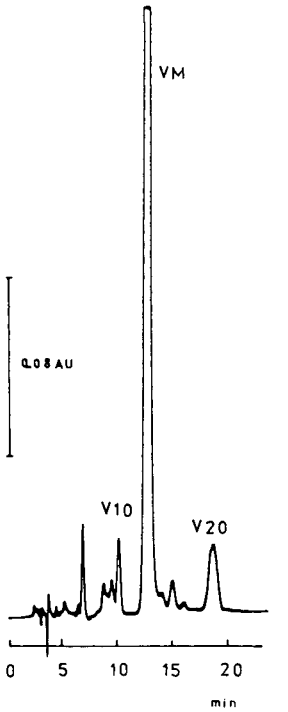

Fig. 5. Chromatogram of *P. vermiculatum* cultivation medium harvested in 144 h. V10 = vermiculic acid; VM = vermiculin; V20 = vermiculinic acid. Column, 150 × 3 mm I.D., Separon SGX C_{18} (7 μm); mobile phase, methanol–water (35:65) (pH 3); flow-rate, 0.4 ml/min; detection wavelength, 230 nm.

spots with iron(III) chloride solution (Table 1).

HPLC on an RP-18 column was used for the determination of the metabolites of *P. vermiculatum*. According to the capacity factors (Figs. 2 and 3), the compounds studied can be divided into three groups. The first group,

Table 2
UV bands of studied metabolites

Compound	M_r	λ (nm) [ε(m²/mol)][a]
Vermilutin	392.4	230 (616)
Mitorubrinol	398.4	216 (3455), 238 (1860), 267 (3456), 306 (1827), 346 (3056)
Vermistatin	328.3	220 (2240), 239 (646), 262 (1024)
Vermilutin	322.2	226 (3645), 248 (2830), 272 (4056), 350 (80), 398 (256)
Dehydroaltenusin	288.3	220 (1967), 241 (976), 252 (990), 276 (378), 298 (540)
Vermixocin A	372.4	220 (6891), 258 (53), 281 (144)
Vermixocin B	414.4	220 (6899), 257 (55), 283 (143)
Funiculosic acid	196.2	233 (1547), 267 (336), 297 (1168)
Methylsorbic acid	126.2	259 (594)
Vermiculinic acid	392.4	230 (720)
Vermiculic acid	196.2	230 (920)

[a] ε = Molar absorptivity (values in parentheses).

characterized by the highest retention, consists of the dioxocine derivatives vermixocin A and B. Vermistatin, vermilutin, methylsorbic acid, mitorubrinol, funiculosic acid and dehydroaltenusin belong to the second group. These compounds can also be discriminated by varying the pH of the mobile phase owing to the acidic character of two metabolites. Funiculosic acid occurs in phthalaldehydic (FAa) and hydroxyphthalidic (FAb) forms (Fig. 4), as was confirmed also by ^{1}H NMR spectrometry [3]. Equilibrium between the two forms occurs after a long period in solution at neutral pH, but after only 1 h in acidic solution under reflux.

The third group is constituted by vermiculin, vermiculic acid and vermiculinic acid. Surprisingly, vermiculin, which has no polar functions in its structure, is little retained by the C_{18} phase. A chromatogram of the cultivation medium of *P. vermiculatum* optimized for vermiculin production is shown in Fig. 5 and that optimized for vermistatin biosynthesis in Fig. 6. All these compounds rarely occurred in one cultivation;

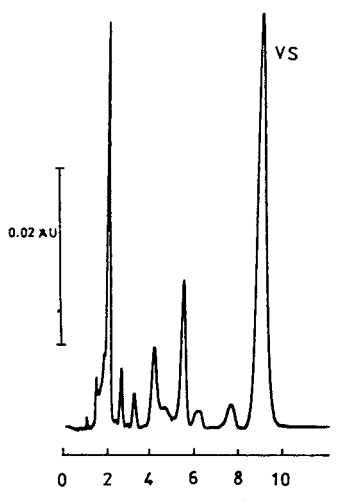

Fig. 6. Chromatogram of extract of cultivation medium optimized for vermistatin production. VS = vermistatin. Column, 150 × 3 mm I.D., Separon SGX C_{18} (7 μm); mobile phase methanol–water (60:40) (pH 3); flow-rate, 0.5 ml/min; detection wavelength, 230 nm.

vermiculin, vermiculinic acid and vermiculin acid, vermilutin, vermixocins, methylsorbic acid funiculosic acid and mitorubrinol are metabolites of *P. vermiculatum* cultivated on a sucrose medium, vermistatin is produced on glucose, only vermixocin A is biosynthesized on a medium containing whey and dehydroaltenusin is a metabolite of a *P. vermiculatum* mutant grown on sucrose. This last compound exhibited the greatest tailing, comparable to that of some flavonoids.

These diverse structures have different UV spectra (Table 2), which can be used for their identification and selective detection in complex mixtures.

4. References

[1] J. Fuska, I. Kuhr and P. Nemec, *J. Antibiot.*, 25 (1972) 208.
[2] J. Fuska, D. Uhrín, B. Proksa, Z. Votický and J. Ruppeldt, *J. Antibiot.*, 39 (1986) 1605.
[3] B. Proksa, D. Uhrín, J. Fuska and E. Michálková, *Collect. Czech. Chem. Commun.*, 57 (1992) 408.
[4] B. Proksa, D. Uhrín, J. Adamcová and J. Fuska, *Phytochemistry*, 31 (1992) 1442.
[5] J. Fuska, B. Proksa, D. Uhrín, L. Marvanová and M. Šturdíková, *Acta Biotechnol.*, 11 (1991) 73.
[6] B. Proksa, D. Uhrín, J. Adamcová and J. Fuska, *J. Antibiot.*, 45 (1992) 1268.
[7] B. Proksa, J. Adamcová and J. Fuska, *Appl. Microbiol. Biotechnol.*, 37 (1992) 443.
[8] B. Proksa and J. Fuska, *Pharmazie*, 47 (1992) 920.
[9] M. Takeuchi, M. Nakajima, T. Ogita, M. Inukai, K. Kodama, K. Furuya, H. Nagaki and T. Haneishi *J. Antibiot.*, 42 (1989) 198.
[10] W.A. Ayer and J.S. Racok, *Can. J. Chem.*, 68 (1990) 2085.
[11] W.A. Ayer and J.S. Racok, *Can. J. Chem.*, 68 (1990) 2095.
[12] O. Filtenborg, J.C. Frisvad and J.A. Svendsen, *Appl. Environ. Microbiol.*, 45 (1983) 581.
[13] J.C. Frisvad and U. Thrane, *J. Chromatogr.*, 404 (1987) 195.
[14] J. Fuska and B. Proksa, *Pharmazie*, 38 (1983) 634.
[15] J.C. Frisvad, O. Filtenborg, R.S. Samson and A.C. Stolk, *Antonie van Leeuwenhoek J. Microbiol. Serol.*, 57 (1990) 179.
[16] W.B. Whalley, *Pure Appl. Chem.*, 7 (1963) 565.

ELSEVIER

Journal of Chromatography A, 665 (1994) 191–195

JOURNAL OF CHROMATOGRAPHY A

Lipid analysis of baker's yeast

Ján Šajbidor*[a], Milan Čertík[b], Jozef Grego[a]

[a]Department of Biochemical Technology, Chemical Faculty, Slovak Technical University, Radlinského 9, 812 37 Bratislava, Slovak Republic

[b]Research Institute of Gerontology, Zámocká ul., P.O. Box 25, 901 01 Malacky, Slovak Republic

Abstract

Commercial baker's yeast was analysed for lipids by TLC and GC. The TLC system of a silica gel plate with *n*-hexane–diethyl ether–acetate acid (70:30:1, v/v/v) allowed the total lipids to be divided into sterol esters (ES), free fatty acids (FFA), triacylglycerols (TAG), diacylglycerols (DAG), free sterols (FS), monoacylglycerols (MAG) and phospholipids (PL). Phospholipids were separated by two-step chromatography with the systems SiO_2 with acetone and SiO_2 with chloroform–methanol–acetic acid–water (25:15:4:2, v/v). The following phospholipids were detected: phosphatidylethanolamine (PE), phosphatidylserine (PS), phosphatidylinositol (PI), phosphatidylcholine (PC) and lysophospholipids (LPL). The fatty acid composition of TAG, ES, FFA, DAG, MAG, PC, PE, PS and PI was investigated by using packed column (15% DEGJ + 3% H_3PO_4) and capillary column (SP 2340) GC, Twenty-two individual fatty acids with carbon chain lengths in the range 12–24 were detected by capillary GC. The presence of squalene, zymosterol, ergosterol and lanosterol in non-saponifiable lipid was proved and the compounds were determined by GC (SE-30).

1. Introduction

There are many reports dealing with analyses of microbial lipids [1,2]. The main interest is focused on lipid classes [3], fatty acids [4] or sterol profile analysis [5]. It is clear that analytical data are necessary for further studies of the physiology [6], taxonomy [7] and biotechnology [8] of yeasts.

A variety of solvent systems have been used to separate simple lipids by TLC on silica gel in one dimension. Those used most frequently contain hexane (or heptane or light petroleum) diethyl ether and acetic (or formic) acid in various proportions. For example, Korte and Casey [9] divided neutral lipids into monoacylglycerols, diacylglycerols, free fatty acids, triacylglycerols and cholesteryl esters using TLC with *n*-heptane–diethyl ether–acetic acid (75:25:4, v/v/v). Bergheim *et al.* [10] recommended the preparative separation of neutral lipids and phospholipids by centrifugally accelerated TLC. This method has not been applied to the preparation of phospholipids, although it is commonly used for other natural products. Non-acidic microbial phospholipids are usefully separated on silica gel plates developed with chloroform–methanol–water (25:10.1, v/v/v), although the solvent system may also contain small amounts of other polar compounds. A mixture of phospholipids was excellently separated using SiO_2 with chloroform–ethanol–water–triethylamine (30:34:8:35, v/v) [9].

Lipids in microorganisms contain a variety of fatty acids differing in chain length, degree of unsaturation, position and configuration of dou-

* Corresponding author.

0021-9673/94/$07.00
SSDI 0021-9673(93)E1217-N

ble bounds and the presence of special functional groups. Augustyn and Kock [11] used capillary columns with different stationary phases spanning a range of polarity for the GC analysis of fatty acids from *Saccharomyces cerevisiae*. Fatty acids were identified by interpretation of picolinyl ester mass spectra without suitable reference standards. Ten fatty acids in the range C_{14}–C_{18} including saturated and monounsaturated acids with precise double-bond localization were found. The fatty acid composition of twenty *Saccharomyces cerevisiae* strains (laboratory and industrial) was investigated by Bendová *et al.* [12]. Methyl esters of fatty acids with carbon chain lengths of 10–28 were separated on SPB-1 by capillary GC.

It is known that the non-saponifiable part of the lipid of *Saccharomyces cerevisiae* contains ergosterol and its biochemical precursors. GC–MS has been used for the identification of $\Delta^{5,7}$-sterols in sterol mixtures [13]. Other methods of sterol analysis by GC were summarized by Itoh *et al.* [14] and Patterson [15].

The aim of this present work was to analyse neutral lipids (by TLC), to identify and determine fatty acids in selected lipid structures (by GC) and to analyse the non-saponifiable lipid isolated from commercial baker's yeast (*Saccharomyces cerevisiae*).

2. Experimental

Commercial baker's yeast (Slovlik Trenčín, Slovak Republic) was extracted by the method of Bligh and Dyer [16].

2.1. TLC of lipids

Precoated silica gel plates (Merck, Darmstadt, Germany) (20 × 20 cm, 0.5-mm layer) were used. A 5-mg amount of the sample [5% lipid solution in chloroform–methanol (1:1)] was applied with a Hamilton syringe as a line of spots 1.5 cm from the lower edge of the silica gel layer. For TLC of neutral lipids a solvent system consisting of *n*-hexane–diethyl ether–acetic acid (70:30:1, v/v/v) was used. Phospholipids were separated by two-step TLC. The plates were first developed in a chamber at ambient temperature with acetone to a height of 18 cm above the origin. After drying, the plates were developed to 17 cm above the origin with chloroform–methanol–acetic acid–water 25:15:4:2 (v/v). The spots were revealed by exposure to iodine vapour.

2.2. GC of fatty acid methyl esters

Lipids containing fatty acids were scraped off from five dry plates (iodine vapour and water traces were removed under reduced pressure), extracted with chloroform–methanol (1:1) and subjected base-catalysed transesterification (sodium methanolate) and acid-catalysed esterification and transesterification (methanolic HCl). Fatty acid methyl esters (FAMEs) were determined by packed or capillary column GC under the conditions outlined below.

Packed column GC

A Chrom 5 chromatograph (Laboratorní přístroje, Prague, Czech Republic) equipped with a flame ionization detector was used; column, 15% DEGJ + 3% H_3PO_4 on Chromaton N AW DMCS (0.125–0.150 mm) (1.8 m × 2 mm I.D) (Lachema, Brno, Czech Republic); column temperature, 180°C; injection port and detection space temperatures, 220°C; carrier gas, nitrogen at 30 ml/min; sample, 1 μl of hexane solution (10 mg FAMEs per ml hexane); integrator, Apex 2.5 (Apex Data, Prague, Czech Republic). The identification of the GC FAME peaks was performed using FAME standards (Supelco, Bellefonte, PA, USA).

Capillary column GC

A Carlo Erba Model 2400 T gas chromatograph equipped with a flame ionization detector was used; column, 78 m × 0.3 mm I.D. glass capillary coated with cyanopropylsiloxane SP 2340 (Supelco); the initial column temperature was 150°C, which was maintained for 3 min, then programmed to 220°C at 3°C/min, the maximum temperature being maintained for a further 9 min before cooling; injection and detection tem-

peratures, 235°C; carrier gas, hydrogen at a linear velocity of 30 cm/s; splitting ratio, 50:1; sample size, 1 μl (solutions in hexane). Peaks were identified by means of known standards (Supelco) and determined with an SP 4000 integrator (Spectra-Physics).

2.3. Saponification of microbial lipids

A 100-mg amount of the lipid from whole cells was hydrolysed with 2 ml of 1 *M* KOH (in 95% ethanol) for 1 h. After cooling, 5 ml water were added and the solution was extracted completely with *n*-hexane (3 × 5 ml). The extract was dried with anhydrous sodium sulphate and the non-saponifiable materials were recovered on removal of the solvent in a rotary evaporator.

2.4. GC of non-saponifiable components

The sample of non-saponifiable lipid was dissolved in 2-propanol (concentration *ca.* 15 mg/ml) and analysed by GC under the following conditions: Chrom 5 chromatograph (Laboratorní přístroje) equipped with a flame ionization detector; column, 10% SE-30 on Chromaton N AW DMCS (0.125–0.150 mm) (1.8 m × 2 mm I.D) (Lachema); column temperature, 260°C; injection port and detection temperatures, 320°C; carrier gas, nitrogen at 30 ml/min; sample, 1 μl of 2-propanol solution: integrator, Apex 2.5 (Apex Data). The identification of the sterol peaks was performed using standards (Sigma, St. Louis, MO, USA).

3. Results and discussion

The total lipid content of *Saccharomyces cerevisiae* has been discussed in many reports [6,17,18]. The wide variation in this content (in the range 3.5–14.7% of lipids, dry mass) depends on various influences including especially growth stage, nutritional aspects and cultivation conditions.

A relatively low content of intracellular lipid in the whole cells of baker's yeast was found (5.3%). The lipid extract from whole cells was separated by TLC using SiO_2 with *n*-hexane–diethyl ether–acetic acid (70:30:1, v/v/v.). Separation in this solvent is carried out according to the polarity of the lipids with the least polar compound migrating furthest. Thus, sterol esters (ES) were near the solvent front (R_F 0.96) followed by triacylglycerol (TAG) (R_F 0.76), free fatty acids (FFA) (R_F 0.65–0.5), free sterols (FS) (R_F 0.25), monoacylglycerols (MAG) (R_F 0.08) and phospholipids (PL) (R_F 0).

Two-step chromatography for polar lipids isolated from whole cells made it possible to separate commonly occurring phospholipid structures such as phosphatidylethanolamine (PE) (R_F 0.51), phosphatidylserine (PS) (R_F 0.43), phosphatidylinositol (PI) (R_F 0.36), phosphatidylcholine (PC) (R_F 0.24) and lysophospholipids (LPL) (R_F 0). Less polar lipids were crowded together at the acetone solvent front.

Myristic (14:0), myristoleic (14:1), palmitic (16:0), palmitoleic (16:1), stearic (18:0), oleic acid (18:1) and linoleic acid (18:2) were detected in the samples analysed by packed column GC.

Table 1
Fatty acid composition of sterol esters (ES), triacylglycerols (TAG), free fatty acids (FFA), diacylglycerols (DAG) and monoacylglycerols (MAG) isolated from baker's yeast

Lipid structure	Fatty acid (%)						
	14:0	14:1	16:0	16:1	18:0	18:1	18:2
ES	0.4	0.6	10.9	34.2	0.8	50.8	2.1
TAG	0.1	0.3	11.4	39.1	2.2	45.0	1.7
FFA	2.1	1.2	21.4	33.6	7.2	33.2	0.6
DAG	0.2	0.2	8.4	31.5	6.8	48.8	3.8
MAG	Trace	0.2	9.9	35.6	7.7	43.1	3.1

Table 2
Fatty acid composition of neutral lipids (NL), phosphatidylethanolamine (PE), phosphatidylserine (PS), phosphatidylinositol (PI) and phosphatidylcholine (PC) isolated from baker's yeast

Lipid structure	Fatty acid (%)						
	14:0	14:1	16:0	16:1	18:0	18:1	18:2
NL	1.1	0.8	13.4	36.1	5.2	41.2	1.8
PE	0.8	0.4	8.9	42.8	1.4	42.1	1.4
PS + PI	0.3	0.7	18.7	35.6	6.8	34.8	1.7
PC	Trace	0.2	16.5	39.1	6.6	32.2	3.9

Although all lipid structures contained identical compounds, the relative amounts of the individual acids varied (Tables 1 and 2). It is interesting that acylglycerols were relatively rich in monoenes (palmitoleic and oleic acid) whereas the fraction of free fatty acids contained mainly saturated fatty acids (palmitic and stearic). Nurminen *et al.* [19] reported a high content of short-chain fatty acids in TAG of *S. cerevisiae* and a similar profile of fatty acids in FFA and TAG. On the other hand, Ng and Laneelle [20] discussed the differences between the content of monoenes in neutral lipids and FFA. Our results showed that the phospholipids contained a higher concentration of 16:1 and a low concentration of 16:0 in comparison with neutral lipids. This observation is in agreement with a previously published report [5].

Table 3 shows the fatty acid composition of yeast lipid analysed by capillary GC. Particularly the analysis of the fatty acid composition on the polar SP 2340 stationary phase allowed us to detect 22 individual fatty acids including their positional and geometrical isomers. It is interesting that in addition to the usual types of acids, the odd-carbon-numbered fatty acids and *trans* isomers of monoenes were found. The presence

Table 3
Fatty acid composition of baker's yeast analysed by capillary GC on an SP 2340 column

Peak No.	Fatty acid	Concentration (%)
1	12:0	0.6
2	14:0	0.1
3	14:1 ω5 *cis*	0.8
4	15:0 *anteiso*	Trace
5	15:0	0.1
6	16:0	10.5
7	16:1 ω7 *trans*	0.1
8	16:1 ω7 *cis*	32.9
9	17:0	0.5
10	17:1 ω8 *cis*	0.2
11	18:0	7.1
12	18:1 ω9 trans	0.1
13	18:1 ω9 *cis*	43.9
14	18:1 ω7 *cis*	Trace
15	19:0	0.1
16	18:2 ω6 *cis*, *cis*	1.1
17	20:0	Trace
18	18:3 ω3 all-*cis*	0.8
19	20:1 ω9 *cis*	Trace
20	21:0	Trace
21	22:0	Trace
22	24:0	0.1

Table 4
Analysis of non-saponifiable lipids of baker's yeast

Peak No.	Retention time (min)	Content (%)	Structure
2	3.9	0.1	Unidentified
3	4.4	1.0	Unidentified
4	6.3	15.1	Squalene
5	8.1	0.2	Unidentified
6	10.5	0.3	Unidentified
7	13.8	0.2	Zymosterol
8	17.3	78.9	Egosterol
9	18.6	0.2	Unidentified
10	21.9	3.7	Lanosterol

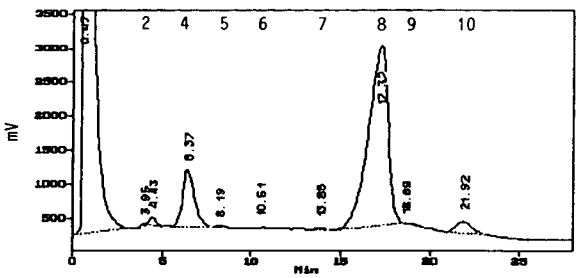

Fig. 1. GC of non-saponifiable lipid from baker's yeasts on an SE-30 packed column. See Table 4 for identification of peaks.

of vaccenic acid in baker's yeast confirmed an earlier observation [21], although its concentration in our sample was extremely low.

Free sterols and steryl esters especially are highly variable components of the yeast cell. Squalene, zymosterol, ergosterol and lanosterol were identified and quantified among nine divided structures from the non-saponifiable lipids of baker's yeast (Table 4, Fig. 1). Considering the earlier reports [6,22], zymosterol is frequently a major component of the steryl ester, but is generally absent in the free sterol component. On the other hand, ergosterol predominates as the free sterol.

4. References

[1] K. Hunter and A.H. Rose, in A.H. Rose and J.S. Harrison (Editors), *The Yeasts*, Academic Press, London, 1971, pp. 211–270.

[2] J.B.M. Rattray, A. Schibeci and D.K. Kidby, *Bacteriol. Rev.*, 39 (1975) 197.

[3] F. Paltauf and J.M. Johnston, *Biochim. Biophys. Acta*, 218 (1970) 424.

[4] L. Kováč, I. Gbelská, M. Poliachová, J. Šubík and V. Kováč, *Eur. J. Biochem.*, 11 (1980) 491.

[5] J.A. Hossack, D.M. Belk and A.H. Rose, *Arch. Microbiol.*, 114 (1977) 137.

[6] J.B.M. Rattray, in C. Ratledge and S.G. Wilkinson (Editors), *Microbial Lipids*, Vol. 1, Academic Press, London, 1988, pp. 555–697.

[7] O.P. Augustyn and J.L.F. Kock, *J. Microbiol. Methods*, 10 (1989) 9.

[8] J. Šajbidor, F. Malík, and H. Kissantalová, *Food Biotechnol.*, 6 (1992) 187.

[9] K. Korte and L.M. Casey, *J. Chromatogr.*, 232 (1982) 47.

[10] S. Bergheim, K.E. Malterud and T. Anthonsen, *J. Lipid Res.*, 32 (1991) 877.

[11] O.P.H. Augustyn, and J.F. Kock, *J. Microbiol. Methods*, 10 (1989) 9.

[12] O. Bendová, V. Richter, B. Janderová and J. Häusler, *Appl. Microbiol. Biotechnol.*, 35 (1991) 810.

[13] S. Popov, I. Stoilov and P. Demirev, *Biomed. Mass. Spectrom.* 11 (1984) 608.

[14] T. Itoh, H. Tani, K. Fukushima, T. Tamura and T. Matsumoto, *J. Chromatogr.*, 234 (1982) 65.

[15] G.W. Patterson, *Anal. Chem.*, 43 (1971) 1165.

[16] E.G. Bligh and W.J. Dyer, *Can. J. Biochem. Physiol.*, 37 (1959) 911.

[17] J. Ahvenainen, *J. Inst. Brew.*, 88 (1982) 367.

[18] A.M. Ramsay and L.J. Douglas, *J. Gen. Microbiol.*, 110 (1979) 185.

[19] T. Nurminen, K. Konttinen and H. Suomalainen, *Chem. Phys. Lipids*, 14 (1975) 15.

[20] K.H. Ng and M.A. Laneelle, *Biochimie*, 59 (1977) 97.

[21] H. Suomalainen and A.J.A. Keränen, *Chem. Phys. Lipids*, 2 (1968) 296.

[22] D.E. Quai and J.M. Haslam, *J. Gen. Microbiol.*, 11 (1979) 343.

ELSEVIER

Journal of Chromatography A, 665 (1994) 197–202

JOURNAL OF CHROMATOGRAPHY A

Effect of the number of sulpho groups on the electrophoretic mobility of sulphonated azo dyes

Jiří Gasparič*, Antonie Sedmíková

Department of Biophysics and Physical Chemistry, Faculty of Pharmacy, Charles University, Heyrovského 1203, 501 65 Hradec Králové, Czech Republic

Abstract

Paper electrophoretic mobilities of azo dyes containing one to six sulpho groups were studied in alkaline (0.1 *M* NaOH) and acidic (30% acetic acid) media. The most significant contribution to the mobility is caused by the presence of the second and third sulpho groups in the original structure. The influence of the fifth and sixth sulpho groups is nearly negligible. The fact that isomers containing the same number of sulpho groups are separated indicates that further factors must be involved. The influence of the presence of the carboxy group and other structural factors was also studied.

1. Introduction

Most reports on the paper electrophoresis of water-soluble azo dyes (for reviews see refs. 1 and 2) have been concerned with practical separations of food colours and did not consider the chemical structures of the dyes. This paper deals with azo dyes, the solubility of which in water is caused by the presence of one or more sulpho groups in their molecules. Dyes with such structures are either acid dyes, used for dyeing of wool, foodstuffs or pharmaceuticals, or direct dyes, used for cotton dyeing or as acid–base indicators.

Four basic structures (A–D, see Tables 1–4) were systematically substituted by one to six sulpho groups or modified in other desired ways in order to find factors that might influence their electrophoretic mobilities.

2. Experimental

2.1. Chemicals

The dyestuffs used within this work were either commercial products with known structures or model compounds prepared by known methods [3]. Their purity was examined by thin-layer chromatography on Silufol sheets, mostly using the mobile phase 1-propanol–ammonia (2:1) [4]. All other chemicals were of analytical-reagent grade.

* Corresponding author.

0021-9673/94/$07.00
SSDI 0021-9673(94)00032-5

2.2. Apparatus

High-voltage electrophoresis was carried out using a Camag HVE instrument and Whatman No. 2 paper (18 × 40 cm), which was connected with the electrodes by double paper bridges (6.5 × 18.5 cm). The operating voltage was 2500 V. Some preliminary experiments were performed using low-voltage electrophoresis. A laboratory made device of the free hanging paper strip in a moist chamber type was used. The distance of the electrodes was 30 cm, the voltage was 300 V and the field strength was 10 V cm^{-1}. Whatman No. 2 paper of 11.5 cm width was used and the operating time was 6 h.

3. Results and discussion

Azo dyes of four structural types (A–D, see Tables 1–4) were used to study some of the structural effects that could influence their electrophoretic mobilities. Our attention was directed to the influence of the number of sulpho groups, the contributions of the carboxy group, the hydroxy group and the electrophoretically inactive substituents and the effect of dimerizing the molecule.

All electrolytes mentioned in previous papers [1,2] were tested in preliminary experiments. Aqueous 0.1 *M* solutions of sodium or potassium hydroxide were found to be the most suitable. The mobilities of the dyes at lower concentrations of the electrolytes, *e.g.*, 0.05 *M* NaOH, were higher and the separations were excellent, but both the mobilities and the form of the spots were strongly affected by the amount of the dyes spotted. The addition of alcohols or glycols did not bring about any improvements. Good separations with well defined spots were also achieved using an organic buffer solution of pH 5.9 according to Savvin and co-workers [5–7] or simply 30% acetic acid. Therefore, 0.1 *M* sodium hydroxide solution was chosen for further work and the two acid electrolytes were used in some complementary experiments.

3.1. Effect of the sulpho group

It has been stated by previous workers [1,8] that the electrophoretic mobility of sulphonated azo dyes is caused by the presence of the sulpho group and is increased with increase in the number of these groups. In fact, the dyes of the basic skeleton but without any sulpho group do not migrate at all (dye I) provided there were no other dissociable groups present. It can be seen from Table 1 and Fig. 1 that the mobility of the dyes increases with increasing number of sulpho groups. A nearly linear increase in mobility is caused by the introduction of the first, second, third and fourth sulpho groups; the fifth and sixth sulpho groups, however, do not bring about any remarkable change in mobility. The highest contribution to the mobility is caused by the second and/or third sulpho groups (see Fig. 2). Similar results can be seen in Fig. 3, where the mobilities are plotted against M/z, where M is the molecular mass of the anion and z the charge. Probably the anions of the dyes may be solvated in aqueous media to different extents and hence calculations based on the number of sulpho groups or molecular masses may not be exactly correct. The fact that isomeric dyes show some differences in mobilities indicates that the contribution of the sulpho group in different positions is not equivalent and that factors other than their number must be involved. It has been shown with anthraquinone dyes [9] that some isomers are separated by electrophoresis that could not have been distinguished by planar chromatography under common conditions.

Analogous results were obtained with type B and C dyes (Tables 2 and 3). The separation in acidic media is also determined by the number of sulpho groups. This means that the sulpho group is completely dissociated under these conditions (pH 1.5 and 5.9).

3.2. Effect of the carboxy group

The carboxy group is also dissociated in alkaline media (0.1 *M* NaOH) and its contribution to the mobility of the dyes is only slightly lower

Table 1
Electrophoretic mobilities of type A azo dyes

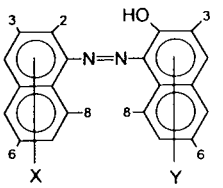

No.	X	Y	M^a	M/z^a	$u \times 10^9$ ($m^2\ V^{-1}\ s^{-1}$)
I	H	H	298.3		0
II	2-SO_3H	–	377.4	377.4	2.31
III	4-SO_3H	–	377.4	377.4	1.42
IV	–	6′-SO_3H	377.4	377.4	1.60
V	4-SO_3H	6′-SO_3H	456.4	228.2	5.51
VI	3,6-$(SO_3H)_2$	–	456.4	228.2	4.09
VII	–	3′,6′-$(SO_3H)_2$	456.4	228.2	3.91
VIII	4-SO_3H	3′,6′-$(SO_3H)_2$	535.5	178.5	7.64
IX	3,6-$(SO_3H)_2$	6′-SO_3H	535.5	178.5	7.28
X	3,6,8-$(SO_3H)_3$	–	535.5	178.5	8.53
XI	–	3′,6′,8′-$(SO_3H)_3$	535.5	178.5	8.36
XII	3,6-$(SO_3H)_2$	3′,6′-$(SO_3H)_2$	614.5	153.6	9.78
XIII	3,6,8-$(SO_3H)_3$	6′-SO_3H	614.5	153.6	11.02
XIV	3,6-$(SO_3H)_2$	3′,6′,8′-$(SO_3H)_3$	692.6	138.5	11.56
XV	3,6,8-$(SO_3H)_3$	3′,6′-$(SO_3H)_2$	692.6	138.5	10.49
XVI	3,6,8-$(SO_3H)_3$	3′,6′,8′-$(SO_3H)_3$	772.6	128.8	11.20

Whatman No. 2 paper, 0.1 *M* NaOH, 2500 V, 62.5 V cm^{-1}, 15 min.
[a] *M* = molecular mass of the dye anion; *z* = charge number.

than that of the sulpho group. Thus, *e.g.*, the mobilities of the corresponding sulpho derivatives are slightly higher than those of the carboxy derivatives: **XXVII** > **XXXIV**; **XXXI** > **XXXV**; **XXXIII** > **XXXVIII**. In acidic media (30% acetic acid) the carboxy group is hardly dissociated and therefore the mobilities of the carboxy deriva-

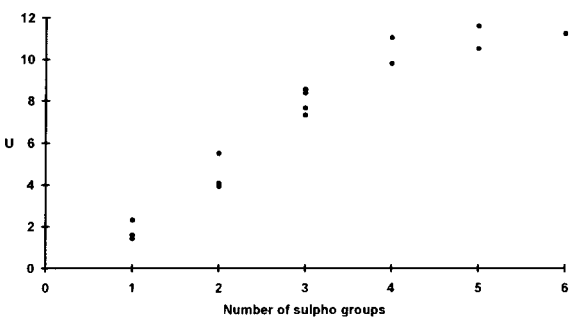

Fig. 1. Dependence of the electrophoretic mobilities ($u \times 10^9$, $m^2\ V^{-1}\ s^{-1}$) of azo dyes on the number of sulpho groups (data from Table 1).

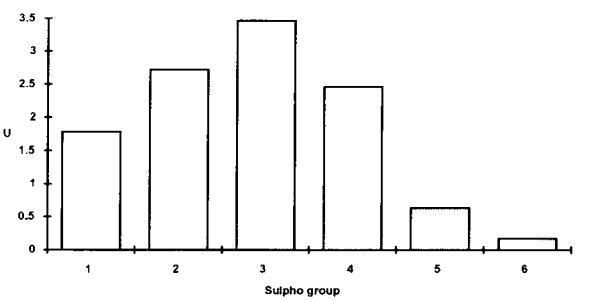

Fig. 2. Schematic presentation of the contributions of the first to sixth sulpho groups to the electrophoretic mobilities of azo dyes ($\Delta u \times 10^9$, $m^2\ V^{-1}\ s^{-1}$; data from Table 1).

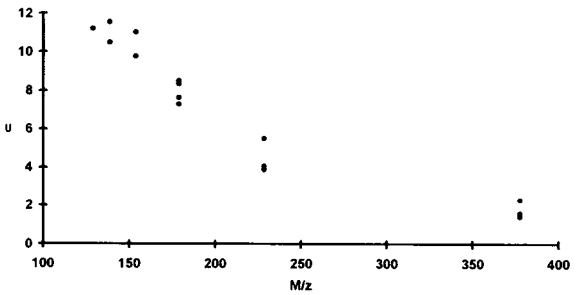

Fig. 3. Dependence on the electrophoretic mobilities ($u \times 10^9$, $m^2\ V^{-1}\ s^{-1}$) of type A azo dyes on the ratio M/z (M = molecular mass, z-charge; data from Table 1).

tives are strongly decreased in comparison with the corresponding sulpho derivatives: the dyes containing a carboxy group have lost the charge and the carboxy group contributes negatively to the mobility by the increase in molecular mass of the dye and as an electrophoretically inactive substituent. Thus, comparison of the electrophoretic migration in alkaline and acidic media could permit the detection of the presence of a carboxy group in the molecule of a dye of unknown structure similarly as reported for acidic anthraquinone dyes [9].

3.3. Effect of the hydroxy group

The hydroxy group contributes to the migration of the azo dyes only when it is dissociated under the experimental conditions used. This is the case with the pyrazolone dyes **XVII** and **XXVI**.

3.4. Effect of electrophoretically inactive substituents

Electrophoretically inactive substituents (compounds **XXXIX–XLIV**) increase the molecular mass of the dye, the charge remaining the same. In Fig. 4 the migration rate of such dyes is plotted against their molecular mass and the dependence obtained applies to compounds containing substituents of the same type; *c.f.*, compound **XLIV**. This is in accordance with the observations of Iijima and Sekido [10].

Table 2
Electrophoretic mobilities of type B azo dyes

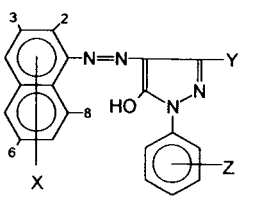

No.	X	Y	Z	M^a	M/z^a	$u \times 10^9$ ($m^2\ V^{-1}\ s^{-1}$)
XVII	H	CH_3	H	328.4	–	0
XVIII	H	CH_3	3′-SO_3H	407.4	407.4	0.35
XIX	4-SO_3H	CH_3	4′-SO_3H	486.5	243.2	2.84
XX	4-SO_3H	CH_3	3′-SO_3H	486.5	243.2	3.91
XXI	3,6-$(SO_3H)_2$	CH_3	3′-SO_3H	565.5	188.5	8.71
XXII	3,6,8-$(SO_3H)_3$	CH_3	3′-SO_3H	644.5	161.1	11.02
XXIII	–	COOH	4′-SO_3H	436.4	218.2	3.56
XXIV	3,6-$(SO_3H)_2$	COOH	4′-SO_3H	594.5	148.6	10.49
XXV	3,6,8-$(SO_3H)_3$	COOH	4′-SO_3H	673.6	134.7	11.02

Whatman No. 2 paper, 0.1 *M* NaOH, 2500 V, 62.5 V cm^{-1}, 15 min.
[a] M = molecular mass of the dye anion; z = charge number.

Table 3
Electrophoretic mobilities of type C azo dyes

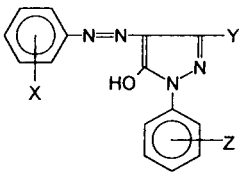

No.	X	Y	Z	M^a	M/z^a	$u \times 10^9$ ($m^2\ V^{-1}\ s^{-1}$)
XXVI	H	CH_3	H	278.3	–	1.78
XXVII	2-SO_3H	CH_3	H	357.4	357.4	4.98
XXVIII	3-SO_3H	CH_3	H	357.4	357.4	4.98
XXIX	4-SO_3H	CH_3	H	357.4	357.4	4.27
XXX	H	CH_3	3′-SO_3H	357.4	357.4	4.09
XXXI	4-SO_3H	CH_3	4′-SO_3H	436.4	218.2	9.60
XXXII	2,5-$(SO_3H)_2$	CH_3	H	436.4	218.2	8.89
XXXIII	2,5-$(SO_3H)_2$	CH_3	3′-SO_3H	515.5	171.8	11.20
XXXIV	2-COOH	CH_3	H	321.3		3.38
XXXV	2-COOH	CH_3	4′-SO_3H	400.4	200.2	7.47
XXXVI	2-COOH	CH_3	3′-SO_3H	400.4	200.2	7.64
XXXVII	H	COOH	4′-SO_3H	386.3	193.1	8.18
XXXVIII	2-SO_3H	COOH	2′-SO_3H	465.4	155.1	8.71
XXXIX	4-CH_3	CH_3	3′-SO_3H	371.4	371.4	3.20
XL	4-Cl	CH_3	3′-SO_3H	391.8	391.8	1.96
XLI	2,4-Cl_2	CH_3	3′-SO_3H	426.2	426.2	1.24
XLII	4-Br	CH_3	3′-SO_3H	436.2	436.2	1.16
XLIII	4-I	CH_3	3′-SO_3H	483.3	483.3	1.07
XLIV	4-C_6H_5	CH_3	3′-SO_3H	433.5	433.5	0.36

Whatman No. 2 paper, 0.1 *M* NaOH, 2500 V, 62.5 V cm^{-1}, 15 min.
[a] *M* = molecular mass of the dye anion; *z* = charge number.

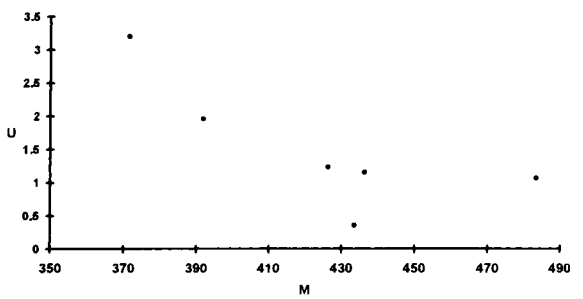

Fig. 4. Dependence of the electrophoretic mobilities ($u \times 10^9$, $m^2\ V^{-1}\ s^{-1}$) of type C azo dyes with electrophoretically inactive substituents on their molecular masses (data from Table 3).

The behaviour of dyes which have a dimeric molecule (**XLV–L**; see Table 4) is also very interesting. Dyes derived from benzidine (**XLV** and **XLVI**) do not migrate at all, which is due to the adsorption of their planar molecules on cellulose (substantivity). Analogous dyes derived from 4,4′-diaminodiphenylmethane (**L**) migrate without problems. The interruption of the conjugation of their double bonds by the methylene group makes these dyes no longer planar, as they can rotate freely round the C–CH_2–C bonds and are therefore no longer substantive. Dyes derived from benzidine-3,3′-disulphonic acid (**XLVII–XLIX**) migrate similarly to the corre-

Table 4
Electrophoretic mobilities of type D azo dyes

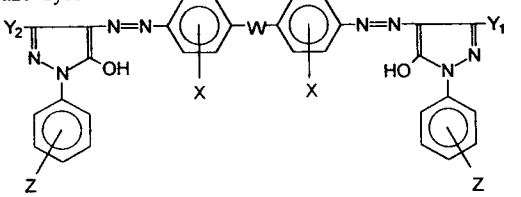

No.	X	W	$Y_1 = Y_2$	Z	M^a	$u \times 10^9$ ($m^2\ V^{-1}\ s^{-1}$)
XLV	–	–	CH_3	3′-SO_3H	712.7	0
XLVI	–	–	COOH	4′-SO_3H	770.7	0
XLVII	3-SO_3H	–	CH_3	–	712.7	3.02
XLVIII	3-SO_3H	–	CH_3	4′-SO_3H	870.9	3.56
XLIX	3-SO_3H	–	COOH	4′-SO_3H	928.8	8.89
L	–	CHC_6H_5	CH_3	4′-SO_3H	802.8	1.96

Whatman No. 2 paper, 0.1 *M* NaOH, 2500 V, 62.5 V cm^{-1}, 15 min.
[a] *M* = molecular mass of the dye anion.

sponding 4,4′-diaminodiphenylmethane derivatives (sulpho groups decrease the substantivity). Their mobilities are slightly lower than those of the half molecules with one sulpho group (*cf.*, Table 3).

4. References

[1] J. Šrámek, in K. Venkataraman (Editor), *The Analytical Chemistry of Synthetic Dyes*, Wiley, New York, 1977, p. 57.
[2] Z. Deyl, in Z. Deyl (Editor), *Electrophoresis. A Survey of Techniques and Applications, Part B: Applications*, Elsevier, Amsterdam, 1983, p. 419.
[3] H.E. Fierz-David and L. Blangey, *Grundlegende Operationen der Farbenchemie*, Springer, Wien, 5. Ausgabe, 1947.
[4] J. Gasparič and J. Churáček, *Laboratory Handbook of Paper and Thin-Layer Chromatography*, Ellis Horwood, Chichester, 1978, p. 307.
[5] S.B. Savvin, R.F. Propiscova, T.G. Akimova and V.P. Dedkova, *Zh. Anal. Khim.*, 24 (1969) 1231.
[6] S.B. Savvin, T.G. Akimova, E.P. Krysin and M.M. Davydova, *Zh. Anal. Khim.*, 25 (1970) 430.
[7] S.B. Savvin, Yu. G. Rozovskii, T.G. Akimova, L.A. Sokolovskaya and E.A. Lichonina, *Zh. Anal. Khim.*, 26 (1971) 164.
[8] V.F. Androsov, L.I. Zaktreger, E.N. Golovanov and K.I. Andreeva, *Izv. Vyssh. Uchebn. Zaved. Tekhnol. Tekst. Prom.*, (1969) 86; *C.A.*, 73 (1970) 16123k.
[9] J. Gasparič, *J. Chromatogr.* 54 (1971) 436.
[10] T. Iijima and M. Sekido, *J. Soc. Dyers Colour.*, 78 (1962) 619.

ELSEVIER

Journal of Chromatography A, 665 (1994) 203–209

JOURNAL OF CHROMATOGRAPHY A

Separation of alkali and alkaline earth metal and ammonium cations by capillary zone electrophoresis with indirect UV absorbance detection

E. Šimuničová, D. Kaniansky*, K. Lokšíková

Department of Analytical Chemistry, Faculty of Natural Sciences, Comenius University, Mlynská Dolina CH-2, 842 15 Bratislava, Slovak Republic

Abstract

Carrier electrolytes combining complexing effects of negatively charged counter ions and electroneutral 18-crown-6 were investigated in the separations of alkali and alkaline earth metal and ammonium cations by capillary zone electrophoresis with indirect UV absorption detection. The use of tartrate with 18-crown-6 at a 0.04 mol l^{-1} concentration permitted the complete resolution of these cations in one electrophoretic run. Benzimidazole served as a visualization co-ion for indirect detection at 254 nm. The separation of some alkali and alkaline earth metal and ammonium cations in rain, tap and mineral water samples illustrates the application potential of the proposed approach.

1. Introduction

Separation methods are widely used in the analysis of alkali and alkaline earth metal and ammonium cations in various types of samples. At present, ion chromatography has a dominant position among these methods. However, capillary electrophoretic techniques have been shown to be promising alternatives for the analysis of this group of cations and capillary isotachophoresis (ITP) [1–10] and capillary zone electrophoresis (CZE) [11–18] seem particularly useful.

The ionic mobilities of alkali and alkaline earth metal and ammonium cations in aqueous electrolyte solutions under non-complexing conditions are close [19–21]. Therefore, some of them (K^+, Rb^+, Cs^+ and NH_4^+, Ca^{2+} and Sr^{2+}, Mg^{2+} and Na^+) are difficult to separate when the ionic mobilities determine their effective mobilities. Although methanol provides favourable differences in the ionic mobilities of the cations of interest [6,7,21], mostly aqueous electrolyte systems introducing complex equilibria are preferred in their electrophoretic separations. Here, negatively charged ligands [1,2,4,8,10,11–13,17,18] or electroneutral crown ethers [3,9,15] have been proposed for separations in the cationic mode. In ITP, some of the alkaline earth metal cations were separated in the anionic mode by converting them into anionically migrating chelates [22].

Only ITP is known to provide a complete electrophoretic resolution of alkali and alkaline earth metal and ammonium cations in one run [10]. Here, the separation is assumed to be due to the formation of weak complexes of the cations with polyethylene glycol. Similar interactions are involved in the electrophoretic sepa-

* Corresponding author.

0021-9673/94/$07.00
SSDI 0021-9673(94)00041-7

rations of these cations when crown ethers are present in the electrolyte systems. However, the results obtained, *e.g.*, for 18-crown-6 in ITP [23], indicate that the differentiating power of this agent differs slightly from that of polyethylene glycol and the formation of mixed zones for some of the cations can be expected. For example, from these data it is predictable that at a concentration of 18-crown-6 in the carrier electrolyte as used by Baechmann *et al.* [15] a complete resolution of Cs^+, K^+, Rb^+ and NH_4^+ is problematic.

This work was aimed at investigating CZE separations of alkali and alkaline earth metal and ammonium cations in which complexing effects of negatively charged ligand(s) and electroneutral crown ethers were combined. It was expected that such a combination of the complexing agents would provide separation conditions suitable for the resolution of the complete group of the cations. Indirect UV absorption detection was chosen to monitor the separations.

2. Experimental

2.1. Instrumentation

A CS Isotachophoretic Analyzer (Labeco-Villa, Spišská Nová Ves, Slovak Republic) was used in the single-column configuration of the separation unit. The column was provided with a 300 μm I.D. capillary tube made of fluorinated ethylene–propylene copolymer (FEP). Its length from the injection point to the detector was 250 mm. The column was connected to a hydrodynamically closed counter-electrode compartment as is current in ITP equipment [21]. The samples were injected with the aid of laboratory-made devices for electromigration injection. A UV spectrophotometric detector [24] was used to monitor the separations at 254 nm.

2.2. Chemicals

The chemicals used for the preparation of the carrier electrolytes were obtained from BDH (Poole, UK), Serva (Heidelberg, Germany), Janssen Chimica (Beerse, Belgium), Sigma (St. Louis, MO, USA), Lachema (Brno, Czech Republic), Reachim (Moscow, Russian Federation), Carlo Erba (Milan, Italy) and Spolana (Neratovice, Czech Republic). Demineralized methylhydroxyethylcellulose (Laboratory of Environmental Analysis, Comenius University, Bratislava, Slovak Republic) was used as an anticonvective additive to the carrier electrolyte. The solutions of the electrolytes were prepared from demineralized water.

Benzimidazole (Lachema), used for the preparations of the carrier electrolytes, was purified by precipitation from a methanolic solution. Other chemicals were used in purities as received.

2.3. Samples

A rain water sample was kindly provided by the Slovak Meteorological Institute (Bratislava, Slovak Republic). Tap water samples were collected in the laboratory in polyethylene sample containers. Mineral waters were purchased in a local supermarket. The samples were injected for analysis without any pretreatment.

3. Results and discussion

3.1. Separation conditions

For already mentioned reasons, the electrolyte systems studied in the CZE separations of alkali and alkaline earth metal and ammonium cations combined the complexing effects of negatively charged counter ions and uncharged 18-crown-6. To achieve a complete resolution of these cations, the choice of the counter-ion constituent(s) and the concentrations of the complexing agents was based on the following considerations.

(i) ITP measurements by Tazaki *et al.* [23] imply that a higher concentration of 18-crown-6 in the carrier electrolyte is favourable as it widens the range of the effective mobilities of the cations and at the same time provides a complete resolution of K^+, Rb^+, Cs^+ and NH_4^+. From these measurements it is also apparent that the effective mobilities of alkaline earth metal

cations should be decreased via an appropriately chosen (complexing) counter-ion constituent to avoid the risk of the formation of mixed zones of these separands with the monovalent cations.

(ii) Although the concentration of crown ether in the carrier electrolyte is not restricted by the electrophoretic separation, the use of indirect detection sets the upper concentration limit for the counter-ion constituent. This is clear from the equation [25] relating the concentration limit of detection (c_{LOD}),

$$c_{LOD} = c_V/(DR \cdot TR) \quad (1)$$

with the concentration of the visualization co-ion (c_V), dynamic reserve (DR) and transfer (displacement) ratio (TR). From this equation it is apparent that favourable detection conditions require a low concentration of the co-ion in the carrier electrolyte and, consequently (electroneutrality), also a low concentration of the (complexing) counter ions.

(iii) The concentration of the complex forming counter ion in the carrier electrolyte has a direct influence on the effective mobilities of the separated cations (see, *e.g.*, refs. 26 and 27). Therefore, weak complexing agents, although providing CZE resolutions of alkaline earth metal cations (see, *e.g.*, refs. 11 and 12), are not convenient for the intended group retardation.

With the above facts in mind, the counter-ion constituents (Table 1) were chosen among the acids with pH buffering capacities at pH ≈ 5.0–6.0 that form complexes with alkaline earth metal cations with stability constants in the range 10^2–10^4 [28].

The effective mobility of the co-ion in the carrier electrolyte should be as close as possible to those of the separated ions [29,30]. In addition, favourable detection conditions require that its concentration in this electrolyte is low (see Eq. 1) while its molar absorptivity at the detection wavelength is high [30,31]. Undoubtedly, these criteria restrict the choice and there is hardly any constituent that meets them for all of the separated cations. The co-ions employed in this work are given in Table 1.

Twenty electrolyte systems based on the constituents listed in Table 1 (each with and without 18-crown-6) were tested [32]. Although several of these systems provided complete resolutions of the cations, only two of them (Table 2) gave

Table 1
Co-ions and counter ions studied as carrier electrolyte constituents in the separation of cations

Ions	Species[a]	Rating	Remarks
Co-ions	Benzimidazole	+	+ = Suitable
	Benzylamine	−	− = Drifts on the baseline, noise of the signal
	Cytosine	−	
	Creatinine	−	
	2,4,6-Collidine	+	
	2-Aminopyridine	−	
Counter ions	ADA	−	+ = Suitable
	PIPES	−	− = Insufficient differentiation
	FMIDA	−	
	HIDA	−	
	Glycolic acid	−	
	Chloroacetic acid	−	
	Iminodiacetic acid	−	
	Tartaric acid	+	
	Citric acid	−[b]	

[a] ADA–N-(2-acetamido)iminodiacetic acid; PIPES = 1,4-piperazinebis(ethanesulphonic) acid; FMIDA = phosphonomethyliminodiacetic acid; HIDA = hydroxyethyliminodiacetic acid.
[b] Strong retardation of doubly charged cations.

Table 2
Electrolyte systems

Parameter	Carrier electrolyte[a]	
	No. 1	No. 2
Solvent	Water	Water
Co-ion	Benzimidazole	Collidine
Concentration (mmol l^{-1})	5	5
Counter ion	Tartrate	Tartrate
pH	5.2	5.2
Additive	HEC; *m*-HEC	HEC; *m*-HEC
Concentration (%, w/v)	0.1; 0.1	0.1; 0.1
Complexing additive	Crown ether	Crown ether
Concentration (mmol l^{-1})	40	40

[a] Collidine = 2,4,6-collidine; HEC = hydroxyethylcellulose; *m*-HEC = methylhydroxyethylcellulose; crown ether = 18-crown-6.

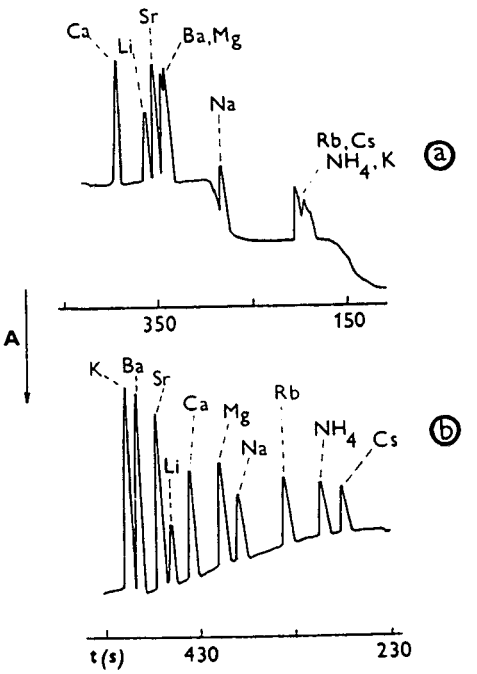

Fig. 1. Electropherograms from the separation of a model mixture (each at a concentration of 10^{-4} mol l^{-1}) in electrolyte system (Table 2): (a) without crown ether; (b) with crown ether (0.04 mol l^{-1}). Driving current, 75 μA; electromigration injection at 50 μA (time = 4 s); FEP capillary column (25 cm × 0.3 mm I.D.). A = decreasing absorption at 254 nm.

an acceptable performance also from the point of view of detection. Strong (often reproducible) drifts of the baselines on the electropherograms and/or increased noise of the detector restricted our choice (see also below).

Ba^{2+}, Ca^{2+}, Sr^{2+} and Mg^{2+} ions migrate in aqueous electrolyte systems under non-complexing conditions or in the presence of weak complexing agents with effective mobilities intermediate between those of K^+ and Na^+ ions [10–12,19–21]. The use of tartrate in the carrier electrolytes changed this migration configuration by decreasing the effective mobilities of the alkaline earth metal cations relative to the other separands (Figs. 1a and 2a). This group retardation was favourable as complete resolutions could be achieved via complexing effects of 18-crown-6 (Figs. 1b and 2b).

From the electropherograms in Fig. 1, it can be seen that the migration times of the cations increased on addition of crown ether to the carrier electrolyte. This is in agreement with the ITP measurements [9,23], which showed that the crown-complexed cations have lower ionic mobilities than the solvated cations. The shorter migration times for Ca^{2+}, Sr^{2+}, Mg^{2+} and Li^+ in electrolyte system 2 [relative to those obtained in the carrier electrolyte without crown ether (Fig. 2a)], however, indicate the opposite effect of the crown complexation. In spite of the fact that competitions of the ligands for the metal cations have to be considered, these results suggest that complexation of the co-ion (collidine) by the crown ether also plays a rôle.

3.2. Separation performance

Drifts of the baseline in CZE separations with indirect UV absorption detection are ascribed to thermal effects due to Joule heating [30,33]. Our experiments carried out in this context (different driving currents) agreed with these findings [32] (see also Fig. 3). On the other hand, the electropherograms in Fig. 1 imply that this need not be the only explanation as the addition of 18-crown-6 to the carrier electrolyte (under other-

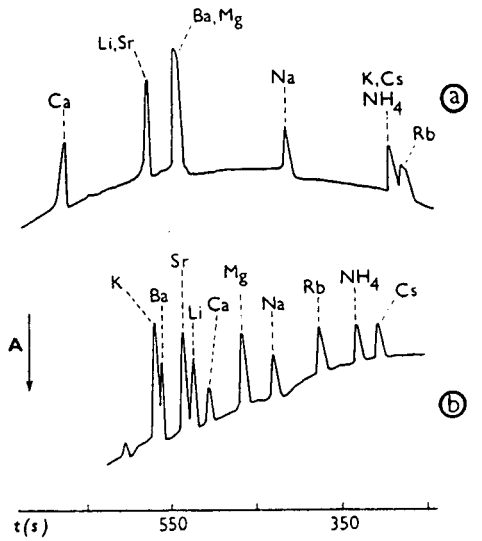

Fig. 2. Electropherograms from the separation of a model mixture (each at a concentration of 10^{-4} mol l^{-1}) in electrolyte system (Table 2): (a) without crown ether; (b) with crown ether (0.04 mol l^{-1}). Other conditions as in Fig. 1.

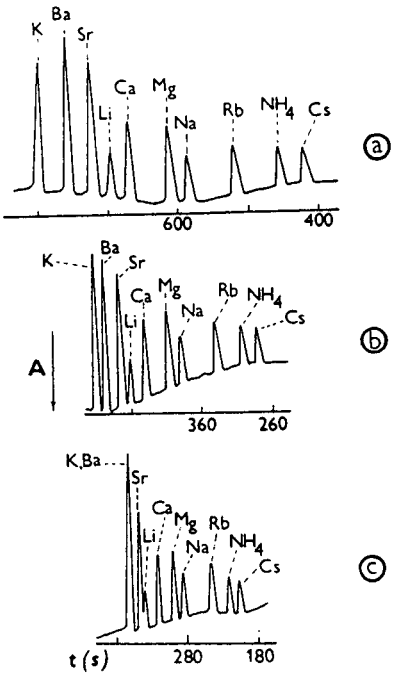

Fig. 3. Effect of the driving current on the CZE separations of the cations. The separations were carried out in electrolyte system 1 (Table 2). (a) 50 μA; (b) 75 μA; (c) 100 μA. Electromigration injection at 40 μA (time = 4 s). Other conditions as in Fig. 1.

wise identical working conditions) improved the drift considerably (Fig. 1). However, for most of the tested systems the effect of the crown ether was not so significant. The electropherograms in Fig. 3 show that the resolutions of K^+ and Ba^{2+} and to a lesser extent Sr^{2+} and Li^+ depended on the driving current. Although decreased separation efficiencies at 10 μA (Table 3) provide a straightforward explanation for the decreased resolutions, different dependences of the effective mobilities of K^+ and Ba^{2+} on temperature should be also taken into the consideration for this particular pair.

The I.D. of the capillary tube employed in this work (300 μm) is less favourable from the point of view of thermal dispersion [34]. For less conductive carrier electrolytes, such as are currently used in separations with indirect detection (see Eq. 1), this need not be a serious disadvantage. The separation efficiencies obtained in our experiments (Table 3) and frontings of the peaks of the most mobile cations suggest that the electromigration dispersion (not related to the I.D. of the column [29]) was mainly responsible for the band broadening. These results also indicate that benzimidazole met the mobility requirements only for less mobile separands. This is a general problem in CZE separations with indirect detection and probably the use of multi-component buffer systems [35] would eliminate this discriminative effect of the carrier electrolytes containing only one co-ionic constituent.

3.3. Application

Examples of CZE separations of practical samples under the proposed separating conditions are shown in Figs. 4 and 5. Although none of these samples contained all of the studied cations at detectable concentrations, the analytical potential of this approach is apparent. For example, it can be seen that the electrolyte systems combining complexation effects of various types of the ligands can provide enhanced selectivities of the separations and, thus, offer a

Table 3
Separation performance parameters obtained at different driving currents

Cation	50 μA		75 μA			100 μA	
	t_m (s)	N/m	t_m (s)	R.S.D. (%)	N/m	t_m (s)	N/m
Cs^+	421.0	46 400	288.0	0.16	43 500	207.5	35 300
NH_4^+	455.9	73 800	303.2	0.15	75 200	221.8	40 380
Rb^+	520.4	70 900	339.1	0.07	60 300	247.3	31 100
Na^+	581.6	84 600	387.3	0.13	122 700	286.6	67 300
Mg^{2+}	615.8	134 600	406.4	0.08	135 100	301.6	74 600
Ca^{2+}	669.7	159 200	438.5	0.05	157 200	322.5	66 200
Li^+	697.4	247 400	461.3	0.09	174 200	341.4	–
Sr^{2+}	724.3	157 200	477.2	0.08	331 500	348.6	–
Ba^{2+}	757.9	292 200	498.0	0.10	361 300	364.3	–
K^+	800.0	325 600	511.1	0.07	380 400	364.3	–

t_m = Migration time; R.S.D. = relative standard deviation for five runs performed within one day; N/m = number of theoretical plates per metre.

way to develop very rapid procedures for the determination of alkali and alkaline earth metal and ammonium cations in various water samples. In this context, a detailed optimization of the composition of the carrier electrolyte is desirable.

Although the within-day reproducibilities of the migration times of the cations were very favourable (Table 3) and their day-to-day fluctuations (1% or slightly less) could be ascribed to small changes in the composition of the carrier electrolyte, an improvement in the quantification is needed.

In spite of the fact that the injection time in

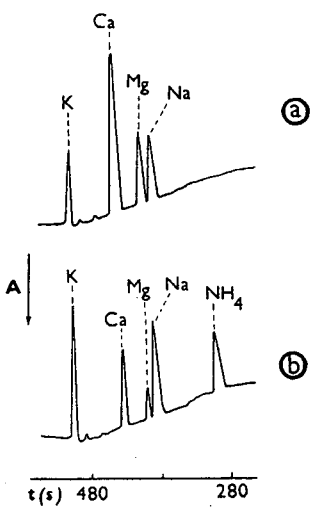

Fig. 4. Electropherograms from the separation of (a) drinking and (b) rain waters. Electrolyte system 1 (Table 2) was used. The separations were carried out with a driving current of 75 μA and electromigration injection was at 40 μA (time = 4 s).

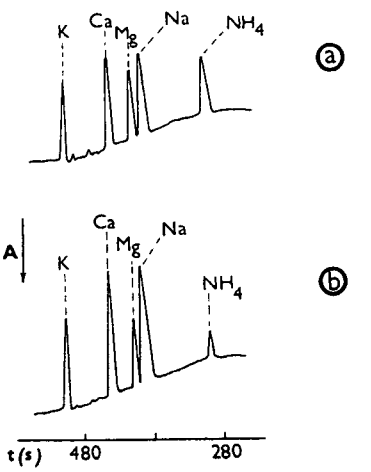

Fig. 5. Electropherograms from the separations of mineral waters in electrolyte system 1 (Table 2). (a) Baldovská mineral water (label concentrations: NH_4^+ = 0.5 ppm, Na^+ = 96.5 ppm, Mg^{2+} = 83.7 ppm, Ca^{2+} = 354.8 ppm, K^+ = 20.0 ppm); (b) Santovská mineral water (label concentrations: NH_4^+ = 0.2 ppm, Na^+ = 372.4 ppm, Mg^{2+} = 82.7 ppm, Ca^{2+} = 440.9 ppm, K^+ = 82.1 ppm). The driving current was 75 μA and electromigration injection was at 40 μA (time = 4 s).

the electromigration injection was carefully controlled (*ca.* 0.1% precision) and the injection current was stabilized to within 0.1% of the preselected value, the relative standard deviations for the peak areas for both model and practical samples were only seldom better than 7–10%. We consider that the main sources of these fluctuations were associated with the sample injection technique (extremely narrow bands of the separands focused at the end of the capillary which is moved from one solution to another). However, further studies along these lines are needed before the full potential of the proposed approach in quantitative analysis can be assessed.

4. Acknowledgement

This work was supported by a grant from the Slovak Grant Agency for Science under contract No. 1/990901/92.

5. References

[1] J. Vacík and I. Muselasová, *J. Chromatogr.*, 320 (1985) 199.
[2] S. Fanali, F. Foret and P. Boček, *Pharmazie*, 40 (1985) 653.
[3] A.A.G. Lemmens, F.M. Everaerts, J.W. Venema and H.D. Jonker, *J. Chromatogr.*, 439 (1988) 423.
[4] I. Matejovič and J. Polonský, *J. Chromatogr.*, 390 (1987) 155.
[5] P.S.L. Janssen and J.W. Nispan, *J. Chromatogr.*, 287 (1984) 166.
[6] P. Pei and D.J. Vonderschmitt, *J. Clin. Chem. Clin. Biochem.*, 26 (1988) 91.
[7] M. Koval', *Thesis*, Comenius University, Bratislava, 1981.
[8] I. Valášková, I. Zelenský, V. Zelenská, A. Komarnicki and D. Kaniansky, *Collect. Czech. Chem. Commun.*, 53 (1988) 515.
[9] F.S. Stover, *J. Chromatogr.*, 298 (1984) 203.
[10] D. Kaniansky, I. Zelenský, I. Valášková, J. Marák and V. Zelenská, *J. Chromatogr.*, 502 (1990) 143.
[11] A. Weston, P.R. Brown, P. Jandik, W.R. Jones and A.L. Heckenberg, *J. Chromatogr.*, 593 (1992) 289.
[12] A. Weston, P.R. Brown, A.L. Heckenberg, P. Jandik and W.R. Jones, *J. Chromatogr.*, 602 (1992) 249.
[13] M. Koberda, M. Konkowski, P. Yangberg, W.R. Jones and A. Weston, *J. Chromatogr.*, 602 (1992) 235.
[14] W. Beck and H. Engelhardt, *Chromatographia*, 33 (1992) 313.
[15] K. Baechmann, J. Boden and I. Haumann, *J. Chromatogr.*, 626 (1992) 259.
[16] J. Morawski, P. Alden and A. Sims, *J. Chromatogr.*, 640 (1993) 359.
[17] M. Chen and R.M. Cassidy, *J. Chromatogr.*, 640 (1993) 425.
[18] Y. Shi and J.S. Fritz, *J. Chromatogr.*, 640 (1993) 473.
[19] K.H. Hellwege, A.M. Schäfer and E. Lax (Editors), *Landolt–Börnstein, Zahlenwerte und Funktionen*, Band II, Teil 7, Springer, Berlin, 6. Aufl., 1960.
[20] R.C. Weast (Editor), *CRC Handbook of Chemistry and Physics*, CRC Press, Boca Raton, FL, 60th ed., 1980.
[21] F.M. Everaerts, J.L. Beckers and Th.P.E.M. Verheggen, *Isotachophoresis: Theory, Instrumentation and Applications*, Elsevier, Amsterdam, 1976.
[22] K. Fukushi and K. Hiiro, *Anal. Sci.*, 2 (1986) 219.
[23] M. Tazaki, M. Takagi and K. Ueno, *Chem. Lett.*, (1982) 639.
[24] P. Havaši and D. Kaniansky, *J. Chromatogr.*, 325 (1985) 137.
[25] E.S. Yeung, *Acc. Chem. Res.*, 22 (1989) 125.
[26] P. Gebauer and P. Boček, *Chem. Listy*, 77 (1983) 483.
[27] T. Hirokawa and Y. Kiso, *J. Chromatogr.*, 242 (1982) 227.
[28] S. Kotrlý and L. Šucha, *Handbook of Chemical Equilibria in Analytical Chemistry*, Ellis Horwood, Chichester, 1985.
[29] F.E.P. Mikkers, F.M. Everaerts and Th.P.E.M. Verheggen, *J. Chromatogr.*, 169 (1979) 1.
[30] F. Foret, S. Fanali, L. Ossicini and P. Boček, *J. Chromatogr.*, 470 (1989) 299.
[31] T. Wang and R.A. Hartwick, *J. Chromatogr.*, 607 (1992) 119.
[32] K. Lokšíková, *Graduation Report*, Comenius University, Bratislava, 1992.
[33] Y. Ma and R. Zhang, *J. Chromatogr.*, 625 (1992) 341.
[34] R. Virtanen, *Thesis*, University of Technology, Helsinki, 1975.
[35] T. Wang and R.A. Hartwick, *J. Chromatogr.*, 589 (1992) 307.

ANALYTICAL BIOTECHNOLOGY

Proceedings of the 4th International Symposium on Analytical Methods, Systems and Strategies in Biotechnology (ANABIOTEC '92), Noordwijkerhout, The Netherlands, 21-23 September 1992

Edited by **C. van Dijk**

Previously published as part of the 1993 subscription to the journals *Analytica Chimica Acta* and *Journal of Biotechnology*

ANABIOTEC '92 focused on the further integration of biotechnology and analytical chemistry. The results of this symposium clearly demonstrated that a substantial progress could be reported in the application of both conventional and new analytical techniques, the latter essentially based on natural analytical tools such as biomolecules. The main themes covered during this meeting are fermentation monitoring, chromatography, instrumental analysis, biosensors and bioanalysis.

A selection of the contents.
Preface.
Process Control. Monitoring and control of recombinant protein production (K. Schügerl *et al.*). Rapid and quantitative analysis of bioprocesses using pyrolysis mass spectrometry and neural networks: application to indole production (R. Goodacre, D.B. Kell). Characterization of a sampling unit based on tangential flow filtration for on-line bioprocess monitoring (T. Buttler, L. Gorton, G. Marko-Varga). Automated monitoring of biotechnological processes using on-line ultrafiltration and column liquid chromatography (N.C. Van de Merbel *et al.*). On-line monitoring of penicillin V during penicillin fermentations: a comparison of two different methods based on flow-injection analysis (M. Carlsen *et al.*). Development of an on-line method for the monitoring of vicinal diketones and their precursors in beer fermentation (C. Mathis *et al.*). Monitoring of fermentation by infrared spectrometry. Alcoholic and lactic fermentations (D. Picque *et al.*).
Chromatography and other Separation Techniques. Chromatographic analysis of biopolymers distribution in "poly-hemoglobin", an intermolecularly crosslinked hemoglobin solution (J. Simoni, G. Simoni, M. Feola). Application of multivariate mathematical-statistical methods for the comparison of the retention behaviour of porous graphitized carbon and octadecylsilica columns (E. Forgács, T. Cserháti, B. Bordás).
Antibodies. Catalytic antibodies: new developments (R. Hilhorst).
Biosensors. Measurements of nitric oxide in biological materials using a porphyrinic microsensor (T. Malinski *et al.*). Reusable fiber-optic-based immunosensor for rapid detection of imazethapyr herbicide (R.B. Wong, N. Anis, M.E. Eldefrawi). Biosensor monitoring of blood lactate during open-heart surgery (M. Kyröläinen *et al.*).
Instrumental Techniques. Introduction to the dielectric estimation of cellular biomass in real time, with special emphasis on measurements at high volume fractions (C.L. Davey *et al.*). Spectral analysis of interactions between proteins and dye ligands (J. Hubble, A.G. Mayes, R. Eisenthal).
Enzymatic Analysis. Preservation of shelf life of enzyme based analytical systems using a combination of sugars, sugar alcohols and cationic polymers or zinc ions (T.D. Gibson, J.N. Hulbert, J.R. Woodward).
Colloidal Carbon Particles. Colloidal carbon particles as a new label for rapid immunochemical test methods: Quantitative computer image analysis of results (A. van Amerongen *et al.*). Author Index.

© 1993 208 pages Hardbound
Price: Dfl. 265.00 (US $ 151.50)
ISBN 0-444-81640-2

ORDER INFORMATION

For USA and Canada
ELSEVIER SCIENCE INC.
P.O. Box 945
Madison Square Station
New York, NY 10160-0757
Fax: (212) 633 3880

In all other countries
ELSEVIER SCIENCE B.V.
P.O. Box 330
1000 AH Amsterdam
The Netherlands
Fax: (+31-20) 5862 845

US$ prices are valid only for the USA & Canada and are subject to exchange rate fluctuations; in all other countries the Dutch guilder price (Dfl.) is definitive. Customers in the European Community should add the appropriate VAT rate applicable in their country to the price(s). Books are sent postfree if prepaid.

ELSEVIER SCIENCE B.V.

TrAC - Trends in Analytical Chemistry: Reference Edition Volume 12: 1993

TrAC Compendium Series Volume 12

The Reference Edition of *Trends in Analytical Chemistry (TrAC)* is a compilation of the archival material reprinted from the regular issues of the journal. *TrAC* provides a topical digest of current developments and new ideas in the analytical sciences. It does so in the form of broadly-based, easy-to-read scientific reviews, backed up by news and other features of interest to the international analytical chemistry community. For subscribers to the library edition of *TrAC*, the reference edition forms an integral part of the annual subscription, but for others it can be purchased individually. It provides informative and stimulating reading for all those who use analytical methods.

This latest volume contains all the archival material published in 1993. It covers a wide range of analytical techniques and applications of interest to academic and research workers in chemistry, biochemistry, clinical chemistry, pharmaceutical chemistry and toxicology.

Contents: *A selection of the Contents.* Single-cell analysis at the level of a single human erythrocyte (B.L. Hogan, E.S. Yeung). Charge-remote fragmentations for structural determination of lipids (J. Adams, M.J. Songer). Recent advances in speciation analysis by capillary gas chromatography-microwave induced plasma atomic emission spectrometry (R. Lobinski, F.C. Adams). Pyrolysis-mass spectrometry under soft ionization conditions (A.C. Tas, J. van der Greef). New developments in glow discharge mass spectrometry (Y. Mei, R.K. Marcus). Enantiomeric separation by micellar electrokinetic chromatography (K. Otsuka, S. Terabe). Liquid chromatographic methods for the chiral separation of β-adrenergic blocking agents (C. Vandenbosch *et al.*). Capillary gel electrophoresis of biopolymers (A.S. Cohen, D.L. Smisek, P. Keohavong). Vibrational spectroscopy - where are we and where are we going? (J.L. Koenig). Capillary electrophoresis of inorganic ions and low-molecular-mass ionic solutes (P.E. Jackson, P.R. Haddad). Mass spectrometric analysis of a GPI-anchored protein: the scrapie prion protein (M.A. Baldwin, A.L. Burlingame, S.B. Prusiner). *In vivo* blood-gas and electrolyte sensors: progress and challenges (M.E. Meyerhoff). Trace analysis in capillary supercritical fluid chromatography: sample introduction (T. Greibrokk, B.E. Berg). Analytical applications of electrified interfaces between two immiscible solutions (P. Vanysek). The use of gas chromatographic detectors in column liquid chromatography (Ch.E. Kientz, U.A.Th. Brinkman). Imaging applications for chemical analysis utilizing charge coupled device array detectors (C.W. Earle *et al.*). Mass spectrometry of proteins (P. Roepstorff).

ELSEVIER SCIENCE

© 1993 592 pages Hardbound
Price: Dfl. 675.00 (US$ 385.75)
ISBN 0-444-81805-7

*An extra supplement is included in this edition - **Directory of Capillary Electrophoresis**:*

- **Over 450 V.I.P.s Worldwide**
- **Complete Addresses, Fax and Phone Numbers, and E-Mail Addresses (where available)**
- **Many Techniques, Applications and Research Topics**
- **Extensive Subject Index.**

This directory forms an integral part of the 1993 subscription to the Library Edition and is also available as a separate publication.

ORDER INFORMATION
ELSEVIER SCIENCE B.V.
P.O. Box 330
1000 AH Amsterdam
The Netherlands
Fax: (+31-20) 5862 845

For USA and Canada
P.O. Box 945
Madison Square Station
New York, NY 10159-0945
Fax: (212) 633 3680

US$ prices are valid only for the USA & Canada and are subject to exchange rate fluctuations; in all other countries the Dutch guilder price (Dfl.) is definitive. Customers in the European Union should add the appropriate VAT rate applicable in their country to the price(s). Books are sent post-free if prepaid.

PUBLICATION SCHEDULE FOR THE 1994 SUBSCRIPTION

Journal of Chromatography A and *Journal of Chromatography B: Biomedical Applications*

MONTH	O 1993	N 1993	D 1993	J	F	M	A	
Journal of Chromatography A	652/1 652/2 653/1	653/2 654/1 654/2 655/1	655/2 656/1 + 2 657/1 657/2	658/1 658/2 659/1 659/2	660/1 + 2 661/1 + 2 662/1 662/2	663/1 663/2 664/1	664/2 665/1 665/2 666/1 + 2 667/1	The publication schedule for further issues will be published later.
Bibliography Section						681/1		
Journal of Chromatography B: Biomedical Applications				652/1	652/2 653/1	653/2 654/1	654/2 655/1	

INFORMATION FOR AUTHORS

(Detailed *Instructions to Authors* were published in *J. Chromatogr. A*, Vol. 657, pp. 463–469. A free reprint can be obtained by application to the publisher, Elsevier Science B.V., P.O. Box 330, 1000 AH Amsterdam, Netherlands.)

Types of Contributions. The following types of papers are published: Regular research papers (full-length papers), Review articles, Short Communications and Discussions. Short Communications are usually descriptions of short investigations, or they can report minor technical improvements of previously published procedures; they reflect the same quality of research as full-length papers, but should preferably not exceed five printed pages. Discussions (one or two pages) should explain, amplify, correct or otherwise comment substantively upon an article recently published in the journal. For Review articles, see inside front cover under Submission of Papers.

Submission. Every paper must be accompanied by a letter from the senior author, stating that he/she is submitting the paper for publication in the *Journal of Chromatography A* or *B*.

Manuscripts. Manuscripts should be typed in **double spacing** on consecutively numbered pages of uniform size. The manuscript should be preceded by a sheet of manuscript paper carrying the title of the paper and the name and full postal address of the person to whom the proofs are to be sent. As a rule, papers should be divided into sections, headed by a caption (*e.g.*, Abstract, Introduction, Experimental, Results, Discussion, etc.) All illustrations, photographs, tables, etc., should be on separate sheets.

Abstract. All articles should have an abstract of 50–100 words which clearly and briefly indicates what is new, different and significant. No references should be given.

Introduction. Every paper must have a concise introduction mentioning what has been done before on the topic described, and stating clearly what is new in the paper now submitted.

Experimental conditions should preferably be given on a *separate* sheet, headed "Conditions". These conditions will, if appropriate, be printed in a block, directly following the heading "Experimental".

Illustrations. The figures should be submitted in a form suitable for reproduction, drawn in Indian ink on drawing or tracing paper. Each illustration should have a caption, all the *captions* being typed (with double spacing) together on a *separate sheet*. If structures are given in the text, the original drawings should be provided. Coloured illustrations are reproduced at the author's expense, the cost being determined by the number of pages and by the number of colours needed. The written permission of the author and publisher must be obtained for the use of any figure already published. Its source must be indicated in the legend.

References. References should be numbered in the order in which they are cited in the text, and listed in numerical sequence on a separate sheet at the end of the article. Please check a recent issue for the layout of the reference list. Abbreviations for the titles of journals should follow the system used by *Chemical Abstracts*. Articles not yet published should be given as "in press" (journal should be specified), "submitted for publication" (journal should be specified), "in preparation" or "personal communication".

Vols. 1–651 of the *Journal of Chromatography*; *Journal of Chromatography, Biomedical Applications* and *Journal of Chromatography, Symposium Volumes* should be cited as *J. Chromatogr.* From Vol. 652 on, *Journal of Chromatography A* (incl. Symposium Volumes) should be cited as *J. Chromatogr. A* and *Journal of Chromatography B: Biomedical Applications* as *J. Chromatogr. B*.

Dispatch. Before sending the manuscript to the Editor please check that the envelope contains four copies of the paper complete with references, captions and figures. One of the sets of figures must be the originals suitable for direct reproduction. Please also ensure that permission to publish has been obtained from your institute.

Proofs. One set of proofs will be sent to the author to be carefully checked for printer's errors. Corrections must be restricted to instances in which the proof is at variance with the manuscript.

Reprints. Fifty reprints will be supplied free of charge. Additional reprints can be ordered by the authors. An order form containing price quotations will be sent to the authors together with the proofs of their article.

Ovomucoid Bonded Column for Direct Chiral Separation

ULTRON ES-OVM

Narrow-Bore Column (2.0 I.D. x 150 mm) for Trace Analyses
Analytical Column (4.6 I.D. , 6.0 I.D. x 150 mm) for Regular Analyses
Semi-Preparative Column (20.0 I.D. x 250 mm) for Preparative Separation

Analysis of Trace FLURBIPROFEN in Metabolite with NARROW-BORE COLUMN

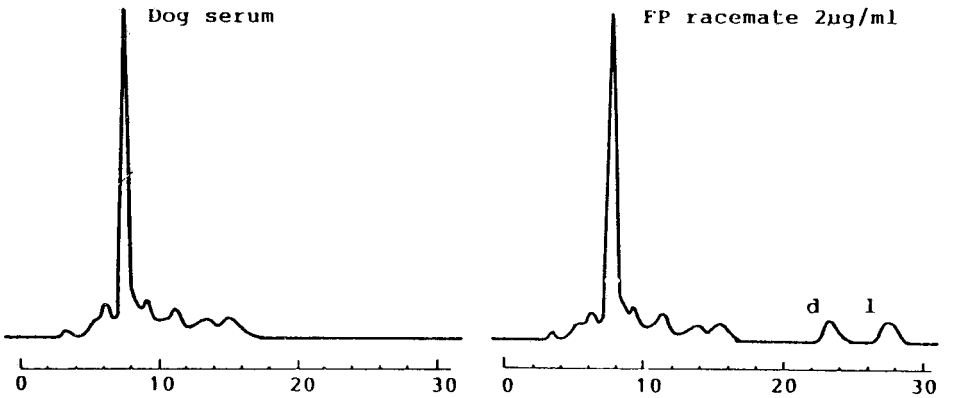

Conditions

Column: ULTRON ES-OVM(2.0I.D. x 150mm)
Mobile Phase: 20mMPhosphate Buffer(pH=3.0)/CH3CN =100/15
Flow Rate: 0.1ml/min
Temperature: 25°C
Injection: 5µl
Detection: UV- 247nm(0.05AUFS)

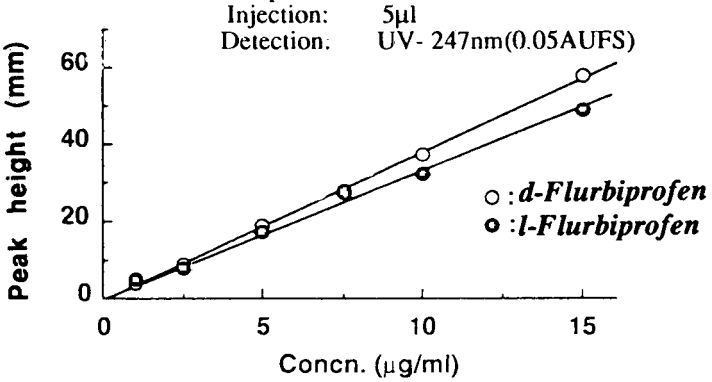

Calibration Curve for Each Enantiomer of Flurbiprofen

SHINWA CHEMICAL INDUSTRIES, LTD.

50 Kagekatsu-cho, Fushimi-ku, Kyoto 612, JAPAN
Phone:+81-75-621-2360 Fax:+81-75-602-2660

In the United States and Europe, please contact:

Rockland Technologies, Inc.

538 First State Boulevard, Newport, DE 19804, U.S.A.
Phone: 302-633-5880 Fax: 302-633-5893

This product is licenced by Eisai Co., Ltd.

16 W.A. 2537